Dankwoord

Vier jaar geleden was ik als naïeve student nog maar pas aan de slag gegaan met mijn doctoraatsproject op het labo longtoxicologie en nu heb ik dit onderzoek neergeschreven, met deze thesis als resultaat. Ik vermeld bewust dat ik nog een naïeve student was. Want al had ik een jaar ervaring als thesisstudent achter de rug, toch merkte ik snel dat zo'n doctoraat meer inhield dan gedacht. De afgelopen jaren waren dus enorm leerrijk en uitdagend, niet enkel binnen mijn onderzoeksdomein, maar ook op mentaal vlak, want teleurstellende resultaten en eindeloze herhalingen maken af en toe ook deel uit van een doctoraat. Gelukkig leerde ik hierdoor te relativeren en stond ik er niet alleen voor. Daarom wil ik de personen die rechtstreeks, of onrechtstreeks, hebben bijgedragen tot dit werk bedanken.

Om te beginnen, wil ik graag mijn promotor professor Peter Hoet bedanken. Bedankt om me te laten starten binnen jouw talentvolle onderzoeksgroep. Ondanks je drukke agenda kon ik op je rekenen en deed je steeds je best om zaken tijdig na te lezen, oplossingen te bieden of samen te zitten als ik er nood aan had. Door je kennis van zaken en jarenlange ervaring binnen toxicologie kon ik vertrouwen op je goede raad. Ook wil ik je bedanken om zo'n gemoedelijke en rustige promotor te zijn, dat maakte het werken zeer aangenaam. Ook mijn co-promotor professor Jeroen Vanoirbeek wil ik bedanken. Je enthousiasme en positivisme zijn ondertussen je handelsmerk, en dit werkte heel motiverend. Met jouw ervaring en hulp voor de muizenstudies, vormden jij en Peter samen een goed begeleidend team tijdens mijn doctoraat. Bedankt, professor Ben Nemery om je nog als inspiratiebron en hoofd van de groep longtoxicologie mee te mogen maken.

I want to thank the members of the jury, professor Guy Joos, professor Arno Gutleb, professor Guy Boeckxstaens and professor Bart Vanaudenaerde, and the chair of the public defense, professor Geert Verbeke, for their critical evaluation of the dissertation and their presence during the public defense.

Enkele mensen wil ik vermelden omwille van de wetenschappelijke samenwerkingen tijdens mijn doctoraat. Rita Derua wil ik bedanken voor de phosphoproteomics analyse in het werk omtrent de barrièreverstoring. Professor Marcel Ameloot en Hannelore Bové, bedankt voor jullie ideeën voor de kleuringen van de epitheelcellen, hopelijk kunnen we binnenkort de grafeen partikels visualiseren. I am very grateful to have had the opportunity to spend a few months in the research institute of Swetox in Sweden. Thanks, Ernesto for hosting me and providing me your insights in co-culturing of cells. I want to thank the whole board of Swetox and especially Åsa Gustafsson for this instructive experience. De micro-CT scan in het muismodel heb ik te danken aan professor Greetje Vande Velde. Je legde me deze techniek geduldig uit en zocht gretig mee naar oplossingen. Ook je aanwezigheid op congres in San Francisco en Hannover vond ik plezant. Anne-Charlotte, merci om je kennis en het protocol van de ILC's met me te delen. Jonathan Cremer wil ik bedanken voor de FACS analyse van de muizenlongen.

Bedankt, Professor Eric Verbeken voor de scoring en foto's van de histologie coupes, en voor je enthousiasme en interesse in mijn werk.

Mijn doctoraat zou niet hetzelfde zijn geweest zonder de goede collega's die hulp boden in het labo of tijdens presentaties, maar daarnaast ook leuke mensen bleken te zijn. Ik heb veel goede herinneringen aan uitstapjes op congressen, Kolonisten van Catan, dansavonden in De Hoorn, teambuildingactiviteiten, Kubb-spelen, Fatty Fridays, kerstfeestjes… en dit komt zeker door jullie!

Lore, jij begeleidde me al vanaf mijn start in het labo, en ook nadien konden we allerlei praktische zaken bij elkaar aftoetsen. Samen op de bureau, in het labo en op congres in Estoril en San Francisco hebben we héél wat grappige momenten bijeen gesprokkeld, en wat afgebabbeld. Hopelijk blijven we dat in de toekomst ook doen! Je was een vaste waarde, en sinds een jaartje weet ik ook dat je het goed doet buiten ons labo, dat wens ik je zeker toe! Tatjana, niet enkel op het werk, maar ook qua woonst ben je mijn buurvrouw. De uitgebreide verhalen over je weekend, training of turnen, deden me plezier. Je 'chillheid' en bedrevenheid zijn een goede combinatie waarmee je een mooi doctoraat zal kunnen afwerken. Veel succes voor de volgende jaren! Hannelore, jij bent ondertussen ook al een jaartje weg op het labo, en dat merkte ik wel. Niet enkel omdat er minder gebabbeld werd over konijnen, maar vooral omdat ik het zonder jou als luisterpaal moest zien te redden. Weet dat ik onze babbels, sportsessies, tv-avonden en naailessen koester. Caro, van klungelen in het labo met 16HBE's tot klungelen met stopcontacten bij de Willy in de kluscursus, dat soort onnozele momenten kennen geen geheimen meer voor ons. Je bent een topper waar ik terecht kon voor praktische hulp (en materiaal), maar nog meer voor de leuke en oprechte babbels. Birger, jou wil ik bedanken voor je open en sociaal gedrag, je flirterige mopjes of complimenten maakten vaak de dag wat vrolijker. De mountainbike tochtjes en dansavonden met jou waren steeds plezant. Birger en Caro, ook bedankt voor jullie koeken en om me niet weg te sturen wanneer ik bij jullie in de bureau kwam hangen als ik weer eens 5 minuten moest wachten. Bedankt, Annelore voor je opgewektheid, en dan vooral als het om zoetigheid ging (je koekjestaart ben ik nog niet vergeten). Jef, bedankt voor je hulpvaardigheid en droge, maar daarom grappige opmerkingen. Enkele onder jullie zijn me komen bezoeken in Stockholm, ik apprecieerde dat enorm en vond het een hele leuke tijd! Valerie, je optimisme is een grote troef en werkte aanstekelijk, Hanne, ik bewonder dat je je eigen ding bent gaan doen. Jullie vormden samen het ontvangstcomité in het begin van mijn doctoraat, bedankt voor de grappige en leuke situaties op die bureau. Deniz, thanks for learning me the tips and tricks of cell culture and taking care of the cells. Manosji, you are growing as post-doc, thanks for your attentive remarks during the meetings. Siva, I appreciate your open and unrestrained way of communicating, thanks for the talks in the cell culture room and your funny behavior after a beer.

Ook Sofie, Kristina, Stephanie, Anke, Laurens, Steven, Stijn, Fien, Elise en An bedankt voor jullie aanwezigheid en leuke middagpauzes, laser- of bowlingavonden, en teambuildingactiviteiten. Thanks Tracy, Tobias, Neel, Anna, Tom, John and Marko for your presence and pleasant lunches, laser or bowling evenings, and teambuilding events. I also want to mention our international visitors Fernanda, Tony, Patrick, Canan and Buket. It was nice to have you around and to share language-related, cultural and culinary differences. Bedankt aan Celine, Allard en Karen om het reilen en zeilen in het labo wat te organiseren. Ook een dikke dankjewel aan Anita en Eline voor het administratieve geregel en bestellingen.

Vrienden zorgden voor de nodige ontspanning en verzetten. Lien, Wannes, Marie, Sine, Lien, Eline, Quinten, Luk, Lore, Stijn en Lotte, ook al woont het merendeel van 'onze hoop' niet meer in Kasterlee, toch ligt daar onze basis en voelt bij jullie zijn een beetje zoals thuis zijn. Tijdens de toffe momenten met jullie was het werkknopje uitdraaien gemakkelijk. Eva en Hanne, het was leuk te weten dat ik ook op jullie kon terugvallen. Anneleen en Charlotte, samen konden we onze doctoraatservaringen delen, wat af en toe zeker deugd deed. Nele, je ving me goed op als nieuwe huisgenoot, door gebeurtenissen met je te delen en Jani programma's te kijken werd het appartement snel een ontspannende thuis na het werk.

Hilde, Stefan, Ine, Francis, Lotte, Wim, Lena, Sander en Margot, ik voelde me meteen heel welkom in jullie familie en genoot van de gezellige momenten samen, bedankt hiervoor.

Mama en papa, jullie staan steeds voor me klaar. Bedankt voor jullie steun, raad en opvang, eender wanneer of waarom ik er nood aan had in de afgelopen jaren. Zonder het vertrouwen en de warmte die jullie me hebben meegegeven zou ik hier niet staan. Thomas en Stijn, al was het soms plagend ('wat ga je nu weer met die muizen of cellen doen?'), ook jullie geloofden in jullie kleine zus. Ergens zal dat geplaag me wel gehard hebben en bijgedragen hebben tot dit resultaat. Ruth en Evelien, bedankt om zo'n goede schoonzussen te zijn, jullie interesse en sympathie apprecieer ik enorm. Ook bedankt bonmama, je zegt altijd 'je doet dat goed', wat een leuke blijk van vertrouwen gaf.

Lieve Dries, ja, jij verdient hier zeker ook een mooie dankjewel. Jouw moeiteloze hulp, gaande van cellen vervoeren, tips voor mooie figuren en teksten nalezen, tot geruststellen en opvrolijken, hebben zeker bijgedragen tot dit resultaat. Het feit dat ik alles met je kan delen en we elkaar goed begrijpen betekent heel veel voor me. We doen niet alles in de gebruikelijke volgorde, en ben benieuwd hoe de dingen verder op ons pad komen, maar met jou erbij zit dat zeker goed!

Sofie

Table of contents

List of abbreviations **i**

Chapter 1:

General introduction **1**

1. The airway barrier 3
2. Asthma 7
3. Irritants and airway hypersensitivity 14

Chapter 2:

Rationale and Aims **27**

Chapter 3:

Effect of irritants on a co-culture model of the airway barrier **33**

Chapter 4:

Contribution of mast cells in irritant-induced airway epithelial barrier impairment *in vitro* **61**

Chapter 5:

Irritant-induced asthma to hypochlorite in mice due to impairment of the airway barrier **83**

Chapter 6:

Airway barrier impairment increases nonspecific airway hyperresponsiveness in mice **115**

Chapter 7:

General Discussion **133**

1. Summary of the findings 135
2. Relevance and limitations 137
3. Future perspectives 149
4. General conclusion 151

Summary **157**

Samenvatting **163**

Scientific acknowledgement, personal contribution and conflict of interest statements **169**

List of publications **173**

Short curriculum vitae **179**

List of abbreviations

ADAM	A disintegrin and metalloproteinase domain-containing protein
AHR	Airway hyperreactivity
AJ	Adherens junctions
ALI	Air liquid interface
AP	Ammonium persulfate
ARDS	Acute respiratory distress syndrome
AUC	Area under the curve
BAL	Broncho-alveolar lavage
BCR	B-cell receptor
BW	Body weight
CCL	C-C motif ligand
CCR	C-C chemokine receptor
CCSP	Club cell secretory protein
CD	Cluster of differentiation
CGRP	Calcitonin gene-related peptide
ClO^-	Hypochlorite
COPD	Chronic obstuctive pulmonary disease
CT	Computed tomography
CYP	Cytochrome P450
Da	Dalton
DAMP	Danger-associated molecular pattern
DC	Dendritic cell
DCP	Double chamber plethysmography
DEP	Diesel exhaust particle
DPPC	Dipalmitoylphosphatidylcholine
EAR	Early phase asthmatic response
EMT	Epithelial-to-mesenchymal transition
FCS	Fetal calf serum
FcεRI	High affinity IgE receptor
FEV1	Forced expiratory volume in 1 second
FITC	Fluorescein isothiocyanate
FVC	Forced vital capacity
G	Graphene
GM-CSF	Granulocyte-macrophage stimulating factor
GNP	Graphene nanoparticle
GO	Graphene oxide
HDM	House dust mite
HMGB	High mobility group box
IFN	Interferon

IgE	Immunoglobulin E
IIA	Irritant-induced asthma
IL	Interleukin
ILC	Innate lymphoid cell
JAM	Junctional adhesion molecule
KO	Knock-out
LAR	Late phase asthmatic response
LDH	Lactate dehydrogenase
MCh	Methacholine
MHC	Major histocompatibility complex
MO	Mineral oil
MMAD	Mass median aerodynamic diameter
NA	Naphthalene
NPFE	Negative pressure-driven forced expiration maneuver
OA	Occupational asthma
OSHA/PEL	Occupational Safety and Health Administration Permissible Exposure Limit
OVA	Ovalbumin
PAMP	Pathogen-associated molecular pattern
ppm	Parts per million
PPR	Pattern recognition receptor
PTM	Post-translational modification
RADS	Reactive airways dysfunction syndrome
ROS	Reactive oxygen species
SP	Sodium persulfate
SP-D	Surfactant protein D
TCR	T-cell receptor
TEER	Transepithelial electrical resistance
TEM	Transmission electron microscopy
Th2	Type 2 T helper cell
TJ	Tight junctions
TLR	Toll-like receptor
TNF	Tumor necrosis factor
TRP	Transient receptor potential
TRPA1	Transient receptor potential ankyrin 1
TRPV1	Transient receptor potential vanilloid 1
TSLP	Thymic stromal lymphopoietin
WEA	Work exacerbated asthma
WHO	World health organization
WST-1	2-(4-Iodophenyl)-3-(4-nitrophenyl)-5-(2,4-disulfophenyl)-2H-tetrazolium
ZO	Zonula occludens

Chapter 1

General introduction

1. The airway barrier

We are continuously exposed to foreign compounds, such as chemicals, fumes, dust and particulates in the air. Upon inhalation, airway epithelial cells are the first cells to have contact with the contaminated air. The airway epithelium forms the interface between the external and internal environment, and plays an essential role in preventing entry of deleterious inhaled substances, and in maintaining homeostasis. Proper functioning of the airway epithelium is crucial in host defense. Alterations in the airway epithelium have been implicated in a number of respiratory diseases, including asthma, rhinosinusitus and chronic obstructive pulmonary disease (COPD).

1.1. The airway epithelium

The luminal surface of the human airway tract is covered with a continuous sheet of epithelial cells, which vary in distribution, abundance and cell type depending on the airway region [1]. Three regions can be identified: the large airways, which start from the trachea until the fifth generation of the bronchial tree, the small airways, which encompass the bronchi until the terminal bronchioles, and the alveoli [2]. Functionally, the airway tract is divided in a conducting zone which carries the inhaled air through the airways, and a respiratory zone which is responsible for gas exchange [1]. The large airways are lined with a pseudostratified epithelium, which gradually becomes columnar and cuboidal in the small airways [3] (Fig. 1). Ciliated cells account for over 50% of all epithelial cells in the conducting airways. The ciliary beating is an important aspect in innate immunity by keeping the airways clean and removing foreign particulates that are trapped in the mucus. Ciliated cells are believed to be terminally differentiated and arise from basal cells, yet a remarkable plasticity and dedifferentiation potential has been suggested [1,3]. Goblet cells secrete mucus in the airway lumen to protect the epithelial surface. In healthy subjects goblet cells are rare, but their number increases in most acute and chronic airway diseases [4]. Basal cells are located underneath the ciliated columnar epithelium. Their most important feature is their capacity to repopulate all the major cell types of the airway epithelium, and are therefore regarded as the airway epithelial precursor cells. Club cells (formerly termed Clara cells) are secretory cells found in the bronchioles, which release their marker club cell secretory protein (CCSP) and surfactant proteins. Club cells express high concentrations of cytochrome P450 monooxygenases, which are enzymes that play an extensive role in the detoxification of inhaled substances. Club cells are a heterogeneous group of cells, of which those located near neuroendocrine bodies and the bronchioalveolar duct junction have progenitor capacity [5]. Following the terminal bronchiole, nearly the whole surface of the alveoli is covered by type I alveolar epithelial cells, which allow gas exchange between the alveoli and blood. Type II alveolar epithelial cells represent the progenitor cells for the alveolar epithelium and produce pulmonary surfactant to keep the alveolar

surface open [6]. Other more rare cell types exist in the lungs: neuroendocrine cells, which sense oxygen levels, irritants and stretch in the airway and signal this information to other lung cells and the central nervous system; tuft cells, which are thought to act as immune sensors; and recently identified pulmonary ionocytes, which express multiple ion-transport genes and might function to maintain normal solute concentrations [7].

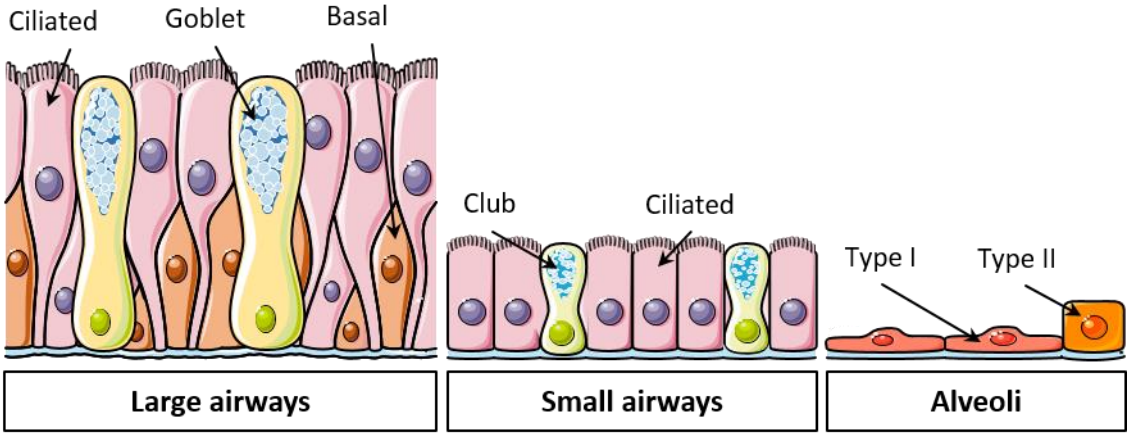

Figure 1. Representation of airway epithelium in different regions of the lung.
In the large airways, the major cell types are columnar ciliated, goblet and basal cells. In the small airways cuboidal ciliated cells and club cells are mainly found. In the alveoli, type I and type II cells are the major cell types. Adapted from Crystal *et al.* [3].

1.2. Barrier function of the airway epithelium

The human respiratory epithelium is an important part of the innate immune system. It functions to trap inhaled pathogens and particulate material in the secreted mucus, which is swept away from the lungs via coordinated beating of the cilia on airway epithelial cells [1]. Respiratory epithelial cells produce antimicrobial substances, as well as release chemokines and cytokines upon stimulation of the pattern recognition receptors (PPR) on their surface to mount protective responses upon insult [6,8]. Airway epithelial cells also create a physical barrier that prevents entry of potentially harmful agents to the host by the intercellular junctional complexes that are formed between neighboring cells [1]. The intercellular junctional complexes consist of the most apical located tight junctions (TJ) and the underlying adherens junctions (AJ) (Fig. 2). While TJ regulate the paracellular transport of ions and certain molecules across epithelia, AJ initiate and mediate cell-cell adhesion. The intercellular junctions not only regulate airway permeability, but also establish the apical-basolateral cell polarity and are involved in numerous signal transduction cascades. TJs are composed of several transmembrane proteins, such as occludin, junctional adhesion molecule (JAM), multiple claudins, and cytoplasmic scaffolding proteins, such as zonula occludens (ZO)-1, 2, 3 and cingulin. The principal proteins in AJs are E-cadherin, β-catenin and α-catenin [9,10]. Intercellular junctional complexes are dynamic structures that enhance/limit airway permeability depending on the stimulus [2]. Environmental exposures such as inhaled allergens, air pollution particles, ozone, cigarette smoke, and respiratory viruses have been

shown to impair the epithelial barrier function by affecting TJ and/or AJ [9]. In addition, certain inflammatory cytokines, such as tumor necrosis factor (TNF)-α, interferon (IFN)-γ, interleukin (IL)-4 and IL-13 have been reported to induce barrier dysfunction via reduced or altered junctional protein expression, or junction complex disassembly [11–13]. In asthma, evidence for epithelial barrier defects is emerging. In 2011, Xiao and colleagues demonstrated that in bronchial biopsies and bronchial epithelial cells of asthmatics, propagated *in vitro* at air liquid interface (ALI), the expression of ZO-1 is reduced, epithelial resistance is lower and permeability is increased, compared to in non-asthmatics [14]. In addition, reduced expression of TJ components in asthma has been described [10]. Airway barrier dysfunction has also been implicated in other respiratory diseases, such as cystic fibrosis, rhinitis and COPD, which all points to a crucial role of airway barrier integrity in maintaining respiratory health[9,13,15,16].

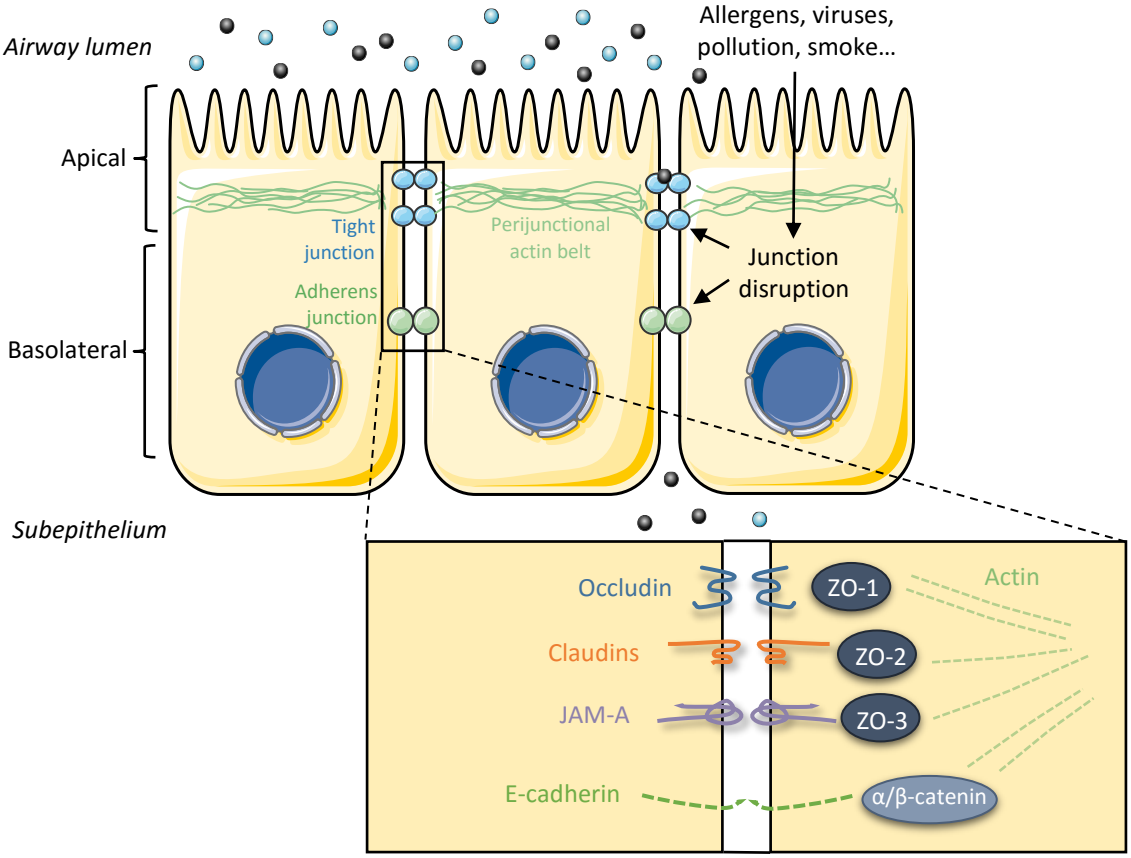

Figure 2. Organization of junctional structures in the respiratory epithelium
Epithelial cells are connected to each other via tight (blue) and adherens (green) junctions. The inset shows an enlarged scheme of protein-protein interactions in the intercellular junctions, including interaction of zonula occludens (ZO) and α/β-catenin with the intracytoplasmic domains and actin cytoskeleton. Figure adapted from Rezaee and Georas [10].

1.3. Naphthalene model of airway barrier impairment

Naphthalene (NA) is a polycyclic aromatic hydrocarbon, broadly known as the main ingredient of traditional mothballs. NA is present in coal tar, crude oil and is used as chemical intermediate in many manufacturing processes. NA is also found in vehicle exhaust and tobacco smoke, making it a ubiquitous environmental pollutant. In experimental set-ups, intra-peritoneal (i.p.) injection with 200 mg NA per kg body weight (BW) in mice is described as a good model of airway epithelial damage and repair [17]. Parenteral administration of NA results in dose-dependent, highly selective injury to the club cells in the airways of mice: low doses (50-100 mg/kg BW) only affect the distal airways, but both distal and larger proximal airways are affected at higher doses (≥ 300 mg/kg BW). In addition to the lesions observed in the lung, high doses of naphthalene (400 mg/kg BW) induce injury to the nasal epithelium of the mouse. Hepatic toxicity is absent and injury of the kidney only occurs at very high doses (400-600 mg/kg BW) of the compound [18,19]. The toxicity of NA requires metabolic activation to the reactive 1,2-naphthalene epoxide by cytochrome P450 monooxygenases. In mice, club cells are the main cellular site of the cytochrome P450 (CYP) isozyme 2F2 which activates NA with high selectivity and at high rate. The human orthologue, CYP2F1, converts NA at a significantly lower selectivity and rate, which explains the substantially larger susceptibility to NA in mice compared to in humans [19–22]. NA-induced airway injury evolves from club cell vacuolization and swelling, to cell death and cellular exfoliation within 24 hours. As response, the surviving progenitor cells quickly start to proliferate, after which these cells migrate and differentiate to normal club cells within 14 days [17,20,22].

The NA-model of airway injury has been used to study various aspects of airway epithelial damage and repair, as well as, implicated for models of asthma or fibrosis [17,23–28].

2. Asthma

Asthma is a chronic airway disease, characterized by reversible expiratory airflow limitation, non-specific airway hyperreactivity (AHR) and airway inflammation leading to airway remodeling. The symptoms of asthma include recurrent wheezing, shortness of breath, chest tightness and cough [29]. Patients with asthma experience these symptoms following exposure to non-specific stimuli such as cold air, exercise, air pollution or tobacco smoke, defining asthma a as condition of airway hypersensitivity [30].

According to a global health survey organized by the world health organization (WHO), the current global asthma prevalence among adults (18-45 year) is 4.5%, leading to an estimation of 315 million individuals with asthma worldwide. The prevalence varies greatly between countries, with the highest prevalence observed in resource-rich countries (for example a prevalence of 21.5% in Australia) [31]. Since asthma is one of the most common chronic diseases, asthma associated morbidity and mortality has become a major threat to public health and considerable burden for public health care [29,32].

Asthma is a complex disorder, driven by an interplay between genetic and environmental factors. Atopy, the genetic predisposition to develop antibodies against common environmental allergens, is a major risk factor to develop allergic asthma. Genome-wide association studies revealed various susceptibility genes for asthma such as the genes for IL-33, IL-1 receptor ligand 1, disintegrin and metalloproteinase domain-containing protein (ADAM) 33, and thymic stromal lymphopoietin (TSLP), but these explain only a limited part of the hereditary component of the disease [30,33,34]. Environmental risk factors such as viral infections (especially during childhood), environmental allergens, air pollution, tobacco smoke and lifestyle (e.g. living on a farm, diet, exercise) have a prominent role in asthma development and exacerbations [29,30].

Given its heterogeneity, the term asthma evolved from a single disease entity, to a broad term encompassing several distinct subgroups. The age at which a patient develops asthma symptoms defines the type of asthma. Childhood-onset asthma has generally an allergic origin, whereas in adult-onset asthma multiple subtypes exist [35]. In the clinic, severity and responsiveness to corticosteroids is a decisive feature. The type of inflammation, i.e. eosinophilic, neutrophilic or paucigranulocytic has long been considered as an important differentiator in asthma [36]. Within adult asthma, subgroups can be identified based on the causal/related stimuli such as in allergic asthma, aspirin-exacerbated asthma, menses-related asthma or occupational asthma (Fig. 3) [29,35]. Currently considerable attention is drawn for molecular phenotyping based on the disease pathway. This has led to identification of asthma subgroups based on the presence of the cytokines IL-4, IL-5 and IL-13, which were initially known to originate from type 2 T helper (Th2) cells, but have shown to be also produced by basophils,

mast cells and type 2 innate lymphoid cells (ILC). The type 2 cytokine high asthma is strongly linked with eosinophilia and is often mediated via allergic sensitization, whereas non-type 2 asthma defines a much broader asthma spectrum [29,36].

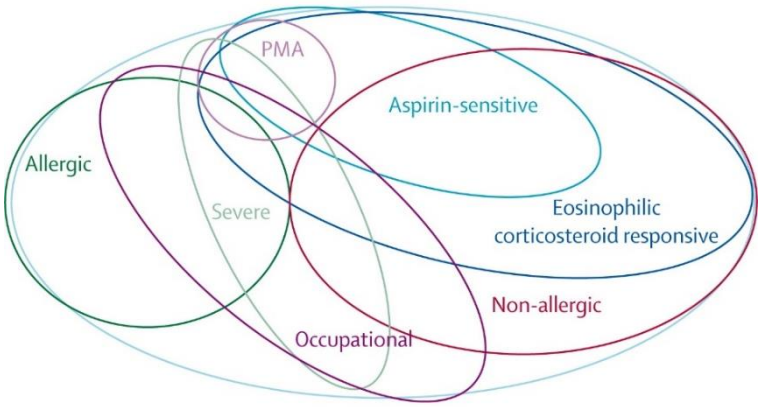

Figure 3. Venn diagram approach to identify phenotypes in adult-onset asthma
PMA=perimenstrual asthma. Figure from Wenzel [35]

2.1. Pathogenesis of allergic asthma

2.1.1. Immunological mechanism

In allergic asthma, the initial step in the pathogenesis is the recognition of an allergen by specialized antigen-presenting airway dendritic cells (DCs). Signals derived from the respiratory epithelium following exposure to allergens, irritants or microbes are the main stimuli that drive DC maturation and migration towards the lung [37]. DCs express receptors of the innate immune system that allow to capture the inhaled allergen, and subsequently process it into small peptides. Via the major histocompatibility complex (MHC) class II these peptides are presented to the T cell receptors (TCR) of naïve T cells located in the draining lymph node. Epithelial-derived signals program DCs to polarize naïve T cells towards Th2-type T cells [29,38]. A subset of these Th2 cells migrate to the B cell follicle to facilitate immunoglobulin class switching towards immunoglobulin E (IgE), while another subset migrates back to the airway mucosa to elicit the classical Th2 response via the release of pro-allergenic cytokines, such as IL-4, IL-5, IL-9, IL-13 and granulocyte-macrophage stimulating factor (GM-CSF) (Fig. 4) [39]. In addition, type 2 ILCs, are activated by the allergen-induced epithelial signals and release Th2 cytokines such as IL-5, IL-9 and IL-13 [40].

Once sensitized, the reintroduced allergen is recognized by the circulating allergen-specific IgE, which leads to cross-linking of the allergen to the mast cell via the high affinity IgE receptor (FcεRI). The activated mast cells release histamine, serotonin, prostaglandin D_2 and leukotriene C_4. These mediators are responsible for the early phase asthmatic response (EAR) that lasts for 5-90 minutes after allergen exposure and is characterized by contraction of the airway smooth muscle cells,

increased mucus secretion and vasodilation [29]. Three to twelve hours later, the EAR is followed by a late phase asthmatic response (LAR), which is caused by recruitment and activation of leukocytes (especially eosinophils) by the Th2 cytokines, which increase the airway responsiveness and inflammation [37].

Repetitive and longstanding stress, either from the mediators (cytokines, matrix metalloproteases and growth factors) released by inflammatory cells, or mechanically due to the bronchoconstriction, can result in airway wall remodeling. The structural changes in asthma include increase of airway smooth muscle mass, epithelial cell hyperplasia, goblet cell metaplasia, thickening of the basement membrane, neuronal proliferation and angiogenesis, resulting in permanent alterations in lung functioning [29,41].

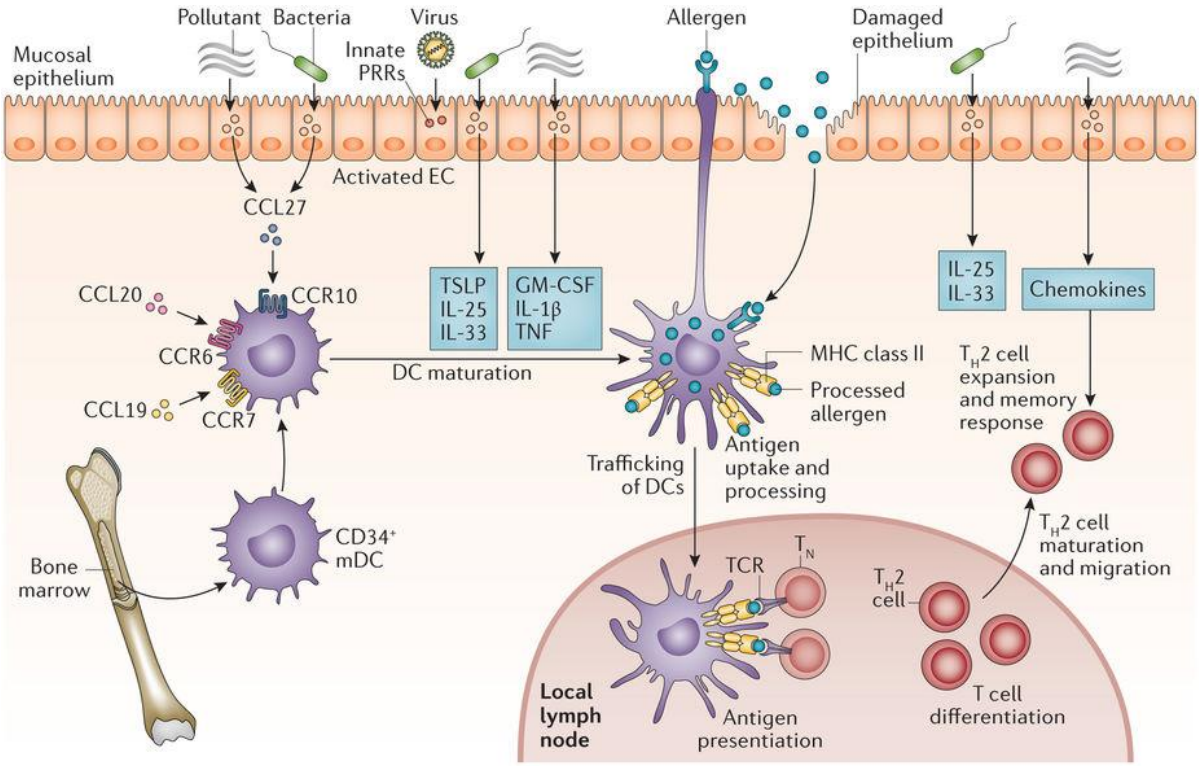

Figure 4. Mechanism of sensitization during the induction of allergic asthma
Infection (bacterial and viral), pollutants and allergens can perturb the airway epithelium, leading recruitment of dendritic cells (DCs). After allergen capture, the allergen is processed and presented by the DCs to naïve T cells in the local lymph node. T helper 2 (Th2) polarization of T cells is influenced by epithelial-derived signals. Abbreviations: PPR, pattern recognition receptor; EC, epithelial cell; CCL, CC-chemokine ligand; CCR, CC-chemokine receptor; TSLP, thymic stromal lymphopoietin; GM-CSF, granulocyte-macrophage colony-stimulating factor; TNF, tumor necrosis factor; MHC, major histocompatibility complex; TCR, T-cell receptor. Figure from Holgate et al. [29]

2.1.2. Cells involved in the immunological mechanism

As described above, the pathophysiology of allergic asthma involves both the innate and adaptive arms of the immune system. Although allergic asthma is generally considered as a disease mainly driven by adaptive immune responses via Th2-cell activation, the innate immune system has been recognized to play a crucial role. Innate immune cells serve as early responders upon first contact with allergens and direct the subsequent generated adaptive responses. In the next section, the innate immune cells investigated in this dissertation are discussed, while being aware that various other innate immune cells involved in allergic asthma are currently not considered.

Epithelial cells

For inhaled allergens to elicit an immune response, they have to pass the filtering in the upper airways and escape the mucociliary clearance, to reach the airway epithelium. Although it was long considered as merely a physical barrier to inhaled allergens, it has become clear that airway epithelial cells control many aspects in lung immunology and asthma [42]. Airway epithelial cells express PPRs including Toll-like receptors (TLRs), NOD-like receptors, C-type lectins and protease-activated receptors (PAR) on their surface to recognize and respond quickly to pathogen-associated molecular patterns (PAMPs) found in microbes, and danger-associated molecular patterns (DAMPS) released upon tissue damage, cell death or cellular stress (Fig. 4). Using these PPRs epithelial cells can sense the allergens and recruit immune cells such as DCs, ILC2s, Th2 cells, basophils and eosinophils via secretion of the chemokines C-C motif ligand (CCL) 22, CCL 17 and eotaxins CCL 11 and CCL 24 [40]. Triggering of the PPRs by allergen exposure also leads to the release of pro-Th2 cytokines IL-33, IL-25, GM-CSF and TSLP, which activate DCs to promote Th2 polarization and activate ILC2s, basophils, eosinophils, and mast cells [6,40]. In addition, epithelial cells can release DAMPs such as ATP, uric acid, high mobility group box (HMGB)-1, IL-1α and IL-33 which promote airway inflammation upon exposure to certain allergens [42]. In asthmatics, the barrier function of the respiratory epithelium is compromised [14,37]. This can be the result of intrinsic barrier defects (i.e. genetic polymorphisms in genes associated with the airway epithelium) or due to induced defects on the epithelium. Many allergens (such as house dust mite, cockroach and fungi) have protease activity and cleave the TJ between epithelial cells [6,10]. In addition, respiratory viruses and air pollutants, such as ozone, tobacco smoke and diesel particles induce oxidative stress, which has detrimental effects on the airway epithelium [9]. Consequently, inhaled allergens and particles penetrate more easily into the airway tissue, which facilitates the interaction with DCs.

Dendritic cells

Due to their sentinel and antigen presenting function, dendritic cells (DCs) are important immune cells that bridge the innate and adaptive immunity. Different subtypes of DCs coexist in the lungs, which are broadly devided into conventional DCs (cDC) and plasmacytiod DCs (pDCs). Among the cDCs cluster of differentiation (CD) $11b^+$ DCs are necessary and sufficient to induce allergic sensitization, whereas $CD103^+$ DCs have the capacity to induce tolerance to inhaled allergens [43]. pDCs control overt airway inflammation via incuction of regulatory T cells [44]. Monocyte-derived DCs (moDCs) arise during inflammation when monocytes are recruited to the local tissues and differentiate into inflammatory DCs that produce chemokines and cytokines that promote Th2 immunity [45,46]. Pulmonary DC are densely distributed near the respiratory epithelium, where they are ideally placed to sample the airway lumen for inhaled antigens [38]. Upon uptake of foreign agents and depending on signals derived from the epithelium, DCs mature by upregulating MHC II and costimulatory molecules such as OX40L, CD80 and CD86. Meanwhile they migrate towards the draining lymph node where they process and present the antigen to naïve T cells to induce a polarized T cell response. The outome of this response depens on signals derived from the airway epithelium upon contact with the allergen. Recognition of allergens such as house dust mite (HDM), cockroach or aspergillus fumigatus spores by the PPR on airway epithelial cells results in the release of the pro-Th2 cytokines TSLP, IL-25, IL-1α, IL-33 and GM-CSF that program DCs to polarize naïve T cells towards Th2-type T cells (Fig. 4) [43]. In addition, environmental risk factors that are associated with development of asthma including cigarette smoking, exposure to ambient particulate matter, exposure to high ozone concentrations or exposure to respiratory syncytial virus have been shown to interfere with the epithelial-DC crosstalk due to, among others, their detrimental effects on the airway barrier integrity [47].

Mast cells

Mast cells are innate immune cells that are particularly abundant at sites exposed to the environment, such as the skin and mucosal surfaces, where they have a role in host defense and maintenance of tissue homeostasis [48]. They are characterized by their ability to rapidly release pre-formed mediators (including histamine, serotonin and proteases) from their granules, secrete newly synthesized lipid mediators (including leukotriene C4 and prostaglandin D2) and production and secretion of cytokines (including TNF-α, IL-3, IL-4, IL-5, IL-6 and GM-CSF) and chemokines (including CCL2, CCL3, CXCL2 and CXCL8) upon activation [49–51]. The best-known mechanism of mast cell activation is via cross-linking of IgE bound to FcεRI on the surface of the mast cell, leading to the allergic cascade. Mast cells however express a large set of receptors, such as TLRs, hormone receptors, G-protein-coupled receptors, neuropeptide receptors, lipid receptors and alarmin receptors, allowing them to respond appropriately to not only allergic stimuli [52].

Innate lymphoid cells

Innate lymphoid cells (ILC) are recently discovered innate immune cells that play an important role in tissue homeostasis, repair and remodeling, in particular at barrier surfaces [53]. Unlike adaptive lymphoid immune cells, ILCs lack T- and B-cell receptors (TCR and BCR respectively), and therefore are antigen nonspecific. ILCs, however, respond rapidly to a wide variety of environmental triggers that induce release of cytokines such as IL-33, IL-25, TSLP and IL-1β in epithelial cells and other immune cells [54]. Based on their expression of effector cytokines and transcription factors, ILCs are classified into three groups: ILC1, ILC2 and ILC3. Remarkably, these groups mirror the phenotypic and functional characteristics of the respective T cell subsets (Th1, Th2 and Th17), and can be regarded as their innate counterparts [55]. Type 1 ILCs represent noncytotoxic IFN-γ producing cells, which have been implicated in Crohn's disease and COPD [55]. ILC2s are activated by IL-33 and IL-25 derived from epithelial cells in response to injury or stimulation of the PPRs. In murine models for asthma, ILC2s, like Th2 cells, produce IL-5, IL-9 and IL-13 and hereby mediate eosinophilia, goblet cell metaplasia and AHR, even in absence of the adaptive immune system [43,54]. Type 3 ILCs comprise a more heterogeneous group, which release IL-17, IL-22, GM-CSF and TNF-α, depending on the tissue-derived signals. Although a pivotal role for ILC2s in the pathogenesis of allergic asthma has clearly been demonstrated, ILCs could also considerably contribute to the development of non-allergic forms of asthma [54].

2.1.3. Neuronal mechanism

Besides an immunological mechanism, the neuronal system also plays a role in the asthmatic response. The upper and lower airways are innervated by sensory neurons that sense and respond to potential harmful substances in the environment [56]. Transient receptor potential (TRP) channels recognize and respond to a wide variety of stimuli (temperature, chemical compounds, pH, mechanical and oxidative stress) to maintain homeostasis and orchestrate protective responses [57]. Activation of the TRP channels results in the release of neuropeptides such as substance P, neurokinin A and calcitonin gene-related peptide (CGRP). These neuropeptides exert inflammatory and immune-modulatory effects such as smooth muscle contraction, vasodilatation, mucus secretion, degranulation of mast cells and chemo-attraction of eosinophils and neutrophils, summarized as neurogenic inflammation [58]. TRP channel activation leading to neurogenic inflammation is presumed to be crucial in causing cough, airway constriction and AHR in asthma [59]. The subtypes transient receptor potential ankyrin 1 (TRPA1) and transient receptor potential vanilloid 1 (TRPV1) are widely expressed in the respiratory tract and have been implicated in asthma pathogenesis [57]. TRPA1 is an important sensor of noxious stimuli, including noxious cold (<17°C), spicy foods (mustard oil, garlic, cinnamon) and irritants [60]. TRPA1 agonists in the environment include ozone, agents present in vehicle exhaust, air pollution and cigarette smoke and chemical irritants such as isocyantes and chlorine derivatives [56]. In rodent models

of both allergic and non-allergic asthma, TRPA1 has been shown to contribute to the development of AHR and airway inflammation [61–63]. TRPV1 can be activated by capsaicin, the pungent component of chili peppers, high temperatures (> 43°C) and acidosis (pH < 5.9) [60]. Studies on the role of TRPV1 in asthma, using rodent models, provided less clear results [62–64].

3. Irritants and airway hypersensitivity

The lungs play a crucial role in immunity by sensing inhaled pathogens, particles and chemical substances, and responds only to those that are harmful to the host. This mechanism has evolved over millions of years, since primitive humans were also exposed to airborne particles and chemicals in the form of wind-blown dusts, volcanic ash, fire smoke and pollens. The recent dramatic increase in chemicals, combustion-derived particles and engineered nanoparticles in the air, together with a change in lifestyle (i.e. diet and smoking) apparently puts a lot of stress on the pulmonary defense system, which might partly explain the increase in asthma prevalence the past decades [65]. Environmental factors associated with asthma prevalence are domestic indoor exposures (e.g. cleaning agents, indoor smoking, pet dander), ambient outdoor exposures (e.g. ozone, NO_2, particulate matter), as well as specific occupational exposures (e.g. wheat flour, spray paint, chlorine) [66].

3.1. Work-related asthma

As mentioned above, asthma can be identified based on the specific exposures/conditions that trigger the development of asthma (Fig. 3). Occupational asthma (OA) is asthma caused by exposure to a specific agent present in the work environment, while work exacerbated asthma (WEA) is defined as worsening of pre-existing asthma due to work-related exposures [67]. Occupational asthma and work exacerbated asthma are both included under the broader term of work-related asthma (Fig. 5). The population-attributable risk of work-related exposures has been estimated to be approximately 17% of all adult asthma cases, which is equivalent to an incidence of new-onset occupational asthma of 250 - 300 cases per 1 million people per year [68]. Occupational asthma can further be subdivided into sensitizer-induced occupational asthma and irritant-induced occupational asthma. Sensitizer-induced occupational asthma develops after an asymptomatic latency period, during which allergic sensitization towards the specific causal agent develops (Fig. 4). Irritant-induced asthma occurs after inhalation of respiratory irritants in absence of immune sensitization and accounts for less than 10% of occupational asthma cases [69].

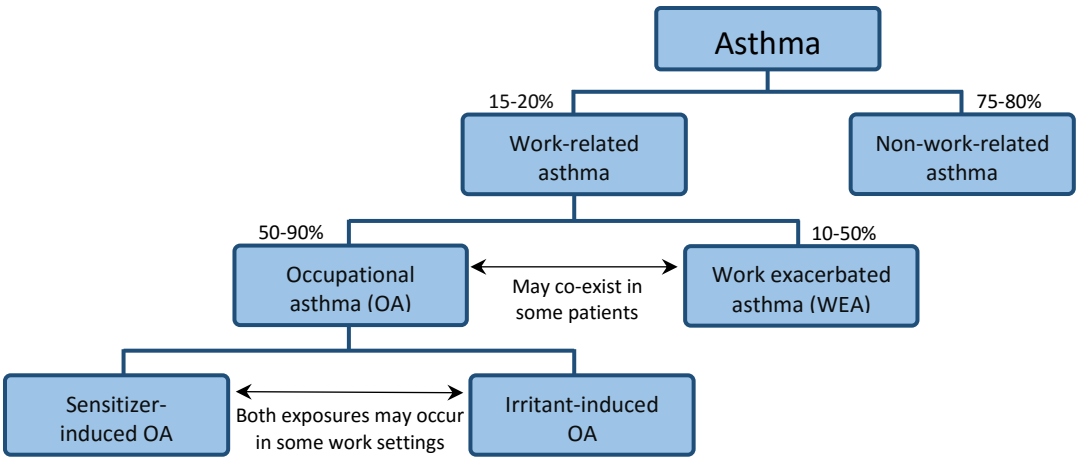

Figure 5. Subdivision of work-related asthma
Asthma is subdivided based on place of encounter, new-onset or not, and type of the causal agent. The relative prevalence of each subtype of asthma is indicated in percentage. Figure adapted from Trivedi *et al.* [67].

3.2. Irritant-induced asthma

Irritant-induced asthma (IIA) has been used to describe an asthmatic syndrome that is caused by exposure to agents that can act as respiratory irritants when inhaled [70]. An irritant is a non-corrosive chemical that causes a non-immunologic, reversible inflammatory reaction upon direct contact with the skin, eyes, nose or respiratory system [71]. Often, exposure to respiratory irritants occurs during work (which is why it has been classified as subset of occupational asthma) although it can also occur in non-occupational indoor and outdoor environments and domestic settings [70]. The best-defined subset of irritant-induced asthma was initially described by Brooks in 1985 [72]. The term reactive airways dysfunction syndrome (RADS) was introduced to describe a persistent respiratory condition defined by sudden occurrence of asthma-like symptoms within 24 hours after exposure to a single, very high concentration of an irritant agent.

IIA is demonstrated by airflow limitation (reduced forced expiratory volume in 1 second (FEV1)) on spirometry or non-specific bronchial hyperresponsiveness to methacholine/histamine [73]. Typical asthma symptoms including cough, wheeze and dyspnea are present. In the strict criteria defined for RADS, these symptoms should appear within 24 hours after a high irritant exposure, yet in other cases these symptoms can develop after a latency period. Treatment in an emergency facility or physician office following accidental exposure can be necessary [74]. Only a few clinical presentations are different in IIA compared to sensitizer-induced OA. In IIA, coughing is a predominant symptom and bronchial obstruction responds less well to bronchodilators (Brooks and Bernstein 2011). The long-term outcome for subjects with IIA is at least as poor as that for subjects with sensitizer-induced OA [74]. In a follow up study of 35 subjects with RADS only 17% had normal airway responsiveness at follow up [75].

3.2.1. Causes

The originally reported cause of IIA/RADS was allocated to a single high-level exposure to irritating vapors, fumes or smoke [72]. This form of acute onset IIA is most often caused by accidental exposure to irritant substances, e.g. after spills of volatile compounds, accidental release of irritants under pressure, explosion or accidental fire with release of complex mixtures [73]. Agents that have been associated with RADS include chlorine gas, ammonia, acids, sulfur dioxide, formaldehyde, isocyanates, diesel exhaust and dust (more specifically World Trade Center alkaline dust) [71,73].

Several clinical reports have described the development of asthma in subjects exposed to multiple high, yet not massive levels or irritant agents. These exposures mainly included 'puffs' or 'gassings' of chlorine, sulfur dioxide and ozone in industrial settings [73].

In addition, due to continuous exposure to irritants present in the work environment, certain persons might develop IIA. The most persuasive evidence for development of IIA because of chronic exposure is provided by epidemiologic studies of workers exposed to cleaning agents [76]. The frequent use of bleach (hypochlorite), ammonia and degreasing sprays has been consistently been associated with asthma in cleaning personnel [77,78]. Other reported occupational settings associated with development of IIA are swimming pools (lifeguards, swimming athletics) and automobile garages [79–83]. Although a clear causal relationship between irritant exposure and the development of asthma is weak on individual basis, continuous low dose exposure at the workplace (or non-work related settings) should not be neglected. This was pointed out in a large-scale epidemiological study in Estonian adults in which it was reported that 17% of individuals having asthma were repeatedly exposed to low levels of irritants in their workplace [84]. In addition, a recent study with data from three large European cohorts found a positive and significant association between lifetime occupational exposure to low molecular weight agents or irritants and adult-onset asthma [33].

3.2.2. Possible pathogenic mechanisms

Pathological observations from animal studies and bronchial biopsies in patients, pointed out that epithelial cells, which are the first line of cells in contact with irritants suffer the greatest injury from irritant exposure [71]. Bronchial biopsies in patients with RADS show denuded epithelium, inflammatory changes, submucosal edema and collagen deposition in the bronchial wall [73,74]. Similarly, epithelial denudation, increased broncho-alveolar lavage (BAL) protein concentrations and neutrophilic lung inflammation were found in murine studies [85–87]. Human studies focusing on the long-term changes in IIA documented both eosinophilic and neutrophilic inflammation, as well as marked airway remodeling. The inflammatory and remodeling mediators did not differ from those seen in allergic OA, yet basement membrane thickness (sub-epithelial fibrosis) was more prominent in patients with

IIA[75,88]. Altogether, the pathologic changes observed during the acute phase resembles a toxic mechanism, while the long term-phase is similar to allergic OA [73].

The underlying mechanism of IIA remains poorly understood, yet it is clear that irritant exposure can damage the bronchial epithelial cells. The cellular injury causes oxidative stress in the epithelial cells, which has been implicated in asthma [66]. Irritant-induced epithelial damage triggers the secretion of cellular mediators that recruit and activate underlying immune cells [89]. Release of inflammatory cytokines and DAMPS from stressed epithelial cells can activate the innate immune system via PPRs [66]. Due to epithelial damage, the bronchial epithelium loses its protective barrier function. This leads enhanced penetration of inhaled particles into the subepithelial compartment, which will facilitate their encounter with the residing immune cells [73]. Also, it exposes the nerve endings of sensory nerves in the airways, leading to neurogenic inflammation due to activation by chemical irritants. TRPA1 channels respond to various environmental irritants, including acrolein, tear gas, vehicle exhaust, ozone and hypochlorite, suggesting a crucial role for TRPA1 and neurogenic inflammation in IIA [73]. Following airway epithelial damage, the airway epithelium reestablishes a normal epithelial sheet. Possibly, in IIA the irritant-induced injury is improperly repaired (because of a genetic susceptibility or because of repetitive or massive injury), leading to persistent structural changes that explain the chronic airway hypersensitivity [71].

3.3. Chlorine and chlorine derivatives

Chlorine is a widely used chemical in industry and society. Due to its high oxidizing potential chlorine is used as disinfectant in e.g. swimming pools or cleaning products, as bleaching agent in e.g. pulp and paper mills, and as reagent in the chemical industry. Exposure to chlorine can occur during routine swimming pool attendance, frequent and misuse of domestic cleaners, accidental spills or transportation accidents, or as chemical weapon [85,90]. Chlorine gas is highly reactive, decomposing in various chlorine derivatives upon contact with water or organic matter, which are an expected cause for chlorine-induced health effects. When added to water, hydrogen chloride (HCl) and hypochlorous acid (HOCl) are synthesized. Hypochlorous acid can further dissociate into hydrogen (H^+) and the reactive anion hypochlorite (ClO^-), which is often used as household bleach or swimming pool disinfectant, in conjunction with sodium (NaClO). Hypochlorous acid (HOCl) and nitrogen, originating from ammonia compounds in sweat and urine of swimmers, form chloramines, which in the air can be recognized as the pungent smell of ‘chlorine’ in swimming pools [85]. Depending on the concentration and duration of exposure, chlorine can exert a variety of detrimental effects. The primary cause of chlorine’s toxicity originates from the direct contact with the respiratory epithelium, which leads to oxidative tissue injury in the lung [85,91]. Acute symptoms following high-level chlorine inhalation in humans include dyspnea, nausea, pulmonary edema, airway obstruction and acute respiratory distress

syndrome (ARDS) [90]. Most humans fully recover from chlorine-induced lung injury, yet others develop chronic respiratory symptoms which can be defined as RADS [75]. In addition, continuous low dose exposure to chlorine due to specific occupations such as in professional swimmers, lifeguards and cleaning personnel, has been associated with higher prevalence of respiratory symptoms and asthma, making chlorine the most prevalent cause of IIA [82,92–97].

3.4. Persulfate salts

Persulfate salts are reactive chemical compounds with strong oxidizing capacity, which are widely used in various manufacturing processes in chemical, pharmaceutical, electronic, photographic, food, and especially cosmetic industries [98]. Persulfate salts including ammonium, sodium and potassium persulfate, are important components of bleaching powders (10-20%) to increase the hair porosity during bleaching [99]. Hairdressers are frequently exposed to persulfate salts especially while mixing the hair-bleaching powders, which form dust easily [100,101]. Persulfates can act as allergens and airway irritants and subsequently have been identified as the main causal agent in contact dermatitis and occupational asthma in hairdressers [102,103]. Although the association between exposure to persulfate salts and development of asthma has clearly been established, the mechanisms for the hypersensitive airway disorders in hairdressers have not yet fully been elucidated [102,104,105].

3.5. Diesel exhaust particles

During the last hundred years, the level of exposure to combustion-derived particles increased dramatically due to industrialization and globalization processes such as increased traffic and urbanization. Diesel exhaust particles (DEP) produced by diesel-fueled engines are a major component of particulate atmospheric pollution, especially in urban areas. DEPs consist of a carbonaceous core that adsorbs a mixture of metals, especially copper, zinc and iron, and organic compounds such as poly-aromatic hydrocarbons. The primary diesel particle sizes between 10 and 30 nm in diameter, but these can also agglomerate and form particles between 60 to 100 nm of diameter [106,107]. The rise in particulate air pollution coincides with an increase in respiratory and cardiovascular mortality and morbidity [108]. More specifically, living close to heavily trafficked roads has been associated with adverse effects on people's health [109–112]. Due to their small size, inhaled DEP can reach the bronchiolar and alveolar region of the lung, where they can exert local effects as well as induce systemic effects after translocation to the bloodstream [106,107]. It is widely accepted that DEPs induce oxidative stress which, depending on the level, induces an antioxidant defense response (at low levels of oxidative stress), initiates a pro-inflammatory mechanism (at intermediate levels of oxidative stress) or exert cytotoxic effects (at high levels of oxidative stress) [113,114]. Generation of reactive oxygen species (ROS), inflammation and damage onto the epithelial cells, which via the release cytokines and chemokines

activates immune cells, is considered a key step in the development of detrimental health effects associated with diesel exhaust exposure [111,112].

3.6. Graphene nanoparticles

Graphene is a single-atom thick, two-dimensional sheet of carbon atoms arranged in a honeycomb lattice. Due to this unique structure, graphene is gifted with exceptional properties concerning electronic conductivity, thermal stability and mechanical strength [116]. Since its discovery in 2004, graphene nanoparticles (GNPs) have drawn considerable attention, and research and applications for graphene materials have emerged rapidly. These applications include structural composites, battery electrodes, capacitators, printable inks, as well as biosensors and drug delivery facilitators. Along with the increase in applications, graphene is manufactured in larger volumes and thus unintentional occupational or environmental exposure becomes more likely [117]. GNPs are produced as dry powders, making inhalation a realistic route of human exposure. The platelet-like shape of graphene raises concerns for respiratory health. GNPs have a small aerodynamic diameter that allows them to penetrate deeply until the lower airways. A study using human airway replicas indicated that most of the inhaled GNPs would enter the lower tracheobronchial airways [118]. Sanchez *et al.* calculated that GNPs will deposit at different regions of the respiratory tract depending on the lateral dimensions and layer number of graphene. It was found that the smallest graphene platelets (0,5 µm) with limited layer number (less than 10) could have considerable deposition in the alveolar region [119]. The platelet-like shape, and high aspect ratio and biopersistence (characteristics they share with asbestos fibers) warns that GNPs could be difficult to handle by alveolar macrophages leading to inflammation, frustrated phagocytosis, failed clearance and possible translocation through the air-blood barrier [116,120,121].

References

1. Ganesan, S., Comstock, A. T. & Sajjan, U. S. Barrier function of airway tract epithelium. *Tissue Barriers* **1,** e24997 (2013).
2. Wittekindt, O. H. Tight junctions in pulmonary epithelia during lung inflammation. *Pflugers Arch.* **469,** 135–147 (2017).
3. Crystal, R. G., Randell, S. H., Engelhardt, J. F., Voynow, J. & Sunday, M. E. Airway Epithelial Cells. *Proc. Am. Thorac. Soc.* **5,** 772–777 (2008).
4. Gras, D., Chanez, P., Vachier, I., Petit, A. & Bourdin, A. Bronchial epithelium as a target for innovative treatments in asthma. *Pharmacol. Ther.* **140,** 290–305 (2013).
5. Hogan, B. L. M. *et al.* Repair and Regeneration of the Respiratory System: Complexity, Plasticity, and Mechanisms of Lung Stem Cell Function. *Cell Stem Cell* **15,** 123–138 (2014).
6. Gandhi, V. D. & Vliagoftis, H. Airway epithelium interactions with aeroallergens: role of secreted cytokines and chemokines in innate immunity. *Front. Immunol.* **6,** 147 (2015).
7. Travaglini, K. J. & Krasnow, M. A. Profile of an unknown airway cell. *Nature* **560,** 313 (2018).
8. Parker, D. & Prince, A. Innate immunity in the respiratory epithelium. *Am. J. Respir. Cell Mol. Biol.* **45,** 189–201 (2011).
9. Rezaee, F. & Georas, S. N. Breaking Barriers. New Insights into Airway Epithelial Barrier Function in Health and Disease. *Am. J. Respir. Cell Mol. Biol.* **50,** 857–869 (2014).
10. Georas, S. N. & Rezaee, F. Epithelial barrier function: at the frontline of asthma immunology and allergic airway inflammation. *J. Allergy Clin. Immunol.* **134,** 509–520 (2014).
11. Saatian, B. *et al.* Interleukin-4 and interleukin-13 cause barrier dysfunction in human airway epithelial cells. *Tissue Barriers* **1,** e24333 (2013).
12. Hardyman, M. A. *et al.* TNF-α-mediated bronchial barrier disruption and regulation by src-family kinase activation. *J. Allergy Clin. Immunol.* **132,** 665–675.e8 (2013).
13. Soyka, M. B. *et al.* Defective epithelial barrier in chronic rhinosinusitis: The regulation of tight junctions by IFN-γ and IL-4. *J. Allergy Clin. Immunol.* **130,** 1087–1096.e10 (2012).
14. Xiao, C. *et al.* Defective epithelial barrier function in asthma. *J. Allergy Clin. Immunol.* **128,** 549–556.e12 (2011).
15. Heijink, I. H., Noordhoek, J. A., Timens, W., van Oosterhout, A. J. M. & Postma, D. S. Abnormalities in airway epithelial junction formation in chronic obstructive pulmonary disease. *Am. J. Respir. Crit. Care Med.* **189,** 1439–1442 (2014).
16. Shaykhiev, R. & Crystal, R. G. Early events in the pathogenesis of chronic obstructive pulmonary disease. Smoking-induced reprogramming of airway epithelial basal progenitor cells. *Ann. Am. Thorac. Soc.* **11 Suppl 5,** S252-258 (2014).
17. Greeley, M. A., Van Winkle, L. S., Edwards, P. C. & Plopper, C. G. Airway trefoil factor expression during naphthalene injury and repair. *Toxicol. Sci. Off. J. Soc. Toxicol.* **113,** 453–467 (2010).
18. Plopper, C. G., Suverkropp, C., Morin, D., Nishio, S. & Buckpitt, A. Relationship of cytochrome P-450 activity to Clara cell cytotoxicity. I. Histopathologic comparison of the respiratory tract of mice, rats and hamsters after parenteral administration of naphthalene. *J. Pharmacol. Exp. Ther.* **261,** 353–363 (1992).
19. Buckpitt, A. *et al.* Naphthalene-Induced Respiratory Tract Toxicity: Metabolic Mechanisms of Toxicity. *Drug Metab. Rev.* **34,** 791–820 (2002).
20. Buckpitt, A. *et al.* Relationship of cytochrome P450 activity to Clara cell cytotoxicity. IV. Metabolism of naphthalene and naphthalene oxide in microdissected airways from mice, rats, and hamsters. *Mol. Pharmacol.* **47,** 74–81 (1995).
21. Plopper, C. G., Cranz, D. L., Kemp, L., Serabjit-Singh, C. J. & Philpot, R. M. Immunohistochemical Demonstration of Cytochrome P-450 Monooxygenase in Clara Cells throughout the Tracheobronchial Airways of the Rabbit. *Exp. Lung Res.* **13,** 59–68 (1987).
22. Van Winkle, L. S., Johnson, Z. A., Nishio, S. J., Brown, C. D. & Plopper, C. G. Early events in naphthalene-induced acute Clara cell toxicity: comparison of membrane permeability and ultrastructure. *Am. J. Respir. Cell Mol. Biol.* **21,** 44–53 (1999).
23. Aoshiba, K. *et al.* A murine model of airway fibrosis induced by repeated naphthalene exposure. *Exp. Toxicol. Pathol. Off. J. Ges. Toxikol. Pathol.* **66,** 169–177 (2014).
24. Karagiannis, T. C. *et al.* Molecular model of naphthalene-induced DNA damage in the murine lung. *Hum. Exp. Toxicol.* **31,** 42–50 (2012).

25. López, I. P. *et al.* Involvement of Igf1r in Bronchiolar Epithelial Regeneration: Role during Repair Kinetics after Selective Club Cell Ablation. *PloS One* **11,** e0166388 (2016).
26. Royce, S. G. *et al.* Mechanistic insights into the contribution of epithelial damage to airway remodeling. Novel therapeutic targets for asthma. *Am. J. Respir. Cell Mol. Biol.* **50,** 180–192 (2014).
27. Royce, S. G., Patel, K. P. & Samuel, C. S. Characterization of a novel model incorporating airway epithelial damage and related fibrosis to the pathogenesis of asthma. *Lab. Investig. J. Tech. Methods Pathol.* **94,** 1326–1339 (2014).
28. Yildirim, A. O. *et al.* Keratinocyte growth factor protects against Clara cell injury induced by naphthalene. *Eur. Respir. J.* **32,** 694–704 (2008).
29. Holgate, S. T. *et al.* Asthma. *Nat. Rev. Dis. Primer* **1,** 15025 (2015).
30. Lemanske, R. F. & Busse, W. W. Asthma: clinical expression and molecular mechanisms. *J. Allergy Clin. Immunol.* **125,** S95-102 (2010).
31. To, T. *et al.* Global asthma prevalence in adults: findings from the cross-sectional world health survey. *BMC Public Health* **12,** 204 (2012).
32. Bousquet, J., Bousquet, P. J., Godard, P. & Daures, J.-P. The public health implications of asthma. *Bull. World Health Organ.* **83,** 548–554 (2005).
33. Rava, M. *et al.* Genes Interacting with Occupational Exposures to Low Molecular Weight Agents and Irritants on Adult-Onset Asthma in Three European Studies. *Environ. Health Perspect.* **125,** 207–214 (2017).
34. Martinez, F. D. & Vercelli, D. Asthma. *Lancet Lond. Engl.* **382,** 1360–1372 (2013).
35. Wenzel, S. E. Asthma: Defining of the persistent adult phenotypes. *Lancet* **368,** (2006).
36. Gauthier, M., Ray, A. & Wenzel, S. E. Evolving Concepts of Asthma. *Am. J. Respir. Crit. Care Med.* **192,** 660–668 (2015).
37. Holgate, S. T. Innate and adaptive immune responses in asthma. *Nat. Med.* **18,** 673–683 (2012).
38. Hammad, H. & Lambrecht, B. N. Dendritic cells and airway epithelial cells at the interface between innate and adaptive immune responses. *Allergy* **66,** 579–587 (2011).
39. Kudo, M., Ishigatsubo, Y. & Aoki, I. Pathology of asthma. *Front. Microbiol.* **4,** 263 (2013).
40. Hammad, H. & Lambrecht, B. N. Barrier Epithelial Cells and the Control of Type 2 Immunity. *Immunity* **43,** 29–40 (2015).
41. Hirota, N. & Martin, J. G. Mechanisms of Airway Remodeling. *Chest* **144,** 1026–1032 (2013).
42. Lambrecht, B. N. & Hammad, H. The airway epithelium in asthma. *Nat. Med.* **18,** 684–692 (2012).
43. Lambrecht, B. N. & Hammad, H. The immunology of asthma. *Nat. Immunol.* **16,** 45–56 (2015).
44. de Heer, H. J. *et al.* Essential role of lung plasmacytoid dendritic cells in preventing asthmatic reactions to harmless inhaled antigen. *J. Exp. Med.* **200,** 89–98 (2004).
45. Plantinga, M. *et al.* Conventional and monocyte-derived CD11b(+) dendritic cells initiate and maintain T helper 2 cell-mediated immunity to house dust mite allergen. *Immunity* **38,** 322–335 (2013).
46. Vroman, H., Hendriks, R. W. & Kool, M. Dendritic Cell Subsets in Asthma: Impaired Tolerance or Exaggerated Inflammation? *Front. Immunol.* **8,** (2017).
47. Lambrecht, B. N. & Hammad, H. Biology of lung dendritic cells at the origin of asthma. *Immunity* **31,** 412–424 (2009).
48. Frossi, B., Mion, F., Tripodo, C., Colombo, M. P. & Pucillo, C. E. Rheostatic Functions of Mast Cells in the Control of Innate and Adaptive Immune Responses. *Trends Immunol.* **38,** 648–656 (2017).
49. Moon, T. C., Befus, A. D. & Kulka, M. Mast cell mediators: their differential release and the secretory pathways involved. *Front. Immunol.* **5,** 569 (2014).
50. Mukai, K., Tsai, M., Saito, H. & Galli, S. J. Mast cells as sources of cytokines, chemokines, and growth factors. *Immunol. Rev.* **282,** 121–150 (2018).
51. Marshall, J. S. Mast-cell responses to pathogens. *Nat. Rev. Immunol.* **4,** 787–799 (2004).
52. Redegeld, F. A., Yu, Y., Kumari, S., Charles, N. & Blank, U. Non-IgE mediated mast cell activation. *Immunol. Rev.* **282,** 87–113 (2018).
53. Yu, S., Kim, H. Y., Chang, Y.-J., DeKruyff, R. H. & Umetsu, D. T. Innate lymphoid cells and asthma. *J. Allergy Clin. Immunol.* **133,** 943–950; quiz 51 (2014).
54. Kim, H. Y., Umetsu, D. T. & Dekruyff, R. H. Innate lymphoid cells in asthma: Will they take your breath away? *Eur. J. Immunol.* **46,** 795–806 (2016).
55. Kortekaas Krohn, I. *et al.* Emerging roles of innate lymphoid cells in inflammatory diseases: Clinical implications. *Allergy* (2017). doi:10.1111/all.13340
56. Geppetti, P., Patacchini, R. & Nassini, R. Transient receptor potential channels and occupational exposure. *Curr. Opin. Allergy Clin. Immunol.* **14,** 77–83 (2014).

57. De Logu, F., Patacchini, R., Fontana, G. & Geppetti, P. TRP functions in the broncho-pulmonary system. *Semin. Immunopathol.* **38,** 321–329 (2016).
58. Groneberg, D. A., Quarcoo, D., Frossard, N. & Fischer, A. Neurogenic mechanisms in bronchial inflammatory diseases. *Allergy* **59,** 1139–1152 (2004).
59. Barnes, P. J. Neurogenic inflammation in the airways. *Respir. Physiol.* **125,** 145–154 (2001).
60. Grace, M. S., Baxter, M., Dubuis, E., Birrell, M. A. & Belvisi, M. G. Transient receptor potential (TRP) channels in the airway: role in airway disease. *Br. J. Pharmacol.* **171,** 2593–2607 (2014).
61. Hox, V. *et al.* Crucial role of transient receptor potential ankyrin 1 and mast cells in induction of nonallergic airway hyperreactivity in mice. *Am. J. Respir. Crit. Care Med.* **187,** 486–493 (2013).
62. Devos, F. C. *et al.* Neuro-immune interactions in chemical-induced airway hyperreactivity. *Eur. Respir. J.* **48,** 380–392 (2016).
63. Caceres, A. I. *et al.* A sensory neuronal ion channel essential for airway inflammation and hyperreactivity in asthma. *Proc. Natl. Acad. Sci. U. S. A.* **106,** 9099–9104 (2009).
64. Rehman, R., Bhat, Y. A., Panda, L. & Mabalirajan, U. TRPV1 inhibition attenuates IL-13 mediated asthma features in mice by reducing airway epithelial injury. *Int. Immunopharmacol.* **15,** 597–605 (2013).
65. Georas, S. N. & Upham, J. Environmental exposures and innate immunity in the lung. *J. Environ. Immunol. Toxicol.* **2,** 1–3 (2014).
66. Malo, J.-L. *et al.* An official American Thoracic Society Workshop Report: presentations and discussion of the fifth Jack Pepys Workshop on Asthma in the Workplace. Comparisons between asthma in the workplace and non-work-related asthma. *Ann. Am. Thorac. Soc.* **12,** S99–S110 (2015).
67. Trivedi, V., Apala, D. R. & Iyer, V. N. Occupational asthma: diagnostic challenges and management dilemmas. *Curr. Opin. Pulm. Med.* **23,** 177–183 (2017).
68. Torén, K. & Blanc, P. D. Asthma caused by occupational exposures is common - a systematic analysis of estimates of the population-attributable fraction. *BMC Pulm. Med.* **9,** 7 (2009).
69. Labrecque, M. Irritant-induced asthma. *Curr. Opin. Allergy Clin. Immunol.* **12,** 140–144 (2012).
70. Tarlo, S. M. Irritant-induced asthma in the workplace. *Curr. Allergy Asthma Rep.* **14,** 406 (2014).
71. Brooks, S. M. & Bernstein, I. L. Irritant-Induced Airway Disorders. *Immunol. Allergy Clin. North Am.* **31,** 747–768 (2011).
72. Brooks, S. M., Weiss, M. A. & Bernstein, I. L. Reactive airways dysfunction syndrome (RADS). Persistent asthma syndrome after high level irritant exposures. *Chest* **88,** 376–384 (1985).
73. Vandenplas, O. *et al.* EAACI position paper: irritant-induced asthma. *Allergy* **69,** 1141–1153 (2014).
74. Brooks, S. M., Malo, J.-L. & Gautrin, D. Irritant-induced asthma and reactive airways dysfunction syndrome. in *Asthma in the workplace* **21,** (2013).
75. Malo, J.-L. *et al.* Long-Term Outcomes of Acute Irritant-induced Asthma. *Am. J. Respir. Crit. Care Med.* **179,** 923–928 (2009).
76. Siracusa, A. *et al.* Asthma and exposure to cleaning products - a European Academy of Allergy and Clinical Immunology task force consensus statement. *Allergy* **68,** 1532–1545 (2013).
77. Folletti, I., Siracusa, A. & Paolocci, G. Update on asthma and cleaning agents. *Curr. Opin. Allergy Clin. Immunol.* **17,** 90–95 (2017).
78. Casas, L. & Nemery, B. Irritants and asthma. *Eur. Respir. J.* **44,** 562–564 (2014).
79. Rosenman, K. D. *et al.* Swimming facilities and work-related asthma. *J. Asthma Off. J. Assoc. Care Asthma* **52,** 52–58 (2015).
80. Bernard, A., Nickmilder, M., Voisin, C. & Sardella, A. Impact of chlorinated swimming pool attendance on the respiratory health of adolescents. *Pediatrics* **124,** 1110–1118 (2009).
81. Nordberg, G. F. *et al.* Lung function in volunteers before and after exposure to trichloramine in indoor pool environments and asthma in a cohort of pool workers. *BMJ Open* **2,** (2012).
82. Romberg, K., Tufvesson, E. & Bjermer, L. Asthma is more prevalent in elite swimming adolescents despite better mental and physical health. *Scand. J. Med. Sci. Sports* **22,** 362–371 (2012).
83. Adewole, F., Moore, V. C., Robertson, A. S. & Burge, P. S. Diesel exhaust causing low-dose irritant asthma with latency? *Occup. Med. Oxf. Engl.* **59,** 424–427 (2009).
84. Dumas, O. *et al.* Occupational irritants and asthma: an Estonian cross-sectional study of 34,000 adults. *Eur. Respir. J.* **44,** 647–656 (2014).
85. White, C. W. & Martin, J. G. Chlorine gas inhalation: human clinical evidence of toxicity and experience in animal models. *Proc. Am. Thorac. Soc.* **7,** 257–263 (2010).
86. Martin, J. G. *et al.* Chlorine-induced injury to the airways in mice. *Am. J. Respir. Crit. Care Med.* **168,** 568–574 (2003).

87. Jonasson, S., Koch, B. & Bucht, A. Inhalation of chlorine causes long-standing lung inflammation and airway hyperresponsiveness in a murine model of chemical-induced lung injury. *Toxicology* **303,** 34–42 (2013).
88. Takeda, N. *et al.* Long-term pathologic consequences of acute irritant-induced asthma. *J. Allergy Clin. Immunol.* **124,** 975–981.e1 (2009).
89. Maestrelli, P., Boschetto, P., Fabbri, L. M. & Mapp, C. E. Mechanisms of occupational asthma. *J. Allergy Clin. Immunol.* **123,** 531-542-544 (2009).
90. Hoyle, G. W. & Svendsen, E. R. Persistent effects of chlorine inhalation on respiratory health. *Ann. N. Y. Acad. Sci.* (2016). doi:10.1111/nyas.13139
91. Wigenstam, E., Elfsmark, L., Koch, B., Bucht, A. & Jonasson, S. Acute respiratory changes and pulmonary inflammation involving a pathway of TGF-β1 induction in a rat model of chlorine-induced lung injury. *Toxicol. Appl. Pharmacol.* **309,** 44–54 (2016).
92. Bernard, A., Nickmilder, M., Voisin, C. & Sardella, A. Impact of chlorinated swimming pool attendance on the respiratory health of adolescents. *Pediatrics* **124,** 1110–1118 (2009).
93. Jacobs, J. H. *et al.* Exposure to trichloramine and respiratory symptoms in indoor swimming pool workers. *Eur. Respir. J.* **29,** 690–698 (2007).
94. Folletti, I., Zock, J.-P., Moscato, G. & Siracusa, A. Asthma and rhinitis in cleaning workers: a systematic review of epidemiological studies. *J. Asthma Off. J. Assoc. Care Asthma* **51,** 18–28 (2014).
95. Zock, J.-P., Vizcaya, D. & Le Moual, N. Update on asthma and cleaners. *Curr. Opin. Allergy Clin. Immunol.* **10,** 114–120 (2010).
96. Nordberg, G. F. *et al.* Lung function in volunteers before and after exposure to trichloramine in indoor pool environments and asthma in a cohort of pool workers. *BMJ Open* **2,** (2012).
97. Rosenman, K. D. *et al.* Swimming facilities and work-related asthma. *J. Asthma Off. J. Assoc. Care Asthma* **52,** 52–58 (2015).
98. Pang, S. & Fiume, M. Z. Final report on the safety assessment of Ammonium, Potassium, and Sodium Persulfate. *Int. J. Toxicol.* **20 Suppl 3,** 7–21 (2001).
99. Kamath, Y. K. & Ruetsch, S. B. Reduction-induced surface modification of human hair. *J. Cosmet. Sci.* **61,** 1–12 (2010).
100. Nielsen, J. *et al.* Dust-free bleaching powder may not prevent symptoms in hairdressers with bleaching-associated rhinitis. *J. Occup. Health* **58,** 470–476 (2016).
101. Nilsson, P. T. *et al.* Characterization of Hairdresser Exposure to Airborne Particles during Hair Bleaching. *Ann. Occup. Hyg.* **60,** 90–100 (2016).
102. Tarlo, S. M. & Lemiere, C. Occupational asthma. *N. Engl. J. Med.* **370,** 640–649 (2014).
103. Cruz, M.-J. *et al.* Assessment of the sensitization potential of persulfate salts used for bleaching hair. *Contact Dermatitis* **60,** 85–90 (2009).
104. De Vooght, V. *et al.* Ammonium persulfate can initiate an asthmatic response in mice. *Thorax* **65,** 252–257 (2010).
105. Cruz, M. J. *et al.* Persistence of respiratory and inflammatory responses after dermal sensitization to persulfate salts in a mouse model of non-atopic asthma. *Allergy Asthma Clin. Immunol.* **12,** 26 (2016).
106. Steiner, S., Bisig, C., Petri-Fink, A. & Rothen-Rutishauser, B. Diesel exhaust: current knowledge of adverse effects and underlying cellular mechanisms. *Arch. Toxicol.* **90,** 1541–1553 (2016).
107. Klein, S. G. *et al.* Endothelial responses of the alveolar barrier in vitro in a dose-controlled exposure to diesel exhaust particulate matter. *Part. Fibre Toxicol.* **14,** 7 (2017).
108. Anderson, J. O., Thundiyil, J. G. & Stolbach, A. Clearing the air: a review of the effects of particulate matter air pollution on human health. *J. Med. Toxicol. Off. J. Am. Coll. Med. Toxicol.* **8,** 166–175 (2012).
109. Schwarze, P. E. *et al.* Inflammation-related effects of diesel engine exhaust particles: studies on lung cells in vitro. *BioMed Res. Int.* **2013,** 685142 (2013).
110. Baccarelli, A. *et al.* Living near major traffic roads and risk of deep vein thrombosis. *Circulation* **119,** 3118–3124 (2009).
111. Nuvolone, D. *et al.* Geographical information system and environmental epidemiology: a cross-sectional spatial analysis of the effects of traffic-related air pollution on population respiratory health. *Environ. Health Glob. Access Sci. Source* **10,** 12 (2011).
112. Riley, S., Wallace, J. & Nair, P. Proximity to major roadways is a risk factor for airway hyper-responsiveness in adults. *Can. Respir. J.* **19,** 89–95 (2012).
113. Li, N. *et al.* Use of a stratified oxidative stress model to study the biological effects of ambient concentrated and diesel exhaust particulate matter. *Inhal. Toxicol.* **14,** 459–486 (2002).

114. Baulig, A. *et al.* Involvement of reactive oxygen species in the metabolic pathways triggered by diesel exhaust particles in human airway epithelial cells. *Am. J. Physiol. Lung Cell. Mol. Physiol.* **285,** L671-679 (2003).
115. Lehmann, A. D., Blank, F., Baum, O., Gehr, P. & Rothen-Rutishauser, B. M. Diesel exhaust particles modulate the tight junction protein occludin in lung cells in vitro. *Part. Fibre Toxicol.* **6,** 26 (2009).
116. Ou, L. *et al.* Toxicity of graphene-family nanoparticles: a general review of the origins and mechanisms. *Part. Fibre Toxicol.* **13,** 57 (2016).
117. Arvidsson, R., Molander, S. & Sandén, B. A. Review of Potential Environmental and Health Risks of the Nanomaterial Graphene. *Hum. Ecol. Risk Assess. Int. J.* **19,** 873–887 (2013).
118. Su, W.-C., Ku, B.-K., Kulkarni, P. & Cheng, Y. S. Deposition of Graphene Nanoparticles in Human Upper Airways. *J. Occup. Environ. Hyg.* **13,** 48–59 (2016).
119. Sanchez, V. C., Jachak, A., Hurt, R. H. & Kane, A. B. Biological Interactions of Graphene-Family Nanomaterials: An Interdisciplinary Review. *Chem. Res. Toxicol.* **25,** 15–34 (2012).
120. Mao, L., Hu, M., Pan, B., Xie, Y. & Petersen, E. J. Biodistribution and toxicity of radio-labeled few layer graphene in mice after intratracheal instillation. *Part. Fibre Toxicol.* **13,** 7 (2016).
121. Schinwald, A., Murphy, F. A., Jones, A., MacNee, W. & Donaldson, K. Graphene-Based Nanoplatelets: A New Risk to the Respiratory System as a Consequence of Their Unusual Aerodynamic Properties. *ACS Nano* **6,** 736–746 (2012).

Chapter 2

Rationale and aims

Via inhalation, humans are continuously exposed to gasses, dust, chemicals and particles in the air. Some of these environmental agents have irritant properties, triggering a reversible inflammatory reaction, compromising coughing, wheezing, decreased breathing frequency and increased mucus production, upon direct contact with the respiratory system. Persistence of these symptoms is indicative of irritant-induced asthma (IIA), a condition of airway hypersensitivity induced by exposure to respiratory irritants. Although it is clinically similar to well-established allergic asthma, the underlying mechanism of IIA is largely unknown.

The first cells encountered by the inhaled air are the airway epithelial cells. As a first line of defense, epithelial cells are tightly connected throughout the airways, creating a mechanical barrier that limits the entry of inhaled particles to the host. Barrier integrity is achieved by the intercellular junctional complexes that form between neighboring cells. Loss of barrier integrity by dysfunction of these complexes therefore might increase the entry of potentially noxious agents to the host. In addition, this can serve as a trigger for the airway epithelium to release signals, which can activate innate immune cells. In this context, mast cells might be activated in a non-IgE dependent fashion, dendritic cells (DCs) might receive signals that alter their maturation and functioning, and the recently identified innate lymphoid cells (ILCs) might be recruited. Activation of these innate immune cells induces the production and release of various inflammatory mediators that can mediate airway responses.

We hypothesize that respiratory irritants can affect the airway barrier integrity, which will facilitate the passage of noxious agent to the host, and trigger the epithelium, leading to recruitment and activation of innate immune cells that can mediate airway hypersensitivity. In this dissertation, we aimed to study the effects of respiratory irritants on the airway epithelial barrier, and to investigate the contribution of impaired airway barrier functioning in the development of airway hypersensitivity. To accomplish this, two major aims were defined:

Part I. Study the effect of environmental irritants on the airway epithelial barrier – *in vitro*

The human respiratory epithelium forms the primary interface with the surrounding environment. Environmental irritants including ozone, diesel exhaust particles (DEP) and cigarette smoke can have negative effects on airway epithelial cells and impair the epithelial barrier. The response of the epithelium is not only determined by the epithelial cells, but is also shaped by its surrounding cells. By exposing mono- and co-cultures of cells at the airway barrier to different types of environmental irritants, we aimed to investigate the effects of environmental agents on barrier function, permeability and signaling.

Via the intercellular junctional complexes formed between neighboring cells, the airway epithelium creates a mechanical barrier that prevents entry inhaled noxious agents to the host. In **chapter 3**, we

used a co-culture consisting of endothelial cells, bronchial epithelial cells and monocytes to mimic the thin lung-blood barrier. This tri-culture was exposed to two types of graphene nanoparticles (graphene and graphene oxide), a chemical irritant (hypochlorite) and two chemical sensitizers with irritant properties (ammonium and sodium persulfate), in order to study their effects on the airway epithelial barrier and functioning of the intercellular junctional complexes.

Mast cells are located just underneath the epithelial barrier and are one of the important first-hand responders of the innate immune system due to their numerous receptors, including receptors for PAMPs and DAMPs on their surface, and their potential to release mediators. In **chapter 4**, we aimed to investigate whether environmental agents can activate mast cells, either directly, or via danger signals derived from the exposed epithelium, and whether activated mast cells, via their release of mediators, could affect barrier functioning. In this chapter, mono- and co-cultures of bronchial epithelial cells and mast cells were exposed to the nanoparticles graphene and graphene oxide, the common combustion-derived particle diesel exhaust and the widely used disinfectant hypochlorite.

Part II. Study airway hypersensitivity following airway barrier impairment – *in vivo*

As a first line of defense, the airway epithelium suffers greatly from irritant-induced damage. We combined a mouse model of airway epithelial damage (using i.p. injection with naphthalene) with airway exposure to the common environmental irritant hypochlorite. Hereby we aimed to mimic an accidental exposure to a high concentration of harmful compounds (e.g. accidental spills in the workplace), leading to epithelial barrier dysfunction and subsequent recovery, followed by daily-life exposures to irritants. The hypothesis that initial airway damage due to high-level exposure to harmful compounds and (partial) repair will result in airway hypersensitivity after exposure to non-irritant concentrations of hypochlorite, was investigated. In **chapter 5**, mice received a single intra-peritoneal (i.p.) injection of naphthalene followed by a single intranasal (i.n.) challenge of hypochlorite. In **chapter 6**, a more intense treatment protocol was utilized, which consisted of a two barrier impairment events with naphthalene and successive endotracheal challenges of hypochlorite.

In addition, we wanted to obtain mechanistic insights in the development of IIA by determining dendritic cell (DC) and innate lymphoid cell (ILC) populations in the lung. Pulmonary DCs are crucial mediators in regulating immune responses in the lung and bridge the innate and adaptive immune responses. As they are located at the vicinity of the external environment, environmental exposure might affect DC biology. ILCs are nonspecific and react to a wide range of innate signals. Recently, ILCs have been shown to exist in the lungs and play a role in the pathophysiology of asthma and allergic inflammation. In **chapter 5**, we studied the involvement of DCs and ILCs in hypochlorite induced airway hypersensitivity due to airway barrier impairment.

Chapter 3

Effect of irritants on a co-culture model of the airway barrier

Sofie Van Den Broucke, Rita Derua, Jeroen Vanoirbeek, Peter Hoet

Abstract

Via inhalation we are continuously exposed to environmental irritants which can induce adverse health effects, such as irritant-induced asthma (IIA). The airway epithelium forms the first barrier encountered by these agents. We investigated the effect of environmental irritants on the airway epithelial barrier *in vitro*.

The airway epithelial barrier was mimicked using a co-culture model, consisting of bronchial epithelial cells (16HBE) and monocytes (THP-1) seeded on the apical side of a permeable support, and human lung microvascular endothelial cells (HLMVEC) grown on the basal side. Upon exposure to graphene (G) and graphene oxide (GO) in a suspension with fetal calf serum (FBS) or dipalmitoylphosphatidylcholine (DPPC), ammonium persulfate (AP), sodium persulfate (SP) and hypochlorite (ClO^-), the transepithelial electrical resistance (TEER) and flux of fluorescent labelled dextrans (FD4-flux), was determined. Integrity of the tight junctions (TJ) was evaluated by immunofluorescent staining of zonula occludens 1 (ZO-1) and occludin. Using phosphoproteomics of the membrane-associated proteins, alterations in phosphorylation due to irritant-exposure were assessed.

Exposure to graphene nanoparticles (GNPs) induced an immediate negative effect on the epithelial barrier, whereas ClO^- only had a negative impact after 24h of exposure. AP and SP did not affect the barrier properties. In a suspension using DPPC, GNPs had a limited effect on the epithelial barrier function. The TJ network showed less connected ZO-1 and occludin staining in GNP-exposed co-cultures. Functional analysis of the phosphoproteomics data indicated that proteins in the adherens junction (AJ) and TJ pathways had an altered phosphorylation due to GNP exposure.

To conclude, we demonstrated that different types of environmental irritants have different effects on the airway epithelial barrier and that for GNPs this depends on the method of suspension. The negative effect of GNPs on the epithelial barrier can be explained by the slightly altered the TJ organization which could be caused by alterations in the phosphorylation level of proteins in the AJ and TJ pathway.

Introduction

The airway epithelium is located at the interface between the internal and external environment and therefore plays an important role in host defense [1]. Via intercellular junctional complexes the airway epithelial cells are tightly connected and create a first barrier to the outside world. Intercellular junctions are dynamic structures that confer a loose structure when ions, solutes or immune cells have to pass the epithelial layer, yet also establish an impenetrable fence to harmful agents [2,3]. Intercellular junctional complexes consist of apically localized tight junctions (TJ) which regulate paracellular transport of ions and small molecules and establish an apical-lateral polarity, and the underlying adherens junctions (AJ) which are important for initiation and maintenance of cell-cell adhesion. TJs are made up of adhesive transmembrane proteins (e.g. claudin, occludin and junction adhesion molecule (JAM) families), actin-binding cytoplasmic proteins (e.g. zonula occludens (ZO) proteins 1, 2 and 3) and associated scaffolding proteins. The principal proteins in AJs are the cadherin and nectin transmembrane protein family and intracellular β-catenin, α-catenin and p120 catenin [4,5].

Various types of environmental agents, such as allergens, pollution particles and respiratory tract viruses can impair the epithelial barrier integrity by disturbing the intercellular junctional complexes, and therefore lead to detrimental health consequences [4,5]. Dysregulation of the TJ and AJ has been implicated in a variety of pulmonary conditions, including asthma, rhinosinusitis and COPD [6–8]. In the current study we aimed to investigate the effect of different types of environmental irritants on the airway epithelium. Exposure to respiratory irritants, either once a high dose or repeatedly lower doses, can result in the development of an asthmatic syndrome termed irritant-induced asthma (IIA) [9,10]. Because the airway epithelium is the first line of cells that come into contact with respiratory irritants, its response upon irritant exposure might provide insight in the first steps towards development to IIA.

Since their discovery, graphene nanoparticles (GNPs) have gained considerable attention and research and applications have emerged rapidly [11,12]. Graphene consist of a single-atom thick, two-dimensional sheet of carbon atoms, resulting in a unique platelet-like shape. The GNP sheets are able to penetrate deep into the lungs, where they pose a possible risk for respiratory health [13,14]. Various studies investigated the toxicity of GNPs *in vitro*, however their effect on the epithelial barrier has not been studied before [13,15–18].

Chlorine is a widely handled oxidizing chemical that upon inhalation can exert a variety of respiratory symptoms, including IIA [19]. The detrimental consequences of chlorine inhalation stem from the direct contact with the respiratory epithelium, which leads to oxidative tissue injury in the lung [20,21]. Hypochlorite (ClO^-) is a chlorine derivative that is often used as household bleach or swimming pool disinfectant, of which we aimed to study the effect on the airway barrier *in vitro*.

Persulfate salts are reactive chemical compounds that are an important component of hair bleaching powders [22]. They have been identified as the main causal agent in occupational asthma in hairdressers, yet the mechanism for this hypersensitive airway disorder has not been elaborately elucidated and investigated *in vitro* [23–26].

Materials and methods

Reagents

Dulbecco's Modified Eagle Medium (DMEM), Dulbecco's Modified Eagle Medium: Nutrient Mixture F-12 (DMEM/F12), Hank's Balanced Salt Solution (HBSS) without Ca^{2+} and Mg^{2+}, Dulbecco's phosphate buffered saline (DPBS) with Ca^{2+} and Mg^{2+}, penicillin-streptomycin, L-glutamine, amphotericin B, fetal calf serum (FCS) from Gibco™, were all purchased via ThermoFisher (Gent, Belgium). Microvascular Endothelial Cell Growth Medium, Transwell® membrane inserts, WST-1 cell proliferation reagent, ammonium persulfate, sodium persulfate, 4kDa size fluorescein isothiocyanate (FITC)-dextran, Phenylmethylsulfonyl fluoride (PMSF) and phosSTOP™ were purchased from Sigma-Aldrich (Overijse, Belgium). Sodium hypochlorite with 13% active chlorine was purchased from Across Organics (Geel, Belgium).

Cell culture

The human bronchial epithelial cells were 16HBE14o- cells (16HBE), cultured in DMEM/F12 medium supplemented with 5% FCS, 100 U/mL penicillin, 100 U/mL streptomycin, 2mM L-glutamine and 2,5 µg/mL aphotericin. THP-1 cells (a human acute monocytic cell line) were cultured in in RPMI medium supplemented with 10% FCS, 100 U/mL penicillin, 100 U/mL streptomycin, 2mM L-glutamine and 2,5 µg/mL amphotericin. Human lung microvascular endothelial cells (HLMVEC) were purchased from Cell applications Inc. and cultured in human lung microvascular endothelial cell growth medium supplemented with 100 U/mL penicillin, 100 U/mL streptomycin, 1 µg/mL amphotercin. The cells were incubated at 37°C, in a humidified atmosphere containing 5% CO_2. When confluent the 16HBE and HLMVEC cells were released enzymatically (0.05% trypsin-EDTA) and transferred to a new culture flask. The medium was renewed every 2-3days.

Exposure conditions

Graphene nanoparticles (GNPs) were purchased from Graphene-supermarket.com. Graphene (G) has a lateral dimension of 2 to 8 µm and consists of 3 to 8 graphene monolayers based on the manufacturer's description. Graphene oxide (GO) has a flake size of 0.5 to 5 µm and contains 80% of graphene oxide monolayers. Figure 1 shows the Raman spectra of G and GO provided from the manufacturer. For G the high intense peak at 1583 cm^{-1} (G band) and a low intense peak between 2500 and 3000 cm^{-1} (2D band) indicate that the provided G consists of multiple layers of graphene (Fig. 1a). The Raman spectrum of GO shows the graphene characterizing peak at 1586 cm^{-1} (G band) and a peak between 1270 and 1450 cm^{-1} (D band) that indicates the different structure in the graphene layer due to the oxygen binding (Fig. 1c). Transmission electron microscopy (TEM) images of the G and GO particles in suspension with 2% FCS are shown in figure 1. The particle dimensions stated by the

manufacturer correspond to the dimensions observed on the acquired TEM images. Based on the 'darkness' of the particles, it can be visualized that the G sheets mostly consisted of multiple layers, and few monolayers were present (Fig. 1b). For GO aggregated monolayers as well as monolayers were observed (Fig. 1d).

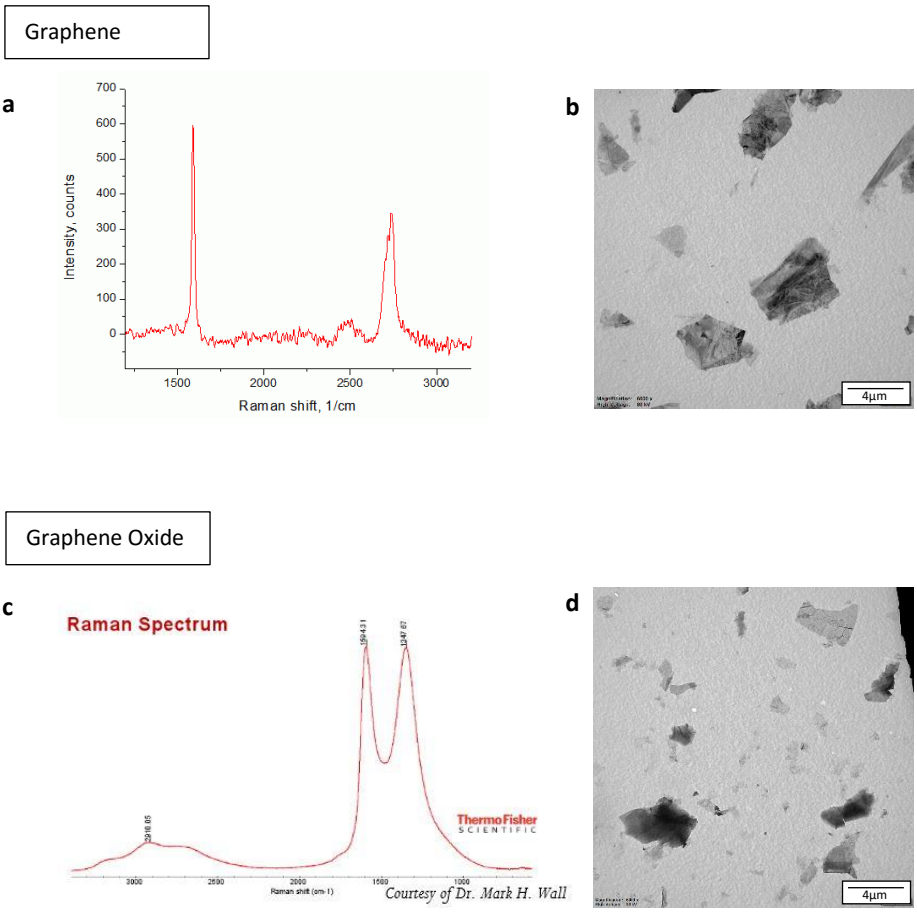

Figure 1. Characterization of G and GO NPs
Raman spectrum provided from the manufacturer of a) G and c) GO. Representative transmission electron spectroscopy (TEM) images of b) G and d) GO.

Two methods were used to disperse the GNPs: one using FCS to obtain a stable suspension that is routinely used for carbon-based NPs and another using the artificial pulmonary surfactant dipalmitoylphosphatidylcholine (DPPC) to mimic more the *in vivo* situation where NP would come in contact with the lung lining fluid. For the method using FCS the GNPs were weighed and dispersed in sterile water (Baxter) containing 2 vol % FCS (= dispersion medium) at a concentration of 2.56 mg/mL. These stock suspensions were dispersed using a Microson ultrasonic cell disruptor (Microsonix, Newton, USA), equipped with a disruptor horn, in a glass beaker on ice during 16 minutes at 730 watt. Intermediate concentrations were made in the dispersion medium and afterwards diluted tenfold in the culture medium to obtain final concentrations. The suspension with DPPC was based on

recommendations in Wallace *et al*. [27]. The GNPs were suspended to a stock with a concentration of 1mg NP in 2.5mg/mL DPPC/saline solution (0.25 wt % DPPC), to form DPPC-coated GNPs. The surfactant dispersion was prepared at 37 °C by ultrasonically mixing DPPC in physiological saline at 2.5 mg DPPC/1 mL saline for 15 minutes using a bath sonicater (Branson 1510, Danbury, USA). The GNPs were mixed into the surfactant suspension with a concentration of 1 mg NP in 2.5 mg/mL DPPC/saline and ultrasonically mixed for 1 hour in a bath sonicator, final concentrations were prepared in culture medium.

The levels of endotoxin in the sample suspensions were evaluated using the Endosafe®-PTS Limuluss Amoebocyte Lysate (LAL) assay according to the manufacturer's instructions. The sensitivity of the assay we used was 0.05 EU/mL.

To prepare the final ammonium persulfate (AP) and sodium persulfate (SP) solutions for the experiments, AP and SP salts were weighed and dissolved in culture medium containing 0.2% FCS.

Sodium hypochlorite with 13% active chlorine (act. Cl) was dissolved and diluted in dispersion medium, to obtain final concentrations that are expressed as parts per million (ppm) of act. Cl in the final hypochlorite (ClO^-) solution.

Cytotoxicity measurements

In order to determine sub-toxic concentrations for exposure in the co-culture, two different cytotoxicity assays were performed on 16HBE monocultures: the lactate dehydrogenase (LDH) and the 2-(4-Iodophenyl)-3-(4-nitrophenyl)-5-(2,4-disulfophenyl)-2H-tetrazolium (WST-1) assay. The cells were seeded in a 96-well plate at a density of 200 000 cells/cm². The next day, the cells were washed with serum-free culture medium and subsequently exposed to increasing concentrations of G, GO, AP, SP and ClO^-.

After the incubation period of 24 h, the supernatant was removed; the cells were washed twice and lysed using a 0.2% Triton-X solution. LDH was measured in the supernatant and in the lysed cells by spectrophotometry (at 340 nm) after the addition of the measuring mixture (0.458 mg/mL pyruvic acid, 0.532 mg/mL NADH and 0.794 mg/mL $NaHCO^3$ in DPBS).

Cytotoxicity was additionally measured using the WST-1 assay. After 24 hours of incubation, the supernatant was removed, the cells were washed and freshly diluted WST-1 reagent (1/20) was added. The cells were incubated for 1 hour and afterwards the absorbance was measured using spectrophotometry at 450 nm.

Co-culture setup

The HLMVECs were seeded the on the lower side of a non-coated polyester Transwell® insert membrane (0.4 µm pore density and 0.33 cm² surface area) in upside down configuration at a density of 45 000 cells/cm². After a two-hour incubation period, the inserts were returned to their original orientation and the 16HBE cells were seeded on the upper side of the insert at a density of 100 000 cells/cm². The cells were grown in their proper culture medium (200 µL apical, 1 mL basolateral), which was renewed every 2-3 days, and microscopically examined. At day 4 after seeding, the THP-1 cells were added to the apical compartment in a 1/10 ratio with the 16HBE cells. The medium in the apical compartment consisted of a mix of 16HBE (9/10) and THP-1 (1/10) medium with 0.2% FCS.

Co-culture exposure

On day 5 in culture, the co-cultures were exposed on the apical compartment of the transwell insert. Concentrations of 64 or 256 µg/mL for G, 16 or 64 µg/mL for GO, 25 or 100 µg/mL for AP or 12.5 or 6.25 µg/mL for SP and 7.5 or 3.75 ppm act. Cl in ClO^- in a medium containing a final concentration of 0.2% FCS were used. Using the suspension with artificial surfactant DPPC co-cultures were exposed to 64 or 128 µg/mL G or GO. Control co-cultures were treated with the vehicle being respectively culture medium containing 0.2% FCS or culture medium containing 0.3125 µg DPPC per mL (=equal amount of DPPC/saline suspension as in highest concentration GNP dispersion added to the cells).

Measurement of the transepithelial electrical resistance (TEER)

The transepithelial electrical resistance (TEER) was measured using the Evom Voltohmmeter supplemented with the End-Ohm chamber or STX2 chopstick (World Precision Instruments Inc.). The resistance of a cell-free transwell insert was subtracted from the resistance measured across each cell layer to obtain the TEER value of the cell layers. Corrections for the surface area were made. Immediately before the exposure, TEER measurements of the co-cultures were made to serve as baseline values. TEER values were measured at 30 minutes, 1, 2, 4, 6 and 24 hours after the start of exposure.

Paracellular flux of fluorescent labelled dextran

Paracellular flux of uncharged molecules was investigated by measuring passage of apically added markers across the cell layer. Fluorescein isothiocyanate (FITC)-conjugated 4kDa-dextran was added to the apical surface at a final concentration of 1mg/mL. After 4 hours of incubation at 37°C, triplicate basolateral samples were taken for assaying on an black 96-well plate. This incubation time was chosen to allow sufficient transport of the FITC-dextran, however this exposure also resulted in a decrease in TEER (due to cytotoxicity of FITC-dextran). Therefore TEER was recorded immediately before adding the FITC-dextran (at 20h after exposure) and these values were related with the changes in flux.

Fluorescence was measured using a fluorescence plate reader (FLUOstar Omega; BMG Labtech, Ortenberg, Germany) with excitation and emission wavelengths of 485 nm and 530 nm, respectively. The flux or change in concentration was calculated by dividing the concentration and volume of the basolateral compartment by the concentration and volume of the apical compartment, and expressed as percentage.

Staining of the intercellular junctional proteins

Integrity of the tight junction was assessed using immunofluorescent staining of proteins zonula occludens 1 (ZO-1) and occludin. After exposure the co-cultures were washed, fixed with ice-cold methanol for 10 minutes at -20°C and permeabilised with 0.3% Triton-X100 for 10 minutes. The co-culture was blocked with 1% BSA solution for 1 hour and incubated successively with Alexa Fluor® 488-conjugated mouse anti-human ZO1 antibody (1/100) and Alexa Fluor® 594-conjugated mouse anti-human Occludin antibody (1/100) for 2 hours in 0.5% BSA solution. The nuclei were counterstained with DAPI (1/500) for 10 minutes. Finally, the membranes were excised from the insert and mounted using ProLong® Gold Antifade Mountant. Images were taken with an Olympus BX61 microscope using the XC30 camera at x40 magnification.

Phosphoproteomics

16HBE cells were exposed to 64mg/mL of G or GO for 24 hours, after this the cells were washed and lysed using the Mem-PER™ Plus membrane protein extraction kit supplemented with 1mM Phenylmethylsulfonyl fluoride (PMSF) and phosSTOP™ to extract the membrane-associated proteins, according to the manufacturers' instructions. Membrane protein concentrations were determined using the Pierce bicinchoninic acid (BCA) protein assay.

180 µg of membrane fraction lysates were subjected to reduction (5 mM DTT) and alkylation (25 mM iodoacetamide) followed by precipitation [28]. The proteins were digested overnight using 4 µg trypsin at 37°C in 200mM ammonium bicarbonate, 5% acetonitrile, 0.01 % ProteaseMax (Promega). The resulting peptides were desalted with C18 Micro Spin Columns (Harvard Apparatus) and subjected to phosphopeptide enrichment on IMAC beads (PHOS-Select iron affinity gel, Sigma). The resulting peptides were desalted with C18 ZipTip pipette tips (Millipore) and subjected to high-resolution LC-MS/MS using an Ultimate 3000 nano UPLC system interfaced with a Q Exactive hybrid quadrupole-orbitrap mass spectrometer via an EASY-spray (C-18, 50 cm) column (Thermo Fisher Scientific).

Progenesis software (Nonlinear Dynamics) was used for relative quantification of peptides. Peptides were identified by MASCOT (Matrix Science) using SwProt_trEMBL_homo sapiens (71 785 sequences) as a database via Proteome Discoverer 2.2 software, incorporating Percolator for peptide validation and ptmRS for PTM localization. Following search parameters were used: phosphorylation (STY) in

combination with oxidation (M) as variable modifications and carbamidomethylation (C) was used as a fixed modification. Three missed cleavages were allowed for trypsin digestion. Peptide tolerance was set at 10 ppm and MS/MS tolerance at 20 mmu. Only peptides with a high (PEP < 0.01) and middle (PEP < 0.05) identification confidence were taken into account.

The peptide and protein abundancies of the NP-exposed cells were divided by those of the control cells, to quantify the change in phosphorylation. If the ratio of phosphopeptide abundance of the NP-exposed cells compared to that of the control cells was larger or equal than 1.5, or smaller or equal than 0.5, these proteins were considered as relevantly hyper- or hypophosphorylated. These unique proteins were selected per type of NP and were further investigated. Functional analysis of the selected proteins was performed using the DAVID web-tool for their involvement in cell pathways using the Kyoto Encyclopedia of Genes and Genomes (KEGG) database (https://www.genome.jp/kegg/)[29–31]. As a background, the DAVID-supported 'Homo sapiens' gene set was used.

Statistical analysis

The results are represented as mean ± SD or mean with individual values. Normality distribution was determined using the d'Agostino & Pearson omnibus normality test. When normally distributed, the data were analyzed with a one-way ANOVA followed by Dunnett's multiple-comparison test. When the data were not normal distributed, the Kruksal-Wallis test followed by a Dunn's multiple comparison test was used. Time series of the TEER measurements were analyzed with a two-way ANOVA (Graphpad Prism 5.00, Graphpad Software inc, San Diego, California, USA). A level of $p < 0.05$ was considered significant.

Results

Part A: Effect of different types of irritants on the airway epithelial barrier

Transepithelial electrical resistance (TEER)

Changes in ion permeability of the cell layers due to irritant exposure were examined using measurement of the transepithelial electrical resistance (TEER). Co-cultures were apically exposed to 64 or 256 µg/mL G, 16 or 64 µg/mL GO, 25 or 100 µg/mL AP, 12.5 or 6.25 µg/mL SP, 7.5 or 3.75 ppm act. Cl in ClO^-, or fresh medium (Ctrl). These concentrations were sub-toxic for 16HBE cells, as determined by LDH and WST-1 assay (Fig. 2). TEER was recorded immediately before and at different time points (30 min, 1, 2, 4, 6 and 24 h) after the start of the exposure. Exposure to each tested concentration of G resulted in an immediate and persistant decrease in TEER compared to the vehicle-exposed control (Fig. 3a). Exposure to GO also induced a significant immediate decrease in TEER, which stayed significantly lower than the control for a concentration of 64 µg/mL (Fig. 3b). When the co-cultures were exposed to AP or SP this did not result in changes in TEER compared to the control co-culture (Fig. 3c and d). Both concentrations of active chlorine in ClO^- initially did not alter the TEER, yet 24 hours after the start of the exposure a significant decrease in TEER compared to the control was found (Fig. 3e).

Flux of fluorescent-labelled dextran

To investigate whether environmental irritants can alter the paracellular transport of small molecules, we determined the flux of an apically added fluorescent-labelled 4kDa-dextran (FD4) across the cell layers. The co-cultures were exposed identically as described above for 20 hours, after which the TEER was recorded and the flux was measured (after a 4h incubation period to allow passage). Permeability for FD4 was significantly larger than in the control condition after exposure to 256 µg/mL of G and 64 µg/mL of GO (Fig. 4a). Other tested concentrations of G and GO, and both concentrations ClO^-, AP and SP did not significantly alter the FD4-flux after 24 hours of exposure. The significant changes in FD4-flux where accompanied with significant decreases in the TEER (Fig. 4b).

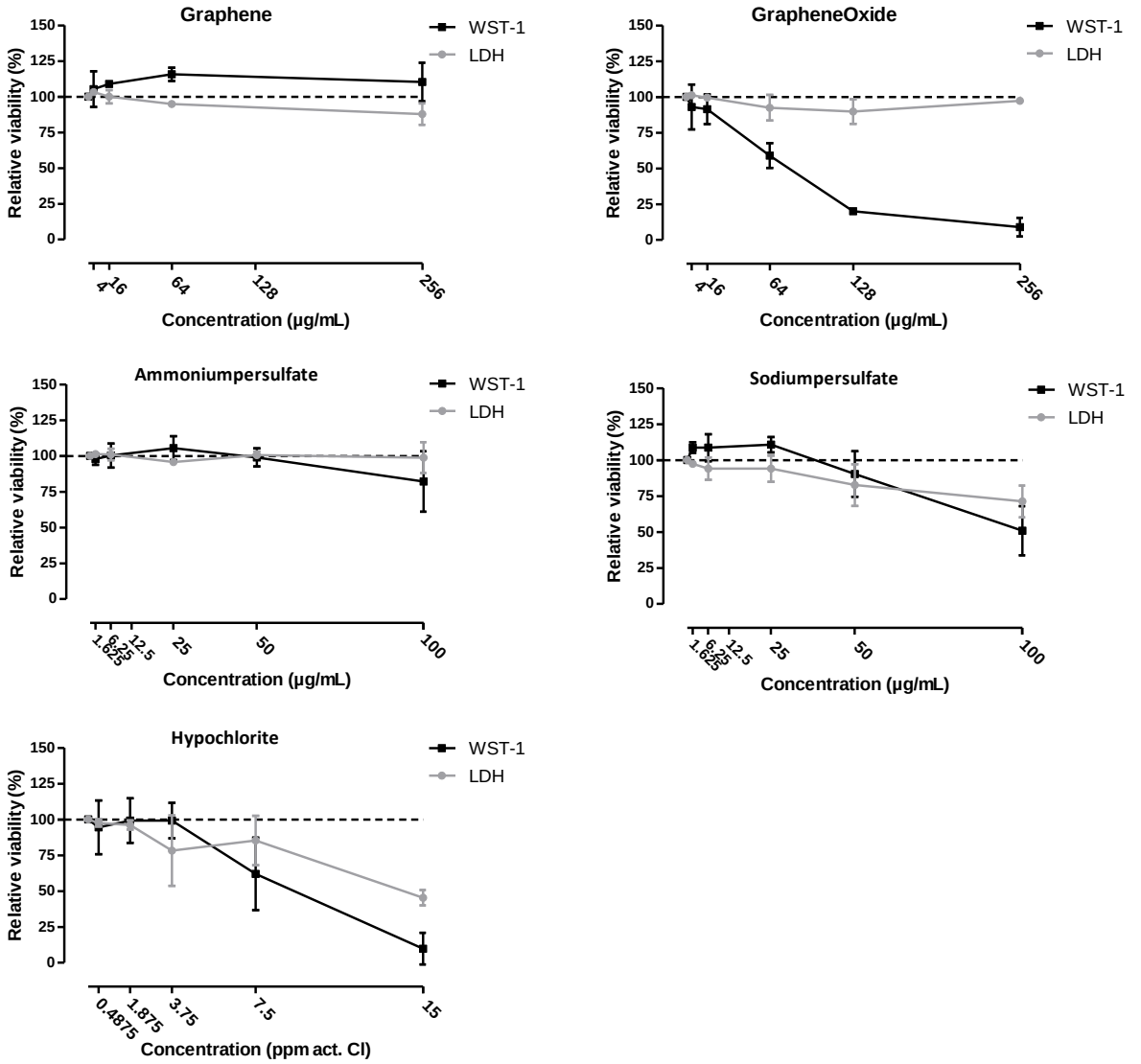

Figure 2. WST-1 and LDH assays of 16HBE cells exposed to G, GO, AP, SP and ClO^-

The 16HBE cells were exposed to increasing concentrations of the agents for 24 hours. Afterwards the cell viability was evaluated using the WST-1 and LDH assay. Mean ±SD, n = 2-3, each experiment was performed in triplicate.

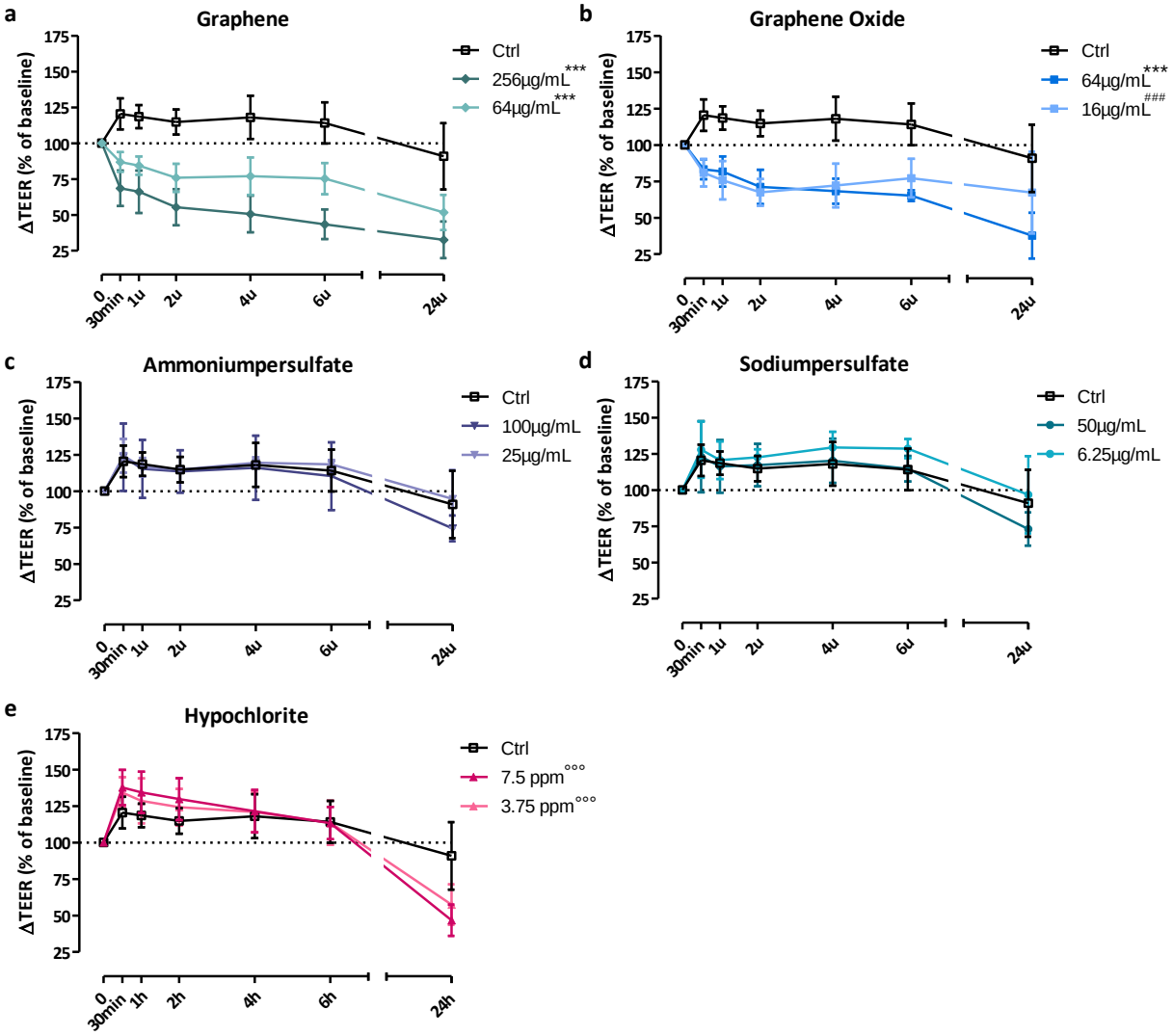

Figure 3. TEER measurements of co-cultures exposed to G, GO, AP, SP and ClO⁻
The TEER values are normalized and represented as percentages of the baseline value. Significant different at * all time points, at # some time points and at ° 24h after the start of exposure compared to the vehicle control. p<0.001: 3 symbols. Mean ± SD, n=3-7, each experiment was performed in duplicate.

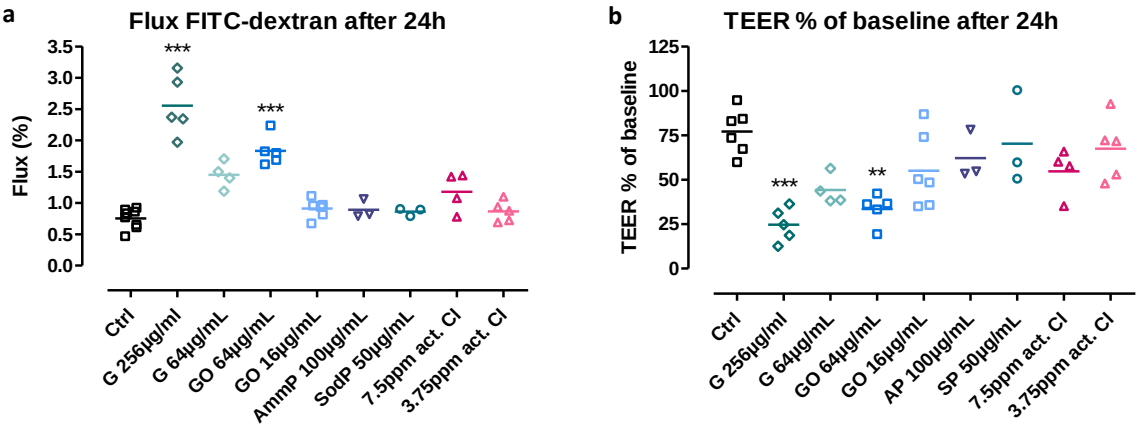

Figure 4. FITC-dextran transport (a) and TEER (b) of co-cultures exposed to G, GO, SP, AP and ClO⁻
** p<0.01, *** p<0.001 compared to the vehicle control. Mean ± SD, n=3-8; each experiment was performed in duplicate

Part B: Altered effect of GNPs on the airway epithelial barrier with different suspension method

Transepithelial electrical resistance (TEER)

Concentrations of 128 or 64 µg/mL G and GO were suspended in the more physiologically relevant suspension using artificial surfactant, and added onto the apical side of the co-cultures. These concentrations were found to be sub-toxic as determined after 24h of exposure by LDH and WST-1 assay on 16HBE monocultures (Fig. 5). As described above, TEER was measured before and at repeated time points after the start of exposure. The TEER of co-cultures exposed to G did not alter compared with the vehicle-exposed co-culture (Fig. 6a). Exposure to GO induced a steady decrease in TEER, and was only significantly reduced compared to the control after 24h of exposure to a concentration of 128µg/mL GO (Fig. 6b).

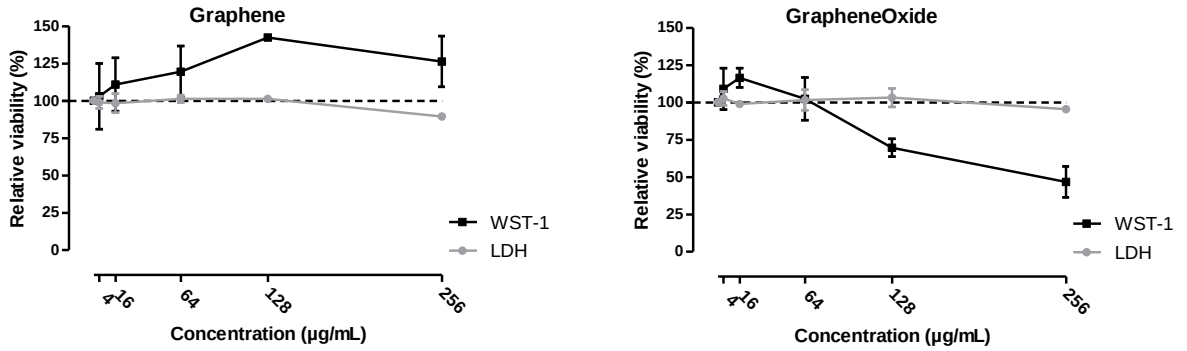

Figure 5. WST-1 and LDH assays of 16HBE cells exposed to G and GO suspended using DPPC
The 16HBE cells were exposed to increasing concentrations of the agents for 24 hours. Afterwards the cell viability was evaluated using the WST-1 and LDH assay. Mean ±SD, n = 2-3, each experiment was performed in triplicate.

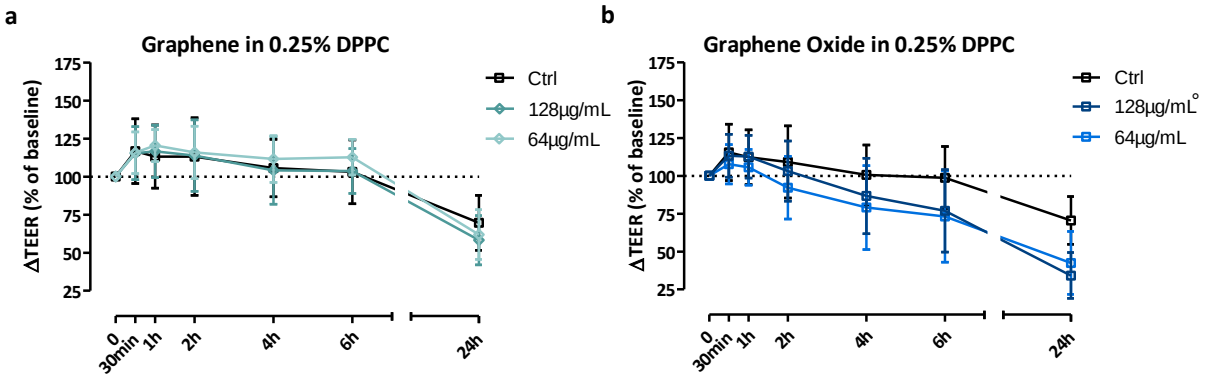

Figure 6. TEER measurements of co-cultures exposed to G and GO suspended using DPPC
The TEER values are normalized and represented as percentages of the baseline value. Significant different at ° 24h after the start of exposure compared to the vehicle control. $p<0.05$: 1 symbol. Mean ± SD, n=4-5, each experiment was performed in duplicate.

Flux of fluorescent-labelled dextran

Permeability of the airway barrier was determined by measuring of FD4-transport, 24 hours after exposure to GNPs in the surfactant suspension. Exposure to the tested concentrations of G did not alter the FD4-flux, whereas both of the tested concentrations GO did induce a significant increase in FD4-flux compared to the vehicle-control (Fig. 7a). These changes in flux were reflected by significant decreases in TEER after 24 h of exposure (Fig. 7b).

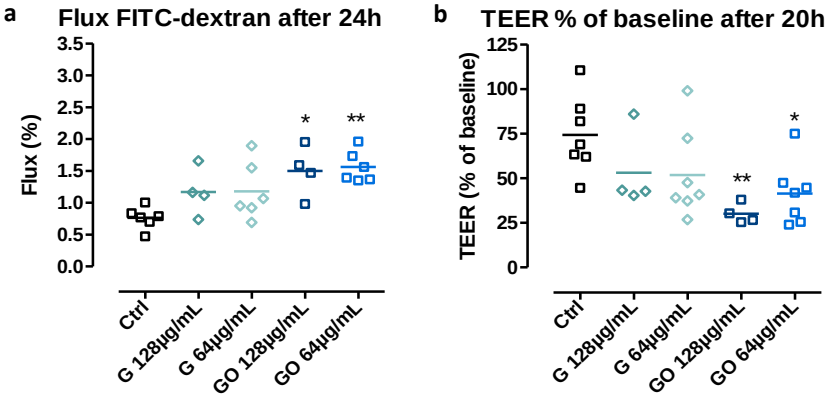

Figure 7. FITC-dextran transport (a) and TEER (b) of co-cultures exposed to G and GO suspended using DPPC
*p<0.05, ** p<0.01 compared to the vehicle control. Mean ± SD, n= 4-7; each experiment was performed in duplicate

Part C: Effect of GNPs on the airway epithelium

Staining of Tight junction (TJ) proteins

In order to investigate whether G or GO exposure disturbed the intercellular junctional complexes, the co-cultures were immunostained for two tight junction markers, zonula occludens 1 (ZO-1) and occludin. Twenty-four hours after the start of the exposure, the vehicle-treated control co-culture showed an intact TJ network with a nicely connected ZO-1 and occludin staining (Fig. 8). After exposure to 128 µg/mL G and GO in the FCS suspension the TJ proteins were still present, but showed a more disorganized pattern with interruptions in the ZO-1 and occludin staining (Fig. 8).

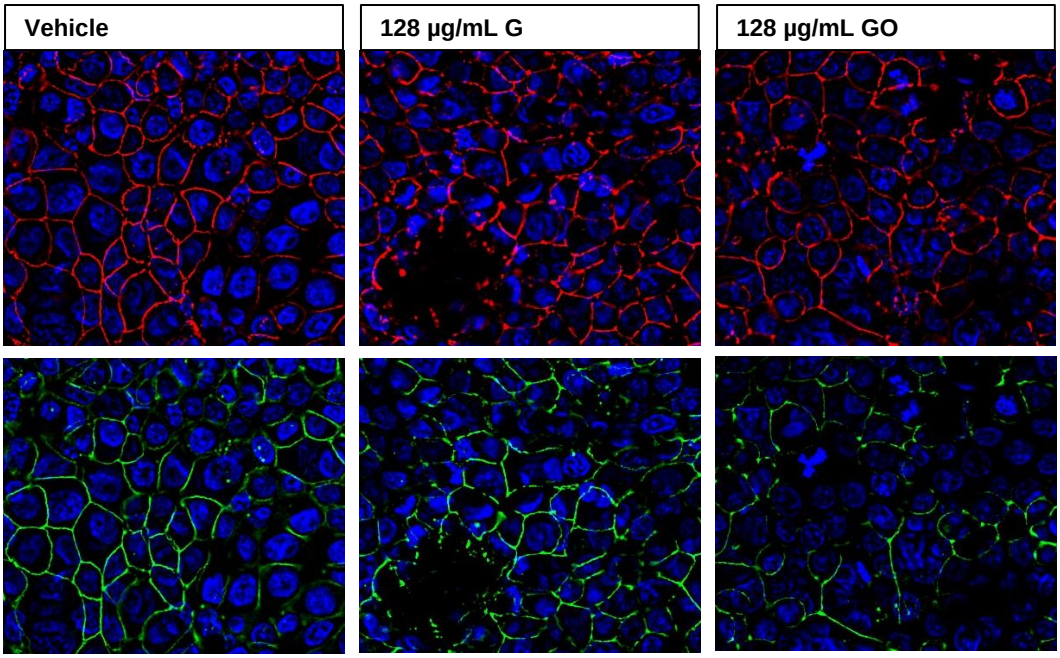

Figure 8. Immunofluorescent staining of TJ in co-cultures exposed to G and GO suspended using 0.2% FCS Representative images from co-cultures apically exposed to vehicle, 128 µg/mL graphene and 128 µg/mL graphene oxide suspended using 0.2% FCS. Immunofluorescent staining for Occludin (red) and ZO-1 (green), cell nuclei were counterstained with DAPI (blue).

Phosphoproteomics of membrane-associated proteins

Since the phosphorylation of intercellular junctional proteins might influence their functioning, and thus the barrier integrity, we investigated the phosphorylation level of the membrane-associated proteins after 24h of exposure to 64 µg/mL G and GO suspended with FCS. Of the large number of identified phosphopeptides, those that had a relevant alteration in phosphorylation level (i.e. a NP-exposed/Ctrl ratio in phosphopepetide abundancies ≤ 0.5 or ≥ 1.5) were taken into consideration. For the cells exposed to G, we identified 242 unique phosphoproteins that had a relevant change in phosphorylation level compared to the control. In cells exposed to GO, 246 phosphoproteins were correspondingly identified. Per type of exposure the identified differently phosphorylated proteins were functionally analyzed to determine their contribution in pathways associated with barrier integrity. As demonstrated in Table 1, the top 5, based on p-value, out of the 15 significatnly enriched KEGG pathways (p-value <0.05) for G included 'Spliceosome', 'Adherens junction', 'RNA transport', 'Ribosome biogenesis in eukaryotes' and 'Tight junction'. For GO the top 5 out of 17 significantly enriched KEGG pathways included 'Spliceosome', 'Tight junction', Adherens junction', 'RNA transport' and 'Cell adhesion molecules', as listed in Table 2.

Figure 9 shows a simplified and combined version of the TJ and AJ pathways provided from the KEGG database. The 15 differently phosphorylated proteins in the TJ and AJ pathways due to G, GO or both GNP exposure are depicted in colored boxes. TJ are essential to establish cell polarity and create a

selective permeable barrier. The proteins Crumbs, PALS1 and PATJ constitute together the cell polarity complex in epithelial cells. TJ establish cell-cell contacts via transmembrane proteins of the claudin, occludin or junctional adhesion molecules (JAM) family and a cytoplasmic 'plaque' consisting different proteins that form a complex and connect to the actin cytoskeleton. AJ are responsible for cellular adhesion in different types of tissues, hereby maintaining tissue architecture and limiting cell movement and proliferation. Cadherin is an essential cell adhesion molecule in AJ. The cytoplasmic tail of cadherin binds β-catenin, which in turn binds α-catenin that connects to the actin cytoskeleton. Catenin-δ stabilizes the cadherin/β-catenin complex at the cell membrane. Phosphorylation of β-catenin and δ-catenin by receptor protein tyrosine kinases (RPTKs) and cytoplasmic protein tyrosine kinases (PTKs, e.g. Fer, Fyn, Yes and Src), negatively affects the integrity of the cadherin/catenin complex, leading to its dissociation. The integrity of this complex is positively regulated by dephosphorylation by protein tyrosine phosphatases and, by phosphorylation by casein kinase II. Changes in β-catenin phosphorylation affects cell-cell adhesion and influences the cellular location of β-catenin, which if not associated with cadherin can degrade or signal as free β-catenin to initiate gene expression. Nectins also function as cell adhesion molecules and transduce signals that reorganize the actin cytoskeleton, regulate AJ formation and strengthen cell-cell adhesion.

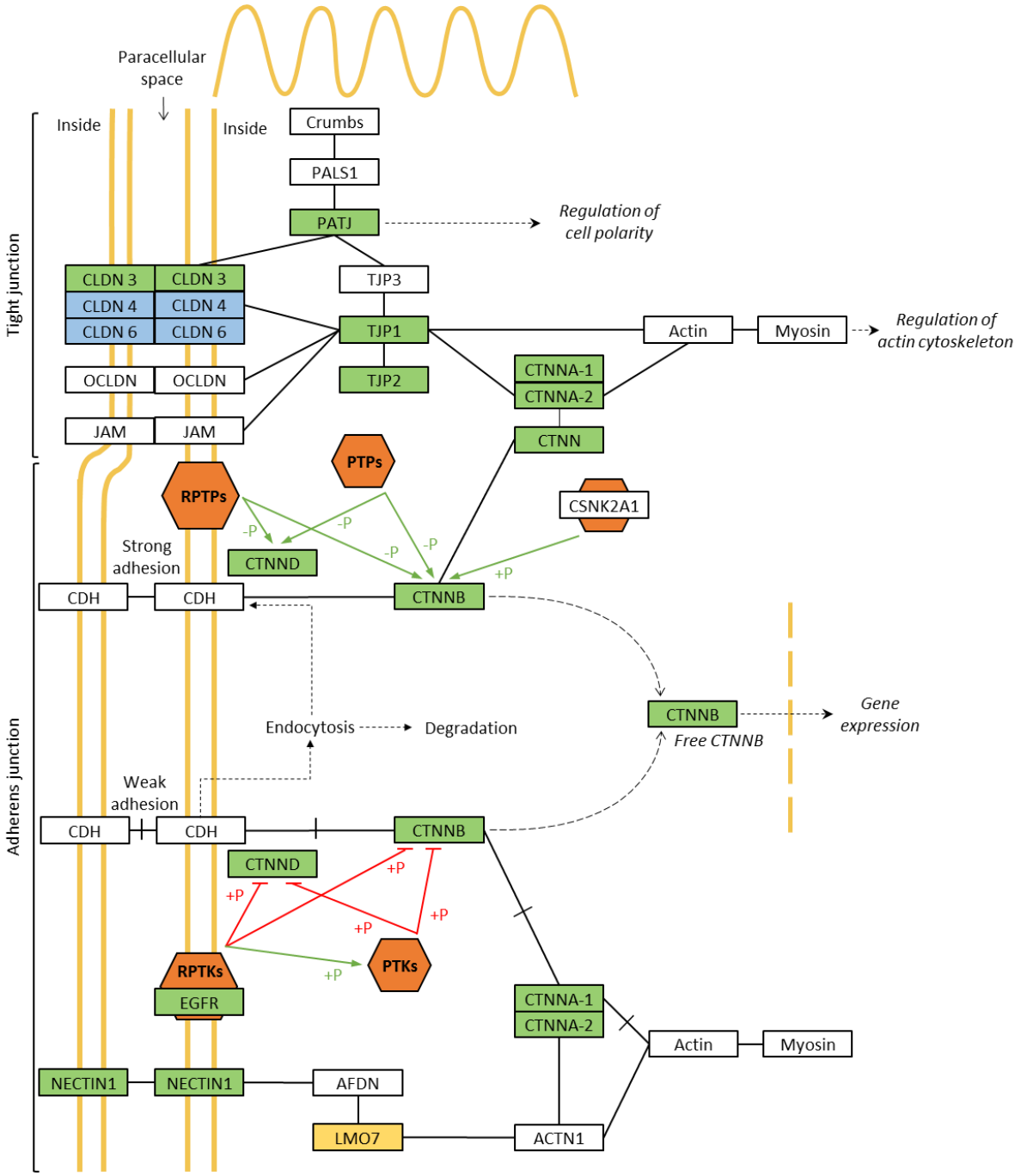

Figure 9. Overview of differentially phosphorylated proteins in TJ and AJ pathways
The proteins that were differently phosphorylated due to exposure to G, GO or both GNPs are depicted respectively in yellow, blue or green boxes. Proteins that were unaffected are depicted in white boxes. The orange hexagons represent protein kinases or phosphatases. '+P' and '-P' indicate respectively phosphorylation and de-phosphorylation, if this promotes the function of the targeted protein a green arrow is drawn, if this hinders the function of the targeted protein a red arrow in drawn. RPTP, receptor protein tyrosine phosphatase; PTP, protein tyrosine phosphatase; RTPK, receptor protein tyrosine kinase; PTK, protein tyrosine kinase. The figure is a simplified and combined version of the TJ and AJ pathway from the KEGG database.

Table 1

Functional classification of the differentially phosphorylated proteins by graphene exposure (fold change ≥ 1.5 or ≤ 0.5). Fifteen of the enriched pathways had a p-value <0.05. The table lists the top 5 out of these enriched pathways.

No.	Full gene name	Gene ID	p-value	Enrichment	FDR
	Spliceosome		**6,92E-13**	**10,28**	**8,15E-10**
1	Apoptotic chromatin condensation inducer 1	ACIN1			
2	Calcium homeostasis endoplasmic reticulum protein	CHERP			
3	DEAH-box helicase 16	DHX16			
4	Heterogeneous nuclear ribonucleoprotein C (C1/C2)	HNRNPC			
5	Heterogeneous nuclear ribonucleoprotein K	HNRNPK			
6	Pre-mRNA processing factor 38A	PRPF38A			
7	RNA binding motif protein 17	RBM17			
8	RNA binding motif protein 8A	RBM8A			
9	X-linked RNA binding motif protein X-linked	RBMX			
10	Squamous cell carcinoma antigen recognized by T-cells 1	SART1			
11	Small nuclear ribonucleoprotein U5 subunit 200	SNRNP200			
12	Serine and arginine rich splicing factor 4	SRSF4			
13	Serine and arginine rich splicing factor 6	SRSF6			
14	Serine and arginine rich splicing factor 9	SRSF9			
15	THO complex 2	THOC2			
16	Transformer 2 alpha homolog	TRA2A			
17	Transformer 2 beta homolog	TRA2B			
18	Ubiquitin specific peptidase 39	USP39			
	Adherens junction		**3,40E-05**	**8,56**	**0,04**
1	Catenin alpha 1	CTNNA1			
2	Catenin alpha 2	CTNNA2			
3	Catenin beta 1	CTNNB1			
4	Catenin delta 1	CTNND1			
5	Epidermal growth factor receptor	EGFR			
6	Lim domain 7	LMO7			
7	Nectin cell adhesion molecule 1	NECTIN1			
8	Tight junction protein 1	TJP1			
	RNA transport		**3,72E-04**	**4,41**	**0,44**
1	Apoptotic chromatin condensation inducer 1	ACIN1			
2	FMR1 autosomal homolog 2	FXR2			
3	Nucleoporin 88	NUP88			
4	Nucleoporin 93	NUP93			
5	Nucleoporin 98	NUP98			
6	Pinin desmosome associated protein	PNN			
7	RNA binding motif protein 8A	RBM8A			
8	Serine and arginine repetitive matrix 1	SRRM1			
9	THO complex 2	THOC2			
10	THO complex 5	THOC5			
	Ribosome biogenesis in eukaryotes		**8,95E-04**	**6,11**	**1,05**
1	Dyskerin pseudouridine synthase 1	DKC1			
2	NOP56 ribonucleoprotein	NOP56			
3	NOP58 ribonucleoprotein	NOP58			
4	Treacle ribosome biogenesis factor 1(TCOF1)	TCOF1			
5	UTP 14 small subunit processome component	UTP14A			
6	UTP 18 small subunit processome component 18	UTP18			
7	5'-3' exoribonuclease 2	XRN2			
	Tight junction		**1,96E-03**	**4,43**	**2,29**
1	Claudin 3	CLDN3			
2	Catenin alpha 1	CTNNA1			
3	Catenin alpha 2	CTNNA2			
4	Catenin beta 1	CTNNB1			
5	Cortactin	CTTN			
6	Crumbs cell polarity complex component	PATJ			
7	Tight junction protein 1	TJP1			
8	Tight junction protein 2	TJP2			

Table 2

Functional classification of differentially phosphorylated proteins by graphene oxide exposure (fold change ≥ 1.5 or ≤ 0.5). Seventeen of the enriched pathways had a p-value <0.05. The table lists the top 5 out of these enriched pathways.

No.	Full gene name	Gene ID	p-value	Enrichment	FDR
	Spliceosome		**1,75E-12**	**9,74**	**2,08E-09**
1	Apoptotic chromatin condensation inducer 1	ACIN1			
2	Calcium homeostasis endoplasmic reticulum protein	CHERP			
3	DEAH-box helicase 16	DHX16			
4	Heterogeneous nuclear ribonucleoprotein C (C1/C2)	HNRNPC			
5	Heterogeneous nuclear ribonucleoprotein K	HNRNPK			
6	Pre-mRNA processing factor 38A	PRPF38A			
7	RNA binding motif protein 8A	RBM8A			
8	X-linked RNA binding motif protein X-linked	RBMX			
9	Squamous cell carcinoma antigen recognized by T-cells 1	SART1			
10	Small nuclear ribonucleoprotein U5 subunit 200	SNRNP200			
11	Serine and arginine rich splicing factor 10	SRSF10			
12	Serine and arginine rich splicing factor 4	SRSF4			
13	Serine and arginine rich splicing factor 6	SRSF6			
14	Serine and arginine rich splicing factor 9	SRSF9			
15	THO complex 2	THOC2			
16	Transformer 2 alpha homolog	TRA2A			
17	Transformer 2 beta homolog	TRA2B			
18	Ubiquitin specific peptidase 39	USP39			
	Tight junction		**1,01E-04**	**5,25**	**0,12**
1	Claudin 3	CLDN3			
2	Claudin 4	CLDN4			
3	Claudin 6	CLDN6			
4	Catenin alpha 1	CTNNA1			
5	Catenin alpha 2	CTNNA2			
6	Catenin beta 1	CTNNB1			
7	Cortactin	CTTN			
8	Crumbs cell polarity complex component	PATJ			
9	Tight junction protein 1	TJP1			
10	Tight junction protein 2	TJP2			
	Adherens junction		**4,02E-04**	**7,10**	**4,75E-01**
1	Catenin alpha 1	CTNNA1			
2	Catenin alpha 2	CTNNA2			
3	Catenin beta 1	CTNNB1			
4	Catenin delta 1	CTNND1			
5	Epidermal growth factor receptor	EGFR			
6	Nectin cell adhesion molecule 1	NECTIN1			
7	Tight junction protein 1	TJP1			
	RNA transport		**5,57E-04**	**4,18**	**0,66**
1	Apoptotic chromatin condensation inducer 1	ACIN1			
2	Eukaryotic translation initiation factor 5B	EIF5B			
3	FMR1 autosomal homolog 2	FXR2			
4	Nucleoporin 93	NUP93			
5	Nucleoporin 98	NUP98			
6	Pinin desmosome associated protein	PNN			
7	RNA binding motif protein 8A	RBM8A			
8	Serine and arginine repetitive matrix 1	SRRM1			
9	THO complex 2	THOC2			
10	THO complex 5	THOC5			
	Cell adhesion molecules (CAM)		**7,04E-04**	**4,56**	**0,83**
1	Claudin 3	CLDN3			
2	Claudin 4	CLDN4			
3	Claudin 6	CLDN6			
4	Major histocompatibility complex class I A	HLA-A			
5	Major histocompatibility complex class I B	HLA-B			
6	Major histocompatibility complex class I C	HLA-C			
7	L1 cell adhesion molecule	L1CAM			
8	Myelin protein zero like 1	MPZL1			
9	Nectin cell adhesion molecule 1	NECTIN1			

Discussion

In the current study, we demonstrated that different types of environmental irritants have different effects on an *in vitro* model of the airway epithelial barrier. As evaluated by TEER and FD4-flux, the nanoparticles G and GO immediately had a negative impact on the epithelial barrier, whereas ClO^- only had a negative impact after 24h of exposure. Exposure to AP and SP did not alter the barrier properties. In addition, we showed that the negative effect of the GNPs on the epithelial barrier was influenced by the method of suspension. With a physiologically more relevant suspension method using DPPC, GNPs had a somewhat lower (but not significant) effect on the epithelial barrier. Next, evaluation of the TJ network using immunofluorescent staining of ZO-1 and occludin, indicated that co-cultures exposed to G or GO had a slightly less connected TJ network. In a large set of membrane-associated proteins, we found using phosphoproteomics that the proteins in the AJ and TJ pathways were significantly hypo- or hyperphosphorylated due to GNP exposure, which therefore provides an explanation for the observed negative effect on the airway epithelial barrier.

In the first part of this study, we evaluated the effect of different types of environmental agents on the airway epithelial barrier. An intact epithelial barrier is crucial, since disruption will enhance the permeability, which will lead to increased penetration of potentially harmful agents towards the host. It was found that the GNPs had an immediate and persistent negative effect on the airway epithelial barrier. The oxidizing chemicals sodium and ammonium persulfate did not have a negative effect on the barrier with the used concentrations. Exposure to hypochlorite impaired the barrier only after 24 hours of exposure. Transepithelial electrical resistance (TEER) measures the passage of ions and small molecules across the cell layers, whereas the flux of fluorescent-labeled dextrans determines the paracellular transport of macromolecules [32]. In our experiments, these two parameters corresponded well and showed significant changes in FD4-flux and TEER for the highest tested concentration of G and GO. According to the WST-1 and LDH assay to determine cytotoxicity due to environmental exposure in 16HBE, these concentrations were non-cytotoxic.

In a second part, we demonstrated that the negative effect of GNPs on the airway barrier *in vitro* was influenced by the method of suspension. If suspended with DPPC, G and GO affected the barrier in a much lesser extent than if suspended with FCS. Since NPs have the tendency to agglomerate (i.e. form loose associations between the primary particles) and sediment when diluted in aqueous culture medium for *in vitro* nanotoxicity studies, there is a need to stably disperse NP [33]. Different dispersion strategies exist and these can alter the bioavailability of the NP, and thus affect its toxicity. As suspension method, we sonicated the GNPs in 2% FCS in distilled water with a probe sonicator, and further diluted this tenfold in cell culture medium for addition to the cells. This method resulted in a

stable and uniform dispersion for the GNPs. However, since inhalation is the main exposure target during the manufacture and processing of NP, this is not a physiologically relevant suspension [34,35]. Within the lung, the bronchioles and alveoli are covered by pulmonary surfactant, that will come into contact with inhaled NP [36]. Dipalmitoylphosphatidylcholine (DPPC) is the major phospholipid in the lung surfactant and the artificial form has been used as a biocompatible dispersive agent [27,33,34,37]. Phospholipids have the feature to form bilayers on hydrophilic surfaces and monolayers on hydrophobic surfaces. In our study we used a concentration of 2.5 mg DPPC per 1mg NP (w/w) in saline to suspend the GNPs in a bath sonicator. According to Wallace et al. this concentration is required to assure complete bilayer coverage of NP with high specific surface area (such as e.g. carbon nanotubes and GNPs) [27]. It is expected that in the DPPC suspension the hydrophobic G was covered with a phospholipid monolayer and the more hydrophilic GO was covered with a phospholipid bilayer. Due to this DPPC coverage both NPs had no negative effect on the barrier integrity, in contrast to the FCS suspended GNPs. Possibly phospholipid coverage 'protected' the cells from direct interactions with the GNPs that might affect the barrier integrity. This is in contrast to findings with CNTs, which had an increased bioavailability and thus increased toxicity when dispersed using DPPC [34]. Dispersion of silica NPs with DPPC, however lead to a reduced toxic potential [33,38,39]. In addition to these alterations due to GNP coverage, bath sonication is a gentle method to disperse NPs, and might not break up all the agglomerates, and thus reduce interaction between the primary particle and the cells.

Third, we further wanted to investigate the interaction of the GNPs with the epithelium. To investigate whether G and GO could destroy the intercellular junctions, we stained for the TJ proteins occuldin and ZO-1. These are important TJ proteins that surround epithelial cells in a belt-like manner. After exposure to G and GO, the organization of the TJ belts was slightly altered, and still clearly present. The fact that the deposited G and GO particles appear black on the images makes it difficult to distinguish 'disorganization of the TJ network' from the black particles. Attempts to quantify our observations on the images were therefore unsuitable, making this only an indicative finding. In addition, not only the expression of the intercellular junctional proteins, but also their post-translational modifications (PTMs) determine the proper functioning of these proteins.

In a way to screen for alterations in a large set of proteins of the intercellular junctions, we performed a phosphoproteome analysis. Phosphorylation is a dynamic and important PTM that has been shown to regulate folding, binding, location and stability of intercellular junction proteins [40]. Using a proteome analysis on the membrane-associated proteins we could evaluate a large set of proteins, providing us substantial information on the alterations due to NP exposure. Selecting the proteins that were significantly hypo- or hyperphosphorylated, indicated that graphene oxide altered a slightly larger number of proteins than graphene. Functional analysis of these selected proteins, revealed that for

both G and GO the KEGG pathways AJ and TJ were found in the top five of significantly enriched pathways, which was in line with our hypothesis that GNP exposure might affect AJ and TJ protein functions. For some specific proteins in these pathways, phosphorylation of specific residues is crucial in their function to maintain cell adhesion via interacting with different proteins (see Fig. 9). Phosphorylation of tyrosine residues in occludin, E-cadherin, ZO-1 and β-catenin have repeatedly been associated with an increased barrier permeability, because of a reduced interaction between the proteins [40–42]. In our dataset of AJ and TJ proteins that were significantly more phosphorylated, tyrosine phosphorylation was only found at Tyr865 in catenin δ-1. This is a known phosphorylated residue, which however has not been described to cause barrier alterations. Not only tyrosine phosphorylation is of importance for interactions between proteins of the AJ or TJ pathway. Phosphorylation of serine at position 641 in α-catenin has been described to disturb the binding between α-catenin and β-catenin, resulting in increased transcriptional activity of β-catenin, as well as, reduced association of the cadherin/β-catenin complex with the actin skeleton [43]. In our experiments, G exposure increased the phosphorylation at Ser641 in catenin α-1, which might result in 'looser' AJ that contribute to the decreased barrier function. Similarly, we found increased serine phosphorylation at residues 552 and 191 in β-catenin, which has been shown to cause its dissociation from the cell-cell contacts and stabilization of β-catenin in the nucleus respectively, and thus could be involved in the observed impaired barrier function [44,45].

In conclusion, in an *in vitro* model of the airway epithelial barrier the nanoparticles G and GO had a negative impact on the barrier properties. This negative effect on the epithelial barrier was influenced by the method of suspension. To explain the negative impact of GNPs on the epithelial barrier, we evaluated whether the TJ proteins ZO-1 and occuldin were affected. A less organized TJ network was observed after exposure to G and GO, but since the deposited GNP appeared black on the images, this observation was difficult to verify. Using phosphoprotemics, we revealed that the phosphorylation status of proteins of the AJ and TJ pathway changed due to GNP exposure, which could explain the observed negative impact of the GNPs on the epithelial barrier.

Acknowledgments: This project was supported by a grant from the University of Leuven Research Council (GOA/14/011).

Conflict of interest: The authors declare no conflict of interest.

References

1. Ganesan, S., Comstock, A. T. & Sajjan, U. S. Barrier function of airway tract epithelium. *Tissue Barriers* **1,** e24997 (2013).
2. Nava, P., Kamekura, R. & Nusrat, A. Cleavage of transmembrane junction proteins and their role in regulating epithelial homeostasis. *Tissue Barriers* **1,** e24783 (2013).
3. Wittekindt, O. H. Tight junctions in pulmonary epithelia during lung inflammation. *Pflugers Arch.* **469,** 135–147 (2017).
4. Rezaee, F. & Georas, S. N. Breaking Barriers. New Insights into Airway Epithelial Barrier Function in Health and Disease. *Am. J. Respir. Cell Mol. Biol.* **50,** 857–869 (2014).
5. Georas, S. N. & Rezaee, F. Epithelial barrier function: at the frontline of asthma immunology and allergic airway inflammation. *J. Allergy Clin. Immunol.* **134,** 509–520 (2014).
6. Xiao, C. *et al.* Defective epithelial barrier function in asthma. *J. Allergy Clin. Immunol.* **128,** 549–556.e12 (2011).
7. Soyka, M. B. *et al.* Defective epithelial barrier in chronic rhinosinusitis: The regulation of tight junctions by IFN-γ and IL-4. *J. Allergy Clin. Immunol.* **130,** 1087–1096.e10 (2012).
8. Heijink, I. H., Noordhoek, J. A., Timens, W., van Oosterhout, A. J. M. & Postma, D. S. Abnormalities in airway epithelial junction formation in chronic obstructive pulmonary disease. *Am. J. Respir. Crit. Care Med.* **189,** 1439–1442 (2014).
9. Brooks, S. M., Weiss, M. A. & Bernstein, I. L. Reactive airways dysfunction syndrome (RADS). Persistent asthma syndrome after high level irritant exposures. *Chest* **88,** 376–384 (1985).
10. Brooks, S. M., Malo, J.-L. & Gautrin, D. Irritant-induced asthma and reactive airways dysfunction syndrome. in *Asthma in the workplace* **21,** (2013).
11. Ou, L. *et al.* Toxicity of graphene-family nanoparticles: a general review of the origins and mechanisms. *Part. Fibre Toxicol.* **13,** 57 (2016).
12. Arvidsson, R., Molander, S. & Sandén, B. A. Review of Potential Environmental and Health Risks of the Nanomaterial Graphene. *Hum. Ecol. Risk Assess. Int. J.* **19,** 873–887 (2013).
13. Sanchez, V. C., Jachak, A., Hurt, R. H. & Kane, A. B. Biological Interactions of Graphene-Family Nanomaterials: An Interdisciplinary Review. *Chem. Res. Toxicol.* **25,** 15–34 (2012).
14. Su, W.-C., Ku, B.-K., Kulkarni, P. & Cheng, Y. S. Deposition of Graphene Nanoparticles in Human Upper Airways. *J. Occup. Environ. Hyg.* **13,** 48–59 (2016).
15. Bianco, A. Graphene: Safe or Toxic? The Two Faces of the Medal. *Angew. Chem. Int. Ed.* **52,** 4986–4997 (2013).
16. Horváth, L. *et al.* Evaluation of the toxicity of graphene derivatives on cells of the lung luminal surface. *Carbon* **64,** 45–60 (2013).
17. Chang, Y. *et al.* In vitro toxicity evaluation of graphene oxide on A549 cells. *Toxicol. Lett.* **200,** 201–210 (2011).
18. Park, E.-J. *et al.* Toxic response of graphene nanoplatelets in vivo and in vitro. *Arch. Toxicol.* **89,** 1557–1568 (2015).
19. Hoyle, G. W. & Svendsen, E. R. Persistent effects of chlorine inhalation on respiratory health. *Ann. N. Y. Acad. Sci.* (2016). doi:10.1111/nyas.13139
20. Wigenstam, E., Elfsmark, L., Koch, B., Bucht, A. & Jonasson, S. Acute respiratory changes and pulmonary inflammation involving a pathway of TGF-β1 induction in a rat model of chlorine-induced lung injury. *Toxicol. Appl. Pharmacol.* **309,** 44–54 (2016).
21. White, C. W. & Martin, J. G. Chlorine gas inhalation: human clinical evidence of toxicity and experience in animal models. *Proc. Am. Thorac. Soc.* **7,** 257–263 (2010).
22. Kamath, Y. K. & Ruetsch, S. B. Reduction-induced surface modification of human hair. *J. Cosmet. Sci.* **61,** 1–12 (2010).
23. De Vooght, V. *et al.* Ammonium persulfate can initiate an asthmatic response in mice. *Thorax* **65,** 252–257 (2010).
24. Cruz, M.-J. *et al.* Assessment of the sensitization potential of persulfate salts used for bleaching hair. *Contact Dermatitis* **60,** 85–90 (2009).
25. Cruz, M. J. *et al.* Persistence of respiratory and inflammatory responses after dermal sensitization to persulfate salts in a mouse model of non-atopic asthma. *Allergy Asthma Clin. Immunol.* **12,** 26 (2016).
26. Tarlo, S. M. & Lemiere, C. Occupational asthma. *N. Engl. J. Med.* **370,** 640–649 (2014).

27. Wallace, W. E. *et al.* Phospholipid lung surfactant and nanoparticle surface toxicity: Lessons from diesel soots and silicate dusts. *J. Nanoparticle Res.* **9,** 23–38 (2007).
28. Wessel, D. & Flügge, U. I. A method for the quantitative recovery of protein in dilute solution in the presence of detergents and lipids. *Anal. Biochem.* **138,** 141–143 (1984).
29. Huang, D. W., Sherman, B. T. & Lempicki, R. A. Systematic and integrative analysis of large gene lists using DAVID bioinformatics resources. *Nat. Protoc.* **4,** 44–57 (2009).
30. Huang, D. W., Sherman, B. T. & Lempicki, R. A. Bioinformatics enrichment tools: paths toward the comprehensive functional analysis of large gene lists. *Nucleic Acids Res.* **37,** 1–13 (2009).
31. Kanehisa, M. & Goto, S. KEGG: kyoto encyclopedia of genes and genomes. *Nucleic Acids Res.* **28,** 27–30 (2000).
32. Matter, K. & Balda, M. S. Functional analysis of tight junctions. *Methods San Diego Calif* **30,** 228–234 (2003).
33. Ratoi, M., Hoet, P. H. M., Crossley, A. & Dobson, P. Impact of lung surfactant on wettability and cytotoxicity of nanoparticles. *RSC Adv.* **4,** 20573–20581 (2014).
34. Herzog, E. *et al.* Dispersion medium modulates oxidative stress response of human lung epithelial cells upon exposure to carbon nanomaterial samples. *Toxicol. Appl. Pharmacol.* **236,** 276–281 (2009).
35. Maynard, A. D. *et al.* Exposure to carbon nanotube material: aerosol release during the handling of unrefined single-walled carbon nanotube material. *J. Toxicol. Environ. Health A* **67,** 87–107 (2004).
36. Foucaud, L., Wilson, M. R., Brown, D. M. & Stone, V. Measurement of reactive species production by nanoparticles prepared in biologically relevant media. *Toxicol. Lett.* **174,** 1–9 (2007).
37. Porter, D. *et al.* A biocompatible medium for nanoparticle dispersion. *Nanotoxicology* **2,** 144–154 (2008).
38. Wallace, W. E. *et al.* Suppression of Inhaled Particle Cytotoxicity by Pulmonary Surfactant and Re-Toxification by Phospholipase: Distinguishing Properties of Quartz and Kaolin. *Ann. Occup. Hyg.* **32,** 291–298 (1988).
39. Hamilton, R. F., Thakur, S. A. & Holian, A. Silica binding and toxicity in alveolar macrophages. *Free Radic. Biol. Med.* **44,** 1246–1258 (2008).
40. Van Itallie, C. M. & Anderson, J. M. Phosphorylation of tight junction transmembrane proteins: Many sites, much to do. *Tissue Barriers* **6,** e1382671 (2018).
41. Olivera, D., Knall, C., Boggs, S. & Seagrave, J. Cytoskeletal modulation and tyrosine phosphorylation of tight junction proteins are associated with mainstream cigarette smoke-induced permeability of airway epithelium. *Exp. Toxicol. Pathol. Off. J. Ges. Toxikol. Pathol.* **62,** 133–143 (2010).
42. Rao, R. K., Basuroy, S., Rao, V. U., Karnaky Jr, K. J. & Gupta, A. Tyrosine phosphorylation and dissociation of occludin-ZO-1 and E-cadherin-beta-catenin complexes from the cytoskeleton by oxidative stress. *Biochem. J.* **368,** 471–481 (2002).
43. Ji, H. *et al.* EGF-induced ERK activation promotes CK2-mediated disassociation of alpha-Catenin from beta-Catenin and transactivation of beta-Catenin. *Mol. Cell* **36,** 547–559 (2009).
44. Fang, D. *et al.* PHOSPHORYLATION OF β-CATENIN BY AKT PROMOTES β -CATENIN TRANSCRIPTIONAL ACTIVITY. *J. Biol. Chem.* **282,** 11221–11229 (2007).
45. Wu, X. *et al.* Rac1 activation and subsequent β-catenin phosphorylation controls nuclear localization of β-catenin during canonical Wnt signaling. *Cell* **133,** 340–353 (2008).

Chapter 4

Contribution of mast cells in irritant-induced airway epithelial barrier impairment *in vitro*

Sofie Van Den Broucke, Jeroen Vanoirbeek, Ernesto Alfaro-Moreno, Peter Hoet

Abstract

The airway epithelium is continuously exposed to environmental irritants, which can cause adverse effects such as irritant-induced asthma (IIA). Mast cells are located at the vicinity of the airway epithelial barrier and have the ability to respond to variety of stimuli. We aimed to investigate whether mast cells influence the response of the epithelium upon irritant exposure.

To study the contribution of mast cells in irritant-induced epithelial barrier impairment, three different seeding conditions, i.e. bronchial epithelial cells (16HBE) only, 16HBE with mast cells (HMC-1's) basolaterally and 16HBE with HMC-1's apically were established. Upon exposure to the environmental irritants, graphene (G), graphene oxide (GO), diesel exhaust particles (DEPs) or hypochlorite (ClO^-) the transepithelial electrical resistance (TEER) and paracellular flux of fluorescent labelled dextrans was determined, along with the release of mediators. Identical experiments were conducted with the Ca^{2+} ionphore ionomycin.

A significant and permanent decrease in TEER was observed after exposure to G and GO, whereas DEP and ClO^- induced a transient decrease in TEER that restored to control level within 24h. This response pattern was similar in all different seeding conditions. FITC-dextran transport after 24h of exposure increased for G and GO in each of the tested seeding conditions, while no change was induced by DEP or ClO^- exposure compared to the control. Upon irritant exposure 16HBE and HMC-1 cells did not release TSLP, IL-33 or IL-1α, and histamine, IL-6 or IL-8 respectively. The alteration in epithelial barrier integrity upon treatment with ionomycin was not affected by HMC-1 cells. A limited amount of IL-6 and IL-8 was released by ionomycin-exposed HMC-1 cells.

To conclude, we found that mast cells (HMC-1) did not influence the epithelial barrier integrity upon environmental exposure, and thus currently do not provide additional information for the underlying mechanism of IIA.

Introduction

Humans are continuously exposed to a variety environmental irritants, such as gases, chemicals and particles in the air. Exposure to these agents in our living and work environment has been associated with development of asthma [1–3]. More specifically, in irritant-induced asthma (IIA), asthmatic symptoms arise and persist after inhalation of respiratory irritants, without involvement of adaptive immune sensitization [4–6]. The first cells in contact with inhaled noxious agents are the airway epithelial cells that form a tight mechanical barrier to prevent entry of harmful agents to the host. Upon inhalation of irritants, the epithelium likewise suffers the largest from the irritant-induced damage, resulting in impairment of the airway barrier, which has been suggested as an underlying mechanism of IIA [5]. Epithelial cells are also central in shaping the initial host defense by interacting with the surrounding immune cells.

Due to their location close to the interface with external environment, and their ability to rapidly release bioactive mediators, mast cells are important first-hand responders to possible detrimental insults [7]. In allergic asthma mast cells play a crucial role by secreting vasoactive and bronchoconstrictive mediators and initiating the synthesis and release of pro-inflammatory cytokines, upon cross-linking of immunoglobulin E (IgE) to the high affinity IgE receptor (FcεRI) on mast cells [8]. Mast cells can however respond to a variety of stimuli in a non-IgE dependent fashion [9]. Via pattern recognition receptors mast cells can recognize exogenous danger signals in the form of microbial, fungal and viral products, as well as endogenous danger signals emitted by injured tissue. Mast cells also express receptors for a number of inflammatory mediators, such as several cytokines and alarmins, which results in mast cell activation upon binding of the ligand.

In the current study we wanted to investigate whether environmental agents can activate mast cells, either via direct interaction with the mast cells, or via danger signals released from epithelial cells, and whether activated mast cells, via their release of mediators affect the barrier integrity for a possible contribution to the development of IIA.

A diverse set of environmental agents was chosen to study. Due to their unique platelet-like shape graphene (G) and graphene oxide (GO), can penetrate deep into the lungs and pose a possible risk for respiratory health[10,11]. Since the number of applications for these nanoparticles is firmly growing, we wanted to consider their irritant properties [12]. Exposure to combustion-derived particles, such as diesel exhaust particles (DEPs), is omnipresent in our current living environment. Various studies have shown that DEPs have immune modulating effects in allergic rhinitis and asthma [13–18]. DEPs also have irritant properties and have been reported as a cause of IIA, making this an interesting agent to study with respect to irritant-induced responses [19,20]. Chlorine is a widely used chemical irritant of which increased

exposure is associated with development of IIA [21–24]. In the current study, we investigated the interaction between the respiratory irritants and cells at the airway barrier in order to gain insight in the pathogenesis of IIA.

Materials and methods

Reagents

Dulbecco's Modified Eagle Medium (DMEM), Dulbecco's Modified Eagle Medium: Nutrient Mixture F-12 (DMEM/F12), Hank's Balanced Salt Solution (HBSS) without Ca^{2+} and Mg^{2+}, Dulbecco's phosphate buffered saline (DPBS) with Ca^{2+} and Mg^{2+}, penicillin-streptomycin, L-glutamine, amphotericin B, fetal calf serum (FCS) from Gibco™, Hyclone™ Iscove's Modified Dulbecco's Medium (IMDM) with L-glutamine and HEPES and PrestoBlue® cell viability reagent were all purchased via ThermoFisher (Göteborg, Sweden). Transwell® membrane inserts, 1-thioglycerol, WST-1 cell proliferation reagent and 4kDa size fluorescein isothiocyanate (FITC)-dextran were purchased from Sigma-Aldrich (Stockholm, Sweden).

Cell culture

The human bronchial epithelial cells were 16HBE14o- cells (16HBE), cultured in DMEM/F12 supplemented with 5% FCS, 100 U/ml penicillin, 100 U/ml streptomycin, 2mM L-glutamine and 2,5 µg/ml amphotericin. Human mast cell line-1 (HMC-1) cells were cultured in IMDM supplemented with 10% FCS, 100 U/ml penicillin, 100 U/ml streptomycin, 2mM L-glutamine, 2,5 µg/ml amphotericin and 1.2 mM α-thioglycerol. The cells were incubated at 37°C, in a humidified atmosphere containing 5% CO_2. When confluent the 16HBE cells were released enzymatically (0.05% trypsin-EDTA) and transferred to a new culture flask. The medium was renewed every 2-3 days.

Exposure conditions

The graphene nanoparticles (GNPs) were purchased from Graphene-supermarket.com and were the same as those used in chapter 3 of this dissertation. Graphene (G) has a lateral dimension of 2 to 8 µm and consists of 3 to 8 graphene monolayers based on the manufacturer's description. Graphene oxide (GO) has a flake size of 0.5 to 5 µm and consists for 80% of GO monolayers. Diesel exhaust particles (DEP) were obtained from the US National Institute of Standards and Technology (NIST-SRM2975, from forklift) and were fully characterized (https://nemo.nist.gov/srmors/view_detail.cfm?srm=2975). The GNPs and DEPs were weighed and dispersed in sterile water (Baxter) containing 2 vol% FCS (= dispersion medium) at a concentration of 2.56 mg/ml (GNPs) or 1mg/ml (DEP). These stock suspensions were dispersed using an ultrasonic cell disruptor (Vibra-cell VCX 130, Newtown, US), equipped with a disruptor horn, in a glass beaker on ice during 16 minutes at 730 watt. Intermediate concentrations were made in the dispersion medium and afterwards diluted 10-fold in the culture medium to obtain final concentrations. Household bleach with 2.6% active chlorine (Klorin Original) was used as hypochlorite solution (ClO^-) and dissolved in dispersion medium for intermediate solutions. Final concentrations were tenfold lower and prepared in culture medium, and expressed as

parts per million (ppm) of active chlorine (act. Cl) in the final solution. Ionomycin was purchased from ThermoFisher as ionomycin calcium salt and dissolved to a stock concentration in $HBSS^-$, and final concentrations were prepared in culture medium.

Cytotoxicity measurements

16HBE cells were seeded in a 96-well plate at a density of 200 000 cells/cm². The next day, the cells were rinsed with serum-free culture medium and subsequently exposed to increasing concentrations of G, GO, DEP or ClO^- for 24h. For WST-1 assay, the supernatant was removed, cells were washed and freshly diluted WST-1 reagent (1/20) was added. The cells were incubated for 1h and the absorbance was measured spectrophotometrically at wavelength 450nm. For PrestoBlue® assay, supernatant was removed, cells were washed and Presto Blue reagent (20µL) was added to the cells with fresh culture medium. The cells were incubated for 1h and fluorescence was measured with excitation and emission at respectively 560 and 590 nm.

Co-culture setup and exposure

In order to study the effect of environmental irritants on the epithelium and the interaction between epithelium and mast cells, three different seeding conditions were established. 16HBE cells were seeded as a monoculture on transwell inserts, to observe the effect on the epithelial barrier itself. HMC-1 cells were added in the basolateral compartment of the well with a 16HBE monolayer on the transwell insert, to mimic the normal *in vivo* situation. To simulate a situation of inflammation, where mast cells are recruited to the lumen of the lung, HMC-1 cells were added on top of the 16HBE monolayer in the transwell insert.

16HBE cells were seeded and grown on Transwell® inserts (0.4 µm pore density and 0.33 cm² surface area) until the transepithelial electrical resistance (TEER) reached at least 200 Ω.cm². Then, depending on the condition, HMC-1 cells were added to the basolateral compartment (16HBE/HMC-1 Basolateral) or to the apical compartment (HMC-1 Apical/16HBE) in a 1/10 ratio with 16HBE cells, or supplied with fresh medium (16HBE only). The medium in the co-cultures consisted of a mix of HMC-1 (1/10) and 16HBE (9/10) medium with 0.2% FCS. Twenty-four hours after addition of the HMC-1 cells (or vehicle for 16HBE only condition), co-cultures were exposed on the apical side of the transwell to 32 and 64 µg/mL G or GO, 5 and 25 µg/mL DEP, 3 and 30 ppm act. Cl, 1µg/mL ionomycin or fresh culture medium (Ctrl).

Measurement of the transepithelial electrical resistance (TEER)

The transepithelial electrical resistance (TEER) was measured using the Evom Voltohmmeter supplemented with the End-Ohm chamber or STX2 chopstick (World Precision Instruments Inc.). The resistance of a cell-free transwell insert was subtracted from the resistance measured across each cell layer to obtain the TEER value of the cell layers. Corrections for the surface area were made. Immediately before the exposure, TEER measurements of the co-cultures were made to serve as baseline values. TEER values were measured at 45 min, 1.5, 3, 6 and 24h after the start of exposure.

Paracellular flux of fluorescent labelled dextran

Twenty-four hours after the start of the exposure, supernatant of apical and basolateral compartment was removed and collected. The transwell inserts were placed in fresh culture medium and 1mg/mL FITC-dextran solution in culture medium was added to the apical compartment. After 4 hours of incubation at 37°C, triplicate basolateral samples were taken for assaying on a black 96-well plate. Fluorescence was measured using a fluorescence plate reader (Tecan Infinite M200Pro, Männedorf, Switzerland) with excitation and emission wavelengths of 485 nm and 530 nm, respectively. The flux or change in concentration was calculated by dividing the concentration and volume of the basolateral compartment with the concentration and volume of the apical compartment.

Qualitative cytokine determination

As a preliminary experiment to assess cytokine release towards the basolateral compartment of the transwell, supernatant of the basolateral compartment of the 16HBE/HMC-1 Basolateral culture was analyzed by a semiquantitative cytokine determination technique (Proteome Profiler, Human Cytokine Array Kit; R&D Systems Inc., Minneapolis, USA). The obtained autoradiographs were imaged and analyzed using ImageJ software. The relative density of each dot was calculated based on the internal controls on the membrane.

Quantitative cytokine determination

Cell culture supernatant and cell lysates of HMC-1 monocultures were collected after different incubation periods (15min, 45min, 1h30, 3h, 6h, 24h) of exposure to 32 and 64 µg/mL G or GO, 5 and 25 µg/mL DEP, 3 and 30 ppm act. Cl, 1µg/mL ionomycin or fresh culture medium (Ctrl), and stored at -80°C. Histamine was assayed in the undiluted sample collected after 15min of exposure with a histamine ELISA kit (Human his ELISA kit; Nordic BioSite AB, Täby, Sweden, limit of detection 1.563 ng/mL) according to the manufacturer's instructions. The samples collected after 6h and 24h of exposure were used undiluted to determine IL-6 and IL-8 via sandwich ELISA (ThermoFisher, limit of detection for both 2pg/mL) according to the manufacturer's recommendations.

16HBE monocultures were exposed to 32 and 64 µg/mL G or GO, 5 and 25 µg/mL DEP, 3 and 30 ppm act. Cl, 1µg/mL ionomycin or fresh culture medium (Ctrl) for different incubation periods (15min, 45min, 1h30, 3h, 6h, 24h) and supernatant was collected and stored (-80°C). Interleukin (IL)-1α, IL-33 and thymic stromal lymphopoietin (TSLP) release after 6h or 24h of exposure was determined via sandwich ELISA in undiluted samples (all Human Duoset ELISA, R&D Systems Inc., Minneapolis, USA, limit of detection respectively 7.81 pg/mL, 23.4 pg/mL and 31.2 pg/mL) according to the manufacturer's instructions.

Statistical analysis

The results are represented as mean ± SD or mean with individual values. Normality distribution was determined using the d'Agostino & Pearson omnibus normality test. When normally distributed, the data were analyzed with a one-way ANOVA followed by Dunnett's multiple-comparison test. When the data were not normal distributed, the Kruksal-Wallis test followed by a Dunn's multiple comparison test was used. Time series of the TEER measurements were analyzed with a two-way ANOVA (Graphpad Prism 5.00, Graphpad Software inc, San Diego, California, USA). A level of $p < 0.05$ was considered significant.

Results

Environmental irritants altered the epithelial barrier integrity, independently of the presence of HMC-1 cells

To determine relevant non-cytotoxic concentrations for the experiments to evaluate barrier integrity, WST-1 and Prestoblue assays were performed on 16HBE cells. Figure 1 shows that 24 hours of exposure to concentrations of 16 to 128 µg/mL of G and 5 to 100 µg/mL of DEP did not affect the cell viability in either of the assays. Starting from a concentration of 64 µg/mL of GO, a significant decrease in viability was observed with the WST-1 assay. The highest concentration of ClO^- destroyed most of the 16HBE cells.

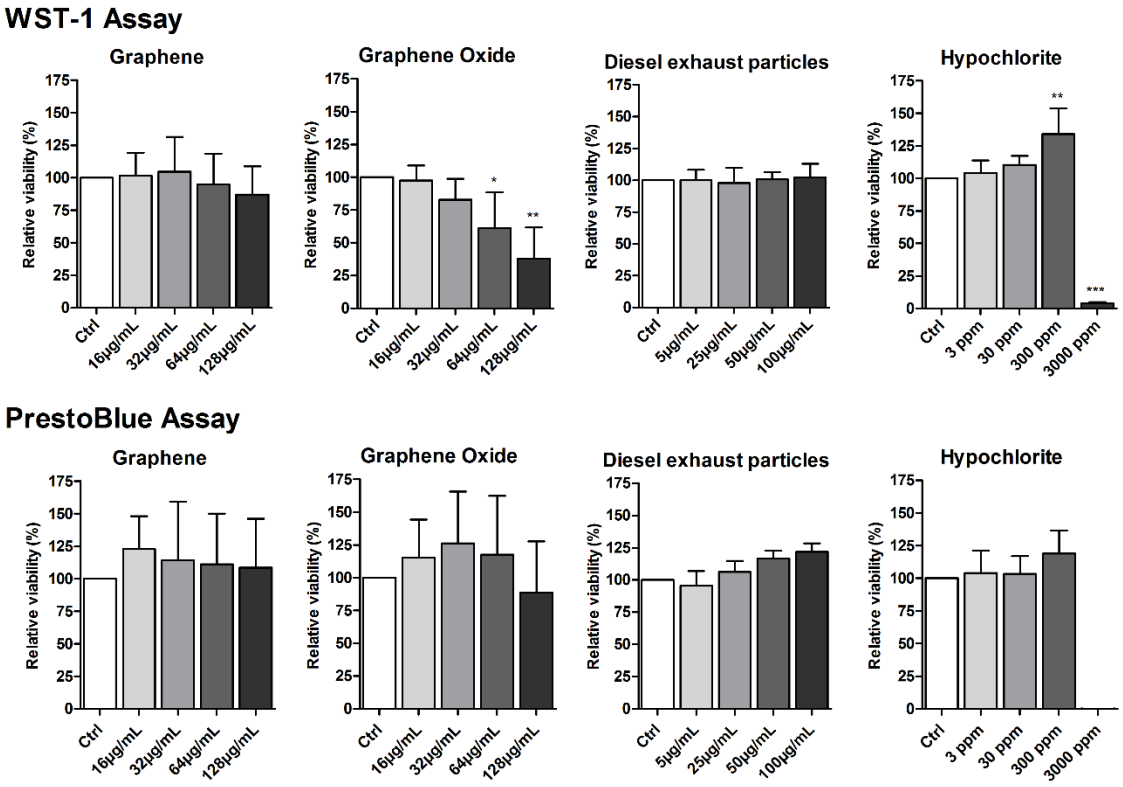

Figure 1. Relative viability of 16HBE cells exposed to increasing concentrations of G, GO, DEP and ClO^-
16HBE cells were exposed to increasing concentrations of the agents for 24 h. Afterwards the cell viability was evaluated using the WST-1 and PrestoBlue assay. *p<0.05, **p<0.01, ***p<0.001 compared to the vehicle control Mean ± SD, n=3-4.

Twenty-four hours after addition of the HMC-1 cells (or fresh medium for 16HBE only), cultures were exposed on the apical side of a transwell insert to 32 and 64 µg/mL G or GO, 5 and 25 µg/mL DEP or 3 and 30 ppm act Cl., or culture medium (Ctrl). As a measure of barrier integrity, TEER was determined before and at repeated time points (45 min, 1.5, 3, 6 and 24h) after start of the exposure in the different co-cultures (Fig. 2). In a culture of only 16HBE cells, a concentration of 32 and 64 µg/mL of G

and GO induced an immediate and persistent decrease in TEER compared to the vehicle control (Fig. 2a). The DEP concentration of 5 and 25 µg/mL induced an initial drop in the TEER-value, which returned nearly to baseline level within 24h of exposure. Exposure to 3 and 30ppm act. Cl in hypochlorite also resulted in a transient decrease in the TEER, which almost returned to the control level 24h after the start of the exposure. Adding HMC-1 cells to the basolateral compartment of the 16HBE culture resulted in similar changes in TEER (Fig. 2b). Exposure to any concentration of G and GO caused a persistently low TEER, while exposure to DEP and ClO^- only temporarily decreased the TEER. Co-culturing HMC-1's on top of the 16HBE similarly did not alter the response pattern compared to the 16HBE only condition (Fig. 2c). G and GO induced a permanently low TEER, while DEP and ClO^- induced a less strong and transient decrease in TEER compared to the vehicle control.

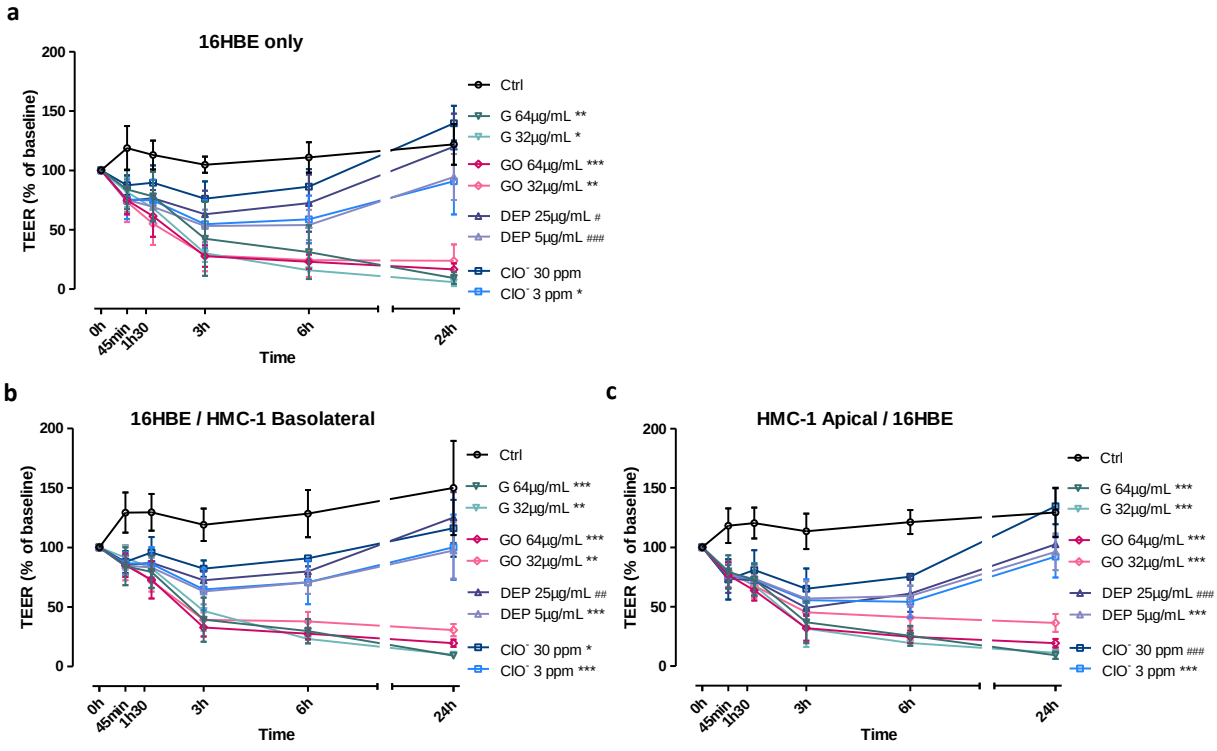

Figure 2. TEER changes over time in different seeding conditions
Cultures were exposed on the apical side of a transwell insert to 32 or 64µg/mL graphene (G) or graphene oxide (GO), 5 or 25 µg/mL diesel exhaust particles (DEP) or 3 or 30 ppm act. Cl in hypochlorite (ClO^-). TEER was measured afterwards at different time points (45min, 1h30min, 3h, 6h, 24h). Three different seeding conditions were used; only 16HBE seeded on an insert (16HBE only, a), 16HBE seeded on an insert and HMC-1 in basolateral compartment (16HBE / HMC-1 Basolateral, b) or 16HBE seeded on an insert and HMC-1 cells on the apical compartment (HMC-1 Apical / 16HBE, c). The TEER values are normalized and represented as percentages of the baseline value. Significant different at * all time points and # at some time points compared to the vehicle control. $p<0.05$: 1 symbol, $p<0.01$: 2 symbols, $p<0.001$: 3 symbols. Mean ± SD, n= 3-6.

Permeability of the epithelial barrier was determined by means of FITC-dextran (4kDa) transport, 24 hours after exposure to 32 and 64 µg/mL G or GO, 5 µg/mL DEP or 3 ppm act. Cl. In a culture with only 16HBE cells on the transwell insert, 24h of exposure to G induced a significant increase, and GO induced a non-significant increase in FD4-flux compared to the vehicle control (Fig. 3a). In the same co-culture, exposure of 5 µg/mL DEP and 3ppm act. Cl did not result in an increase in barrier permeability. If HMC-1 cells were added to the basolateral compartment of the 16HBE culture, G and GO induced similar changes in FD4-flux than on 16HBE cells only (Fig. 3b). Exposure to 5µg/mL DEP and 3ppm act. Cl did not alter the barrier permeability. Similarly, addition of HMC-1 cells to the apical compartment resulted in increased FD4-flux after exposure to G and GO, whereas DEP and ClO^- minimally altered the barrier permeability (Fig. 3c).

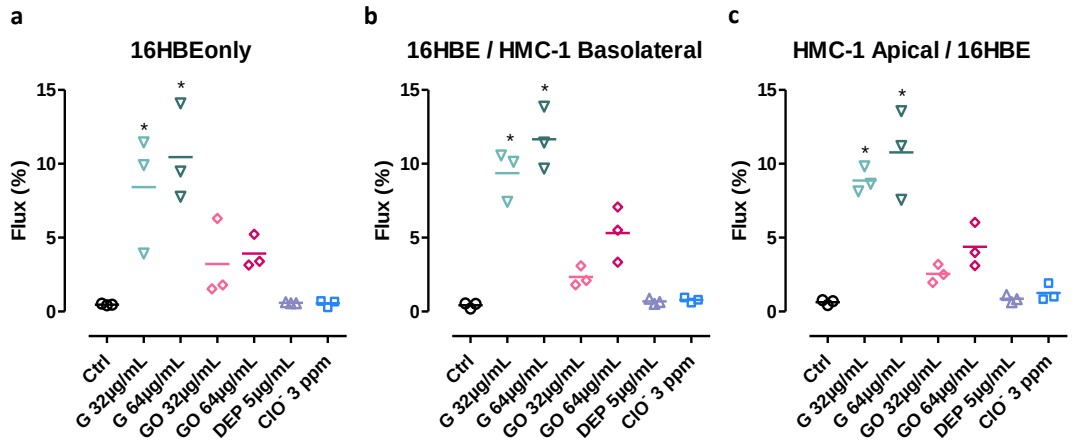

Figure 3. FITC-dextran flux after 24h of exposure in different seeding conditions
Cultures were exposed on the apical side of a transwell insert to 32 or 64µg/mL graphene (G) or graphene oxide (GO), 5 µg/mL diesel exhaust particles (DEP) or 3 ppm act. Cl in hypochlorite (ClO^-). FITC-dextran was added 24h after the start of the exposure (i.e. time point of last TEER measurement), and incubated for 4h to assess transport over the cell layer. Three different seeding conditions were used; only 16HBE seeded on an insert (16HBE only, a), 16HBE seeded on an insert and HMC-1 in basolateral compartment (16HBE / HMC-1 Basolateral, b) or 16HBE seeded on an insert and HMC-1 cells on the apical compartment (HMC-1 Apical /16HBE, c)* $p<0.05$, ** $p<0.01$ compared to the vehicle control. Mean ± individual values, n= 3.

Environmental irritants did not stimulate 16HBE and HMC-1 cells

Semi-quantitative analysis of the basolateral sample of irritant-exposed co-cultures for presence of cytokines, indicated that very limited amount of cytokines were released towards the basolateral side of the cell layer (Suppl. Fig. 1). The danger signals IL-33 and TSLP were not detectable in the supernatant of 16HBE monocultures collected after 6 and 24 hours of exposure to the environmental agents. After 24 hours of exposure, IL-1α release was low and did not differ between the different exposure conditions (generally a release of around 20 pg/mL – data not shown). IL-1α was undetectable in the supernatant collected after 6 hours of exposure.

Determination of histamine in supernatant and lysate of HMC-1 cells exposed for 15 min to irritants yielded values under the limit of detection (data not shown). HMC-1 cells did not release or produced IL-6 and IL-8 after 24 hours of exposure to irritants (values under the limit of detection).

The mast cell activator ionomycin had a minimal effect on the HMC-1 cells

The cell cultures were exposed apically to 1 µg/mL of the calcium ionophore ionomycin, which is a selective mast cell activator. According to the WST-1 assay, this concentration is between one that stimulated proliferation of the 16HBE cells, and one that induced strong cellular toxicity (Suppl. Fig. 2). TEER measurement in a culture with only 16HBE cells at different time points after the start of the exposure indicates that there was an initial increase in TEER due to ionomycin exposure, which decreases again to baseline level after 24 hours (Fig. 4a). With HMC-1 cells in the basolateral compartment or apical compartment in 1/10 ratio with 16HBE cells, the TEER pattern after ionomycin exposure remained the same (Fig. 4b and c). Twenty-four hours after exposure to 1µg/mL ionomycin, FITC-dextran transport did not differ compared to the vehicle control in either of the culture conditions (Fig. 5).

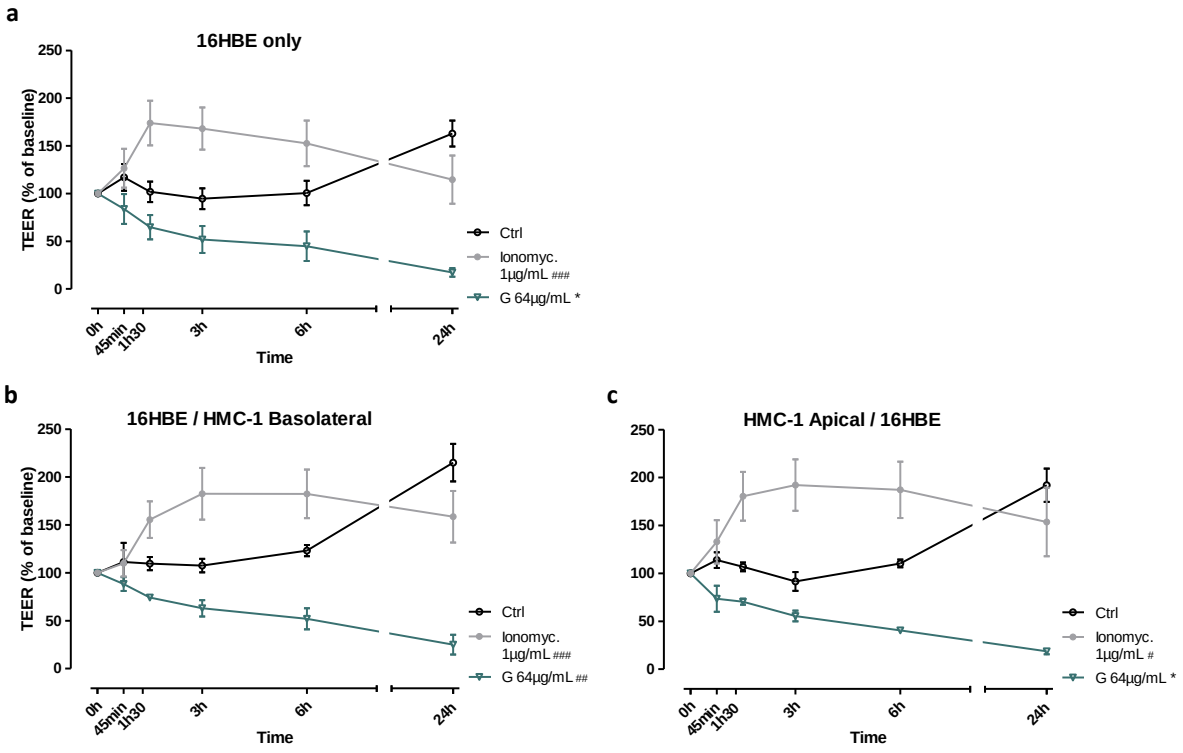

Figure 4. TEER changes over time in different seeding conditions
Cultures were exposed on the apical side of a transwell insert to 1µg/mL ionomycin or 64µg/mL graphene (G). TEER was measured afterwards at different time points (45min, 1.30, 6, 6 and 24h). Three different seeding conditions were used; only 16HBE seeded on an insert (16HBE only, a), 16HBE seeded on an insert and HMC-1 in basolateral compartment (16HBE / HMC-1 Basolateral, b) or 16HBE seeded on an insert and HMC-1 cells on the apical compartment (HMC-1 Apical / 16HBE, c). Significant different at * all time points and # at some time points compared to the vehicle control. p<0.05: 1 symbol, p<0.01: 2 symbols, p<0.001: 3 symbols. Mean ± SD, n= 4-5.

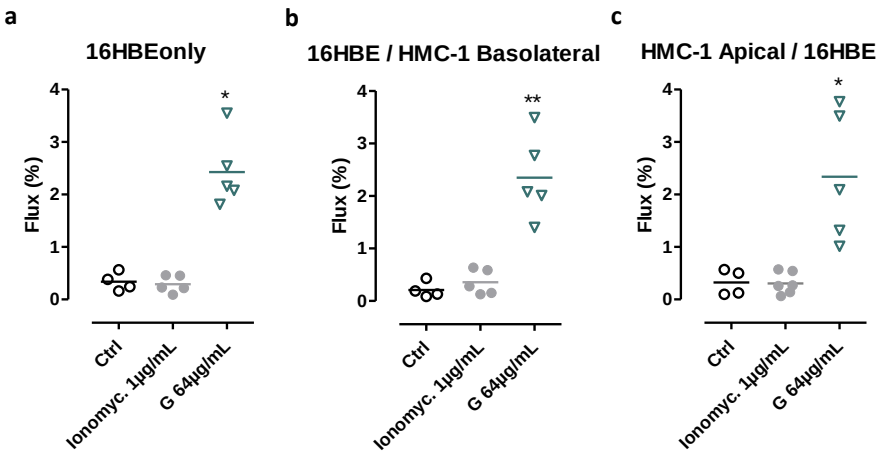

Figure 5. FITC-dextran flux after 24h of exposure in different seeding conditions
Cultures were exposed on the apical side of a transwell insert to 1µg/mL ionomycin or 64µg/mL graphene (G). FITC-dextran was added 24h after the start of the exposure (i.e. time point of last TEER measurement), and incubated for 4h to assess transport over the cell layer. Three different seeding conditions were used; only 16HBE seeded on an insert (16HBE only, a), 16HBE seeded on an insert and HMC-1 in basolateral compartment (16HBE / HMC-1 Basolateral, b) or 16HBE seeded on an insert and HMC-1 cells on the apical compartment (HMC-1 Apical /16HBE, c)* $p<0.05$, ** $p<0.01$ compared to the vehicle control. Mean ± individual values, n= 4-5.

Histamine determination, to assess mast cell degranulation, in supernatant and lysate of HMC-1 cells exposed for 15 min to 1µg/mL ionomycin, resulted in values under the limit of detection (data not shown). After exposure to 1µg/mL ionomycin for 24h, IL-8 and IL-6 were present in the supernatant (resp. 96.08 ± 1.87 pg/mL and >100pg/mL) and the lysate (resp. 69.13 ± 0.39 pg/mL and 9.91 ± 2.78 pg/mL) of the HMC-1 cells.

Discussion

In this study, we investigated the effect of environmental agents on the epithelial barrier and their interaction with mast cells, to investigate the possible contribution in the development of IIA. In a monoculture of 16HBE cells, sub-toxic concentrations of G and GO induced a persistent decrease in TEER, whereas sub-toxic concentrations of DEP and ClO^- induced a transient decrease in TEER. Contrary to our expectations, adding HMC-1 cells on the basolateral or apical side of the 16HBE monolayer, resulted in similar changes in TEER upon irritant-exposure. In line with the TEER measurements, FITC-dextran transport was elevated 24 hours after start of the exposure to G and GO, and was equal to the control for exposure to DEP and ClO^-, in each of the tested seeding conditions. The Ca^{2+} ionophore ionomycin transiently increased the epithelial barrier properties (increase in TEER, equal FD4-flux), independently of the presence of mast cells. To study mast cell activation after environmental exposures, histamine release was determined on HMC-1 monocultures, but this was absent after all exposures. Release of the pro-inflammatory cytokines IL-6 and IL-8 was only present in ionomycin-exposed HMC-1 cells. 16HBE cells did not release signals of inflammation or danger upon irritant- and ionomycin-exposure, as evaluated by qualitative and IL-1α, IL-33 and TSLP specific assays.

The environmental agents used in our experiments clearly altered epithelial barrier functioning. On a monolayer of 16HBE cells, exposure to the nanoparticles G and GO resulted in a persistent impairment of the barrier, whereas exposure to DEP and ClO^- resulted in an initial decreased barrier function, which recovered within 24h. This indicates that depending on the irritant agent, different mechanisms cause barrier impairment. Altered epithelial barrier functioning due to irritant-induced tissue injury, such as exposure to ozone, ambient particulate matter and diesel exhaust, has been previously described [25]. Mast cells have the ability to sense tissue damage via recognition of danger signals released from injured cells [9]. These alarmins, such as IL-1α, IL-33 and TSLP, can activate mast cells [26–28] . In the current study, the level of IL-1α, IL-33 and TSLP in supernatants of 16HBE monocultures was not changed after environmental exposure. Absence of these alarmins proved that no extensive damage was caused by the tested concentrations of the irritants, as also shown by the viability assays on 16HBE monocultures. Consistent with this data, mast cell activation via signals derived from the irritant-exposed epithelium was absent in the co-culture experiments.

In order to study mast cell activation upon G, GO, DEP and ClO^- exposure, histamine, a biogenic amine stored in secretory granules of the mast cell, was determined in HMC-1 supernatant. In none of the tested conditions, histamine was present. Mast cell activation not only involves mast cell degranulation, but also includes production of various pro-inflammatory cytokines, including IL-6 and IL-8 [7,29]. However, we did not detect IL-6 or IL-8 release from irritant-exposed HMC-1 cells. A few

studies have described mast cell activation by chemicals (e.g. ammonium persulfate [30]), metals (e.g. silver [31]) or air pollution (e.g. acrolein [32], sodium sulfite [33] and DEP [18]). As a common pathway, these agents induced reactive oxygen species (ROS) in the mast cells, which modifies the phosphorylation status of key proteins in mast cell signaling, which results in mast cell degranulation and cytokine production [34]. It cannot be ruled out that G, GO, DEP and ClO^- induced ROS in the HMC-1 cell, yet this clearly did not cause mast cell activation in the current experiment.

The absence of a mast cell response upon environmental exposure is probably due to the specific mast cell line that we used. HMC-1 cells are the first reported stable human mast cell line, derived in 1988 from peripheral blood of a patient with mast cell leukemia [35]. HMC-1 cells however, represent an immature type of mast cells, since they contain only moderate amounts of histamine, do not express functional FcεRI and thus fail to respond to IgE, and have reduced levels of trypase [35–37]. Morphologically HMC-1 contain a limited amount of granules, which not resemble those in mature mast cells [35]. In our experiments, we did not find histamine or the pro-inflammatory cytokines IL-6 and IL-8 in the supernatants of irritant-exposed HMC-1 cells. The fact that stimulation with the Ca^{2+} ionphore ionomycin, also failed to induce histamine release, suggests that the unresponsiveness of HMC-1 cells upon environmental exposure could partly be due to their immaturity. IL-6 and IL-8 release did occur after 24 hours of stimulation with ionomycin, this (and previous reports) indicates that the HMC-1 cell can respond to mast cell activators, by initiating cytokine production [36,38–40]. Other models for human mast cells are the mast cell lines LAD2, LUVA, ROSA $^{KIT\ WT}$ (which all have their own advantages and drawbacks) or primary human mast cells derived from tissue, blood or bone marrow [41–44]. Based on our findings, environmental agents do not affect mast cell responses, however, we cannot exclude that other responses could be observed using another mast cell model.

This study demonstrates that the environmental irritants G, GO, DEP and ClO^- alter the epithelial barrier function via different mechanisms. Addition of mast cells to mimic either a healthy state or diseased state at the epithelial barrier did not alter the response pattern. Upon exposure to environmental irritants, the 16HBE cells were not stimulated to release danger signals that could influence surrounding immune cells. The environmental irritants their selves had no effect on mast cell activation, which can be due to the immature state of the HMC-1 mast cell line. To conclude, in the current study we found that environmental agents do not directly or indirectly, activate mast cells. Due to the inactivated (or immature) state of the mast cells, these did not influence the epithelial barrier integrity upon environmental exposure, and thus currently do not provide additional information for the underlying mechanism of IIA.

Acknowledgments: This project was partly executed at SweTox, Södertälje, Sweden in the view of a Junior Mobility program grant received from the University of Leuven Research Council (JUMO/16/056). This project was further supported by a grant from the University of Leuven Research Council (GOA/14/011).

Conflict of interest: The authors declare no conflict of interest.

Supplementary figures

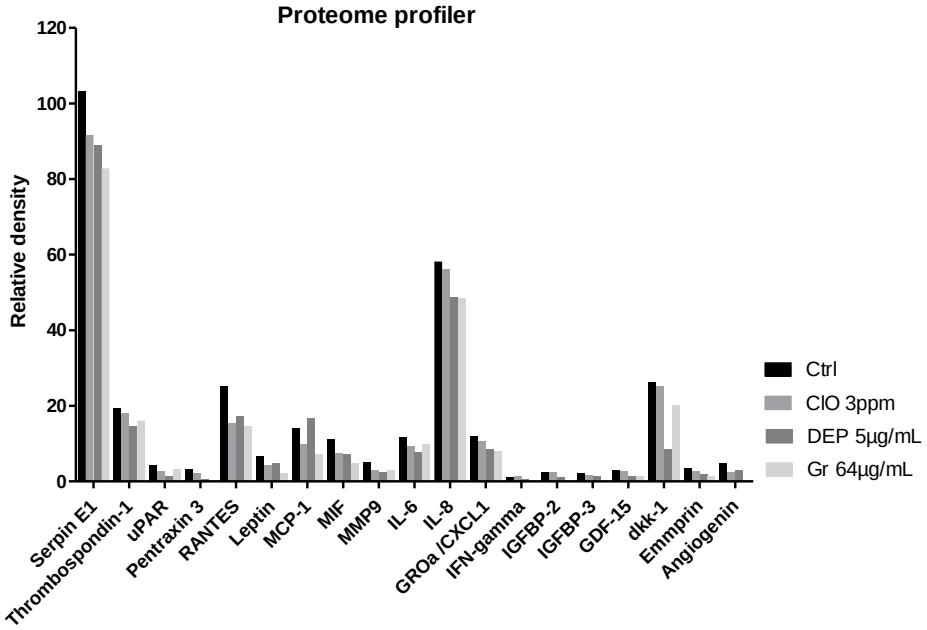

Supplementary Figure 1. Qualitative determination of cytokines
Cytokines were determined in supernatant of basolateral compartment of 16HBE/HMC-1 co-culture exposed for 24h to vehicle, 3ppm of act. Cl, 5 µg/mL DEP and 64 µg/mL G, with a proteome array. The graph demonstrates the calculated density per cytokine on the scanned autoradiographs.

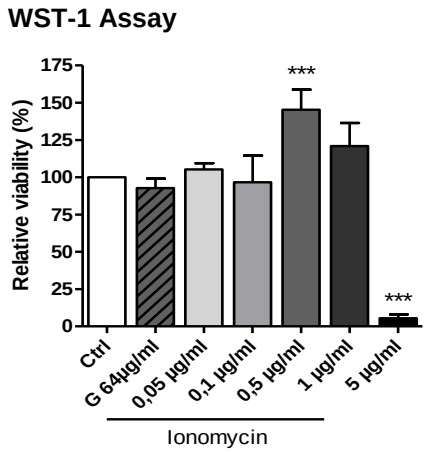

Supplementary Figure 2. Viability of 16HBE cells exposed to increasing concentrations of Ionomycin
16HBE cells were exposed to increasing concentrations of ionomycin for 24 h. Afterwards the cell viability was evaluated using the WST-1 assay. 16HBE cells were exposed to 64 µg/mL graphene as a reference agent. ***p<0.001compared to the vehicle control. Mean ± SD, n= 4.

References

1. Guarnieri, M. & Balmes, J. R. Outdoor air pollution and asthma. *Lancet Lond. Engl.* **383,** 1581–1592 (2014).
2. Dumas, O. *et al.* Occupational irritants and asthma: an Estonian cross-sectional study of 34,000 adults. *Eur. Respir. J.* **44,** 647–656 (2014).
3. Holgate, S. T. *et al.* Asthma. *Nat. Rev. Dis. Primer* **1,** 15025 (2015).
4. Brooks, S. M., Weiss, M. A. & Bernstein, I. L. Reactive airways dysfunction syndrome (RADS). Persistent asthma syndrome after high level irritant exposures. *Chest* **88,** 376–384 (1985).
5. Vandenplas, O. *et al.* EAACI position paper: irritant-induced asthma. *Allergy* **69,** 1141–1153 (2014).
6. Brooks, S. M. & Bernstein, I. L. Irritant-Induced Airway Disorders. *Immunol. Allergy Clin. North Am.* **31,** 747–768 (2011).
7. Moon, T. C., Befus, A. D. & Kulka, M. Mast cell mediators: their differential release and the secretory pathways involved. *Front. Immunol.* **5,** 569 (2014).
8. Barnes, P. J. Cellular and molecular mechanisms of asthma and COPD. *Clin. Sci. Lond. Engl. 1979* **131,** 1541–1558 (2017).
9. Redegeld, F. A., Yu, Y., Kumari, S., Charles, N. & Blank, U. Non-IgE mediated mast cell activation. *Immunol. Rev.* **282,** 87–113 (2018).
10. Sanchez, V. C., Jachak, A., Hurt, R. H. & Kane, A. B. Biological Interactions of Graphene-Family Nanomaterials: An Interdisciplinary Review. *Chem. Res. Toxicol.* **25,** 15–34 (2012).
11. Su, W.-C., Ku, B.-K., Kulkarni, P. & Cheng, Y. S. Deposition of Graphene Nanoparticles in Human Upper Airways. *J. Occup. Environ. Hyg.* **13,** 48–59 (2016).
12. Arvidsson, R., Molander, S. & Sandén, B. A. Review of Potential Environmental and Health Risks of the Nanomaterial Graphene. *Hum. Ecol. Risk Assess. Int. J.* **19,** 873–887 (2013).
13. Maes, T. *et al.* Mouse models to unravel the role of inhaled pollutants on allergic sensitization and airway inflammation. *Respir. Res.* **11,** 7 (2010).
14. Diaz-Sanchez, D., Tsien, A., Fleming, J. & Saxon, A. Combined diesel exhaust particulate and ragweed allergen challenge markedly enhances human in vivo nasal ragweed-specific IgE and skews cytokine production to a T helper cell 2-type pattern. *J. Immunol. Baltim. Md 1950* **158,** 2406–2413 (1997).
15. Saxon, A. & Diaz-Sanchez, D. Air pollution and allergy: you are what you breathe. *Nat. Immunol.* **6,** 223–226 (2005).
16. Provoost, S. *et al.* Diesel exhaust particles stimulate adaptive immunity by acting on pulmonary dendritic cells. *J. Immunol. Baltim. Md 1950* **184,** 426–432 (2010).
17. De Grove, K. C. *et al.* Dysregulation of type 2 innate lymphoid cells and TH2 cells impairs pollutant-induced allergic airway responses. *J. Allergy Clin. Immunol.* **139,** 246–257.e4 (2017).
18. Diaz-Sanchez, D., Penichet-Garcia, M. & Saxon, A. Diesel exhaust particles directly induce activated mast cells to degranulate and increase histamine levels and symptom severity. *J. Allergy Clin. Immunol.* **106,** 1140–1146 (2000).
19. Adewole, F., Moore, V. C., Robertson, A. S. & Burge, P. S. Diesel exhaust causing low-dose irritant asthma with latency? *Occup. Med. Oxf. Engl.* **59,** 424–427 (2009).
20. Deering-Rice, C. E. *et al.* Electrophilic components of diesel exhaust particles (DEP) activate transient receptor potential ankyrin-1 (TRPA1): a probable mechanism of acute pulmonary toxicity for DEP. *Chem. Res. Toxicol.* **24,** 950–959 (2011).
21. White, C. W. & Martin, J. G. Chlorine gas inhalation: human clinical evidence of toxicity and experience in animal models. *Proc. Am. Thorac. Soc.* **7,** 257–263 (2010).
22. Hoyle, G. W. & Svendsen, E. R. Persistent effects of chlorine inhalation on respiratory health. *Ann. N. Y. Acad. Sci.* (2016). doi:10.1111/nyas.13139
23. Evans, R. B. Chlorine: state of the art. *Lung* **183,** 151–167 (2005).
24. Bernard, A. Chlorination products: emerging links with allergic diseases. *Curr. Med. Chem.* **14,** 1771–1782 (2007).
25. Rezaee, F. & Georas, S. N. Breaking Barriers. New Insights into Airway Epithelial Barrier Function in Health and Disease. *Am. J. Respir. Cell Mol. Biol.* **50,** 857–869 (2014).
26. Lunderius-Andersson, C., Enoksson, M. & Nilsson, G. Mast Cells Respond to Cell Injury through the Recognition of IL-33. *Front. Immunol.* **3,** (2012).
27. Nagarkar, D. R. *et al.* Airway epithelial cells activate TH2 cytokine production in mast cells through IL-1 and thymic stromal lymphopoietin. *J. Allergy Clin. Immunol.* **130,** 225–232.e4 (2012).
28. Bradding, P. & Arthur, G. Mast cells in asthma – state of the art. *Clin. Exp. Allergy* **46,** 194–263 (2016).

29. Mukai, K., Tsai, M., Saito, H. & Galli, S. J. Mast cells as sources of cytokines, chemokines, and growth factors. *Immunol. Rev.* **282,** 121–150 (2018).
30. Pignatti, P. *et al.* Oxidative activity of ammonium persulfate salt on mast cells and basophils: implication in hairdressers' asthma. *Int. Arch. Allergy Immunol.* **160,** 409–419 (2013).
31. Yoshimaru, T., Suzuki, Y., Inoue, T., Niide, O. & Ra, C. Silver activates mast cells through reactive oxygen species production and a thiol-sensitive store-independent Ca2+ influx. *Free Radic. Biol. Med.* **40,** 1949–1959 (2006).
32. Hochman, D. J., Collaco, C. R. & Brooks, E. G. Acrolein induction of oxidative stress and degranulation in mast cells. *Environ. Toxicol.* **29,** 908–915 (2014).
33. Collaco, C. R., Hochman, D. J., Goldblum, R. M. & Brooks, E. G. Effect of sodium sulfite on mast cell degranulation and oxidant stress. *Ann. Allergy Asthma Immunol. Off. Publ. Am. Coll. Allergy Asthma Immunol.* **96,** 550–556 (2006).
34. Frossi, B., Rivera, J., Hirsch, E. & Pucillo, C. Selective activation of Fyn/PI3K and p38 MAPK regulates IL-4 production in BMMC under nontoxic stress condition. *J. Immunol. Baltim. Md 1950* **178,** 2549–2555 (2007).
35. Butterfield, J. H., Weiler, D., Dewald, G. & Gleich, G. J. Establishment of an immature mast cell line from a patient with mast cell leukemia. *Leuk. Res.* **12,** 345–355 (1988).
36. Möller, A. *et al.* Human mast cells produce IL-8. *J. Immunol. Baltim. Md 1950* **151,** 3261–3266 (1993).
37. Guhl, S., Babina, M., Neou, A., Zuberbier, T. & Artuc, M. Mast cell lines HMC-1 and LAD2 in comparison with mature human skin mast cells--drastically reduced levels of tryptase and chymase in mast cell lines. *Exp. Dermatol.* **19,** 845–847 (2010).
38. Kandere-Grzybowska, K. *et al.* IL-1 induces vesicular secretion of IL-6 without degranulation from human mast cells. *J. Immunol. Baltim. Md 1950* **171,** 4830–4836 (2003).
39. Zhao, Y. *et al.* Inhibitory effects of budesonide, desloratadine and dexamethasone on cytokine release from human mast cell line (HMC-1). *Inflamm. Res.* **53,** 664–669 (2004).
40. Meade, C. J., Worrall, L., Hayes, D. & Protin, U. Induction of interleukin 8 release from the HMC-1 mast cell line: synergy between stem cell factor and activators of the adenosine A(2b) receptor. *Biochem. Pharmacol.* **64,** 317–325 (2002).
41. Laidlaw, T. M. *et al.* Characterization of a novel human mast cell line that responds to stem cell factor and expresses functional FcεRI. *J. Allergy Clin. Immunol.* **127,** 815-822–5 (2011).
42. Kirshenbaum, A. S. *et al.* Characterization of novel stem cell factor responsive human mast cell lines LAD 1 and 2 established from a patient with mast cell sarcoma/leukemia; activation following aggregation of FcepsilonRI or FcgammaRI. *Leuk. Res.* **27,** 677–682 (2003).
43. Saleh, R. *et al.* A new human mast cell line expressing a functional IgE receptor converts to tumorigenic growth by KIT D816V transfection. *Blood* **124,** 111–120 (2014).
44. Arock, M., Le Nours, A., Malbec, O. & Daëron, M. Ex vivo and in vitro primary mast cells. *Methods Mol. Biol. Clifton NJ* **415,** 241–254 (2008).

Chapter 5

Irritant-induced asthma to hypochlorite in mice due to impairment of the airway barrier

Sofie Van Den Broucke, Lore Pollaris, Anne-Charlotte Jonckheere, Tatjana Decaesteker, Jonathan Cremer, Greetje Vande Velde, Erik Verbeken, Benoit Nemery, Jeroen Vanoirbeek, Peter Hoet

Based on:
Irritant-induced asthma to hypochlorite in mice due to impairment of the airway barrier. *Archives of Toxicology*, January 2018; 92 (4):1551-1561

Abstract

Inhalation of commonly present irritants, such as chlorine and chlorine derivatives, can cause adverse respiratory effects, including irritant-induced asthma (IIA). We hypothesize that due to airway barrier impairment, exposure to hypochlorite (ClO^-) can result in airway hypersensitivity.

C57Bl/6 mice received an intra-peritoneal (i.p.) injection of the airway damaging agent naphthalene (NA, 200 mg/kg body weight) or vehicle (mineral oil, MO). *In vivo* micro-computed tomography (CT) images of the lungs were acquired before and at regular time points after the i.p. treatment. After a recovery period of 14 days an intranasal (i.n.) challenge with 0.003% active chlorine (in ClO^-) or vehicle (distilled water, H_2O) was given, followed by assessment of the breathing frequency. One day later, pulmonary function, along with pulmonary inflammation was determined. Lung permeability was assessed by means of total broncho-alveolar lavage (BAL) protein content and plasma surfactant protein (SP) D levels. Dendritic cells (DC) and innate lymphoid cells (ILC) were assessed in the lungs.

In vivo micro-CT imaging revealed enlargement of the lungs and airways early after NA treatment, with a return to normal at day 14. When challenged i.n. with ClO^-, NA-pretreated mice immediately responded with a sensory irritant response. Twenty-four hours later, NA/ClO^- mice showed airway hyperreactivity (AHR), accompanied by a neutrophilic and eosinophilic inflammation. NA administration followed by ClO^- induced airway barrier impairment, as shown by increased broncho-alveolar lavage (BAL) protein and plasma surfactant protein (SP)-D concentrations; histology revealed epithelial denudation. Moreover, the NA-induced barrier impairment resulted in recruitment of monocyte-derived DCs (moDC) to the lung and an additional insult with ClO^- upregulated the pulmonary ILC 2 population.

These data proves that NA-induced lung impairment renders the lungs of mice more sensitive to an airway challenge with ClO^-, confirming the hypothesis that incomplete barrier repair, followed by irritant exposure results in airway hypersensitivity.

Introduction

The airway epithelium forms the primary interface with the outside environment and is, therefore, the first target site for injury after exposure to noxious agents, including chemical irritants and particulate matter. Airway epithelial cells form a tight protective barrier, preventing penetration of harmful agents to the host [1]. Dysfunction of the airway barrier has been described in a number of respiratory diseases, such as chronic obstructive pulmonary disease (COPD), rhinitis and asthma [2–7]. In addition, exposure to agents affecting the airway barrier has been associated with increased risk for asthma exacerbations[8].

Chlorine is a widely used chemical irritant, occurring in different industrial setting, such as pulp and paper mills where it is used as bleaching agent; in swimming pools, predominantly for disinfection; and at home, as cleaning agent [9,10]. When added to water, chlorine (Cl_2) rapidly converts to hypochlorous acid (HOCl) and the reactive anion hypochlorite (ClO^-). Chlorine inhalation can damage the airway mucosa and results in wheezing, cough and dyspnea. Acute symptoms following high dose exposure include pulmonary edema, temporary airflow dysfunction and adult respiratory distress syndrome (ARDS). Moreover, airway hyperreactivity (AHR) can arise and persist, making chlorine an important cause of reactive airways dysfunction syndrome (RADS), which is a respiratory condition defined by sudden occurrence of asthma-like symptoms within 24 hours after exposure to a single, high concentration of an irritant agent [11–13]. Moreover, repeated exposure to lower levels of irritants, including chlorine, may also lead to asthmatic symptoms developed after a latency period. This type of asthma is defined as irritant-induced asthma (IIA) and arises without immunologic sensitization to the causal agent [14]. Up to date, the underlying mechanism of IIA remains largely unknown, yet increased airway permeability has been suggested as a contributor to development of the hypersensitivity [15,16].

Administration of naphthalene (NA) in mice has been put forward as a well-established model of airway epithelial damage and repair [17–19]. The toxicity of NA depends on metabolic activation to a reactive epoxide intermediate by cytochrome P450 (CYP) monooxygenases. In mouse lungs, the non-ciliated bronchiolar (club) cells are the main cellular site of CYP2F2, the CYP enzyme responsible for NA metabolization [19–21]. Since club cells are the predominant epithelial cells present in the distal airways of mice, NA administration is a highly effective approach to induce selective damage to the distal airways in mice.

In this study, we used the NA model to damage the respiratory barrier and allowed repair of the barrier for 14 days. Subsequently, we exposed mice with a seemingly intact epithelial barrier to a common environmental irritant hypochlorite (ClO^-) via the airways. Hereby, we aim to mimic human accidental

exposures to high levels of damaging compounds (e.g. accidental spills in the workplace), followed by daily-life exposures to irritant chemicals. Our hypothesis is that due to the incomplete repair increased airway permeability develops, after which airway exposure to non-irritant concentrations of hypochlorite will result in increased airway sensitivity, as in IIA.

Materials and methods

A complete description of the materials and methods is available in the supplement.

Animals and treatment protocol

Seven-week old male C57Bl/6J mice were obtained from Envigo (Horst, The Netherlands) and were housed in a conventional animal house with 12h dark/light cycles. They were kept in individually ventilated cages (IVC) and received lightly acidified water and pelleted food *ad libitum*. The Animal Ethics Committee of the University of Leuven approved all experimental procedures (Project N°. P236-2014).

Preliminary experiment

A preliminary study was performed in order to validate and characterize the mouse model of induced airway barrier impairment, in which an intra-peritoneal (i.p.) injection with naphthalene (NA) in a dose of 200 mg/kg body weight (BW) is mostly used and proved to target the bronchioles in mice [18]. Therefore C57Bl/6 mice received 200 mg/kg body weight (BW) of NA dissolved in mineral oil (MO, vehicle) (10mL/kg BW) or vehicle only (10 mL/kg) with an i.p. injection on day 0 and were scarified 1, 2, 3, 7, 14 or 21 days later. Body weight was recorded before (day 0) and at regular time points until the sacrifice. On the day of sacrifice blood, broncho-alveolar lavage (BAL) fluid and lung tissue were collected.

Full experiment

Based on the preliminary, a combination protocol was conducted. On day 0, C57Bl/6 mice were injected i.p. with NA in a dose of 200 mg/kg BW dissolved in MO (vehicle) (10 mL/kg BW) or vehicle only (10 mL/kg BW). Before the start of the treatment (day -1) and at different time points after the NA administration (day 1, 4, 7, 10, 13), micro-CT images of the mice lungs were generated. On day 14, the mice received an intranasal (i.n.) instillation (40µL) with 0.003% active chlorine (dosed as sodium hypochlorite in distilled water) or distilled water (H_2O). The administered concentration of chlorine is tenfold higher than the concentration found in public swimming pool water (3ppm). The early ventilatory response was recorded immediately following the i.n. challenge. One day later, lung function was assessed followed by an autopsy to collect blood, BAL fluid and lung tissue.

Four different treatment groups were included: MO/H_2O, MO/ClO^-, NA/H_2O, NA/ClO^-. The first abbreviation refers to the i.p. injection on day 0, being mineral oil (MO) or naphthalene (NA) and the second abbreviation refers to the i.n. challenge on day 14, including distilled water (H_2O) or hypochlorite (ClO^-).

Efficacy of the NA-treatment was evaluated based on the body weight of the mice. It was anticipated that if mice did not show a 10% decrease in body weight the i.p. injection with NA was not successful and thus a NA-dependent response could not be expected. This was confirmed by fewer alterations in the airways and lungs as observed on the longitudinal micro-CT images for these animals. These mice were therefore excluded from the dataset.

Lung imaging and image analysis and quantification

To acquire the *in vivo* lung micro-CT scans, mice were anesthetized with 1.5-2 % isoflurane in 100% oxygen. Micro-CT images of free-breathing animals were obtained using a small-animal micro-CT scanner (SkyScan 1278, Bruker microCT, Kontich, Belgium) according to a previously validated scan protocol [22]. The respiratory-gated four-dimensional micro-CT data were retrospectively gated, reconstructed, visualized and processed to quantify the images (TSort, NRecon, DataViewer, CTan, ImageJ).

Early ventilatory response

The breathing frequency of the mice was recorded 5 min before (baseline measurement) and 60 min after the i.n. instillation in a double chamber plethysmograph (DCP) (EMKA Technologies, Paris, France).

Pulmonary function

The pulmonary function was measured 24h after the i.n. instillation using the flexiVent™ FX system (SCIREC, Montreal, Canada), as described previously [23]. Briefly, airway reactivity (Newtonian resistance, Rn) was assessed using a forced oscillation perturbation 'Quick prime-3' (QP-3) and forced expiratory volumes (forced vital capacity, FVC and forced expiratory volume in 0.1 seconds, $FEV_{0.1}$) were determined using a negative pressure-driven forced expiratory volume (NPFE) perturbation. Parameters were acquired before (baseline) and after nebulization of increasing concentrations of methacholine (Mch, 0-40 mg/mL).

Inflammatory, permeability and histopathological determinations

Immediately after the lung function measurements, plasma was collected to measure surfactant protein (SP) D concentration by ELISA in a 1 in 4 dilution (Duoset ELISA R&D Systems Inc., DY6839-05, limit of detection 62.5µg/mL) according to the manufacturers' instructions. The left lung was clamped, collected and weighed to obtain dry/wet weight ratio. The right lung was lavaged and the collected fluid was analyzed for total and differential cell counts. Protein concentration was determined on the cell-free BAL supernatant using the Bradford method. Histology was performed on the right lung after fixation with 4% paraformaldehyde.

Lung single cell suspension and flow cytometry

After rinsing the pulmonary circulation, the lungs of the mice were collected, minced and incubated for 45 min at 37°C in digestion medium. Red blood cells were lysed with ammonium chloride buffer.

For dendritic cell (DC) staining, two million cells were preincubated with anti-CD16/CD32 and stained with the Zombie Aqua™Fixable Viability Kit. Combinations of anti-mouse fluorochrome-conjugated mAbs against CD45, CD11c, MHC II, CD11b, CD103, CD64 and Siglec-H were used to label the cells. A representative gating for the DCs is shown in supplementary figure 3. For innate lymphoid cell (ILC) staining, four million cells were stained Fixable Viability Dye eFluor™ 780 and preincubated with anti-CD16/CD32. Combinations of anti-mouse fluorochrome-conjugated mAbs against CD45, CD127, CD117, CD90.2, KLGR-1, NK1.1, CD11b, CD19, CD3e, CD45RB, CD5, CD94, Gr-1, TCRγδ and Ter-119 were used to label the cells. Supplementary figure 4 demonstrates a representative gating for the ILCs. Data acquisition was performed on a LSR Fortessa flow cytometer running DIVA software (BD Biosciences, Erembodegem, Belgium). Cell populations and subpopulations were analyzed with Flowjo software.

Results

NA-treatment resulted in changes indicating club cell death and alterations in airway permeability

In a preliminary experiment, we characterized the NA-induced changes at different time points following the NA- i.p. injection. A substantial weight loss was observed, which returned to normal values within 14 days after the NA-injection (Fig. 1a). Treatment with NA damaged the respiratory tract, as shown by an increased number of dead cells and elevated protein content in the BAL fluid of NA-treated mice on days 1 to 3, compared to MO-treated mice (Fig. 1b and d). Mice treated with NA also showed elevated levels of the pulmonary protein surfactant protein (SP) D in their plasma, compared to the MO-treated mice (Fig. 1c). Both groups of mice had only a minor influx of inflammatory cells towards the lungs, as characterized by a limited presence of neutrophils and eosinophils in the BAL fluid (data not shown). Lung wet-to-dry weight ratio was determined, but did not differ between control and NA-treated mice (Fig. 1e). Fourteen days after the NA-injection these parameters stabilized i.e. returned to control conditions.

Pretreatment with NA resulted in enlargement of the lungs and airways

Mice were scanned longitudinally by *in vivo* micro-CT. The micro-CT images showed a moderate enlargement of the lungs and increased likelihood of finding spots of increased density in the NA-treated mice (Fig. 2a). Quantification of these parameters, partially confirmed these observations (Fig. 2b-f). Following the NA-injection, the mice demonstrated a significant increase in the total and air lung volume at day 7 (Fig. 2b and c). Lung tissue volume did not alter in time depending on the treatment (Fig. 2d). Aerated lung volume significantly increased in the NA-treated mice on days 1 and 7 (Fig. 2e). Visual inspection of the micro-CT scans suggested that the large airways of NA-treated mice were broadened. Calculation of the surface area of the trachea showed that after NA treatment, the large airways of the mice broadened significantly (Fig. 2f). Based on the longitudinal micro-CT images, the lungs and airways of the NA-treated mice returned to normal 13 days after the i.p. injection.

ClO^--challenge resulted in a transient decrease in breathing frequency in NA-pretreated mice

Fourteen days after the i.p. injection, the mice received an i.n. challenge with distilled water (H_2O) or 0.003% active chlorine in hypochlorite (ClO^-) and breathing frequency was recorded. Regardless of their pretreatment, mice receiving an i.n. instillation with distilled water showed no change in breathing frequency (groups MO/H_2O and NA/H_2O, Fig. 3). Also the mice pretreated with MO and instilled with ClO^-, did not show an alteration in breathing frequency (group MO/ClO^-). However, if pretreated with NA, the instillation with ClO^- did result in a transient decrease in breathing frequency (group NA/ClO^-).

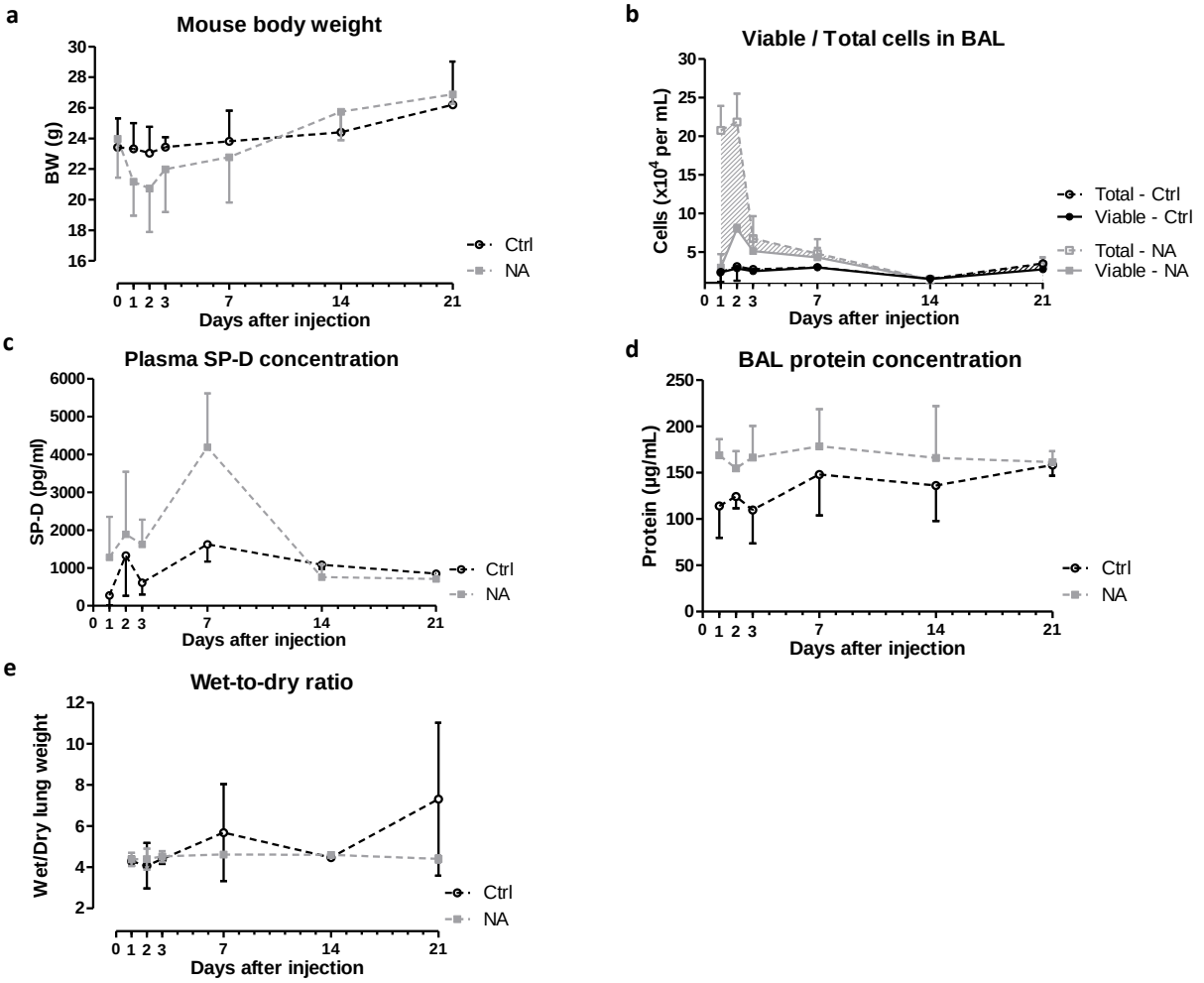

Figure 1. NA-induced changes in body weight, BAL fluid, plasma and lung weight over time
Mice were i.p. treated with vehicle (Ctrl) or naphthalene (NA) on day 0 and scarified 1, 2, 3, 7, 14 or 21 days later. Body weight was recorded before (day 0) and at regular time points until the sacrifice (a). Total and viable cells counted in the BAL fluid are shown in b) with respectively open and closed symbols and dashed area identifying the death cells per treatment condition. SP-D concentration was determined in the plasma of mice using ELISA (c). Protein concentration in the BAL fluid for each treatment group at the respective time of sacrifice is shown in d). Wet-to-dry weight ratio of the left lung lobe is shown in e). Data is presented as mean ± SD. n=2-4 per group.

Pretreatment with NA resulted in increased lung volumes

By applying the NFPE perturbation of the flexiVent, a change in lung volumes depending on pretreatment was found. Mice that received an i.p. injection of NA at the start of the experiment had a significantly increased FVC (groups NA/H_2O and NA/ClO^-, Fig. 4a) on day 15. NA-treatment affected less the $FEV_{0.1}$ as indicated in figure 4b. Mch provocation did not have an additional effect on these changes (data not shown).

ClO^--challenge induced airway hyperreactivity in NA-pretreated mice

Twenty-four hours after the airway challenge an increased Mch response was observed in the NA/ClO^- treated mice. Mice pretreated with NA and receiving a challenge of ClO^- showed significantly increased Rn at high Mch concentrations compared to the MO/H_2O group (Fig. 4c).

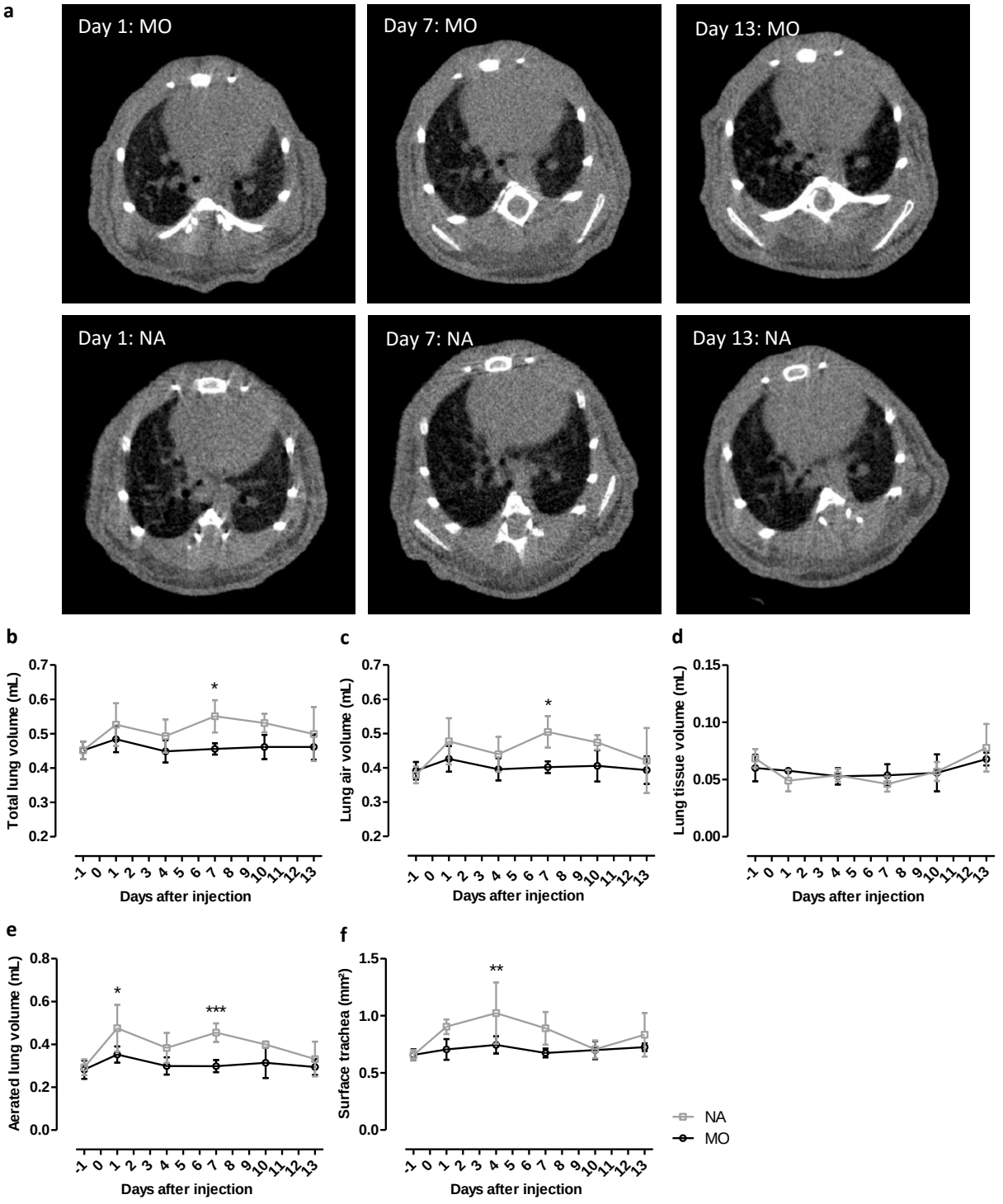

Figure 2. Longitudinal *in vivo* micro-CT images and quantification

Mice were scanned with micro-CT before (day -1) and at regular time points after the i.p. injection (day 1, 4, 7, 10 and 13) with MO or NA. Representative transverse micro-CT images of a MO-(top) and NA- (bottom) treated C57Bl/6 mouse acquired 1, 7 and 13 days (left to right) after treatment (a). The position of the shown images was chosen at 100 z-positions after the first bifurcation of the airways. As i.n. treatment with H_2O or ClO^- took place on day 14, only the i.p. injection defined the two treatment groups i.e. MO versus NA. By manual delineating VOI's on the micro-CT images, three lung volumes were established: total lung volume, lung tissue volume and lung air volume (respectively b, c, d). The volume of connected air is represented in e). Panel f demonstrates the quantification of the surface of the trachea of the mice. Data is represented as mean ± SD. *p < 0.05, **p < 0.01 and ***p < 0.001 compared to MO as analyzed by repeated measures two-way ANOVA excluding day -1. n= 5 per group.

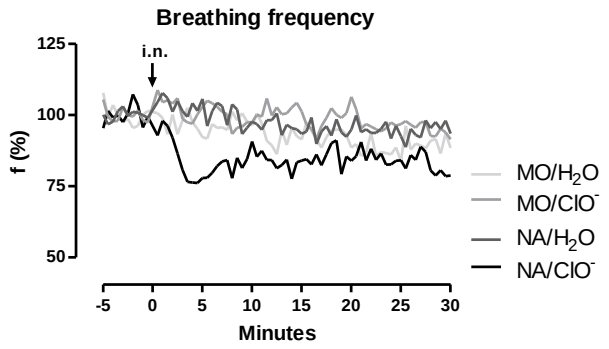

Figure 3. Early ventilatory response following i.n. challenge

The ventilatory response was monitored during 5 min before (baseline) and 60 min after instillation with either distilled water (H_2O) or 0,003% active chlorine in hypochlorite (ClO^-). The mean values of breathing frequency (f) against time per group before and 30 minutes after the instillation (indicated by arrow) are shown. Data is normalized by baseline values, which are represented as 100 %. n= 5-7 per group.

ClO^--challenge increased the airway inflammation, permeability and epithelial damage in NA-pretreated mice

On day 15, mice of all treatment groups had similar body weight (Suppl. Fig. 1). Analysis of the BAL fluid did not demonstrate ongoing cell death (viable vs. total cell count in BAL fluid – data not shown). Differential cell count of the BAL fluid showed a negligible pulmonary inflammation in the NA/H_2O group. However, combining the NA-treatment with ClO^- airway exposure augmented the pulmonary inflammation, as shown by significant increases in neutrophils and eosinophils (group NA/ClO^-, Fig. 5a). Additionally, an increased BAL protein concentration was found in the NA/ClO^- mice (Fig. 5b). The concentrations of SP-D proteins in plasma was significantly increased in the NA-injected and ClO^--challenged mice, compared to the control group (Fig. 5c). Lung wet-to-dry weight ratio did not differ between the treatment groups (Suppl. Fig. 2). Histological abnormalities including epithelial denudation and inflammation at the bronchovascular bundle, alveoli and veins were present in some of the NA-pretreated mice, while the MO-mice had no or only mild signs of inflammation (Fig. 5h). There were no signs of increased smooth muscle cells, alveolar widening or emphysema (data not shown). Blinded scoring by an experienced pathologist indicated that the changes in epithelial denudation and inflammation were statistically increased in the NA/ClO^- group (Fig. 5d-g).

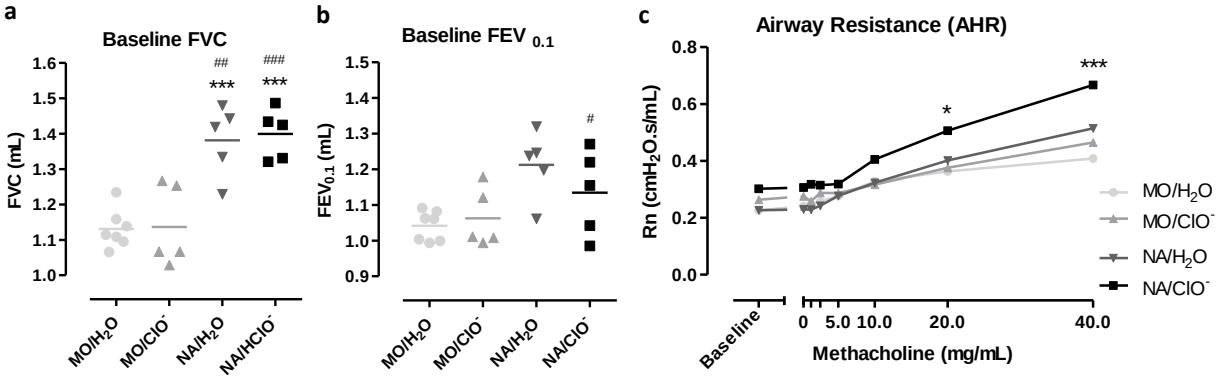

Figure 4. Pulmonary function 24h after the i.n. challenge

Twenty-four hours after the i.n. instillation, lung function was assessed by negative pressure-driven forced expiration (NFPE) maneuvers and forced oscillations were performed to at baseline and after each Mch concentration (0-40 mg/mL). Individual and mean group baseline values for FVC and FEV $_{0.1}$ are shown in a) and b). The mean dose-response for Rn against the Mch concentration is shown in c). **$p < 0.01$ and ***$p < 0.001$ compared to MO/H_2O, $^{\#}p < 0.05$, $^{\#\#}p < 0.01$, $^{\#\#\#}p < 0.001$ compared to MO/ClO^-. n= 5-7 per group.

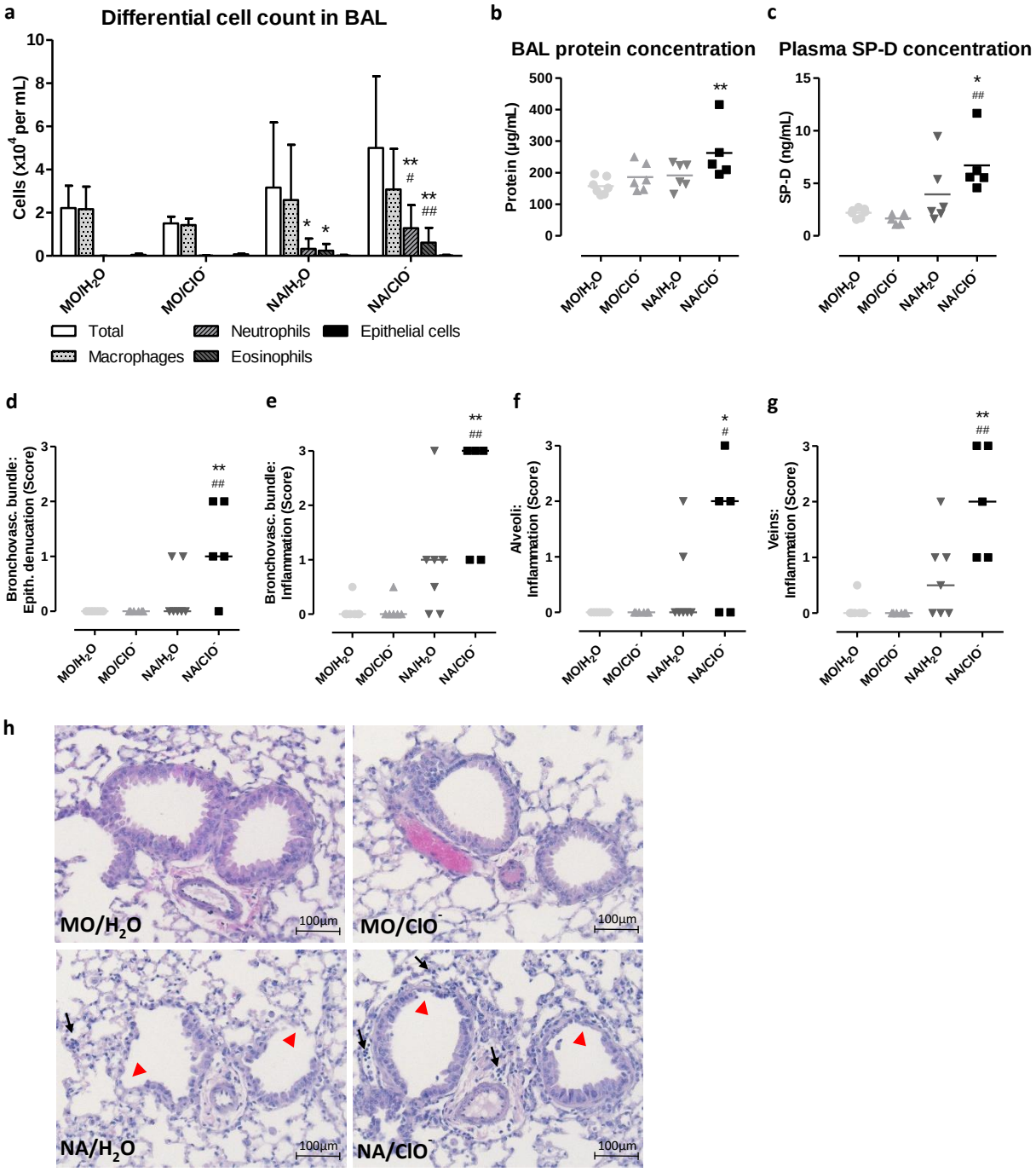

Figure 5. Inflammatory, permeability and histopathological parameters on day 15
Immediately after lung function measurements the blood was collected, the right lung was lavaged (for BAL fluid analysis) and isolated (for histological analysis). The total cell count and total numbers of macrophages, neutrophils, eosinophils and epithelial cells determined in the BAL fluid are shown in a). Data is presented as mean ± SD. Individual and mean group values of the protein concentration in the BAL fluid, is shown in b). The individual and group mean plasma SP-D concentrations, measured with ELISA, are shown in c). H&E stained sections of the right lung were scored from 0 to 3 in for d) epithelial denudation, inflammation at the e) bronchovascular bundle, f) alveoli and g) veins. The individual scores and group median are depicted on the graphs. Representative images taken with 200x amplification are shown for each treatment group (h). Red arrowheads indicate epithelial denudation and black arrows indicate inflammation.*p < 0.05, **p < 0.01 compared to MO/H_2O and $^{\#}p < 0.05$, $^{\#\#}p < 0.01$ compared to MO/ClO^-. n= 4-7 per group.

Pretreatment with NA recruited monocyte-derived dendritic cells (moDC) towards the lungs

The total number of cells collected from the total lung digest showed that significantly higher numbers of cells could be collected from the NA/H_2O and NA/ClO^- -treated mice (Fig. 6a). The percentage of macrophages within the viable leukocyte population did not alter between the treatment groups (Fig. 6b). NA/H_2O and NA/ClO^- -treated mice had a significantly higher percentage of DC compared to the MO/ClO^- -treated mice (Fig. 6c). The moDC subpopulation was significantly increased in the NA/H_2O and NA/ClO^- groups (Fig. 6e).

ClO^- challenge induced a shift within the innate lymphoid cell (ILC) population towards type 2 ILCs

The percentage of ILCs within the viable leukocyte population was not significantly different among the treatment groups (Fig. 6d). For the NA/ClO^- -treated mice a significant increase in the percentage of type 2 ILCs and significant decrease in the percentage of type 3 ILCs was found (Fig. 6f).

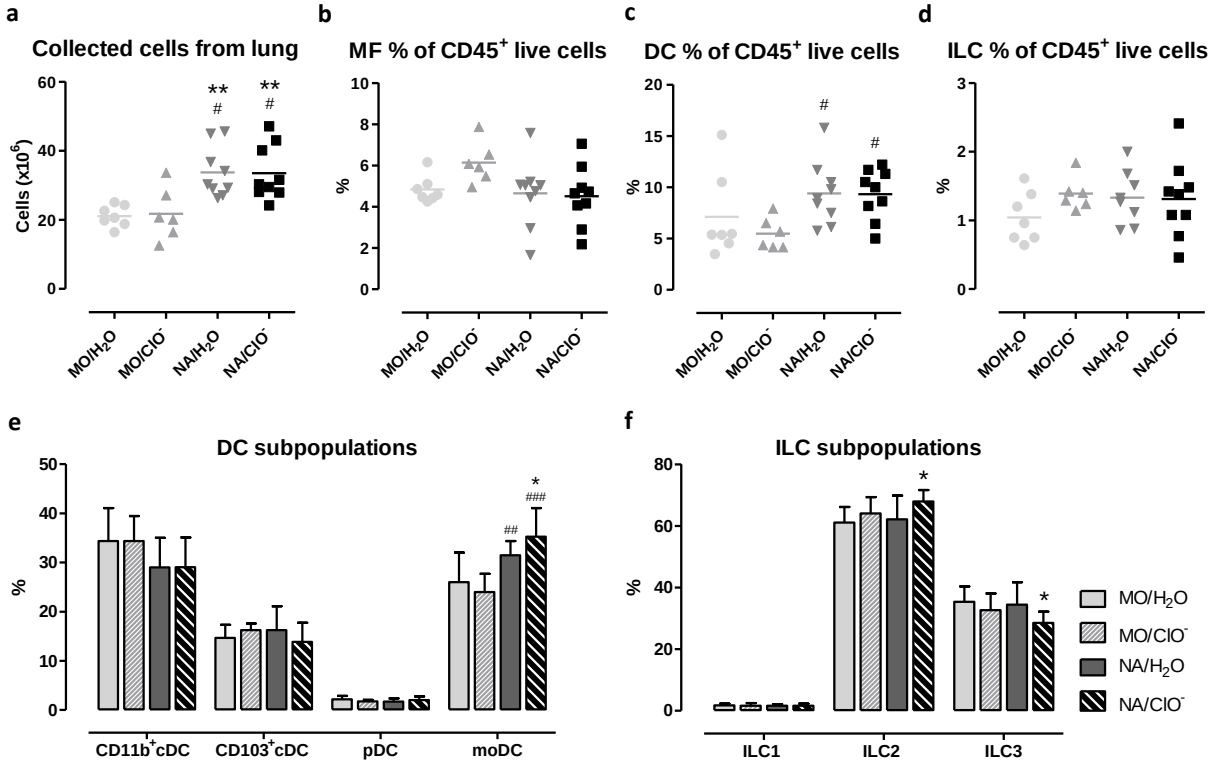

Figure 6. Total collected cells, macrophages, DCs and ILCs in the lung
The total amount of cells collected from the lung digest is shown in a). Cell types were identified using flow cytometry as b) macrophages (MF) ($CD45^+$, $CD11c^{high}$ and high-autofluorescent), c) DCs ($CD45^+$, low-autofluorescent, $CD11c^{high}$ and MHC^+) and d) ILCs ($CD45^+$, Lin^-, $CD90.2^+$ and $CD127^+$). Data is presented as mean with individual values. DC subpopulations are shown in e) as $CD11b^+$ and $CD103^-$ cDCs, $CD11b^-$ and $CD103^+$ cDCs, $CD11^-$ and $SiglecH^+$ pDCs and $CD11b^+$, $CD103^-$ and $CD64^+$ moDCs. ILC subpopulations are shown in f) as ILC1 ($KLRG\text{-}1^{neg}$ and $NK1.1^+$), ILC2 ($KLRG\text{-}1^+$) and ILC3 ($KLRG\text{-}1^{neg}$ and $NK1.1^-$). Cell subpopulations are shown as mean ± SD. *$p < 0.05$, **$p < 0.01$ compared to MO/H_2O and $^{\#}p < 0.05$, $^{\#\#}p < 0.01$, $^{\#\#\#}p < 0.001$ compared to MO/ClO^-. n=6-9 per group.

Discussion

We hypothesized that targeted damage to the airway epithelium, with only partial repair, followed by airway exposure to an irritant compound would result in increased sensitivity of the airways. To test this hypothesis, we combined the mouse model of NA-induced airway epithelial injury with an airway exposure to the common chemical irritant hypochlorite.

I.p. injection with NA in C57Bl/6 mice was characterized by an early, transient decrease in body weight, an increase in plasma SP-D levels and an increase in dead cells and protein content in BAL fluid, which returned to control levels within 14 days. Also, for the first time, we describe temporary enlargement of the lungs and airways due to NA treatment, as evaluated by longitudinal *in vivo* micro-CT images. When challenged i.n. with ClO^- 14 days after the i.p. injection with NA, mice responded with an immediate decrease in breathing frequency. Twenty-four hours later, these mice showed AHR, pulmonary inflammation and histological alterations of the epithelium, along with increased airway permeability as indicated by elevated BAL protein and plasma SP-D concentrations in this group.

Chlorine gas and chlorine-related compounds are ubiquitous respiratory irritants, which cause injury to the respiratory epithelium resulting in early loss of epithelial cells and denudation of the mucosa [24–26]. Recovery from chlorine-induced injury might be insufficient leading to persisting sequelae including sub-epithelial fibrosis, mucus hyperplasia and non-specific AHR [11]. Studies in which mice were exposed to chlorine gas, reported damaged airways, epithelial denudation, increased BAL protein concentrations, along with neutrophil and macrophage influx and AHR [24–29]. It should be noted that these observations were made in murine studies using nose-only exposures to relatively high concentrations of chlorine gas (50 to 800 ppm). In our study, we administered only 0.003% active chlorine (dosed in sodium hypochlorite) in the nose to mimic low dose chlorine exposures in humans.

We used the club cell-selective toxicity of NA to induce airway epithelial injury combined with increased airway permeability. Previous research demonstrated that an i.p. injection of 200mg/kg BW of NA in mice results in airway injury that evolves from club cell vacuolization and swelling, to cell death and cellular exfoliation within 24 hours. As response, the surviving progenitor cells quickly start to proliferate, after which these cells migrate and differentiate to normal club cells within 14 days [19,30,31]. The NA-model of airway injury has been used to study various aspects in airway epithelial damage and repair [30–34].

First, we wanted to validate whether the NA-induced airway epithelial injury resulted in increased ‘inside out’ permeability, by determining the protein concentration in the BAL fluid of mice. A preliminary experiment, showed substantial increase in BAL protein concentration the first days following the injection with NA. Fourteen days later, no differences could be seen in the BAL protein

concentration of NA- compared to MO-treated mice. Nevertheless, when NA-pretreated mice were exposed to ClO^- at this time point, the BAL protein level did increase. Secondly, the concentration of SP-D was determined in the plasma of mice, as a marker of 'outside in' permeability. SP-D is mainly synthesized and secreted into the lungs by the alveolar type II cells and bronchiolar club cells of the respiratory epithelium [35]. Plasma SP-D levels have, therefore, been suggested as markers for lung injury and pulmonary inflammation, and they have been found to be increased in human lung diseases such as asthma and COPD [36–39]. Whether elevated serum levels of SP-D reflect increased leakage towards the circulation due to impairment of the respiratory barrier or reflects increased synthesis, has not been elucidated [35,36,39]. In our preliminary study, plasma SP-D levels of the mice peaked 7 days after the NA-treatment, returning to control levels within the next 7 days. Again, it was found that the challenge with ClO^- in NA-pretreated mice affected the barrier integrity, as demonstrated by the increased plasma SP-D concentration in the NA/ClO^- group on day 15. Based on these two parameters we conclude that NA treatment increased airway permeability. Although this alteration is restored within 14 days, treatment with NA rendered the respiratory epithelium more vulnerable to the injurious effects of irritating agents, as seen by the increased permeability after the ClO^- challenge. In addition, the epithelium of NA/ClO^- mice was severely affected, as quantified by scoring for 'denudation' of the epithelium on H&E stained lung sections.

Immediately following the i.n. instillation with ClO^-, mice pretreated with NA displayed a decrease in breathing frequency, while mice receiving the ClO^- challenge following MO-treatment did not. The absence of a decrease in breathing frequency immediately following intranasal instillation with ClO^- in the MO/ClO^- group indicates that a concentration of 0.003% active chlorine in hypochlorite is not irritant to naïve C57Bl/6 mice. However, in NA-pretreated mice the same concentration of active chlorine did induce an early sensory irritant response. The RD_{50} (i.e. exposure concentration producing a 50% respiratory rate decrease) of chlorine, defined by Alarie et al., is 9.3 ppm [40]. The absence of a decrease in breathing frequency in our naïve mice can be explained by the intranasal instead of the gas exposure which makes our dosing low, since there is a reduced availability of free chlorine in the hypochlorite solution. Apparently, the respiratory epithelium of NA-treated mice remained more susceptible for the adverse effects of ClO^-, thus allowing ClO^- to penetrate more easily trough the respiratory mucosa to reach the trigeminal nerves and provoke the observed respiratory response. Involvement of the transient receptor potential (TRP) channels in the development of hypochlorite-induced airway responses has been demonstrated by Hox *et al.* In mice sensitized to ovalbumin (OVA) and challenged with ClO^- it was found that AHR did not develop in TRPA1 knock-out mice and ClO^- generated a Ca^{2+} influx in TRPA1-transfected cells, suggesting that the observed early ventilatory response is mediated via TRPA1 stimulation [41].

Non-specific AHR is one of the key hallmarks of asthma. Only the NA/ClO^- mice developed AHR towards Mch one day after the airway challenge. Previous studies using NA in mice reported AHR 12 or 24 hours following the NA administration, while being absent at later time points, as we also observed in our NA/H_2O group [32,42,43]. In line with the literature, AHR was not expected to develop following a single i.n. challenge with a low concentration of active chlorine [41,44]. Limited information is available on the type of pulmonary inflammation present in patients with IIA. In our combination model, a significant increase of neutrophils and eosinophils in BAL fluid was observed one day after the ClO^- instillation. H&E stained sections of NA/ClO^-- treated mice lungs showed inflammation at the bronchovascular bundle, alveoli and veins. These data demonstrate that one day after the i.n. challenge with ClO^- two important characteristics of asthma, i.e. AHR and pulmonary inflammation, only develop in mice with, previously damaged but seemingly intact airway barrier (NA-pretreated mice). This confirms our hypothesis that selective epithelial damage followed by an airway challenge results in hypersensitivity of the airways.

Longitudinal micro-CT imaging showed that as a primary response upon the NA-induced airway injury, the total lung volumes increased and the large airways broadened. Total lung volume increased without increase in tissue volume, demonstrating that NA-treatment does not induce inflammation nor fibrosis. Since NA selectively kills the club cells, the main sites of cytotoxicity are the bronchioles [19]. However, using micro-CT scanning, we also observed significant changes in the large airways of these mice. This suggests that the NA-induced damage in the distal regions of the lung can result in compensation at the proximal parts of the respiratory tract, by broadening the large airways, as seen by the increased surface area of the trachea. During a recovery period of 13 days these macroscopic alterations returned to control levels, suggesting a repair from the NA-toxicity.

Fifteen days after the i.p. injection, both mouse groups treated with NA showed increased FVC at baseline. Apparently the lungs of NA mice appear restored on *in vivo* micro-CT, but increased volumes of air can still be 'pulled', by the negative pressure-driven forced expiration maneuver (NPFE), from the lungs at this time point. This contradiction can be explained by the fact that during the micro-CT scanning mice breathe spontaneously with a low vital capacity (VC), whereas during the NPFE maneuver air is intensively forced from the lungs to determine the FVC. This finding reveals that although macroscopically the mice appear recovered, functionally the lungs are still altered 15 days after the NA-treatment.

DCs play a crucial role in allergic asthma by sampling and presenting the allergen to naïve T cells, in order to induce a Th2 cell mediated immune response [45,46]. Given their location in close proximity with the airway epithelial cells, DCs receive signals from the stimulated epithelium, which influences their activation and the generated immune response [47]. Not only allergens, but also pollutants such as diesel

exhaust particles can alter DC biology by acting on the epithelial cells, to promote allergic immune responses [48,49]. Since little is known on the involvement of DC in IIA, we wanted investigated the DC recruitment in our model of IIA induced by epithelial barrier impairment. Fourteen days after the initial barrier impairment with NA, DCs were augmented in the lungs of the mice. In both NA-pretreated mouse groups there was a significant increase in the monocyte-derived DC (moDC) population. Unlike the $CD11b^+$ and $CD103^+$ conventional DCs (cDCs) or plasmacytiod DCs (pDCs), moDCs arise during inflammation when monocytes are recruited to the local tissues and differentiate into moDCs [50]. This indicates that although there is a recovery period of 14 days after the NA-insult, the epithelium is still in an inflammatory state that attracts/preserves the accumulation of moDCs. In a model of HDM-induced asthma moDCs could induce Th2 cell mediated immunity when a high dose HDM was given and mainly functioned to produce proinflammatory chemokines [50]. Further research is necessary to identify the moDC-specific signals that are released from the NA-impaired epithelium, and to elucidate whether the moDCs release pro-inflammatory chemokines that contribute to the observed immune response.

Innate lymphoid cells (ILCs) are recently identified innate immune cells that respond to a variety of environmental stimuli, including viruses, allergens, diesel exhaust particles or ozone [51–55]. ILC are mainly found at barrier surfaces where they respond to these triggers via release of innate signals, such as IL-33, IL-25, TSLP and IL-1β, from the epithelial cells [55]. Based on their cytokine release and function, ILCs have been divided into type 1, 2 and 3, which mirror the adaptive T-cell counterparts (Th1, Th2 and Th17 respectively) [56]. Since lung ILCs are antigen non-specific and strategically located near the airway epithelial barrier, we wanted to study their contribution in our model. The total number of ILCs in the lungs did not alter between the different treatment groups. However, in the NA/ClO^- treatment group, we observed a significant shift of type 3 ILCs towards type 2 ILCs. Type 2 ILCs are activated in response to innate cytokines released from a stimulated airway epithelium and are able to mediate eosinophilia, goblet cell metaplasia, AHR and IL-5 and IL-13 release, even in absence of the adaptive immune system [53,54,57]. Respiratory irritants such as diesel exhaust particles, ozone and chlorine can insult the airway epithelial barrier, which can result in the release of these innate cytokines [51,52]. The observed increase in ILC2 population in the NA/ClO^- group is probably mediated via the (previously) impaired airway epithelium and a specific signal derived from the ClO^- exposure. The resulting ILC2 recruitment towards the lung might play an important role in the observed airway response in our model.

In conclusion, NA-induced lung impairment renders the lungs of C57Bl/6 mice more sensitive to an airway challenge with ClO^-, resulting in a sensory irritant response immediately following the airway exposure, as well as development of AHR and pulmonary inflammation one day later. NA-

administration transiently increased the airway permeability and left the epithelium more vulnerable for the barrier-affecting effects of ClO^-. Disturbance of the respiratory barrier increases the penetration of chemical substances to the host and hereby facilitates their interaction with inflammatory cells in the sub-epithelial compartment. We demonstrated that airway barrier impairment attracts inflammatory DCs towards the lung and that an additional insult with ClO^- upregulates the pulmonary ILC 2 population. Hereby we provide evidence that these cells contribute to the observed response. Further research is necessary to elucidate via which signals these cells are recruited, and to which extent they mediate the airway hypersensitivity in IIA. Taken together these findings confirm our hypothesis that selective airway epithelial damage, with apparent good repair, followed by an airway challenge with an irritant agent results in airway hypersensitivity, as seen in IIA.

Acknowledgments: This project was supported by a grant from the University of Leuven Research Council (GOA/14/011, STG/15/024 and C24/17/061) and a grant of the Flemish Research Foundation (research grant 1504912N).

Conflict of interest: The authors declare no conflict of interest.

Supplementary materials and methods

Reagents

Naphthalene (99%, CAS 91-20-3), mineral oil and acetyl-β-methylcholine chloride (≥ 98%) were obtained from Sigma-Aldrich (Bornem, Belgium). Sodium hypochlorite (10-15% active chlorine, CAS 7681-52-9) was purchased from ACROSS Organics (Geel, Belgium). Pentobarbital (Nembutal®) from Ceva Santé Animale (Brussel, Belgium) was obtained via the animalium of the University of Leuven.

Lung imaging and image analysis and quantification

For the acquisition of the *in vivo* lung micro-CT scans, mice were anesthetized with 1.5-2 % isoflurane in 100% oxygen. According to a previously validated scan protocol, respiratory-gated four-dimensional (4D) micro-CT images of free-breathing animals were acquired using a small-animal micro-CT scanner (SkyScan 1278, Bruker microCT, Kontich, Belgium) [22]. Scan parameters were as follows: 50 kV X-ray source voltage combined with a 1 mm aluminum filter, 918 µA source current and 55 ms exposure time per projection. Nine projections per position were acquired with steps of 0.9° increments over a total angle of 180°, resulting in an estimated dose of 716 mGy (per scan) and scanning time of 8 min. Four phases of the breathing cycle were tracked using a camera and subdivided based on the time course of the breathing pattern. This yielded 4D data, i.e. four reconstructed 3D datasets with 50 µm isotropic voxel size. Repeated lung micro-CT using this protocol does not induce radiotoxic damage to the lungs of mice [58].

Micro-CT data were retrospectively gated, reconstructed, visualized and processed using software provided by the manufacturer (TSort, NRecon, DataViewer, CTan). Total lung volume was determined by quantifying the number of voxels in a volume of interest (VOI) covering the lung consisting of regions of interest (ROIs) that were manually delineated on the transversal images, thereby avoiding the heart and main blood vessels. Lung tissue volume was distinguished from the total lung volume by setting a fixed greyscale threshold and quantifying the number of voxels within this selection of the previously determined VOI. Subtracting the lung tissue volume by total lung tissue revealed the lung air volume. Quantification of the aerated lung volume was performed using a custom written automated algorithm that was applied to all datasets as defined, validated, and described previously [59]. The surface area of the trachea was determined for each mouse on a fixed z-position, i.e. 10 steps above the first bifurcation, of the airways. The image generated for quantification of the aerated lung volume was opened with the ImageJ software. After making the image binary, the trachea was selected and the total area was quantified in pixels using the 'Analyze particles' plugin.

The retrospectively gated micro-CT data generated images on four different phases of the breathing cycle (i.e. end of inspiration, end of expiration and intermediate phases). All data reported here was

obtained using images from the end-expiratory breathing phase and likewise provide information on this phase of the breathing cycle.

Early ventilatory response

The respiratory response upon the airway challenge was recorded in a double chamber plethysmograph (DCP) (EMKA Technologies, Paris, France). Breathing frequency (f) was registered 5 min before (baseline measurement) and 60 min after the intranasal instillation, as a measure of sensory irritation. For each individual mouse, the breathing frequency was plotted against time and normalized to their average baseline value (data expressed as percentage of average baseline value). The area under the curve (AUC) for the period after the instillation was calculated to perform statistical analysis.

Pulmonary function

Twenty-four hours after the i.n. challenge, the pulmonary function was assessed using the flexiVent™ FX system (SCIREC, Montreal Qc, Canada). The system was designed to concurrently measure forced oscillations and forced expiration parameters, as described previously [23]. Briefly, the system operated with flexiWare™ 7.2 software and was equipped with a FX1 module, a negative pressure forced expiration (NPFE) extension for mice and a small particle size Aeroneb® Lab nebulizer (2.5-4 µm; Aerogen, Galway, Ireland). Mice were anesthetized with an intraperitoneal injection of pentobarbital (70 mg/kg BW, Nembutal ®). Once sufficiently anesthetized, a tracheotomy was performed to insert a 18-gauge metal cannula. Mice were quasi-sinusoidally ventilated with a tidal volume of 10 mL/kg and a frequency of 150 breaths/min to mimic spontaneous breathing.

At the start of the experiment, two successive deep inflations were applied to maximally inflate the lungs to a pressure of 30 cmH_2O in order to open the lungs.

Next, to determine airway responsiveness, a protocol to evaluate the pulmonary function was initiated. An aerosol containing increasing concentrations of the bronchoconstrictive agent methacholine (MCh) (0, 1.25, 2.5, 5, 10, 20, 40 mg/mL in saline) was nebulized for 5 sec. After the aerosol exposure, the forced oscillation perturbation 'Quick Prime-3' (QP3), generating forced oscillations with a frequency between 1-20.5 Hz during 3 sec, was executed five times. The reported central airway resistance (Rn) for each concentration is the average of these five measurements. After the sequence, a NPFE perturbation was performed to measure the forced vital capacity (FVC) and forced expiratory volume in 0.1 seconds ($FEV_{0.1}$) at each concentration.

If the coefficient of determination (COD) of a measurement was lower than 0.9, the measurement was excluded. For each mouse, Rn, FVC and $FEV_{0.1}$ were plotted against Mch concentration and a dose-

response curve was constructed per treatment group. The AUC of the dose-response curve was used to perform statistical analysis.

Rn, FVC and $FEV_{0.1}$ were identically measured prior to any Mch aerosol exposure to determine the baseline values for each mouse.

Inflammatory, permeability and histopathological determinations

During the autopsy, the left lung was clamped and collected afterwards to quantify the wet and dry weight.

The right lung was lavaged, *in situ*, three times with 0.45 mL sterile saline (0.9% NaCl), and the recovered fluid was pooled. The total amount of cells in the BAL fluid was counted using a Bürker hemocytometer. Subsequently the BAL fluid was centrifuged (1000 g, 4°C, 10 min). The supernatant was collected and frozen (-80° C) until further analysis. For differential cell counts, the cells were resuspended in 1 mL saline (0.9% NaCl), afterwards 250 µL of the resuspended cells were spun (300 g, 4°C, 6 min) (Cytospin 3, Shandon, TechGen, Zellik, Belgium) onto microscope slices, air-dried and stained (Diff-Quik® method, Medical Diagnostics, Düdingen, Germany). For each sample, 200 cells were counted to quantify the number of macrophages, eosinophils, neutrophils and epithelial cells.

The protein content in the BAL fluid was determined using the Bradford method with bovine serum albumin as the standard.

The right lung was inflated and collected with a 4% paraformaldehyde solution to fix the lung tissue. The hematoxylin and eosin (H&E) stained sections were scored semi-quantitatively in a blinded manner, by an experienced pathologist for inflammation, epithelial denudation and smooth muscle cells at the broncho-vascular bundle; inflammation, widening and emphysema at the alveoli; and inflammation at the veins.

Mouse surfactant protein (SP) D concentration in plasma was determined with an ELISA kit (Duoset ELISA R&D Systems Inc., DY6839-05) according to the manufacturers' instructions.

Single cell suspension

The pulmonary circulation was rinsed with saline/EDTA to remove the intravascular pool of cells. The lungs were minced and incubated for 45 minutes at 37°C in digestion medium (RPMI 1640 with GlutaMAX™, supplemented with 5% FCS, 0.05mM 2-mercaptoethanol, 100U/mL penicillin-100 mg/mL streptomycin (all from Invitrogen, Merelbeke, Belgium), 1 mg/mL collagenase type 2 (Worthington Biochemical, Lakewood, New York) and 0.02 mg/mL DNase (grade II form bovine pancreas; Boehringer Ingelheim, Ingelheim, Germany)). Red blood cells were lysed with ammonium chloride buffer. Total amount of lung cells were counted using a Bürker hemocytometer.

Flow cytometry

For dendritic cell (DC) staining, two million cells of the single lung suspension were collected and preincubated with anti-CD16/CD32 (Clone 2.4G2, from BD Biosciences, Erembodegen, Belgium). After live/dead staining using the Zombie Aqua™Fixable Viability Kit, cells were labelled with combinations of anti-mouse fluorochrome-conjugated mAbs against CD45 (clone 30-F11), CD11c (clone N418), MHC II (clone M5/114.15.2), CD11b (clone M1/70), CD103 (clone 2E7), CD64 (clone X54-5/7.1) or Siglec-H (clone 551) (all from Biolegend, San Diego, California).

For innate lymphoid cell (ILC) staining, four million cells of the single lung suspension were collected and stained with Fixable Viability Dye eFluor™ 780 (eBioscience, Invitrogen, Merelbeke, Belgium). To minimize non-specific binding, the cells were preincubated with anti-CD16/CD32 (Clone 2.4G2, from BD Biosciences, Erembodegen, Belgium). Combination of anti-mouse fluorochrome-conjugated mAbs against CD45 (clone 30-F11), CD127 (clone SB/199), CD117 (clone 2B8), CD90.2 (clone 53-2.1), KLGR-1 (clone 2F1), NK1.1 (clone PK136), CD11b (clone M1/70), CD19 (clone 1D3), CD3e (clone G4.18), CD45RB (clone 16A), CD5 (clone 53-7.3), CD94 (clone 20d5), Gr-1 (clone RB6-8C5), TCR γδ (clone GL3) and Ter-119 (clone TER-119) (all from BD biosciences, Erembodegem, Belgium).

Data acquisition was performed on a LSR Fortessa flow cytometer running DIVA software (BD Biosciences, Erembodegem, Belgium). Cell populations and subpopulations were analyzed with Flowjo software (BD Biosciences, Ashland, Oregon). The composition of the DC Ab panel and the ILC Ab panel were developed by Lore Pollaris and Anne-Charlotte Jonckheere (unpublished communication).

Data analyses

The data are presented as means with standard deviation (SD). Individual mice are shown with group mean (median for the histology scores). In case of normal distribution, assessed by the Kolmogorov-Smirnov test, Bonferroni multiple comparison *post hoc* test was performed (Graph Pad Prism 5.01. Graphpad Software Inc., San Diego, USA). If data had non-normal distribution, Dunn's multiple comparison *post hoc* test was used. Data of micro-CT parameters (total lung volume, lung air volume, lung tissue volume, aerated lung volume and surface trachea) were analyzed using repeated measures two-way ANOVA excluding day -1, followed by a Bonferroni multiple comparison *post hoc* test. Dose-response curves of the Rn were analyzed using two-way ANOVA followed by a Bonferroni multiple comparison post hoc test. A level of $p < 0.05$ (two tailed) was considered significant.

Supplementary figures

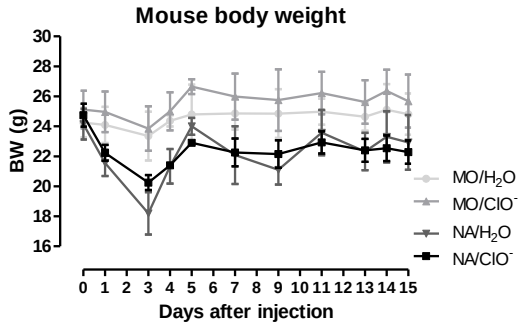

Supplementary figure 1. Time course of changes in body weight
The mice were i.p. treated with vehicle (MO) or naphthalene (NA) on day 0, received an i.n. instillation with distilled water (H_2O) or hypochlorite (ClO^-) on day 14 and were sacrificed one day later. Body weight was recorded before (day 0) and at regular time points until the sacrifice. Data is presented as mean ± SD. n= 5-7 per group.

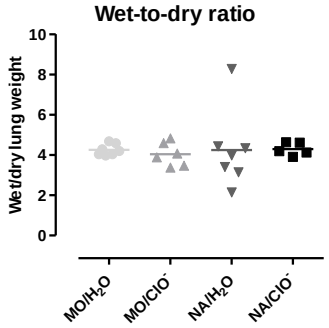

Supplementary figure 2. Wet-to-dry lung weight ratio
Wet-to-dry weight ratio of the left lung lobe is shown. Data is presented as mean with individual mice. n= 5-7 per group.

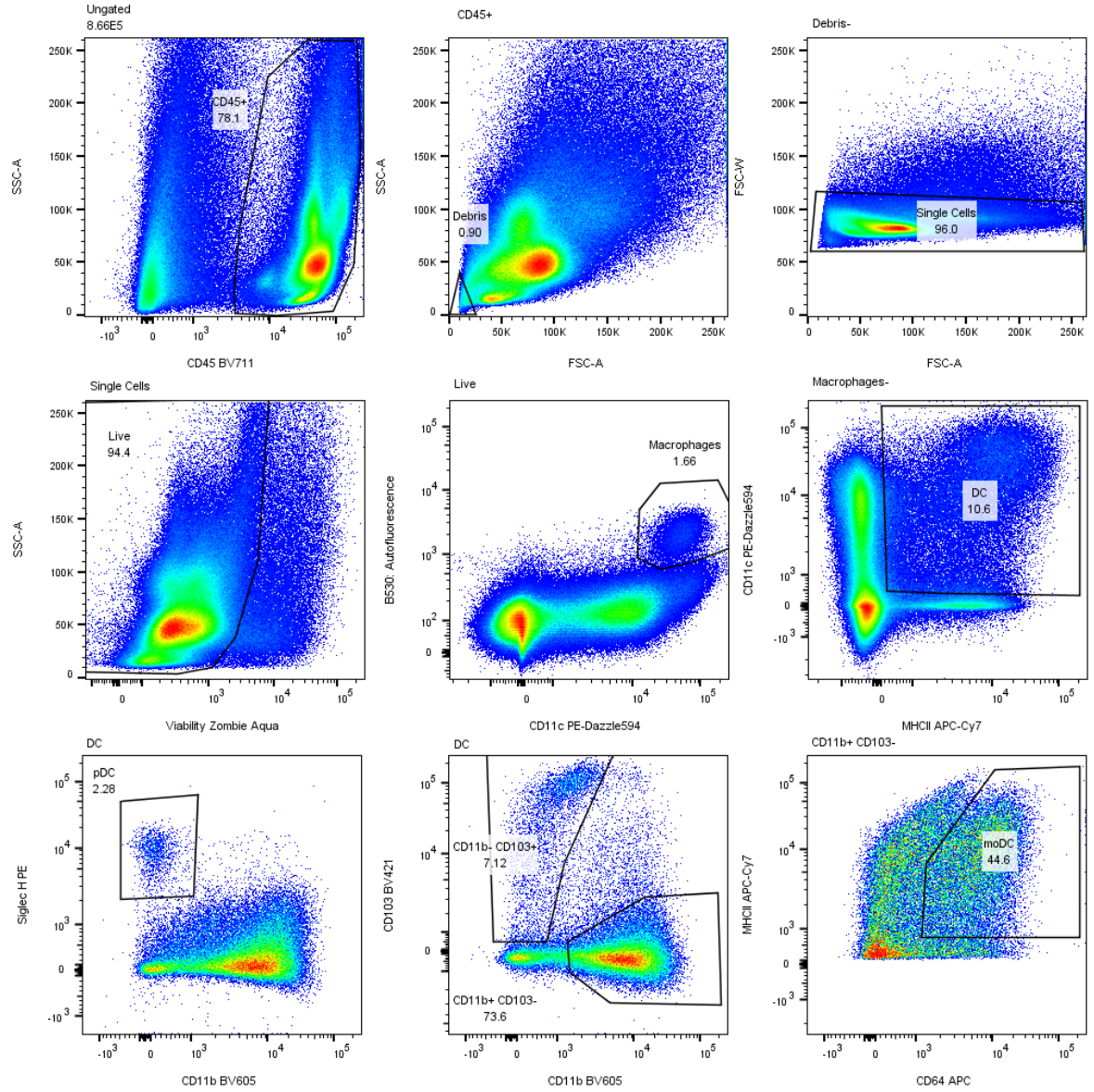

Supplementary figure 3. Representative flow cytometry data and gating strategy for DC populations in lung
DCs were marked as low-autofluorescent, CD11c^{high} and MHC^{+}, CD11c^{high} and high-autofluorescent cells are marked as macrophages. pDCs were gated as CD11^{-} and SiglecH^{+}. cDCs were subdivided into CD11b^{+} and CD103^{-} cells or CD11b^{-} and CD103^{+}. moDC were identified as CD11b^{+},CD103^{-} and CD64^{+}. FCS, forward scatter; SSC, side scatter.

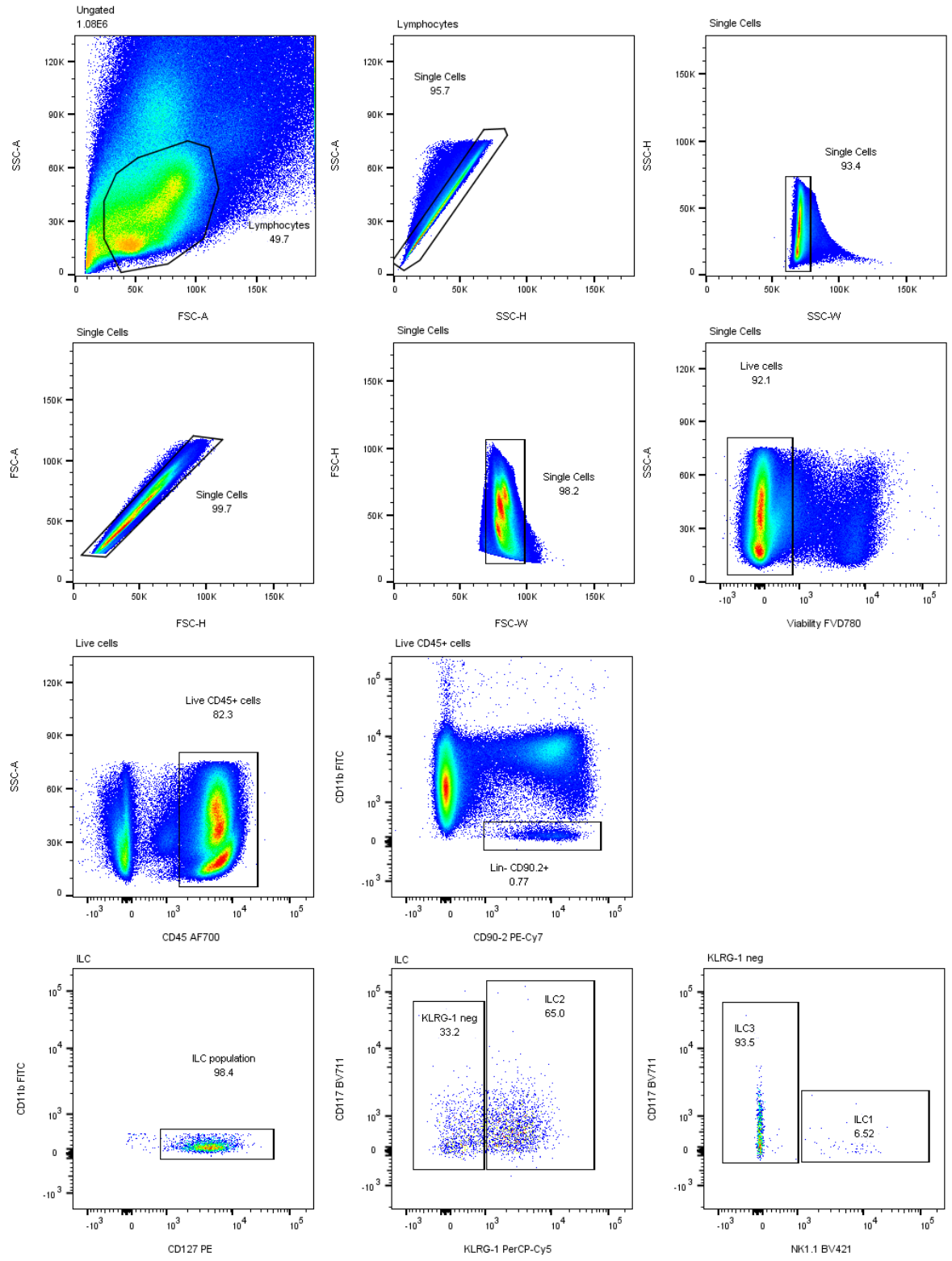

Supplementary figure 4. Representative flow cytometry data and gating strategy for ILC populations in lung
ILCs were identified as Lin- (CD11b, CD19, CD3e, CD45RB, CD5, CD94, Gr-1, TCR γδ and Ter-199), CD90.2^{+} and CD127^{+} cells. ILC2s were marked as KLRG-1^{+}. ILC1s were gated as KLRG-1^{neg} and NK1.1^{+} and ILC3 as KLRG-1^{neg} and NK1.1^{-}. FCS, forward scatter; SSC, side scatter.

References

1. Rezaee, F. & Georas, S. N. Breaking Barriers. New Insights into Airway Epithelial Barrier Function in Health and Disease. *Am. J. Respir. Cell Mol. Biol.* **50,** 857–869 (2014).
2. Georas, S. N. & Rezaee, F. Epithelial barrier function: at the frontline of asthma immunology and allergic airway inflammation. *J. Allergy Clin. Immunol.* **134,** 509–520 (2014).
3. Heijink, I. H., Noordhoek, J. A., Timens, W., van Oosterhout, A. J. M. & Postma, D. S. Abnormalities in airway epithelial junction formation in chronic obstructive pulmonary disease. *Am. J. Respir. Crit. Care Med.* **189,** 1439–1442 (2014).
4. Holgate, S. T. Epithelium dysfunction in asthma. *J. Allergy Clin. Immunol.* **120,** 1233-1244-1246 (2007).
5. Shaykhiev, R. & Crystal, R. G. Early events in the pathogenesis of chronic obstructive pulmonary disease. Smoking-induced reprogramming of airway epithelial basal progenitor cells. *Ann. Am. Thorac. Soc.* **11 Suppl 5,** S252-258 (2014).
6. Soyka, M. B. *et al.* Defective epithelial barrier in chronic rhinosinusitis: The regulation of tight junctions by IFN-γ and IL-4. *J. Allergy Clin. Immunol.* **130,** 1087–1096.e10 (2012).
7. Xiao, C. *et al.* Defective epithelial barrier function in asthma. *J. Allergy Clin. Immunol.* **128,** 549–556.e12 (2011).
8. Bernstein, J. A. *et al.* Health effects of air pollution. *J. Allergy Clin. Immunol.* **114,** 1116–1123 (2004).
9. Evans, R. B. Chlorine: state of the art. *Lung* **183,** 151–167 (2005).
10. Casas, L. *et al.* Use of household cleaning products, exhaled nitric oxide and lung function in children. *Eur. Respir. J.* **42,** 1415–1418 (2013).
11. Hoyle, G. W. & Svendsen, E. R. Persistent effects of chlorine inhalation on respiratory health. *Ann. N. Y. Acad. Sci.* (2016). doi:10.1111/nyas.13139
12. White, C. W. & Martin, J. G. Chlorine gas inhalation: human clinical evidence of toxicity and experience in animal models. *Proc. Am. Thorac. Soc.* **7,** 257–263 (2010).
13. Brooks, S. M., Weiss, M. A. & Bernstein, I. L. Reactive airways dysfunction syndrome (RADS). Persistent asthma syndrome after high level irritant exposures. *Chest* **88,** 376–384 (1985).
14. Vandenplas, O. *et al.* EAACI position paper: irritant-induced asthma. *Allergy* **69,** 1141–1153 (2014).
15. Brooks, S. M. & Bernstein, I. L. Irritant-Induced Airway Disorders. *Immunol. Allergy Clin. North Am.* **31,** 747–768 (2011).
16. Maestrelli, P., Boschetto, P., Fabbri, L. M. & Mapp, C. E. Mechanisms of occupational asthma. *J. Allergy Clin. Immunol.* **123,** 531-542-544 (2009).
17. Buckpitt, A. *et al.* Naphthalene-Induced Respiratory Tract Toxicity: Metabolic Mechanisms of Toxicity. *Drug Metab. Rev.* **34,** 791–820 (2002).
18. Plopper, C. G., Suverkropp, C., Morin, D., Nishio, S. & Buckpitt, A. Relationship of cytochrome P-450 activity to Clara cell cytotoxicity. I. Histopathologic comparison of the respiratory tract of mice, rats and hamsters after parenteral administration of naphthalene. *J. Pharmacol. Exp. Ther.* **261,** 353–363 (1992).
19. Van Winkle, L. S., Johnson, Z. A., Nishio, S. J., Brown, C. D. & Plopper, C. G. Early events in naphthalene-induced acute Clara cell toxicity: comparison of membrane permeability and ultrastructure. *Am. J. Respir. Cell Mol. Biol.* **21,** 44–53 (1999).
20. Buckpitt, A. *et al.* Relationship of cytochrome P450 activity to Clara cell cytotoxicity. IV. Metabolism of naphthalene and naphthalene oxide in microdissected airways from mice, rats, and hamsters. *Mol. Pharmacol.* **47,** 74–81 (1995).
21. Plopper, C. G., Cranz, D. L., Kemp, L., Serabjit-Singh, C. J. & Philpot, R. M. Immunohistochemical Demonstration of Cytochrome P-450 Monooxygenase in Clara Cells throughout the Tracheobronchial Airways of the Rabbit. *Exp. Lung Res.* **13,** 59–68 (1987).
22. Vande Velde, G. *et al.* Longitudinal micro-CT provides biomarkers of lung disease that can be used to assess the effect of therapy in preclinical mouse models, and reveal compensatory changes in lung volume. *Dis. Model. Mech.* **9,** 91–98 (2016).
23. Devos, F. C. *et al.* Forced expiration measurements in mouse models of obstructive and restrictive lung diseases. *Respir. Res.* **18,** 123 (2017).
24. McGovern, T. K. *et al.* Neutrophils mediate airway hyperresponsiveness after chlorine-induced airway injury in the mouse. *Am. J. Respir. Cell Mol. Biol.* **52,** 513–522 (2015).
25. McGovern, T. K. *et al.* Dimethylthiourea protects against chlorine induced changes in airway function in a murine model of irritant induced asthma. *Respir. Res.* **11,** 138 (2010).

26. Tuck, S. A. *et al.* Time course of airway remodelling after an acute chlorine gas exposure in mice. *Respir. Res.* **9,** 61 (2008).
27. Jonasson, S., Koch, B. & Bucht, A. Inhalation of chlorine causes long-standing lung inflammation and airway hyperresponsiveness in a murine model of chemical-induced lung injury. *Toxicology* **303,** 34–42 (2013).
28. Martin, J. G. *et al.* Chlorine-induced injury to the airways in mice. *Am. J. Respir. Crit. Care Med.* **168,** 568–574 (2003).
29. Wigenstam, E., Elfsmark, L., Koch, B., Bucht, A. & Jonasson, S. Acute respiratory changes and pulmonary inflammation involving a pathway of TGF-β1 induction in a rat model of chlorine-induced lung injury. *Toxicol. Appl. Pharmacol.* **309,** 44–54 (2016).
30. Greeley, M. A., Van Winkle, L. S., Edwards, P. C. & Plopper, C. G. Airway trefoil factor expression during naphthalene injury and repair. *Toxicol. Sci. Off. J. Soc. Toxicol.* **113,** 453–467 (2010).
31. Van Winkle, L. S., Buckpitt, A. R., Nishio, S. J., Isaac, J. M. & Plopper, C. G. Cellular response in naphthalene-induced Clara cell injury and bronchiolar epithelial repair in mice. *Am. J. Physiol.* **269,** L800-818 (1995).
32. Karagiannis, T. C. *et al.* Molecular model of naphthalene-induced DNA damage in the murine lung. *Hum. Exp. Toxicol.* **31,** 42–50 (2012).
33. López, I. P. *et al.* Involvement of Igf1r in Bronchiolar Epithelial Regeneration: Role during Repair Kinetics after Selective Club Cell Ablation. *PloS One* **11,** e0166388 (2016).
34. Yildirim, A. O. *et al.* Keratinocyte growth factor protects against Clara cell injury induced by naphthalene. *Eur. Respir. J.* **32,** 694–704 (2008).
35. Crouch, E. C. Surfactant protein-D and pulmonary host defense. *Respir. Res.* **1,** 6 (2000).
36. Benfante, A. *et al.* Asthmatics with high levels of serum surfactant protein D have more severe disease. *Eur. Respir. J.* **47,** 1864–1867 (2016).
37. Fujita, M. *et al.* Serum surfactant protein D is increased in acute and chronic inflammation in mice. *Cytokine* **31,** 25–33 (2005).
38. Pan, T. *et al.* Serum SP-D is a marker of lung injury in rats. *Am. J. Physiol. Lung Cell. Mol. Physiol.* **282,** L824-832 (2002).
39. Winkler, C. *et al.* Comprehensive characterisation of pulmonary and serum surfactant protein D in COPD. *Respir. Res.* **12,** 29 (2011).
40. Alarie, Y., Ferguson, J. S., Stock, M. F., Weyel, D. A. & Schaper, M. Sensory and pulmonary irritation of methyl isocyanate in mice and pulmonary irritation and possible cyanidelike effects of methyl isocyanate in guinea pigs. *Environ. Health Perspect.* **72,** 159–167 (1987).
41. Hox, V. *et al.* Crucial role of transient receptor potential ankyrin 1 and mast cells in induction of nonallergic airway hyperreactivity in mice. *Am. J. Respir. Crit. Care Med.* **187,** 486–493 (2013).
42. Royce, S. G. *et al.* Mechanistic insights into the contribution of epithelial damage to airway remodeling. Novel therapeutic targets for asthma. *Am. J. Respir. Cell Mol. Biol.* **50,** 180–192 (2014).
43. Royce, S. G., Patel, K. P. & Samuel, C. S. Characterization of a novel model incorporating airway epithelial damage and related fibrosis to the pathogenesis of asthma. *Lab. Investig. J. Tech. Methods Pathol.* **94,** 1326–1339 (2014).
44. Hox, V. *et al.* Airway exposure to hypochlorite prior to ovalbumin induces airway hyperreactivity without evidence for allergic sensitization. *Toxicol. Lett.* **204,** 101–107 (2011).
45. Lambrecht, B. N., Salomon, B., Klatzmann, D. & Pauwels, R. A. Dendritic cells are required for the development of chronic eosinophilic airway inflammation in response to inhaled antigen in sensitized mice. *J. Immunol. Baltim. Md 1950* **160,** 4090–4097 (1998).
46. Lambrecht, B. N. & Hammad, H. Biology of lung dendritic cells at the origin of asthma. *Immunity* **31,** 412–424 (2009).
47. Lambrecht, B. N. & Hammad, H. Dendritic cell and epithelial cell interactions at the origin of murine asthma. *Ann. Am. Thorac. Soc.* **11 Suppl 5,** S236-243 (2014).
48. Provoost, S. *et al.* Diesel exhaust particles stimulate adaptive immunity by acting on pulmonary dendritic cells. *J. Immunol. Baltim. Md 1950* **184,** 426–432 (2010).
49. Provoost, S., Maes, T., Joos, G. F. & Tournoy, K. G. Monocyte-derived dendritic cell recruitment and allergic T(H)2 responses after exposure to diesel particles are CCR2 dependent. *J. Allergy Clin. Immunol.* **129,** 483–491 (2012).
50. Plantinga, M. *et al.* Conventional and monocyte-derived CD11b(+) dendritic cells initiate and maintain T helper 2 cell-mediated immunity to house dust mite allergen. *Immunity* **38,** 322–335 (2013).
51. De Grove, K. C. *et al.* Dysregulation of type 2 innate lymphoid cells and TH2 cells impairs pollutant-induced allergic airway responses. *J. Allergy Clin. Immunol.* **139,** 246–257.e4 (2017).

52. Yang, Q. *et al.* Group 2 innate lymphoid cells mediate ozone-induced airway inflammation and hyperresponsiveness in mice. *J. Allergy Clin. Immunol.* **137,** 571–578 (2016).
53. Chang, Y.-J. *et al.* Innate lymphoid cells mediate influenza-induced airway hyper-reactivity independently of adaptive immunity. *Nat. Immunol.* **12,** 631–638 (2011).
54. Klein Wolterink, R. G. J. *et al.* Pulmonary innate lymphoid cells are major producers of IL-5 and IL-13 in murine models of allergic asthma. *Eur. J. Immunol.* **42,** 1106–1116 (2012).
55. Kim, H. Y., Umetsu, D. T. & Dekruyff, R. H. Innate lymphoid cells in asthma: Will they take your breath away? *Eur. J. Immunol.* **46,** 795–806 (2016).
56. Kortekaas Krohn, I. *et al.* Emerging roles of innate lymphoid cells in inflammatory diseases: Clinical implications. *Allergy* (2017). doi:10.1111/all.13340
57. Yu, S., Kim, H. Y., Chang, Y.-J., DeKruyff, R. H. & Umetsu, D. T. Innate lymphoid cells and asthma. *J. Allergy Clin. Immunol.* **133,** 943–950; quiz 51 (2014).
58. Vande Velde, G. *et al.* Longitudinal in vivo microcomputed tomography of mouse lungs: No evidence for radiotoxicity. *Am. J. Physiol. Lung Cell. Mol. Physiol.* **309,** L271-279 (2015).
59. Langhe, E. D. *et al.* Quantification of Lung Fibrosis and Emphysema in Mice Using Automated Micro-Computed Tomography. *PLOS ONE* **7,** e43123 (2012).

Chapter 6

Airway barrier impairment increases nonspecific airway hyperresponsiveness in mice

Sofie Van Den Broucke, Tatjana Decaesteker, Erik Verbeken, Benoit Nemery, Jeroen Vanoirbeek, Peter Hoet

Abstract

Chlorine is a respiratory irritant that causes irritant-induced asthma (IIA). Previously, we showed that airway barrier impairment, followed by a single airway exposure to hypochlorite (ClO^-), results in airway hypersensitivity. In the current study, we aimed to initiate a more robust IIA response.

On days 0 and 14, C57Bl/6 mice received an intra-peritoneal (i.p.) injection with the airway damaging agent naphthalene (NA, 200 mg/kg body weight, BW) or vehicle (mineral oil, MO). After a second recovery period of 14 days, three endotracheal instillations (40µL) of 0.003% active chlorine (in ClO^-) or saline (Sal) were administered on days 28, 31, 34, or the mice were left untreated. One day after the last instillation, lung function was measured, along with evaluation of the pulmonary inflammation, airway permeability and histologic lesions.

After each i.p. injection of NA, a transient decrease in BW of the mice was observed. On day 35, an increased baseline forced vital capacity (FVC) and forced expiratory volume in 0.2 sec ($FEV_{0.2}$) developed due the pre-treatment with NA. In NA-pretreated mice, three successive endotracheal instillations induced airway hyperreactivity (AHR), which was not specifically increased due to ClO^- exposure. Repeated NA-treatment increased the number of neutrophils in the broncho-alveolar lavage (BAL) fluid and subsequent dosing with ClO^- recruited eosinophils. Airway permeability, assessed by the total protein concentration in BAL-fluid and concentration of surfactant protein (SP)-D in serum and BAL-fluid, did not alter between the different treatment groups. Histology revealed fibrotic lesions as a result of the repeated NA-administration, while epithelial denudation and inflammation occurred due to the multiple endotracheal instillations in NA-pretreated mice.

In conclusion, implementing a vigorous treatment protocol, to impair airway barrier function and target an irritant to the lower lung resulted in nonspecific airway hypersensitivity. Repetitive NA-administration lead to a hampered recovery, and by bypassing the nose using endotracheal instillations, increased sensitivity specifically towards ClO^- was not initiated.

Introduction

In the indoor and outdoor environment humans are continuously exposed to gases, fumes, chemicals and particulates in the air, which can adversely affect the respiratory health. Respiratory irritants such as disinfectants, preservatives and cleaning products can trigger a reversible inflammatory response resulting in wheezing, cough, increased mucus secretion and bronchoconstriction upon direct contact with the respiratory system [1]. These symptoms are indicative of irritant-induced asthma (IIA). IIA is defined by development of asthma symptoms after exposure to a single high (defined as reactive airways dysfunction syndrome, RADS) or repeated lower levels of respiratory irritants, without adaptive immunological sensitization towards the causal agent [2]. Chlorine and chlorine derivatives have often been associated with development of IIA. Epidemiological studies showed that certain professions with increased chlorine exposure such as domestic cleaners, lifeguards and professional swimmers have increased risk of developing asthma, airway inflammation, hay fever and allergic rhinitis [3–9]. In mice, airway exposure to chlorine damages the airways, recruits neutrophils and macrophages towards the lung and results in development of airway hyperreactivity (AHR) [10–15].

The underlying mechanism of IIA is largely unknown, yet impaired barrier function of the respiratory epithelium is a plausible mechanism. The airway epithelium is located at the interface between the internal and external environment and forms a tight mechanical barrier to prevent entry of potential harmful agents to the host [16]. Respiratory irritants can impair barrier functioning by damaging the airway epithelium, which is associated with loss of epithelial cells and denudation of the mucosa [2,17]. This leads enhanced infiltration of inhaled agents into the subepithelial compartment, facilitating their encounter with the residing innate immune cells. Activated innate immune cells will induce pro-inflammatory responses that might contribute to the development of asthma [2]. In addition, the irritant-induced epithelial injury might restore improperly, resulting in prolonged airway hypersensitivity [1].

Previously, we showed that impairment of the airway barrier using the club-cell toxicant naphthalene (NA), followed by an intra-nasal (i.n.) exposure to the respiratory irritant hypochlorite (ClO^-) after a recovery period of fourteen days, results in development of IIA [15]. The observed response was characterized by sensory irritation upon airway exposure to the irritant, as well as development of AHR and pulmonary inflammation one day later. In the current study, we aimed to improve our model to induce a more pronounced response. Therefore we replaced the single i.n. challenge, which mainly targets the upper airways, with endotracheal instillation, whereby the lower lungs are more exposed [18,19]. To guarantee sufficient impairment of the epithelial barrier (as reflected by a decrease in body weight of the mouse), NA-treatment was performed twice with each time a recovery period of 14 days [15].

Materials and Methods

Reagents

Naphthalene (99%, CAS 91-20-3), mineral oil and acetyl-β-methylcholine chloride (≥ 98%) were obtained from Sigma-Aldrich (Bornem, Belgium). Sodium hypochlorite (10-15% active chlorine, CAS 7681-52-9) was purchased from ACROSS Organics (Geel, Belgium). Pentobarbital (Nembutal®) from Ceva Santé Animale (Brussel, Belgium) and Isoflurane (Iso-Vet, 1000mg/g) from Dechra Veterinary products NV (Belgium) was obtained via the animalium of the University of Leuven.

Animals and treatment protocol

Seven-week old male C57Bl/6J mice, obtained from Envigo (Horst, The Netherlands), were housed in a conventional animal house with 12h dark/light cycles. They were kept in individually ventilated cages (IVC) and received lightly acidified water and pelleted food *ad libitum*. The Animal Ethics Committee of the University of Leuven approved all experimental procedures (Project N°. P236-2014).

To establish a robust model of airway barrier impairment, mice received twice an intra-peritoneal (i.p.) injection with the club cell toxicant, naphthalene (NA). On days 0 and 14, a dose of 200 mg/kg body weight (BW) NA dissolved in mineral oil (MO, vehicle) (10 mL/kg BW) or vehicle only (10 mL/kg BW) was administered to the mice. After a second recovery period of 14 days, the mice received three endotracheal instillations (40µL) with 0.003% active chlorine (dosed as sodium hypochlorite in saline, ClO^-) or saline (Sal) on days 28, 31, 34, or were left untreated. One day after the last instillation, lung function was assessed followed by an autopsy to collect blood, broncho-alveolar lavage (BAL) fluid and lung tissue.

Six different treatment groups were included: MO, MO/Sal, MO/ClO^-, NA, NA/Sal, NA/ClO^-. The first abbreviation refers to the i.p. injection on days 0 and 14, being mineral oil (MO) or naphthalene (NA) and the second abbreviation refers to the endotracheal challenges on days 28, 31, 34, including non-instilled, saline (Sal) or hypochlorite (ClO^-).

Efficacy of the NA-treatment was evaluated based on the body weight of the mice. It was anticipated that if mice did not show a 10% decrease in body weight after the first or second i.p. injection with NA, the treatment was not successful and thus a NA-dependent response could not be expected, these mice were excluded from the dataset.

Pulmonary function

On day 35, one after the last endotracheal instillation, pulmonary function was assessed using the flexiVent™ FX system (SCIREC, Montreal, Canada), as described previously [20]. Briefly, mice were anesthetized with pentobarbital (70 mg/kg BW, Nembutal®), tracheotomized and ventilated.

At the start of the lung function measurements, two deep inflations (DI) were applied to maximally inflate the lungs. Next, to determine airway responsiveness, an aerosol containing increasing concentrations of the bronchoconstrictive agent methacholine (MCh) (0, 2.5, 5, 10, 20, 40 mg/mL in saline) was nebulized for 10 sec. After the aerosol exposure, the forced oscillation perturbation 'Quick Prime-3' (QP3), was executed five times over 2 minutes. The reported central airway resistance (Rn) for each concentration is the average of the accepted measurements (coefficient of determination (COD) > 0.9). After the sequence, a negative pressure forced expiration (NPFE) perturbation was performed to measure the forced vital capacity (FVC) and forced expiratory volume in 0.2 seconds ($FEV_{0.2}$) at each concentration, followed by a DI to open the lungs again. For each mouse, Rn, FVC and $FEV_{0.2}$ were plotted against Mch concentration and a dose-response curve was constructed per treatment group.

Rn, FVC and $FEV_{0.2}$ were identically measured prior to any Mch aerosol exposure to determine the baseline values for each mouse.

Inflammatory, permeability and histopathological determinations

After measuring lung function, the mice were sacrificed. Blood was collected from retro-orbital plexus, centrifuged (14000g, 4°C, 10 min) and serum samples were stored at -80°C. Surfactant protein (SP)-D concentration in serum and BAL was determined by ELISA using respectively a 1 in 4 and 1 in 1000 dilution (Duoset ELISA R&D Systems Inc., DY6839-05, limit of detection 62.5pg/mL).

The lung was lavaged, *in situ*, three times with 0.7 mL sterile saline (0.9% NaCl), and the recovered fluid was pooled. Total amount of cells in the BAL fluid was counted in a Bürker hemocytometer. The BAL fluid was centrifuged (1000 g, 4°C, 10 min), and the supernatant was stored at -80°C until further analysis. For differential cell counts, the resuspended cells were spun (300 g, 4°C, 6 min) (Cytospin 3, Shandon, TechGen, Zellik, Belgium) onto microscope slices, air-dried and stained (Diff-Quik® method, Medical Diagnostics, Düdingen, Germany). For each sample, 200 cells were counted to quantify the number of macrophages, eosinophils and neutrophils.

The protein content in the cell-free BAL fluid was determined using the Bradford method with bovine serum albumin as the standard.

The left lung was inflated and collected with a 4% paraformaldehyde solution to fix the lung tissue. The hematoxylin and eosin (H&E) stained sections were scored semi-quantitatively in a blinded manner, by an experienced pathologist for inflammation, epithelial denudation and smooth muscle cells at the bronchovascular bundle; inflammation, fibrosis, widening and emphysema at the alveoli; and inflammation at the veins.

Data analyses

The data are presented as means with standard deviation (SD). Individual mice are shown with group mean (median for the histology scores). In case of normal distribution, assessed by the Kolmogorov-Smirnov test, Bonferroni multiple comparison *post hoc* test was performed (Graph Pad Prism 5.01. Graphpad Software Inc., San Diego, USA). If data had non-normal distribution, Dunn's multiple comparison *post hoc* test was used. Time course of the body weight and dose-response curves of the Rn were analyzed using two-way ANOVA. Each treatment group was compared with the respective control group. Within the group with the same pre-treatment (i.e. MO or NA) the different endotracheal instillation treatments were compared (i.e. untreated, Sal or ClO^-). Each endotracheal instillation group (i.e. untreated, Sal or ClO^-) was compared with its respective pre-treatment group (i.e. MO or NA). A level of $p < 0.05$ (two tailed) was considered significant.

Results

Treatment with NA induced a transient decrease in body weight

The first days following each i.p. injection with NA, the mice lost approximately 10% of their original BW (i.e. day 0, before the i.p. injection, Fig. 1). The NA/Sal and NA/ClO^- groups had a significantly lower BW at certain time points, compared to respectively the MO/Sal and MO/ClO^- groups. On day 35, the BW of the treatment groups was similar.

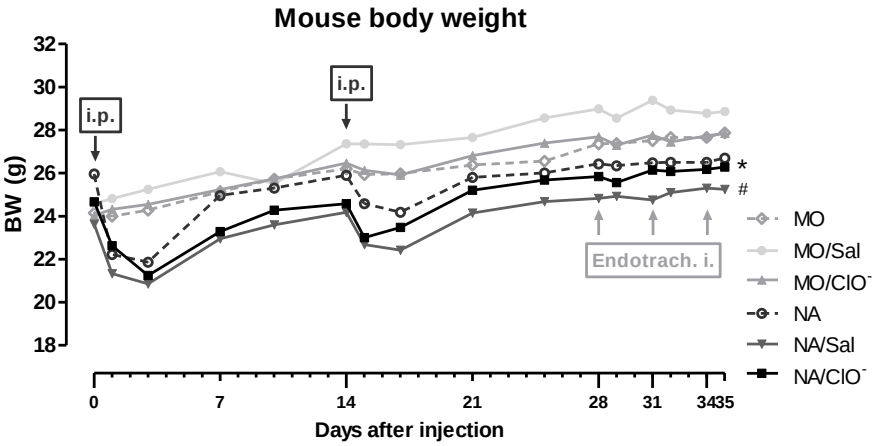

Figure 1. Time course of changes in body weight
Mice were injected intra-peritoneal (i.p.) with vehicle (MO) or naphthalene (NA) on days 0 and 14, received endotracheal instillations (endotrach. i.) with saline (Sal) or hypochlorite (ClO^-), or were not instilled, on days 28, 31, 34 and were sacrificed one day later. Body weight was recorded before (day 0) and at regular time points until the end of the experiment. $^{\#}p < 0.05$ compared to the respective control MO/Sal, $^{*}p < 0.05$ compared to the respective control MO/ClO^-. Data is presented as mean only. n=4-6 per group.

Pretreatment with NA resulted in increased lung volumes and subsequent endotracheal instillations induced airway hyperresponsiveness

The negative pressure forced expiration perturbation on the flexiVent, showed that baseline lung volumes (FVC and $FEV_{0.2}$) of the NA-pretreated mice were higher (Fig. 2a and b). A statistically significant difference was found for the baseline FVC and $FEV_{0.2}$ of the non-instilled NA group and NA/Sal group compared to their respective control group.

The NA/Sal and NA/ClO^--treated mice groups showed significantly increased responsiveness of the large airways after MCh exposure in comparison to their respective MO-pretreated mice group (Fig. 2c). Endotracheal challenge with hypochlorite did not result in a different response within the MO- or NA-pretreated groups respectively. At baseline the airway resistance of the treatment groups did not differ (data not shown).

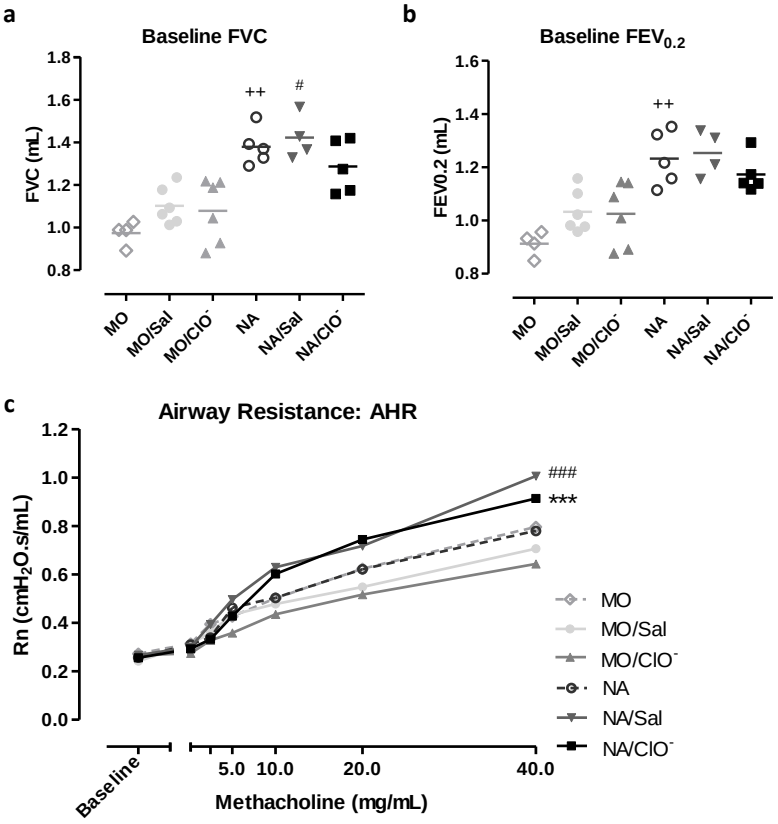

Figure 2. Pulmonary function 24h after the last endotracheal challenge
Twenty-four hours after the last endotracheal instillation, lung function was assessed by negative pressure-driven forced expiration (NFPE) maneuvers and forced oscillations; that were performed at baseline and after each Mch concentration (0-40 mg/mL). Individual and mean group baseline values for FVC and $FEV_{0.2}$ are shown in a) and b). The mean dose-response for Rn against the Mch concentration is shown in c). $^{+}p < 0.05$ and $^{++}p < 0.01$ compared to the respective control MO, $^{\#}p < 0.05$ and $^{\#\#\#}p < 0.001$ compared to the respective control MO/Sal, ***$p < 0.001$ compared to the respective control MO/ClO^{-}. n= 4-6 per group.

NA-pretreatment and ClO^{-}-challenges altered pulmonary inflammation

At the time of sacrifice, no death cells were present in the BAL fluid (data not shown). Differential analysis of the BAL fluid demonstrated a significant influx of neutrophils in the non-instilled NA and NA/Sal-mice compared to their respective control group (Fig. 3). Within the NA-pretreated mice, the NA/ClO^{-} -treated mice had increased numbers of eosinophils compared to the non-instilled NA mice (Fig. 3).

NA-pretreatment and ClO^{-}-challenges minimally altered permeability parameters

The BAL protein concentration was slightly higher in the NA-pretreated mice compared to the MO-pretreated mice, yet no statistical differences where present (Fig. 4a). SP-D concentration in the serum did not differ significantly between the different treatment groups (Fig. 4b). The concentration of SP-D in the BAL-fluid of NA-pretreated mice was higher than that in MO-pretreated mice. This difference was statistically different for the NA compared to the MO groups (Fig.4c).

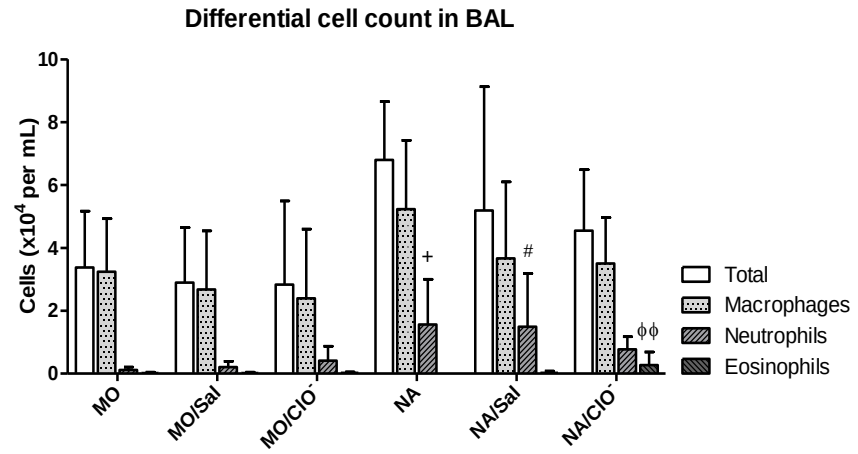

Figure 3. Pulmonary inflammation on day 35
The total cell count and total numbers of macrophages, neutrophils and eosinophils determined in the BAL fluid are shown. Data is presented as mean ± SD. $^{+}p < 0.05$ compared to the respective control MO, $^{\#}p < 0.05$ compared to the respective control MO/Sal, $^{\Phi\Phi}p < 0.01$ compared to NA. n= 4-6 per group.

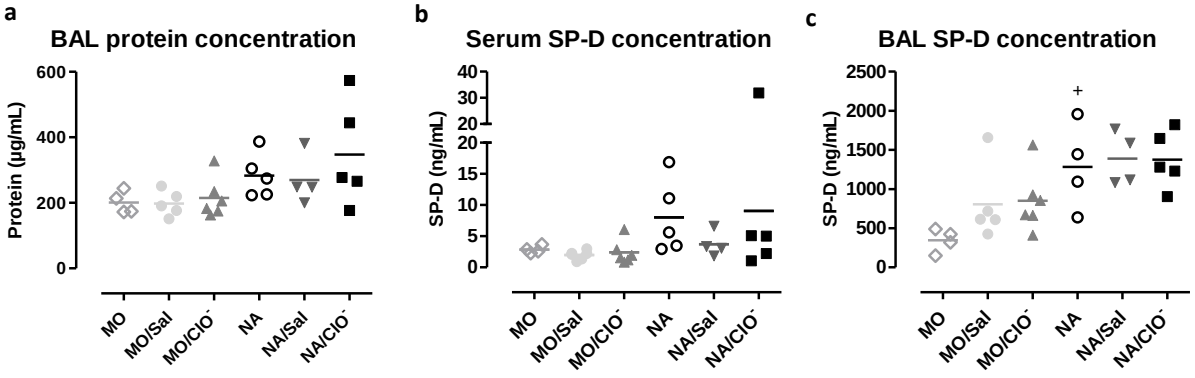

Figure 4. Permeability parameters on day 35
Individual and mean group values of the protein concentration in the BAL fluid, is shown in a). The individual and group mean serum and BAL-fluid SP-D concentrations measured with ELISA, are shown in b) and c). $^{+}p < 0.05$ compared to the respective control MO. n= 4-6 per group.

Endotracheal instillations induced epithelial denudation and inflammatory lesions in NA-pretreated mice

Histological abnormalities including epithelial denudation, inflammation at the bronchovascular bundle, alveoli and veins or interstitial alterations were present in the NA-pretreated mice, while the MO-mice had no or only mild signs of inflammation (Fig. 5f). Signs of increased smooth muscle cells, alveolar widening or emphysema were absent (data not shown). Blinded scoring by an experienced pathologist indicated that epithelial denudation was significantly more present in the NA/Sal and NA/ClO^--mice, compared to their respective control groups (Fig. 5a). The non-instilled NA-mice had like the non-instilled MO-mice no signs of epithelial denudation. NA/ClO^--treated mice, had a significant higher score for inflammation at the bronchovascular bundle than MO/ClO^--treated mice (Fig. 5b). Inflammation at the veins and alveoli was significantly more present in the NA/Sal and NA/ClO^--group,

in comparison with their respective control groups (Fig. 5c and d). Repeated administration of NA induced fibrotic lesions in the NA-pretreated mice, with a statistical higher score in the NA/Sal-group/Sal (Fig. 5e).

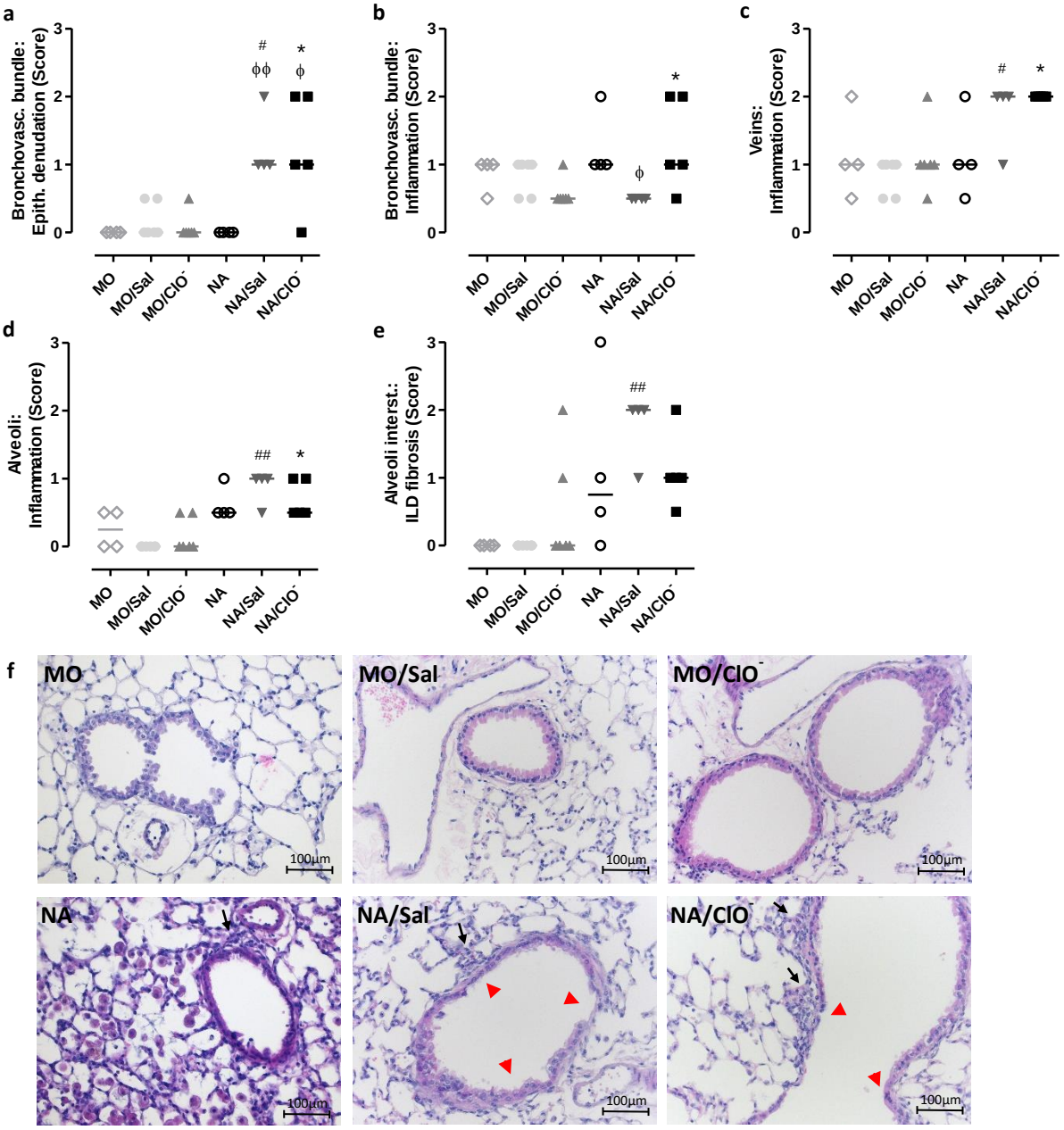

Figure 5. Histology of the lungs on day 35

During autopsy, the left lung was collected for histology and scored from 0 to 3 in for a) epithelial denudation, b), c) and d) inflammation at respectively the bronchovascular bundle, the veins and alveoli, and e) fibrotic lesions in the alveolar interstitium. The individual scores and group median are depicted on the graphs. Representative images of the H&E stained lung sections taken with 200x amplification are shown for each treatment group in f). Red arrowheads indicate epithelial denudation and black arrows indicate inflammation. $^{\#}p < 0.05$ and $^{\#\#}p < 0.01$ compared to the respective control MO/Sal, $^{*}p < 0.05$ compared to the respective control MO/ClO^-, and $^{\Phi}p < 0.05$ and $^{\Phi\Phi}p < 0.01$ compared to NA. n= 4-6 per group.

Discussion

Double airway barrier impairment using NA, with subsequent recovery periods, led to increased functional lung volumes (baseline FVC and $FEV_{0.2}$). In combination with three endotracheal instillations, the NA-pretreated mice developed nonspecific AHR. Exposure to ClO^- at this time point did not augment the airway responses. The inflammatory infiltrate in the BAL fluid indicated an increase in neutrophils due to NA-pretreatment, and an increase in eosinophils due to ClO^--instillation. Airway permeability, assessed by BAL protein concentration and SP-D concentration in serum and BAL, did not consistently differ between the different treatment groups, at this time point. On a histological level, the NA-pretreated mice that were endotracheally instilled had more signs of epithelial denudation and inflammation, than the MO-pretreated mice. Successive treatment with NA induced fibrotic lesions.

In a previous study, we showed that airway barrier impairment, followed by a single i.n. instillation with ClO^- resulted in airway hypersensitivity [15]. Starting from these data, we wanted to initiate a more robust IIA response, by implementing a more rigorous treatment protocol. This consisted of two successive i.p. injections with NA, with each time a recovery period of 14 days, followed by repeated ClO^- exposure, using endotracheal instillation, to target the irritant deeper into the lungs.

In the current study we could only partially confirm the findings made in our previous study. Single as well as successive dosing with NA resulted in an increase in functional lung volumes, indicating that airway barrier impairment results in structural changes in the lungs. However, in our former study mice received only a single i.n. challenge with ClO^- after single pre-treatment with NA developed AHR specifically after exposure to ClO^-, whereas in the current study a double NA-treatment followed by successive endotracheal instillations induced AHR, irrespective of the challenging agent. Two NA-treatments resulted in increased numbers of neutrophils in the BAL-fluid, which was not assessed with non-instilled mice after single airway barrier impairment. ClO^- exposure recruited eosinophils towards the lungs both after a single i.n. and triple endotracheal instillations. Previously, we demonstrated increased BAL protein levels and serum SP-D levels due to combined NA and ClO^--treatment, while these parameters, indicating airway permeability, yielded inconclusive data in the current study. Epithelial denudation and inflammation at the bronchovascular bundle were present in the NA-pretreated mice due to the repetitive endotracheal challenge (irrespective of the challenge agent), while after a single i.n. challenge these lesions were specifically induced by the ClO^--exposure in NA-pretreated mice.

In the current treatment protocol, mice received double i.p. injections with NA, to guarantee sufficient impairment of the airway barrier. Repeated dosing with NA might alter the metabolisation of NA, which might result in altered biological responses. Previous studies have reported that the airway

epithelium of mice appeared normal with only minor epithelial alterations after seven daily exposures to NA. This was explained by decreased expression of cytochrome P450 monooxygenases in the bronchiolar epithelium that are responsible for formation of the toxic NA-epoxide [21–23]. Although not fully investigated, this mechanism is less likely with an interval of 14 days. West et al. demonstrated that after a 96-hour recuperation period, susceptibility to NA had returned [23]. In addition, Aoshiba et al. clearly found epithelial and fibrotic lesions after weekly exposure to NA for 14 weeks [24]. Since there was each time a decrease in BW following the NA-administration and there were epithelial lesions, we can presume that the mice remained sensitive to the harmful effect of NA.

After each barrier impairment with NA, a period of 14 days to recuperate was included. Within this period, after an initial loss of the targeted club cells, the surviving progenitor cells at the bronchioles establish a new epithelial sheet which structurally resembles the normal epithelium [25,26]. We observed that although there was each time a recovery period of 14 days, repeated NA-administration was more difficult to manage for the mice, and they did not fully recover. Irrespective whether the mice received endotracheal challenges or not, NA-pretreated mice had increased numbers of neutrophils, pointing out that 21 days after the last i.p. injection, inflammation due to NA-treatment was still present. On histology, the NA-pretreated mice still had epithelial alterations and signs of inflammation due to the endotracheal challenge 'act'. Both NA-pretreated mice groups that received endotracheal instillations had AHR, indicating that the repeated airway damaging events rendered the mice more sensitive to any kind of airway exposure. In contrast to previous study, the airway response was not additionally augmented specifically to due ClO^- exposure. Possibly, because of the incomplete recuperation, also the vehicle (saline) induced irritation and ClO^--specific airway responses did not develop because the ongoing airway inflammation made it more difficult for the ClO^- to reach the airways. We did observe eosinophil recruitment specifically due to ClO^- exposure, indicating that a distinct inflammatory response is initiated in these mice.

Instead of using an i.n. instillation technique, the mice received three successive endotracheal instillations to dose the solution to the lungs. The distribution of a solution towards the lungs of mice is strongly affected by the delivery method and volume. According to Southampton et al., approximately 40% of the delivered radioactivity is detectable in the lungs of isoflurane-anaesthetized mice after i.n. instillation of 25µL ^{99m}Tc-labelled sulfide colloid (SC) solution, which is extensively lower in unanaesthetized mice (approx. 5%) [18]. In contrast, 60 and 80 % of respectively 25 and 50 µL administered ^{99m}Tc-labelled SC solution reaches the lungs following endotracheal instillation [19]. Although a substantial dose would reach the lower airways and contrary to previous findings, endotracheal instillation did not provoke a vigorous influx of inflammatory cells towards he BAL-fluid in the current study [27]. In both non-instilled and endotracheal instilled mice the level of pulmonary

inflammation was comparable, indicating that repeated NA-treatment resulted in the increase in neutrophils in the BAL-fluid. However, irrespective to the challenging agent, three successive endotracheal treatments led to epithelial denudation and inflammation at the bronchovascular bundle, and induced AHR in NA-pretreated mice. Apparently, deep penetration of the solution by endotracheal instillation, disturbed the epithelium and lungs, and increased the sensitivity of the airways in NA-treated mice.

By dosing the mice with ClO^- via the endotracheal route instead of i.n. route, we by-passed sensing of the chemical by the nose. A crosstalk between nose and lung has been proven, and might play an important role in generation of airway responses. Hens *et al*. demonstrated that although the nose and lungs were separated by tracheostomy, selective nasal allergen provocation still lead to the development of bronchial hyperreactivity in allergic mice [28]. Upregulation of substance P (SP) and neurokinin 1 receptor in the pulmonary nerves, suggest a neuronal mechanism in the communication between nose and lung [28]. Neuronal involvement due to activation of transient receptor potential (TRP) A1 receptors, that are highly expressed on the trigeminal nerve that innervate the nasal cavity, has been shown to play a crucial role in generation of bronchial hyperreactivity in allergic (OVA), chemical (TDI) and irritant (HClO) induced asthma [29–32]. Upon activation of TRPA1, neuropeptides, such as SP, neurokinin A and B are released from the sensory nerves, which induce a local inflammatory response termed 'neurogenic inflammation', that is responsible for mast cell degranulation, vasodilatation, mucus hypersecretion and airway contraction [33,34]. It is very likely that due to the endotracheal instillation, this naso-bronchial crosstalk is absent in the current study, while after the single i.n. instillation with ClO^-, this could explain the observed increased AHR.

In conclusion, a vigorous treatment protocol consisting of repeated administration of NA, to impair the airway barrier, followed by irritant exposure deep into the lungs using successive endotracheal instillations in order to induce IIA, resulted in nonspecific airway hypersensitivity rather than a specific hypersensitivity. This study adds that due to insufficient recuperation from airway barrier impairment, mice become more sensitive to airway exposures, and that sensing of the irritant chemical by e.g. TRP channels in the nose probably plays an important role in the development of specific airway responses.

Acknowledgments: This project was supported by a grant from the University of Leuven Research Council (GOA/14/011 and C24/17/061) and a grant of the Flemish Research Foundation (research grant 1504912N).

Conflict of interest: The authors declare no conflict of interest.

References

1. Brooks, S. M. & Bernstein, I. L. Irritant-Induced Airway Disorders. *Immunol. Allergy Clin. North Am.* **31,** 747–768 (2011).
2. Vandenplas, O. *et al.* EAACI position paper: irritant-induced asthma. *Allergy* **69,** 1141–1153 (2014).
3. Bernard, A., Nickmilder, M., Voisin, C. & Sardella, A. Impact of chlorinated swimming pool attendance on the respiratory health of adolescents. *Pediatrics* **124,** 1110–1118 (2009).
4. Jacobs, J. H. *et al.* Exposure to trichloramine and respiratory symptoms in indoor swimming pool workers. *Eur. Respir. J.* **29,** 690–698 (2007).
5. Folletti, I., Zock, J.-P., Moscato, G. & Siracusa, A. Asthma and rhinitis in cleaning workers: a systematic review of epidemiological studies. *J. Asthma Off. J. Assoc. Care Asthma* **51,** 18–28 (2014).
6. Zock, J.-P., Vizcaya, D. & Le Moual, N. Update on asthma and cleaners. *Curr. Opin. Allergy Clin. Immunol.* **10,** 114–120 (2010).
7. Nordberg, G. F. *et al.* Lung function in volunteers before and after exposure to trichloramine in indoor pool environments and asthma in a cohort of pool workers. *BMJ Open* **2,** (2012).
8. Rosenman, K. D. *et al.* Swimming facilities and work-related asthma. *J. Asthma Off. J. Assoc. Care Asthma* **52,** 52–58 (2015).
9. Romberg, K., Tufvesson, E. & Bjermer, L. Asthma is more prevalent in elite swimming adolescents despite better mental and physical health. *Scand. J. Med. Sci. Sports* **22,** 362–371 (2012).
10. Jonasson, S., Koch, B. & Bucht, A. Inhalation of chlorine causes long-standing lung inflammation and airway hyperresponsiveness in a murine model of chemical-induced lung injury. *Toxicology* **303,** 34–42 (2013).
11. Martin, J. G. *et al.* Chlorine-induced injury to the airways in mice. *Am. J. Respir. Crit. Care Med.* **168,** 568–574 (2003).
12. McGovern, T. K. *et al.* Neutrophils mediate airway hyperresponsiveness after chlorine-induced airway injury in the mouse. *Am. J. Respir. Cell Mol. Biol.* **52,** 513–522 (2015).
13. Tuck, S. A. *et al.* Time course of airway remodelling after an acute chlorine gas exposure in mice. *Respir. Res.* **9,** 61 (2008).
14. Wigenstam, E., Elfsmark, L., Koch, B., Bucht, A. & Jonasson, S. Acute respiratory changes and pulmonary inflammation involving a pathway of TGF-β1 induction in a rat model of chlorine-induced lung injury. *Toxicol. Appl. Pharmacol.* **309,** 44–54 (2016).
15. Van Den Broucke, S. *et al.* Irritant-induced asthma to hypochlorite in mice due to impairment of the airway barrier. *Arch. Toxicol.* (2018). doi:10.1007/s00204-018-2161-8
16. Rezaee, F. & Georas, S. N. Breaking Barriers. New Insights into Airway Epithelial Barrier Function in Health and Disease. *Am. J. Respir. Cell Mol. Biol.* **50,** 857–869 (2014).
17. Brooks, S. M., Malo, J.-L. & Gautrin, D. Irritant-induced asthma and reactive airways dysfunction syndrome. in *Asthma in the workplace* **21,** (2013).
18. Southam, D. S., Dolovich, M., O'Byrne, P. M. & Inman, M. D. Distribution of intranasal instillations in mice: effects of volume, time, body position, and anesthesia. *Am. J. Physiol. Lung Cell. Mol. Physiol.* **282,** L833-839 (2002).
19. Foster, W. M., Walters, D. M., Longphre, M., Macri, K. & Miller, L. M. Methodology for the measurement of mucociliary function in the mouse by scintigraphy. *J. Appl. Physiol. Bethesda Md 1985* **90,** 1111–1117 (2001).
20. Devos, F. C. *et al.* Forced expiration measurements in mouse models of obstructive and restrictive lung diseases. *Respir. Res.* **18,** 123 (2017).
21. Lakritz, J. *et al.* Cellular and metabolic basis of Clara cell tolerance to multiple doses of cytochrome P450-activated cytotoxicants. I: Bronchiolar epithelial reorganization and expression of cytochrome P450 monooxygenases in mice exposed to multiple doses of naphthalene. *J. Pharmacol. Exp. Ther.* **278,** 1408–1418 (1996).
22. West, J. A. A., Winkle, L. S. V., Morin, D., Fleschner, C. A. & Forman, H. J. *Repeated Inhalation Exposures to the Bioactivated Cytotoxicant Naphthalene (NA) Produce Airway-Specific Clara Cell Tolerance in Mice*. (2003).
23. West, J. A., Buckpitt, A. R. & Plopper, C. G. Elevated airway GSH resynthesis confers protection to Clara cells from naphthalene injury in mice made tolerant by repeated exposures. *J. Pharmacol. Exp. Ther.* **294,** 516–523 (2000).

24. Aoshiba, K. *et al.* A murine model of airway fibrosis induced by repeated naphthalene exposure. *Exp. Toxicol. Pathol. Off. J. Ges. Toxikol. Pathol.* **66,** 169–177 (2014).
25. Van Winkle, L. S., Buckpitt, A. R., Nishio, S. J., Isaac, J. M. & Plopper, C. G. Cellular response in naphthalene-induced Clara cell injury and bronchiolar epithelial repair in mice. *Am. J. Physiol.* **269,** L800-818 (1995).
26. Van Winkle, L. S., Johnson, Z. A., Nishio, S. J., Brown, C. D. & Plopper, C. G. Early events in naphthalene-induced acute Clara cell toxicity: comparison of membrane permeability and ultrastructure. *Am. J. Respir. Cell Mol. Biol.* **21,** 44–53 (1999).
27. De Vooght, V. *et al.* Oropharyngeal aspiration: an alternative route for challenging in a mouse model of chemical-induced asthma. *Toxicology* **259,** 84–89 (2009).
28. Hens, G. *et al.* Selective nasal allergen provocation induces substance P-mediated bronchial hyperresponsiveness. *Am. J. Respir. Cell Mol. Biol.* **44,** 517–523 (2011).
29. Devos, F. C. *et al.* Neuro-immune interactions in chemical-induced airway hyperreactivity. *Eur. Respir. J.* **48,** 380–392 (2016).
30. Hox, V. *et al.* Crucial role of transient receptor potential ankyrin 1 and mast cells in induction of nonallergic airway hyperreactivity in mice. *Am. J. Respir. Crit. Care Med.* **187,** 486–493 (2013).
31. Caceres, A. I. *et al.* A sensory neuronal ion channel essential for airway inflammation and hyperreactivity in asthma. *Proc. Natl. Acad. Sci. U. S. A.* **106,** 9099–9104 (2009).
32. Bessac, B. F. *et al.* Transient receptor potential ankyrin 1 antagonists block the noxious effects of toxic industrial isocyanates and tear gases. *FASEB J. Off. Publ. Fed. Am. Soc. Exp. Biol.* **23,** 1102–1114 (2009).
33. Grace, M. S., Baxter, M., Dubuis, E., Birrell, M. A. & Belvisi, M. G. Transient receptor potential (TRP) channels in the airway: role in airway disease. *Br. J. Pharmacol.* **171,** 2593–2607 (2014).
34. Barnes, P. J. Neurogenic inflammation in the airways. *Respir. Physiol.* **125,** 145–154 (2001).

Chapter 7

General discussion

1. Summary of the findings

Part I. Study the effect of environmental irritants on the respiratory epithelial barrier – *in vitro*

The respiratory epithelium is the first barrier encountered by inhaled respiratory irritants. Therefore, we investigated the effects of different environmental irritants on the airway epithelial barrier function *in vitro*.

Effect of irritants on a co-culture model of the airway barrier (chapter 3)

In the first study of this thesis, we demonstrated that different types of environmental irritants have different effects on an *in vitro* model of the airway epithelial barrier. The nanoparticles graphene (G) and graphene oxide (GO) immediately had a negative impact on the epithelial barrier, whereas hypochlorite (ClO^-) only had a negative impact 24 hours after exposure. Both ammonium- and sodium persulfate (AP and SP) salt did not affect the barrier properties. In addition, we showed, that if the graphene nanoparticles (GNPs) were suspended in a presumed more physiologically relevant suspension with dipalmitoylphosphadidylcholine (DPPC), the GNPs had a minimal effect on the epithelial barrier. Next, immunofluorescent staining of ZO-1 and occludin, indicated that co-cultures exposed to G or GO had a slightly less connected tight junction (TJ) network. In a large set of membrane-associated proteins, we found using phosphoproteomics that the proteins in the adherens junction (AJ) and TJ pathways had an altered phosphorylation due to the GNP exposure, thereby providing an explanation for the observed negative effect of the GNPs on the airway epithelial barrier *in vitro*.

Contribution of mast cells in irritant-induced airway epithelial barrier impairment *in vitro* (chapter 4)

To study the possible contribution of mast cells in irritant-induced epithelial barrier impairment, bronchial epithelial cells (16HBE) were cultured alone, or in presence of mast cells (HMC-1) on the basolateral or apical side of the epithelial cell layer, and exposed to the environmental irritants. G and GO had a persistent negative impact on the epithelial barrier, whereas diesel exhaust particles (DEP) and ClO^- transiently affected the epithelial barrier, in each of the tested seeding conditions. Upon exposure to environmental irritants, 16HBE cells did not release danger signals and HMC-1 cells were not activated. The Ca^{2+} ionophore ionomycin minimally altered the barrier function in each of the tested cultures and activated the HMC-1 cells in limited extent. To conclude, due to the inactivated (or immature) state of the HMC-1 cells, these did not influence the epithelial barrier integrity upon environmental exposure, and thus currently do not provide additional information as an underlying mechanism in irritant-induced asthma (IIA).

Part II. Study airway hypersensitivity following airway barrier impairment – *in vivo*

In the second part of this thesis, we investigated whether incomplete repair of the epithelium after targeted damage, would lead to increased airway sensitivity when the lungs are exposed to low levels of irritants, as in IIA. To test this hypothesis, we combined the mouse model of naphthalene (NA)-induced airway epithelial injury with an airway exposure to the common chemical irritant hypochlorite.

Irritant-induced asthma to hypochlorite in mice due to impairment of the airway barrier (chapter 5)

We demonstrated that NA-induced barrier impairment resulted in a temporary enlargement of the lungs and airways, and persistent increased functional lung volumes. ClO^- challenge, after a 14-days period of repair, in NA-pretreated mice resulted in a sensory irritant response immediately following the airway exposure, as well as development of airway hyperresponsiveness (AHR) and pulmonary inflammation one day later. The increase in airway permeability and epithelial denudation after ClO^- exposure indicated that the NA-induced barrier impairment left the epithelium more vulnerable for the irritant effect of ClO^-. Moreover, the NA-induced epithelial dysfunction resulted in recruitment of monocyte-derived dendritic cells (moDCs) to the lung and an additional insult with ClO^- upregulated the pulmonary type 2 innate lymphoid cell (ILC) population. Hereby we proved that NA-induced lung impairment renders the lungs of mice more sensitive to an airway challenge with ClO^-, confirming our hypothesis that incomplete barrier repair, followed by irritant exposure results in airway hypersensitivity.

Airway barrier impairment increases nonspecific airway hyperresponsiveness in mice (chapter 6)

Next, we introduced a more rigorous airway barrier impairment, by doubling the NA treatment, which then was followed by repeated endotracheal exposures to ClO^-. Successive airway barrier impairment transiently decreased the body weight (BW) of mice following each treatment with NA, and resulted in increased the functional lung volumes, neutrophil recruitment towards the lung and epithelial damage after a recovery period. In combination with the endotracheal instillations, repeated airway barrier impairment, resulted in nonspecific AHR. Exposure to ClO^- did not augment the airway responses and epithelial damage, but did increase the number of eosinophils in the lung. Using this treatment protocol the mice were not specifically sensitive to ClO^-, but were more sensitive to nonspecific stimuli.

2. Relevance and limitations

The airway epithelium plays a very important role in the first line defense against inhaled foreign pathogens and irritants. We investigated in detail both *in vitro* (part I, **chapter 3** and **4**) as *in vivo* (part II, **chapter 5** and **6**), the airway epithelial responses after exposure to noxious irritants, to determine a plausible mechanism underlying IIA.

Chlorine is the most common reported cause of IIA [1,2]. Therefore, it was selected as a stressor in both the *in vitro* and *the in vivo* part of this thesis, to evaluate the effect of on the airway epithelial barrier. ClO^- exposure did not clearly result in epithelial barrier impairment in the *in vitro* studies. Using a mouse model of airway barrier impairment with NA, followed by airway exposure to ClO^-, we specifically investigated the effect of hypochlorite exposure *in vivo*. After a single barrier impairment and a single i.n. challenge with hypochlorite, we observed that mice became more sensitive to ClO^-. Airway permeability and epithelial denudation increased due to ClO^- in NA-pretreated mice, indicating that ClO^- was able to alter the epithelial barrier function, but only after a previous epithelial injury. In this respect, it is difficult to link the *in vitro* and *in vivo* findings to each other.

We evaluated in detail the effect of the GNPs on the airway epithelial barrier *in vitro*. Since their discovery, GNPs have gained a lot of attention and the number applications grew, making the risk for human exposure more and more likely. At the same time due to their sheet-like shape, the concern that these particles might have detrimental effects after inhalation rose, and both *in vitro* and *in vivo* studies to evaluate the toxicity of GNPs were undertaken [3]. *In vitro* studies focused mostly on cytotoxicity to different cell types and evaluated ROS generation, inflammation and apoptosis [3–8]. A firm conclusion on the toxicity of the GNPs *in vitro* is however difficult to derive, since this depends on the layer number, lateral dimension, functionalization of the particle, and method of exposure [3,5,9]. We are the first to evaluate the effect of sub-toxic concentrations of GNPs on the airway epithelial barrier functioning. At this stage, we did not evaluate the effect of GNP exposure *in vivo*. Various studies evaluated the pulmonary toxicity of GNPs following airway exposure. Briefly summarized it was found that G and GO induced pulmonary inflammation that can persist and evolve to fibrosis with increasing concentrations, that aggregated G and larger sized GO caused stronger inflammatory responses and that the GNP can retain in the lungs for longer periods [10]. In addition, disruption of the alveolar-capillary barrier and increased alveolar permeability were demonstrated [11,12].

In the first part of this thesis, we investigated the effect of different types of environmental irritants on the airway epithelial barrier *in vitro*, by investigating the resistance and permeability of the cell layer, and investigated alterations in TJ or AJ functioning due to the irritant exposure. In the second part of this thesis, we induced airway epithelial barrier impairment using selective depletion/death of

club cells in the respiratory tract, and investigated the consequences of this barrier impairment on irritant exposure. These approaches are different, but evaluate both relevant mechanisms of epithelial alterations that occur in asthma [13]. Using immunohistochemistry of tissue sections and cultured bronchial epithelial cells, it was demonstrated that TJs are disrupted in asthmatic patients [14]. In addition, impaired proliferation of basal and club cells has been described in asthma, resulting in an impaired repair. The epithelial alterations observed after specific club cell depletion in mice, resemble those found in asthmatic patients [13]. Another approach, that could make a more coherent story, is the administration of the biopolymer chitosan, that transiently opens the TJ between adjacent epithelial cells *in vitro*, as well as *in vivo* [15]. However, its effects on the adaptive immune system might have hampered our aimed irritant-induced observations [16].

In this dissertation, we specifically focused on the effect of respiratory irritants on the airway epithelial barrier and its interaction with cells of the innate immune system to elucidate underlying mechanisms for IIA. Yet, it should be remarked that these mechanisms might also be involved in other chronic lung diseases. In chapter 3, we observed a decrease in epithelial barrier function, suggestive of epithelial-to-mesenchymal transition (EMT) due to NP exposure, and repeated barrier impairment in chapter 6 resulted in fibrotic lesions. EMT and subepithelial fibrosis are structural alterations occurring in asthmatics, as well as in patients with COPD, cystic fibrosis and interstitial lung diseases. It has been suggested that these lung diseases are not that distinct and can be regarded as a single disease entity that has a different outcome depending on endogenous factors and exogenous factors. In this respect, we could put our work in a broader perspective whereby we studied the effect of environmental agents on the airway epithelial barrier, which may be an initiating event in various chronic lung diseases.

2.1. Study the effect of environmental irritants on the airway epithelial barrier – *in vitro*

Modelling the airway epithelial barrier *in vitro*

In order to investigate the effect of environmental irritants on the airway epithelial barrier *in vitro*, a relevant model that mimics the human lung epithelium is essential. Airway epithelial cells *in vitro* are available as continuous cell lines or as primary cells. An advantage of cell lines is their ability to divide infinitely, which makes them easy to expand and cheap to culture, resulting in reproducible data. However, cell lines often fail to recapitulate certain characteristics of an *in vivo* epithelium. Primary epithelial cells in contrast have a limited dividing capacity, yet they retain the capacity to differentiate when cultured at air-liquid interface (ALI), hereby resembling more the *in vivo* epithelium. Disadvantages of primary cells is that the isolation and culturing can be time-consuming and expensive and that donor variability can hamper the results [17]. Various methods and techniques have been developed to create a physiological relevant epithelial barrier of the lung. Monocultures have been

proven valuable in the past and allow for large throughput analysis of compounds, however, they over-simplify the *in vivo* situation, where different cell types communicate with, or are connected to each other. To capture this complex interplay between the distinct cells types of the human airways, co-culture systems have been developed [17–25]. Culturing primary epithelial cell monocultures or co-cultures at air-liquid interface is becoming increasingly conventional. The fact that epithelial cells from bronchial biopsies can differentiate into ciliated, secretory and basal cells, makes that in this method the pseudostratified epithelium is closer mimicked [26,27]. Another advantage of culturing cells at air-liquid is that cells are exposed to air and can, as happens during inhalation, be exposed to airborne compounds. Exposing cells to aerosolized chemicals or particles, reduce the possible alterations that occur while dissolving or suspending the agents in culture medium, and represent the real-life exposure. However, these exposure methods are complex and technical, and require specialized (and expensive) exposure equipment [25].

The epithelial cells used in this project are cells from the bronchial epithelial cell line $16HBE_{14o-}$, that was developed by the transformation and immortalization of normal bronchial epithelial cells obtained from a 1-year-old male heart and lung transplant patient. These cells are cuboidal and form polarized monolayers with extensive TJ belts, which makes this cell line a useful tool to study barrier properties [28,29]. In **chapter 3**, these cells were co-cultured with human lung microvascular endothelial cells (HLMVEC) at the basolateral side of the transwell insert, together with cells of the THP-1 cell line added in a later stage to the apical compartment. We admit that culturing the endothelial cells directly underneath the epithelial cells, is not a perfect mimic for the airway epithelium. In this way, our co-culture has characteristics of the alveolar barrier where epithelial cells and endothelial cells are closely linked to each other and alveolar macrophages represent the main clearance mechanism. We did not use the A549 cell line that represents the alveolar type II cell because they lack the ability to form a strong barrier, which was our main outcome parameter [30,31].

In **chapter 4**, bronchial epithelial cells were cultured together with mast cells of the HMC-1 cell line. The mast cells were seeded underneath or on top of the epithelial layer, to mimic the healthy state where mast cells are located in the subepithelium or a diseased state where mast cells are recruited into the lumen of the airways. By using only two distinct cell types, we could specifically study the interaction between the epithelial barrier and mast cells upon environmental exposure. As discussed in chapter 4, the HMC-1 cells represent an immature type of mast cells and we have to admit that for mast cell responses the use of primary human mast cells would have resulted in conclusions that were more meaningful.

Evaluating the barrier properties in the airway epithelium

Airway epithelial cells create a selectively permeable barrier in which paracellular diffusion of ions and hydrophilic nonionic macromolecules occurs based on charge and size [32]. Transepithelial electrical resistance (TEER) is a measure for ion permeability, as this technique is based on the difference in electric potential due to movements of ions across the cell layer [24]. TEER values are quite variable depending on the culture conditions, therefore we expressed our TEER measurements as percentage of the baseline value. Paracellular permeability of hydrophilic macromolecules is often monitored with fluorescently labelled dextrans, which have the advantage to exist in different sizes, allowing a more elaborate analysis of the barrier permeability [32]. We applied a relatively small 4 kDa sized FITC-labeled dextran on the apical side of the epithelial cell layer and measured, after an incubation period to allow passage, its accumulation in the basolateral compartment using fluorometry. The flux was determined by dividing the volume and FD4-concentration of the basolateral compartment with the volume and FD4-concentration in the apical compartment. It can be noted that the FD4-flux of the exposed co-cultures in chapter 4 is fairly larger than that in chapter 3. This discrepancy can be explained by the fact that in chapter 4 there a no endothelial cells basolateral from the epithelial cells that might hinder the FD4 transport, the FD4-flux was determined 28h after the start of exposure (instead of after 24h) and another fluorescence plater reader was used which might have had more sensitive settings.

Proteins of the TJ and AJ are responsible for the barrier function and cell-cell adhesion in the airway epithelium. Immunofluorecence and confocal microscopy is a widely used technique to visualize the TJ and AJ protein network. In intact epithelial layers the commonly analyzed proteins occludin, cadherin, or ZO-1, 2 or 3 form a honeycomb-like connected network [24]. In chapter 3, the pattern of ZO-1 and occludin staining in the G or GO-exposed co-cultures seemed less connected. Since we used relatively high concentrations of the GNPs, which appear black on the images, we could however not distinguish the ‘disorganisation of the TJ network’ from the particles, which made this a rather subjective finding.

Another method to assess the TJ and AJ proteins, is quantification of these proteins using qPCR or Western Blot. However, sometimes these measures do not reflect the functioning of the proteins, as reduced translation of the mRNA, degradation of the protein or post-translational modifications can occur due to the assessed stimulus [14,33–35]. Altered phosphorylation of TJ and AJ proteins has been associated with altered epithelial barrier function [36,37]. We are the first to use phosphoproteomics to screen for alterations in phosphorylation status of TJ and AJ proteins, to explain the observed reduced barrier function following GNP-exposure in chapter 3. Functional analysis of the differentially phosphorylated proteins in the membrane fraction lysate revealed that indeed the proteins in the TJ and AJ KEGG pathway were significantly enriched. In general, phosphorylation of TJ and AJ proteins on

tyrosine residues is associated with reduced protein-protein interactions and decreased barrier integrity [36–40]. In our dataset, not many tyrosine residues were strongly phosphorylated due to G or GO exposure, suggesting that the GNPs do no induce reduced barrier function via established alterations in phosphorylation. We however did observe increased phosphorylation of serine residues in α-catenin and β-catenin at residues that alter the cadherin-catenin complex association and localization of β-catenin [41–43] . β-catenin is a protein with a dual role, it functions to establish cell-cell contacts by associating with cadherin, but also acts as a transcriptional activator that induces Wnt-mediated gene expression [44]. In this respect, it might be that the observed alterations in phosphorylation induced nuclear localization of β-catenin, where it co-activates Wnt-signaling. β-catenin/Wnt-signaling can, amongst others, induce epithelial-to-mesenchymal transition (EMT), a process in which polarized epithelial cells lose their apical-basal polarity, reorganize their cytoskeleton and acquire a mesenchymal cell phenotype [45]. It remains to be elucidated whether the observed decreased barrier function in G and GO-exposed epithelial cells occurs due to EMT.

Graphene nanoparticles

Graphene and its multiple derivatives are important nanoparticles to evaluate since potential human exposure is becoming more likely with its increasing number of applications. Inhalation is a likely route of exposure during the manufacturing and handling of the GNP powders that can easily from dusts in the air [46].

In **chapter 3** and **4** of this work, we considered the effect of G and GO on the airway epithelial barrier *in vitro.* In both studies the tested concentrations of G induced no cytotoxicity on 16HBE monocultures, whereas GO induced cytotoxicity starting from a concentration of 64µg/mL. GNP-induced impairment of the airway epithelial barrier was also consistent in the two studies, as quantified by an immediate and persisting decrease in TEER and an increase in the flux of fluorescent labelled dextrans.

The concentrations used in the *in vitro* experiments seem high, but should be regarded as a cumulative dose acquired after many years of exposure. If we assume that a employee works 40 years in a manufacturing plant with yearly 200 workdays of 8 hours and inhales 10m³ of air per workday, deposition of the lowest concentration of G (i.e. 64 µg/mL in 200 µL on a surface of 0.33 cm²) into a lung with a surface area of 100 m², would correspond with a concentration of 480 µg/m³ of G in the air of the manufacturing plant. Likewise the other applied concentrations of 64 µg/mL G and 64 and 16 µg/mL GO can be converted into respective air concentrations of 1920 µg/m³ of G and 480 and 120 µg/m³ of GO. Threshold limit values have not been defined for the GNPs specifically but the OSHA/PEL (Occupational Safety and Health Administration, Permissible Exposure Limit) for synthetic graphite (i.e. multiple graphene layers, forming a large structure) is 15 mg/m³ for total dust and 5 mg/m³ for the

respirable faction, which is far above our estimated exposure levels based on the *in vitro* concentrations used [47]. The concentrations that we used were however high for a single dose and sometimes hampered the interpretations of our findings.

To elicit harmful effects in the lungs, particles need to be respirable. The respirability and site of deposition in the airways is determined by the aerodynamic diameter (i.e. the diameter of a spherical particle that has the same settling velocity as another particle regardless of its shape, size or density) of the particle [48]. The particle size distribution and mass median aerodynamic diameter (MMAD) of the used GNPs was determined using the PreciseInhale™ exposure system at the hosting institute in Sweden. G had a MMAD of 4 µm, which is in the respirable fraction of particles that would deposit in the tracheobronchial and alveolar region of the lungs (Fig. 1) [49,50]. For GO a 'dust' of the particles could not be generated, probably due to strong aggregation that made the particles to sticky and large to be able to form a dust. This suggest that the GO powder in this form is less likely to be inhaled.

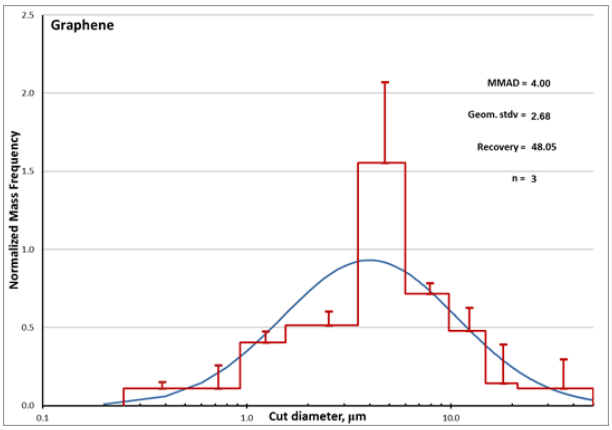

Figure 1. Size distribution of graphene
The size distribution of the graphene was determined using a cascade impactor (Marple Andersen, EnVirREC AB, Sweden). The nanoparticles were aerosolized with the PreciseInhale system (Inhalation Sciences Sweden AB, Stockholm, Sweden) and the aerodynamic size distribution of the nanoparticles were determined with the cascade impactor at a flow rate of 2 L/min as previously described [51,52]. The mass of nanoparticles deposited on the nine stages in the impactor was used to calculate the mass median aerodynamic diameter (MMAD) and the geometric standard deviation (GSD).

Diesel exhaust particles

In **chapter 4** of this thesis, we found that DEPs induced a transient decrease in TEER in 16HBE monocultures as well as, 16HBEs cultured together with HMC-1 cells. In this study, we did not further attempt to explain this transient impairment of the epithelial barrier. Lehman *et al.*, found in a monoculture of 16HBE cells, and not in a tri-culture where macrophages and dendritic cells were added, that exposure to 125 µg/mL DEPs induced a permanent decrease in TEER [29]. Although the quantified amount of occludin mRNA in 16HBE cells was non-significantly reduced compared to the

control, it was concluded that alterations in the TJ protein occludin caused the decreased barrier function.

The concentrations of DEP that we used is 5 and 25-fold lower than that used by Lehman et al. (which maybe explains the reduced and transient alteration in TEER) and is in the range of previous *in vitro* studies investigating the effect of DEP on 16HBE cells [53–57]. Trying to place our *in vitro* concentrations of 5 µg/mL and 25 µg/mL in perspective, we calculated that, taking into account that humans inhale approximately 20 m³ of air per day, respectively 34 and 171 years of exposure to the average $PM_{2.5}$ level of 12µg/m³ in Flanders would result in the *in vitro* concentrations that we used [58]. If we correlate to the yearly threshold limit value determined by the European commission of 25 µg/m³, humans should be exposed for respectively 16.5 and 82 years to this air concentration, to reach our *in vitro* concentrations in their lungs [59]. It can also be noted that average concentrations of $PM_{2.5}$ (and so DEP) in the air differ largely in the world, for example in 2013, a yearly average of 100.75 µg/m³ $PM_{2.5}$ was noted in Beijing, China [60].

The DEPs were obtained from the US National Institute of Standards and Technology (NIST-SRM2975, from forklift) and were fully characterized. Using the Precise Inhale™ particle size distributor, a MMAD of 0.1 µm was determined for the DEPs. Since 0.1 µm was the smallest filter size and the size distribution is not normal, we however expect that most of the DEPs are smaller than 0.1 µm (Fig. 2). This is in line with the actual size of DEPs and is in the range that has considerable deposition in the alveoli and capability of translocating towards the bloodstream [50,61].

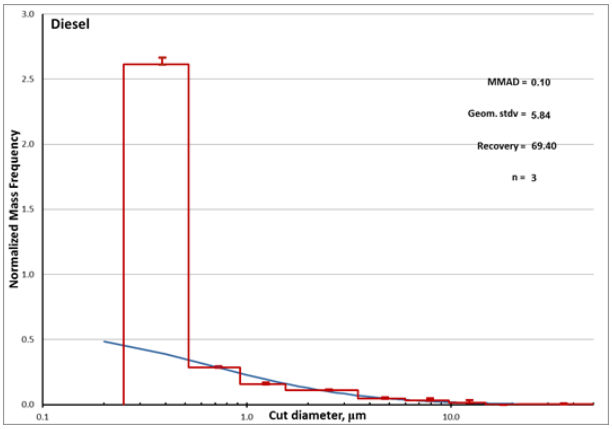

Figure 2. Size distribution of diesel exhaust particles (DEP)
The size distribution of the DEP was determined using a cascade impactor (Marple Andersen, EnVirREC AB, Sweden). The nanoparticles were aerosolized with the PreciseInhale system (Inhalation Sciences Sweden AB, Stockholm, Sweden) and the aerodynamic size distribution of the nanoparticles were determined with the cascade impactor at a flow rate of 2 L/min as previously described [51,52]. The mass of nanoparticles deposited on the nine stages in the impactor was used to calculate the mass median aerodynamic diameter (MMAD) and the geometric standard deviation (GSD).

Chlorine and chlorine derivatives

Since swimming pool attendance is associated with increased risk of developing respiratory disorders, we based the tested concentrations of hypochlorite *in vitro* on this dose of 3 ppm active chlorine present in public swimming pool water [62,63].

In this thesis, we wanted to investigate whether the respiratory irritant chlorine had a negative effect on the airway epithelial barrier *in vitro*. Histological findings in humans and laboratory animals already demonstrated that chlorine injures the airway epithelium, however *in vitro* studies to investigate these mechanisms are sparse [64,65]. This is possibly due to the inert characteristic of chlorine, and its derivatives in water hypochlorous acid (HOCl) and hypochlorite (ClO^-), of being highly reactive. In addition, hypochlorous acid can react with organic nitrogen compounds (such as from the sweat, urine and salvia of humans in swimming pools), to form mono-, di- or trichloramines, which have been associated with increased respiratory symptoms [66,67]. We used an aqueous solution of sodium hypochlorite as a dissolvable analogue for chlorine to expose the cells *in vitro*. However, due to the high reactivity, ClO^- might react with the supplements in the cell culture medium, whereby the exact concentration of chlorine that reaches the cells is unpredictable.

Exposure to ClO^- had a different effect on the airway epithelial barrier in both *in vitro* studies. In **chapter 3** exposure to 3.75 and 7.5 ppm of active chlorine affected the barrier function in a negligible extent, whereas in **chapter 4** exposure to 3 or 30 ppm of active chlorine induced clearly an early decrease in TEER, that normalized within 24 hours of exposure. Beside the difference in concentration used it needs to be noted that different brands of sodium hypochlorite solutions were used in the two studies, which can explain the differences in biological effect. The experiments in chapter 3 were performed with a concentrated sodium hypochlorite solution containing 13 % active chlorine (Across Organics), whereas in chapter 4 we used a commercially available household bleach of 2.6 % active chlorine (KLORIN). It is known that temperature, exposure to light, metal impurities and pH affect the stability of sodium hypochlorite solutions. To maintain hypochlorite ions in the solution, sodium hypochlorite solutions need to be at alkaline pH of around 11. To preserve this pH sodium hydroxide (NaOH) is often added to the sodium hypochlorite solution, which was also the case in both the used solutions. Decomposition of sodium hypochlorite to sodium chloride ($2\ NaClO \rightarrow 2\ NaCl + O_2$) proceeds quicker with high concentrations of active chlorine. Since the Across Organics solution had a higher concentration of active chlorine, which accelerated the decomposition, and was more diluted in culture medium to obtain the desired *in vitro* concentration (which also diluted the alkaline NaOH in a stronger extent) this solution might have had a reduced chlorine activity compared to the household bleach. This provides a plausible explanation for the noted discrepancy between the two *in vitro* studies.

2.2. Study airway hypersensitivity following airway barrier impairment – *in vivo*

Development of a model for IIA to hypochlorite due to impairment of the airway barrier

In the second part of this thesis, we hypothesized that due to an impaired airway epithelial barrier, mice become more sensitive to low concentrations of irritants, resulting in the development of airway hypersensitivity, as in IIA. To impair the airway epithelial barrier, we applied an established protocol of an i.p. injection with 200 mg/kg BW of NA that selectively damages the club cells within the respiratory tract [68,69]. By acquiring micro-CT images of the mouse lungs before and at repeated time points following the NA-treatment in **chapter 5**, we could identify that NA-treatment not only injures the club cells in the epithelium of the lower airways, but that this disturbance also lead to enlargement of the lungs and airways. These structural alterations occurred early following the NA-treatment and seemed to act as a compensation mechanism for the alterations onto the epithelium. Although these structural alterations disappeared within 14 days, increased lung volumes were still detectable at this time point, suggesting that the mice did not recover completely on a functional level. In **chapter 6**, we treated the mice twice with NA, with each time a recovery period of 14 days. At the end of the experiment, we observed again the alterations in forced functional volumes, indicating that this was a robust finding.

In several murine studies using high to moderate level exposure to chlorine gas it was shown that chlorine on itself can induce pulmonary inflammation and AHR [70–76]. We however, used a low concentration of 0.003% active chlorine dosed in a sodium hypochlorite solution that did not induce a sensory irritant airway response or inflammation in naïve mice, as determined in a pilot study. In **chapter 5,** it was clearly demonstrated that due to the impaired airway epithelial barrier, mice did become sensitive to this concentration of active chlorine. We are the first to describe this type of response upon hypochlorite exposure.

A substantial amount of studies investigated the effect of chlorine exposure *in vivo*, here a limited number of publications investigating the mechanisms behind the chlorine-induced asthma is discussed. Hox *et al*. demonstrated the importance of TRPA1 channels and neuro-immune interactions in the development of hypochlorite-induced asthma in mice [77,78]. A single i.n. challenge with sodium hypochlorite solution following OVA resulted in development of AHR in wild-type mice, as well as, in mice lacking the adaptive immune system. TRPA1 KO and mast cell KO mice, however did not develop AHR, indicating that the response upon hypochlorite exposure is mediated by TRPA1-dependent stimulation of the sensory neurons and mast cell activation [78]. Another important mechanism via which chlorine, can mediate airway hypersensitivity is oxidative stress. Treatment with the anti-oxidant dimethylthiourea attenuated chlorine-induced increase in airway responsiveness and pulmonary

inflammation [70]. It is established that chlorine induces oxidative injury onto the airway epithelium. McGovern et al., however postulated that not only the direct oxidative effect on the epithelial cells, but also the generated oxidant stress by the recruited neutrophils could contribute to the development of AHR following chlorine exposure [71]. In a study using chronic low dose exposure to sodium hypochlorite vapor and OVA, Kim *et al.*, found that chlorine exposure increased the expression of IL-33 from epithelial cells and IL-1β from macrophages, suggesting that alarmin-inflammasome activation pathways might be implicated in the pulmonary inflammation and AHR [79].

The used concentration of active chlorine in our studies is tenfold higher than that found in public swimming pool water, but was still considered relevant due to the dosing technique. It is known that when using i.n. instillation in unanaesthetized mice, the actual amount of the applied solution that reaches the lungs is limited, as would occur in **chapter 5** [80]. In **chapter 6**, the mice, however, received three endotracheal instillations, hereby increasing the delivered dose substantially [30]. To perform this instillation the mice were anaesthetized and held vertically. Next, the solution was pipetted just above the epiglottis, and by gasping the tongue and meanwhile closing the nose, the mice were forced to inhale the solution. This technique is not invasive, but might agitate the lungs of the mice. Therefore we initially expected that the observed neutrophilic inflammation in NA-treated and endotracheal instilled (Sal and ClO^-) mice, was caused by the repetitive endotracheal instillations. Using non-instilled mice, it became clear that this was not the case and that the repeated NA-treatment was responsible for the neutrophil influx.

A common finding in both *in vivo* studies, is the increase in pulmonary eosinophils in the NA-treated and ClO^--challenged mice. Eosinophils have long been associated with asthma, and are considered as a hallmark of type 2 immune responses. Type 2 cell-mediated immunity is rich in eosinophils, basophils, mast cells, type 2 T helper (Th2) cells and type 2 ILCs, and has evolved as an immune response that protects against helminths [81]. The fact that we observed an (although not enormous) influx of eosinophils to the lungs, specifically in the mice who had airway epithelial barrier impairment combined with ClO^--exposure, suggest that a type 2 immune mechanism plays a role. The observed shift towards ILC2s in the NA/ClO^--mice in chapter 5 supported this suggestion. This is intriguing because type 2 immunity has mostly been associated with allergic immune responses. Bruselle and colleagues postulated that in allergic asthma, IgE switching in B cells, eosinophilic inflammation and AHR are driven by adaptive Th2 cells that are stimulated to release IL-4, IL-5 and IL-13 after allergen capture by DCs [82]. In contrast, in non-allergic asthma, pollutants, microbes or glycolipids stimulate the epithelium to release innate cytokines that activate ILC 2 cells in an antigen-independent manner. Activated ILC2s produce IL-5 and IL-13, leading to eosinophilia and AHR [82]. Our finding that airway hypersensitivity developed only after airway epithelial barrier impairment strengthens the recent

insight that the airway epithelium and the subsequent evoked innate immune signals underlie non-allergic airway responses and that these can also be considered as type 2 immune response [83].

Dendritic cell and innate lymphoid cell involvement in IIA

Dendritic cells (DCs) play a crucial role in allergic asthma by sampling and presenting the allergen to naïve T cells, in order to induce Th2 cell mediated immune response [84,85]. Given their location near the epithelium, DC receive signals from the exposed epithelium which influences their activation and the generated immune response [85]. In house dust mite (HDM)-induced allergic asthma, recognition of the HDM by TLR4 on airway epithelial cells results in the release of the epithelial cytokines IL-1α, TSLP, IL-25, IL-33 and GM-CSF, which activate DCs to initiate the asthmatic response [83,86,87]. For environmental pollutants such as DEP, cigarette smoke, ozone and toxic gases like NO_2, the epithelial damage and associated release of these cytokines that activate DCs, are an important aspect in their adjuvant action on allergic airway responses [85]. In our single treatment model (**chapter 5**), we wanted to investigate the alterations in DCs upon to impairment of the airway epithelial barrier. Due to NA-induced barrier impairment, increased numbers of DCs, and especially monocyte-derived DCs (moDCs) were found in the lungs of mice. MoDCs are monocytes that are recruited to the lung in C-C chemokine receptor type 2 (CCR2)-dependent fashion and differentiate to moDCs under inflammatory conditions [88,89]. In a study where the adjuvant effect of DEPs was investigated, Provoost *et al.*, demonstrated that upon DEP exposure moDCs were recruited towards the lungs, and this in a CCR2 dependent way [90,91]. Since moDCs poorly migrate to the lymph nodes, their function is not in T cell polarization, but rather in the effector phase, by producing chemokines and cytokines that promote Th2 immunity [88,89]. Since in our model no antigens are available to be captured by the DCs, it is not unlikely that only the inflammatory moDCs increased. The increase in moDCs, even 14 days after the insult, indicates that airway barrier impairment can exert a prolonged inflammatory state in the epithelium and that this is a possible mechanism that increases the sensitivity to irritants in IIA.

Innate lymphoid cells (ILCs) are a recently discovered group of innate immune cells that respond rapidly to a variety of environmental stimuli. Several studies have demonstrated that type 2 ILCs play an important role in allergic asthma [92]. In response to IL-25 and IL-33 released from the stimulated epithelium, ILC2s produce the Th2 cytokines IL-5 and IL-13, which are able to induce lung eosinophilia, mucus hypersecretion and AHR [93,94]. Even in the absence of the adaptive immune system, ILC2s were able to mediate eosinophilia, goblet cells metaplasia, type 2 cytokine production and AHR [95,96]. Since ILCs are antigen non-specific and respond to innate epithelial-derived signals, these cells are potential effector cells in IIA. In our model of IIA to hypochlorite due to epithelial barrier impairment (**chapter 5**), the proportion of type 2 ILCs increased significantly in NA/ClO^--treated mice, which thus might be responsible for the increase in eosinophils and AHR upon ClO^- exposure. We believe that the ILC2s

were recruited to the lungs due to the (previously) impaired airway epithelium and a specific signal derived from the ClO^- exposure. A potential contribution of ILC2 activation upon irritant exposure has been investigated in a limited extent. In a study investigating the adjuvant effect of ozone in aspergillus fumigatus-induced airway responses, Yang *et al.*, demonstrated that ozone upregulated the ILC 2 activator, IL-33 in the lung, and proved that the ILC2s were responsible for the ozone-enhanced AHR in mice [97]. Similarly De Grove *et al*., investigated the contribution of ILC2s in DEP-enhanced allergic airway responses, and found that mainly the adaptive immune system contributed to DEP-enhanced allergic airway inflammation, unlike the ILC2s that only contributed in a limited extent [98]. Although experimental studies are limited, release of mediators, such as IL-33 and IL-25, or DAMPs, such as HMGB1 and uric acid, by irritant-induced epithelial damage might be a first step in the development of IIA via the activation of ILCs that are able to mediate the asthmatic airway responses.

Specific response to hypochlorite?

In **chapters 5** and **6**, we investigated the development of airway hypersensitivity upon inhalation of hypochlorite following impairment of the airway barrier. Chlorine and chlorine derivatives are important irritants to investigate in this respect, as they are the most reported cause of IIA [2]. IIA can however develop after inhalation of different types of irritants, and we could therefore question whether the observed responses in our model are specifically induced by ClO^-. During the course of this PhD, we also performed the barrier impairment and single i.n. challenge protocol with a 1% ammonium persulfate (AP) solution. AP is a known asthmogen, especially in hairdressers, yet it also has irritant properties that might evoke respiratory responses [99–101]. In this respect, we wanted to investigate whether AP could similarly evoke airway hypersensitivity. Consistent with the studies reported in this dissertation, an increase in functional lung volumes due to the NA-treatment was observed. Yet, the short decrease in breathing frequency (which indicates the respiratory irritant properties of AP) and the low level of airway responsiveness was equal for both the MO/AP and NA/AP-treated mice. This indicates that a single challenge with AP after barrier impairment did not enhance the sensitivity of the airways, whereas a single challenge with ClO^- did. This is a relevant observation, as it suggests that ClO^- and AP act differently on the respiratory system. Which might be an interesting aspect to take into account when exploring the mechanisms underlying IIA.

3. Future perspectives

Effect of irritants on a co-culture model of the airway barrier (chapter 3)

In **chapter 3**, we investigated the effect of environmental irritants on the airway epithelial barrier and found that GNPs might decrease the barrier integrity via alterations in the phosphorylation of TJ and AJ proteins. Which specific hypo- or hyperphosphorylated peptides are key within TJ or AJ fine-tuning protein interactions and thus also the barrier function should to be studied in further detail. After identification of such alterations using our phosphoproteomics data, we could verify the altered proteins using phospho-specific western blot.

It would be interesting to understand the interaction between the sheet-like GNPs and the epithelial cells. Using femtosecond-pulsed laser microscopy, in collaboration with the Biomedical Research Institute of Hasselt University, under supervision of Prof. Marcel Ameloot, we could visualize whether the GNPs are internalized or intercalate between the epithelial cells. A preliminary experiment demonstrated that using a concentration of 64 µg/mL of G the amount of deposited G is too large to identify the individual particles, which made it impossible to draw firm conclusions from the acquired images. This experiment can be optimized and repeated using lower concentrations of G, to accurately evaluate the GNP deposition.

Contribution of mast cells in irritant-induced airway epithelial barrier impairment *in vitro* (chapter 4)

We aimed to investigate whether mast cells influence the response of the epithelium upon irritant exposure. We cannot exclude that the absence of an effect of mast cells on the irritant-exposed epithelium in this study was because of the immaturity of the HMC-1 mast cells. Therefore, it would be more appropriate to repeat these experiments using well-differentiated and mature primary mast cells derived from human tissue, blood or bone marrow.

Irritant-induced asthma to hypochlorite in mice due to impairment of the airway barrier (chapter 5)

A model for IIA to hypochlorite due to impairment of the airway epithelial barrier was developed. This model can be used to further identify the mechanisms underlying IIA. We postulate that the observed sensory irritant response and subsequent AHR was initiated by activation of the TRPA1 channels located on the sensory nerves within the nose of the mice, which mediate a neurogenic inflammation. To proof this suggestion, we should subject WT mice treated with a TRPA1 blocker or TRPA1 KO mice to our treatment protocol. It would be interesting to determine which signals are derived from the NA-impaired and ClO^--exposed airway epithelium, as these might explain the recruitment of the moDCs or

ILC2s in this model. To verify the real contribution of the ILCs in our model we could compare the response generated in SCID mice (lacking T- and B-cells) with the response generated in $Rag2^{-/-}$ mice (lacking ILCs, T- and B-cells). The specific role of the type 2 ILCs, could be further investigated using ILC2-deficient mice (which can be achieved by intercrossing $RORa_{fl/fl}$ mice with IL-7 reporter-Cre mice) or adoptive transfer of ILC2s in $Rag2^{-/-}$ mice.

Airway barrier impairment increases nonspecific airway hyperresponsiveness in mice (chapter 6)

In **chapter 6**, we implemented a vigorous treatment protocol, consisting of double barrier impairment with NA, followed by repeated airway exposures to hypochlorite. To verify whether the observed alterations are caused by barrier impairment or by repeated triggering of the lungs using the endotracheal administration route, non-instilled MO- and NA-pretreated mice were included in the study. Unexpectedly the serum SP-D concentration did not increase after double NA-induced barrier impairment. Possibly the club and alveolar type II cells are gone/have reduced levels of SP-D due to the double barrier impairment. Therefore, identification of SP-D on the lung tissue sections using immunohistochemistry and quantification of the SP-D concentration in the BAL fluid to acquire the total SP-D concentration will be valuable.

4. General conclusion

The hypothesis throughout this thesis was, that respiratory irritants can impair the airway epithelial barrier, and that this contributes to the development of airway hypersensitivity. The following aspects can be concluded from this work:

- Environmental irritants can permanently or transiently impair the airway epithelial barrier *in vitro*, yet this depends on the nature of the chemical used, the composition of the chemical solution and the method of suspension. Barrier impairment did not occur via a clear disruption of the TJ proteins, but possibly alterations in the phosphorylation of AJ and TJ proteins explain the altered epithelial barrier function.
- The HMC-1 cells used in this study do not alter the effects of environmental irritants on the airway epithelial barrier.
- Hypochlorite exposure after impairment of the airway epithelial barrier, allowing (partial) repair, results in development of a sensory irritant response, AHR and pulmonary inflammation. Hypochlorite induces epithelial damage and increases the airway permeability, which stimulates ILC2 recruitment towards the lung.
- Successive airway epithelial barrier impairment with NA results in development of nonspecific AHR.

When integrating these findings, several questions concerning IIA have been answered. Respiratory irritants, including nanoparticles, can permanently or transiently impair epithelial barrier functioning. Barrier impairment does not always imply disruption or loss of the intercellular junctional complexes, but alterations in the phosphorylation of these proteins might play a role. Alteration of the airway epithelial barrier by respiratory irritants probably forms the initial trigger for development of IIA. Although mast cells might play a role in IIA via their interaction with the exposed epithelium, we could not elucidate this question with the used mast cell line. We clearly demonstrated that airway barrier impairment increases the sensitivity of the airways in mice. Intranasal exposure to hypochlorite after single barrier impairment resulted in the development of IIA, which was characterized by an increase in type 2 ILCs in the lung. Therefore, also new directions of research relating to irritants and the airway barrier might be considered. It would for example be interesting to study how alterations in phosphorylation of TJ and AJ proteins relate to barrier impairment due to irritant exposure. Investigating how the innate immune system responds and interacts with an impaired airway epithelial barrier would also be valuable in research concerning airway diseases.

References

1. Tarlo, S. M. Irritant-induced asthma in the workplace. *Curr. Allergy Asthma Rep.* **14,** 406 (2014).
2. Vandenplas, O. *et al.* EAACI position paper: irritant-induced asthma. *Allergy* **69,** 1141–1153 (2014).
3. Sanchez, V. C., Jachak, A., Hurt, R. H. & Kane, A. B. Biological Interactions of Graphene-Family Nanomaterials: An Interdisciplinary Review. *Chem. Res. Toxicol.* **25,** 15–34 (2012).
4. Dudek, I., Skoda, M., Jarosz, A. & Szukiewicz, D. The Molecular Influence of Graphene and Graphene Oxide on the Immune System Under In Vitro and In Vivo Conditions. *Arch. Immunol. Ther. Exp. (Warsz.)* **64,** 195–215 (2016).
5. Bianco, A. Graphene: Safe or Toxic? The Two Faces of the Medal. *Angew. Chem. Int. Ed.* **52,** 4986–4997 (2013).
6. Horváth, L. *et al.* Evaluation of the toxicity of graphene derivatives on cells of the lung luminal surface. *Carbon* **64,** 45–60 (2013).
7. Chang, Y. *et al.* In vitro toxicity evaluation of graphene oxide on A549 cells. *Toxicol. Lett.* **200,** 201–210 (2011).
8. Park, E.-J. *et al.* Toxic response of graphene nanoplatelets in vivo and in vitro. *Arch. Toxicol.* **89,** 1557–1568 (2015).
9. Lalwani, G., D'Agati, M., Khan, A. M. & Sitharaman, B. Toxicology of graphene-based nanomaterials. *Adv. Drug Deliv. Rev.* **105,** 109–144 (2016).
10. Ema, M., Gamo, M. & Honda, K. A review of toxicity studies on graphene-based nanomaterials in laboratory animals. *Regul. Toxicol. Pharmacol. RTP* **85,** 7–24 (2017).
11. Li, B. *et al.* Biodistribution and pulmonary toxicity of intratracheally instilled graphene oxide in mice. *NPG Asia Mater.* **5,** e44 (2013).
12. Duch, M. C. *et al.* Minimizing Oxidation and Stable Nanoscale Dispersion Improves the Biocompatibility of Graphene in the Lung. *Nano Lett.* **11,** 5201–5207 (2011).
13. Holgate, S. T. The sentinel role of the airway epithelium in asthma pathogenesis. *Immunol. Rev.* **242,** 205–219 (2011).
14. Xiao, C. *et al.* Defective epithelial barrier function in asthma. *J. Allergy Clin. Immunol.* **128,** 549–556.e12 (2011).
15. Hsu, L.-W. *et al.* Elucidating the signaling mechanism of an epithelial tight-junction opening induced by chitosan. *Biomaterials* **33,** 6254–6263 (2012).
16. Wen, Z.-S., Xu, Y.-L., Zou, X.-T. & Xu, Z.-R. Chitosan Nanoparticles Act as an Adjuvant to Promote both Th1 and Th2 Immune Responses Induced by Ovalbumin in Mice. *Mar. Drugs* **9,** 1038–1055 (2011).
17. Mertens, T. C. J., Karmouty-Quintana, H., Taube, C. & Hiemstra, P. S. Use of airway epithelial cell culture to unravel the pathogenesis and study treatment in obstructive airway diseases. *Pulm. Pharmacol. Ther.* **45,** 101–113 (2017).
18. Alfaro-Moreno, E. *et al.* Co-cultures of multiple cell types mimic pulmonary cell communication in response to urban PM10. *Eur. Respir. J.* **32,** 1184–1194 (2008).
19. Klein, S. G. *et al.* Endothelial responses of the alveolar barrier in vitro in a dose-controlled exposure to diesel exhaust particulate matter. *Part. Fibre Toxicol.* **14,** 7 (2017).
20. Klein, S. G., Serchi, T., Hoffmann, L., Blömeke, B. & Gutleb, A. C. An improved 3D tetraculture system mimicking the cellular organisation at the alveolar barrier to study the potential toxic effects of particles on the lung. *Part. Fibre Toxicol.* **10,** 31 (2013).
21. Rothen-Rutishauser, B., Blank, F., Mühlfeld, C. & Gehr, P. In vitro models of the human epithelial airway barrier to study the toxic potential of particulate matter. *Expert Opin. Drug Metab. Toxicol.* **4,** 1075–1089 (2008).
22. Barosova, H. *et al.* Biological response of an in vitro human 3D lung cell model exposed to brake wear debris varies based on brake pad formulation. *Arch. Toxicol.* **92,** 2339–2351 (2018).
23. Tomašek, I. *et al.* Combined exposure of diesel exhaust particles and respirable Soufrière Hills volcanic ash causes a (pro-)inflammatory response in an in vitro multicellular epithelial tissue barrier model. *Part. Fibre Toxicol.* **13,** 67 (2016).
24. Papazian, D., Würtzen, P. A. & Hansen, S. W. K. Polarized Airway Epithelial Models for Immunological Co-Culture Studies. *Int. Arch. Allergy Immunol.* **170,** 1–21 (2016).
25. Klein, S. G., Hennen, J., Serchi, T., Blömeke, B. & Gutleb, A. C. Potential of coculture in vitro models to study inflammatory and sensitizing effects of particles on the lung. *Toxicol. Vitro Int. J. Publ. Assoc. BIBRA* **25,** 1516–1534 (2011).

26. Karp, P. H. *et al.* An in vitro model of differentiated human airway epithelia. Methods for establishing primary cultures. *Methods Mol. Biol. Clifton NJ* **188,** 115–137 (2002).
27. Pezzulo, A. A. *et al.* The air-liquid interface and use of primary cell cultures are important to recapitulate the transcriptional profile of in vivo airway epithelia. *Am. J. Physiol. - Lung Cell. Mol. Physiol.* **300,** L25–L31 (2011).
28. Heijink, I. H. *et al.* Characterisation of cell adhesion in airway epithelial cell types using electric cell–substrate impedance sensing. *Eur. Respir. J.* **35,** 894–903 (2010).
29. Lehmann, A. D., Blank, F., Baum, O., Gehr, P. & Rothen-Rutishauser, B. M. Diesel exhaust particles modulate the tight junction protein occludin in lung cells in vitro. *Part. Fibre Toxicol.* **6,** 26 (2009).
30. Foster, W. M., Walters, D. M., Longphre, M., Macri, K. & Miller, L. M. Methodology for the measurement of mucociliary function in the mouse by scintigraphy. *J. Appl. Physiol. Bethesda Md 1985* **90,** 1111–1117 (2001).
31. Lehmann, A. D. *et al.* An in vitro triple cell co-culture model with primary cells mimicking the human alveolar epithelial barrier. *Eur. J. Pharm. Biopharm. Off. J. Arbeitsgemeinschaft Pharm. Verfahrenstechnik EV* **77,** 398–406 (2011).
32. Matter, K. & Balda, M. S. Functional analysis of tight junctions. *Methods San Diego Calif* **30,** 228–234 (2003).
33. Hardyman, M. A. *et al.* TNF-α-mediated bronchial barrier disruption and regulation by src-family kinase activation. *J. Allergy Clin. Immunol.* **132,** 665–675.e8 (2013).
34. Sherwood, C. L. *et al.* Arsenic compromises conducting airway epithelial barrier properties in primary mouse and immortalized human cell cultures. *PloS One* **8,** e82970 (2013).
35. Cao, X. *et al.* Tight junction disruption by cadmium in an in vitro human airway tissue model. *Respir. Res.* **16,** 30 (2015).
36. Olivera, D., Knall, C., Boggs, S. & Seagrave, J. Cytoskeletal modulation and tyrosine phosphorylation of tight junction proteins are associated with mainstream cigarette smoke-induced permeability of airway epithelium. *Exp. Toxicol. Pathol. Off. J. Ges. Toxikol. Pathol.* **62,** 133–143 (2010).
37. Van Itallie, C. M. & Anderson, J. M. Phosphorylation of tight junction transmembrane proteins: Many sites, much to do. *Tissue Barriers* **6,** e1382671 (2018).
38. Rao, R. K., Basuroy, S., Rao, V. U., Karnaky Jr, K. J. & Gupta, A. Tyrosine phosphorylation and dissociation of occludin-ZO-1 and E-cadherin-beta-catenin complexes from the cytoskeleton by oxidative stress. *Biochem. J.* **368,** 471–481 (2002).
39. Rao, R. Occludin phosphorylation in regulation of epithelial tight junctions. *Ann. N. Y. Acad. Sci.* **1165,** 62–68 (2009).
40. Dörfel, M. J. & Huber, O. Modulation of Tight Junction Structure and Function by Kinases and Phosphatases Targeting Occludin. *BioMed Research International* (2012). Available at: https://www.hindawi.com/journals/bmri/2012/807356/. (Accessed: 3rd July 2018)
41. Ji, H. *et al.* EGF-induced ERK activation promotes CK2-mediated disassociation of alpha-Catenin from beta-Catenin and transactivation of beta-Catenin. *Mol. Cell* **36,** 547–559 (2009).
42. Wu, X. *et al.* Rac1 activation and subsequent β-catenin phosphorylation controls nuclear localization of β-catenin during canonical Wnt signaling. *Cell* **133,** 340–353 (2008).
43. Fang, D. *et al.* PHOSPHORYLATION OF β-CATENIN BY AKT PROMOTES β -CATENIN TRANSCRIPTIONAL ACTIVITY. *J. Biol. Chem.* **282,** 11221–11229 (2007).
44. Daugherty, R. L. & Gottardi, C. J. Phospho-regulation of β-Catenin Adhesion and Signaling Functions. *Physiol. Bethesda Md* **22,** 303–309 (2007).
45. Lamouille, S., Xu, J. & Derynck, R. Molecular mechanisms of epithelial–mesenchymal transition. *Nat. Rev. Mol. Cell Biol.* **15,** 178–196 (2014).
46. Arvidsson, R., Molander, S. & Sandén, B. A. Review of Potential Environmental and Health Risks of the Nanomaterial Graphene. *Hum. Ecol. Risk Assess. Int. J.* **19,** 873–887 (2013).
47. OSHA Annotated PELs | Occupational Safety and Health Administration. Available at: https://www.osha.gov/dsg/annotated-pels/tablez-1.html#niosh_rel. (Accessed: 12th June 2018)
48. Brown, J. S. Chapter 27 - Deposition of Particles. in *Comparative Biology of the Normal Lung (Second Edition)* (ed. Parent, R. A.) 513–536 (Academic Press, 2015).
49. Fernández Tena, A. & Casan Clarà, P. Deposition of Inhaled Particles in the Lungs. *Arch. Bronconeumol. Engl. Ed.* **48,** 240–246 (2012).
50. Oberdörster, G., Oberdörster, E. & Oberdörster, J. Nanotoxicology: an emerging discipline evolving from studies of ultrafine particles. *Environ. Health Perspect.* **113,** 823–839 (2005).

51. Selg, E. *et al.* Delivering horseradish peroxidase as a respirable powder to the isolated, perfused, and ventilated lung of the rat: the pulmonary disposition of an inhaled model biopharmaceutical. *J. Aerosol Med. Pulm. Drug Deliv.* **23,** 273–284 (2010).
52. Selg, E. *et al.* Dry powder inhalation exposures of the endotracheally intubated rat lung, ex vivo and in vivo: the pulmonary pharmacokinetics of fluticasone furoate. *J. Aerosol Med. Pulm. Drug Deliv.* **26,** 181–189 (2013).
53. Bonvallot, V. *et al.* Organic Compounds from Diesel Exhaust Particles Elicit a Proinflammatory Response in Human Airway Epithelial Cells and Induce Cytochrome p450 1A1 Expression. *Am. J. Respir. Cell Mol. Biol.* **25,** 515–521 (2001).
54. Baulig, A., Sourdeval, M., Meyer, M., Marano, F. & Baeza-Squiban, A. Biological effects of atmospheric particles on human bronchial epithelial cells. Comparison with diesel exhaust particles. *Toxicol. Vitro Int. J. Publ. Assoc. BIBRA* **17,** 567–573 (2003).
55. Baulig, A. *et al.* Involvement of reactive oxygen species in the metabolic pathways triggered by diesel exhaust particles in human airway epithelial cells. *Am. J. Physiol. Lung Cell. Mol. Physiol.* **285,** L671-679 (2003).
56. Schwarze, P. E. *et al.* Inflammation-related effects of diesel engine exhaust particles: studies on lung cells in vitro. *BioMed Res. Int.* **2013,** 685142 (2013).
57. Li, N. *et al.* Use of a stratified oxidative stress model to study the biological effects of ambient concentrated and diesel exhaust particulate matter. *Inhal. Toxicol.* **14,** 459–486 (2002).
58. Fijn stof (PM2,5) jaargemiddelde. *Vlaamse Milieumaatschappij* (2016). Available at: http://www.vmm.be/data/fijn-stof-pm2-5-jaargemiddelde. (Accessed: 12th June 2018)
59. Standards - Air Quality - Environment - European Commission. (2015). Available at: http://ec.europa.eu/environment/air/quality/standards.htm. (Accessed: 12th June 2018)
60. Batterman, S., Xu, L., Chen, F., Chen, F. & Zhong, X. Characteristics of PM2.5 concentrations across Beijing during 2013–2015. *Atmos. Environ.* **145,** 104–114 (2016).
61. Steiner, S., Bisig, C., Petri-Fink, A. & Rothen-Rutishauser, B. Diesel exhaust: current knowledge of adverse effects and underlying cellular mechanisms. *Arch. Toxicol.* **90,** 1541–1553 (2016).
62. Bernard, A. Chlorination products: emerging links with allergic diseases. *Curr. Med. Chem.* **14,** 1771–1782 (2007).
63. Bernard, A., Nickmilder, M., Voisin, C. & Sardella, A. Impact of chlorinated swimming pool attendance on the respiratory health of adolescents. *Pediatrics* **124,** 1110–1118 (2009).
64. White, C. W. & Martin, J. G. Chlorine gas inhalation: human clinical evidence of toxicity and experience in animal models. *Proc. Am. Thorac. Soc.* **7,** 257–263 (2010).
65. Hoyle, G. W. & Svendsen, E. R. Persistent effects of chlorine inhalation on respiratory health. *Ann. N. Y. Acad. Sci.* (2016). doi:10.1111/nyas.13139
66. Florentin, A., Hautemanière, A. & Hartemann, P. Health effects of disinfection by-products in chlorinated swimming pools. *Int. J. Hyg. Environ. Health* **214,** 461–469 (2011).
67. Jacobs, J. H. *et al.* Exposure to trichloramine and respiratory symptoms in indoor swimming pool workers. *Eur. Respir. J.* **29,** 690–698 (2007).
68. Greeley, M. A., Van Winkle, L. S., Edwards, P. C. & Plopper, C. G. Airway trefoil factor expression during naphthalene injury and repair. *Toxicol. Sci. Off. J. Soc. Toxicol.* **113,** 453–467 (2010).
69. Van Winkle, L. S., Johnson, Z. A., Nishio, S. J., Brown, C. D. & Plopper, C. G. Early events in naphthalene-induced acute Clara cell toxicity: comparison of membrane permeability and ultrastructure. *Am. J. Respir. Cell Mol. Biol.* **21,** 44–53 (1999).
70. McGovern, T. K. *et al.* Dimethylthiourea protects against chlorine induced changes in airway function in a murine model of irritant induced asthma. *Respir. Res.* **11,** 138 (2010).
71. McGovern, T. K. *et al.* Neutrophils mediate airway hyperresponsiveness after chlorine-induced airway injury in the mouse. *Am. J. Respir. Cell Mol. Biol.* **52,** 513–522 (2015).
72. Koohsari, H., Tamaoka, M., Campbell, H. R. & Martin, J. G. The role of gamma delta T cells in airway epithelial injury and bronchial responsiveness after chlorine gas exposure in mice. *Respir. Res.* **8,** 21 (2007).
73. Tuck, S. A. *et al.* Time course of airway remodelling after an acute chlorine gas exposure in mice. *Respir. Res.* **9,** 61 (2008).
74. Jonasson, S., Koch, B. & Bucht, A. Inhalation of chlorine causes long-standing lung inflammation and airway hyperresponsiveness in a murine model of chemical-induced lung injury. *Toxicology* **303,** 34–42 (2013).

75. Wigenstam, E., Elfsmark, L., Koch, B., Bucht, A. & Jonasson, S. Acute respiratory changes and pulmonary inflammation involving a pathway of TGF-β1 induction in a rat model of chlorine-induced lung injury. *Toxicol. Appl. Pharmacol.* **309,** 44–54 (2016).
76. Martin, J. G. *et al.* Chlorine-induced injury to the airways in mice. *Am. J. Respir. Crit. Care Med.* **168,** 568–574 (2003).
77. Hox, V. *et al.* Airway exposure to hypochlorite prior to ovalbumin induces airway hyperreactivity without evidence for allergic sensitization. *Toxicol. Lett.* **204,** 101–107 (2011).
78. Hox, V. *et al.* Crucial role of transient receptor potential ankyrin 1 and mast cells in induction of nonallergic airway hyperreactivity in mice. *Am. J. Respir. Crit. Care Med.* **187,** 486–493 (2013).
79. Kim, S.-H., Park, D.-E., Lee, H.-S., Kang, H.-R. & Cho, S.-H. Chronic Low Dose Chlorine Exposure Aggravates Allergic Inflammation and Airway Hyperresponsiveness and Activates Inflammasome Pathway. *PLoS ONE* **9,** (2014).
80. Southam, D. S., Dolovich, M., O'Byrne, P. M. & Inman, M. D. Distribution of intranasal instillations in mice: effects of volume, time, body position, and anesthesia. *Am. J. Physiol. Lung Cell. Mol. Physiol.* **282,** L833-839 (2002).
81. Hammad, H. & Lambrecht, B. N. Barrier Epithelial Cells and the Control of Type 2 Immunity. *Immunity* **43,** 29–40 (2015).
82. Brusselle, G. G., Maes, T. & Bracke, K. R. Eosinophils in the spotlight: Eosinophilic airway inflammation in nonallergic asthma. *Nat. Med.* **19,** 977–979 (2013).
83. Lambrecht, B. N. & Hammad, H. The immunology of asthma. *Nat. Immunol.* **16,** 45–56 (2015).
84. Lambrecht, B. N. & Hammad, H. Biology of lung dendritic cells at the origin of asthma. *Immunity* **31,** 412–424 (2009).
85. Lambrecht, B. N. & Hammad, H. Dendritic cell and epithelial cell interactions at the origin of murine asthma. *Ann. Am. Thorac. Soc.* **11 Suppl 5,** S236-243 (2014).
86. Hammad, H. *et al.* House dust mite allergen induces asthma via Toll-like receptor 4 triggering of airway structural cells. *Nat. Med.* **15,** 410–416 (2009).
87. Willart, M. A. M. *et al.* Interleukin-1α controls allergic sensitization to inhaled house dust mite via the epithelial release of GM-CSF and IL-33. *J. Exp. Med.* **209,** 1505–1517 (2012).
88. Plantinga, M. *et al.* Conventional and monocyte-derived CD11b(+) dendritic cells initiate and maintain T helper 2 cell-mediated immunity to house dust mite allergen. *Immunity* **38,** 322–335 (2013).
89. Vroman, H., Hendriks, R. W. & Kool, M. Dendritic Cell Subsets in Asthma: Impaired Tolerance or Exaggerated Inflammation? *Front. Immunol.* **8,** (2017).
90. Provoost, S., Maes, T., Joos, G. F. & Tournoy, K. G. Monocyte-derived dendritic cell recruitment and allergic T(H)2 responses after exposure to diesel particles are CCR2 dependent. *J. Allergy Clin. Immunol.* **129,** 483–491 (2012).
91. Provoost, S. *et al.* Diesel exhaust particles stimulate adaptive immunity by acting on pulmonary dendritic cells. *J. Immunol. Baltim. Md 1950* **184,** 426–432 (2010).
92. Kim, H. Y., Umetsu, D. T. & Dekruyff, R. H. Innate lymphoid cells in asthma: Will they take your breath away? *Eur. J. Immunol.* **46,** 795–806 (2016).
93. Klein Wolterink, R. G. J. *et al.* Pulmonary innate lymphoid cells are major producers of IL-5 and IL-13 in murine models of allergic asthma. *Eur. J. Immunol.* **42,** 1106–1116 (2012).
94. Halim, T. Y. F. *et al.* Group 2 innate lymphoid cells are critical for the initiation of adaptive T helper 2 cell-mediated allergic lung inflammation. *Immunity* **40,** 425–435 (2014).
95. Chang, Y.-J. *et al.* Innate lymphoid cells mediate influenza-induced airway hyper-reactivity independently of adaptive immunity. *Nat. Immunol.* **12,** 631–638 (2011).
96. Kim, H. Y. *et al.* Innate lymphoid cells responding to IL-33 mediate airway hyperreactivity independently of adaptive immunity. *J. Allergy Clin. Immunol.* **129,** 216-227–6 (2012).
97. Yang, Q. *et al.* Group 2 innate lymphoid cells mediate ozone-induced airway inflammation and hyperresponsiveness in mice. *J. Allergy Clin. Immunol.* **137,** 571–578 (2016).
98. De Grove, K. C. *et al.* Dysregulation of type 2 innate lymphoid cells and TH2 cells impairs pollutant-induced allergic airway responses. *J. Allergy Clin. Immunol.* **139,** 246–257.e4 (2017).
99. Moscato, G. *et al.* Occupational asthma and occupational rhinitis in hairdressers. *Chest* **128,** 3590–3598 (2005).
100. Cruz, M. J. *et al.* Persistence of respiratory and inflammatory responses after dermal sensitization to persulfate salts in a mouse model of non-atopic asthma. *Allergy Asthma Clin. Immunol.* **12,** 26 (2016).
101. De Vooght, V. *et al.* Ammonium persulfate can initiate an asthmatic response in mice. *Thorax* **65,** 252–257 (2010).

Summary

Via inhalation we are continuously exposed to environmental agents, such as gasses, chemicals and particles in the air. The first layer of cells that come into contact with these inhaled agents is the airway epithelium. Airway epithelial cells are closely linked to each other, creating a barrier that prevents entry of inhaled (deleterious) agents to the human body. Proper functioning of the airway epithelial barrier is crucial in host defense and the importance of an intact barrier has already implicated in a number of respiratory diseases, such as asthma, rhinitis and chronic obstructive pulmonary disease, where dysfunction of the epithelium occurs.

Inhalation of irritating agents induces a reversible inflammatory response compromising coughing, wheezing and increased mucus production, persistence of these symptoms is indicative of irritant-induced asthma (IIA). IIA is a subtype of asthma that develops after exposure to irritants, such as chlorine, formaldehyde, strong acids and smoke, without an immunological sensitization towards the causal agent. IIA can arise after acute exposure to high concentrations of respiratory irritants, such as during an explosion, fire or accidental leak. However, continuous exposure to lower levels of irritating agents, such as for example exposure of chlorine in professional swimmers, lifeguards and cleaning personnel, can result in IIA. Currently the mechanisms leading to IIA are poorly known.

The general hypothesis in this dissertation is that environmental irritants can disturb the airway epithelial barrier and that this contributes to the development of airway hypersensitivity, as in IIA. Therefore we first evaluated the effect of different types of irritants on the airway epithelial barrier on an *in vitro* level. In a second part, we tested in mice the hypothesis that due to airway barrier impairment, inhalation of low levels of irritants can result in airway hypersensitivity.

In chapter 3, a co-culture mimicking the airway epithelial barrier was exposed to different types of environmental irritants. This co-culture consisted of bronchial epithelial cells (16HBE) and endothelial cells (HLMVEC) seeded on the opposite sides of a permeable membrane, and monocytes (THP-1) added apically. We found that the nanoparticles graphene and graphene oxide induced an immediate negative effect on the airway epithelial barrier. Hypochlorite only induced a negative effect after 24 hours of exposure, and ammonium and sodium persulfate did not alter the barrier function. Using immunofluorescent staining a less connected tight junction network was observed due to graphene and graphene oxide exposure. By means of phosphoproteomics we found that graphene and graphene oxide altered the level of phosphorylation of proteins from the tight junction and adherens junction pathway, hereby providing an explanation of the reduced barrier function following exposure to graphene and graphene oxide.

Next, we evaluated whether mast cells could influence the response of the airway epithelium upon exposure to environmental irritants (chapter 4). Bronchial epithelial cells (16HBE) were seeded on a

permeable membrane in absence or in presence of mast cells (HMC-1) on the basolateral or apical side, and were exposed to different types of irritants. Irrespective of the seeding condition, graphene and graphene oxide had an immediate and persistent negative effect on the airway epithelial barrier, whereas hypochlorite and diesel exhaust particles only induced a temporary decrease in barrier function. After irritant exposure, the bronchial epithelial cells did not release the 'danger' signals TSLP, IL-33 or IL-1α and the mast cells were not activated. Due to the inactive (or immature) state of the HMC-1 cells, no additional effects of the airway epithelium following irritant exposure was found in these cultures.

In the first *in vivo* study of this thesis, we combined the mouse model of naphthalene-induced airway damage (after a recovery period) with a single intranasal exposure to the common disinfectant hypochlorite (chapter 5). We demonstrated that naphthalene-induced barrier impairment resulted in temporary enlargement of the lungs and airways and in a permanent increase in the functional lung volumes. The challenge with hypochlorite induced a sensory irritant response, as well as, development of airway hyperresponsiveness and pulmonary inflammation. The increased airway permeability and epithelial damage after exposure to hypochlorite indicated that due to barrier impairment the epithelium is more vulnerable for the irritant effect of hypochlorite. Moreover, the naphthalene-induced epithelial dysfunction resulted in the recruitment of monocyte-derived dendritic cells towards the lung and increased the type 2 innate lymphoid cell population because of the additional insult with hypochlorite. We confirmed our hypothesis that due to impairment of the airway epithelial barrier, with partial recovery, the mice became more sensitive for exposure to hypochlorite.

In chapter 6, we implemented a more vigorous treatment protocol, in which mice were treated twice with naphthalene in order to impair the airway barrier, followed by repeated endotracheal instillations with hypochlorite. In this model the functional lung volumes of mice treated with naphthalene also increased. In combination with the endotracheal instillations, the repeated barrier impairment resulted in non-specific airway hyperresponsiveness. The increase in neutrophils in the broncho-alveolar lavage fluid and epithelial damage on histologic sections at the end of the experiment indicated that the mice were not fully recuperated from the repeated barrier impairment. Airway exposure to hypochlorite did not augment the airway responses and epithelial damage, but did increase the number of eosinophils in the lung. Using this more vigorous treatment protocol, specific sensitivity towards hypochlorite did not develop, but the mice did become more sensitive to airway exposure in general.

To conclude, in this thesis we demonstrated that different types of environmental irritants have different effects on the airway epithelial barrier *in vitro*, and that impairment of the airway epithelial

barrier can result in the development of airway hypersensitivity in mice. By studying these mechanisms, we demonstrated that the airway epithelial barrier and its interaction with respiratory irritants are crucial aspects in the development of IIA.

Samenvatting

Wanneer we inademen worden we continu blootgesteld aan stoffen, zoals gassen, chemicaliën en partikels, in de lucht. De eerste lijn van cellen die in contact komen met deze ingeademde lucht, zijn de cellen van het luchtwegepitheel. Luchtwegepitheelcellen zijn nauw met elkaar verbonden en vormen zo een barrière, opdat ingeademde (schadelijke) stoffen het lichaam niet binnendringen. Deze barrière is van cruciaal belang ter bescherming van de mens, en het belang van een intacte barrière werd reeds aangetoond in luchtwegaandoeningen zoals astma, rhinitis en chronisch obstructief longlijden, waar dysfunctie van de luchtwegbarrière plaatsvindt.

Inhalatie van irriterende stoffen induceert een tijdelijke ontstekingsreactie die bestaat uit hoesten, piepende ademhaling en verhoogde mucusproductie, het aanhouden van deze symptomen is indicatief voor irritant-geïnduceerd astma (IIA). IIA is een vorm van astma die optreedt na blootstelling aan irritantia, zoals chlorine, formaldehyde, sterke zuren en rook, zonder ontwikkeling van een immunologische sensitisatie naar de causale stof. IIA kan optreden na een acute blootstelling aan hoge concentraties van irriterende stoffen, zoals tijdens een explosie, brand of accidentele lek. Maar ook continue blootstelling aan lagere concentraties van irriterende stoffen, zoals bijvoorbeeld blootstelling aan chlorine in professionele zwemmers, redders of schoonmaakpersoneel, kan leiden tot IIA. Momenteel zijn de mechanismen die leiden tot IIA maar beperkt gekend.

De algemene hypothese in dit werk is dat omgevingsirritantia de luchtwegbarrière kunnen verstoren en dat dit bijdraagt tot de ontwikkeling van luchtwegovergevoeligheid zoals in IIA. Hiervoor evalueerden we eerst het effect van verschillende soorten irritantia op de luchtwegbarrière op een *in vitro* niveau. In een tweede deel, testen we in muizen de hypothese dat door schade aan het luchtwegepitheel inhalatie van lage concentraties irritantia, kan leiden tot luchtwegovergevoeligheid.

In hoofdstuk 3, werd een co-cultuur die de luchtwegbarrière nabootst blootgesteld aan verschillende soorten omgevingsirritantia. Deze co-cultuur bestond uit bronchiale epitheelcellen (16HBE) en endotheelcellen (HLMVEC) die gezaaid werden aan weerszijden van een permeabel membraan, en monocyten (THP-1) die apicaal werden toegevoegd. Hier toonden we aan dat de nanopartikels grafeen en grafeen oxide onmiddellijk een nadelig effect op de luchtwegbarrière hebben. Hypochloriet veroorzaakte slechts na 24 uur een nadelig effect op de luchtwegbarrière, en ammonium- en natriumpersulfaat veranderden de barrièrefunctie niet. Op basis van immunofluorescente kleuring observeerden we na blootstelling aan grafeen en grafeen oxide, een verminderde aaneenschakeling van de ‘tight junctions’ in de epitheelcellen. Gebruik makend van fosfoproteomics stelden we vast dat door blootstelling aan grafeen en grafeen oxide, proteïnen in de ‘tight junction’ en ‘adherens junction’ pathways een andere graad van fosforylatie kregen, wat een verklaring geeft voor de geobserveerde daling in barrièrefunctie door blootstelling aan grafeen en grafeen oxide.

Vervolgens, evalueerden we of mast cellen een invloed hebben op de respons van het luchtwegepitheel na blootstelling aan irritantia (hoofdstuk 4). Hiervoor werden bronchiale epitheelcellen (16HBE) gezaaid op een permeabel membraan in af- of aanwezigheid van mastcellen (HMC-1) aan de basolaterale zijde of aan de apicale zijde. Deze culturen werden blootgesteld aan verschillende typen van irritantia. Ongeacht de samenstelling van de celcultuur, hadden grafeen en grafeen oxide een onmiddellijk en persistent negatief effect op de luchtwegbarrière, terwijl hypochloriet en diesel partikels slechts een tijdelijke daling in de barrièrefunctie veroorzaakten. Na blootstelling aan de irriterende stoffen zetten de bronchiale epitheelcellen de 'danger' signalen TSLP, IL-33 or IL-1α niet vrij en werden de mast cellen niet geactiveerd. Door de inactieve (of immature) staat van de HMC-1 cellen, werd in deze culturen geen additionele respons van het luchtwegepitheel gevonden na blootstelling aan irritantia.

In de eerste *in vivo* studie van deze thesis combineerden we het muismodel van naftaleen-geïnduceerde luchtwegschade (na een herstelperiode) met een enkelvoudige intranasale blootstelling aan het veelvoorkomend desinfectans hypochloriet (hoofdstuk 5). We toonden aan dat naftaleen-geïnduceerde barrièreverstoring leidde tot een tijdelijke vergroting van de longen en luchtwegen, en tot een permanente toename in de functionele longvolumes. De blootstelling aan hypochloriet induceerde een sensorische irritante ademhalingsrespons, alsook ontwikkeling van bronchiale hyperreactiviteit en pulmonale inflammatie. De toename in luchtwegpermeabiliteit en epitheliale schade na blootstelling aan hypochloriet gaf aan dat door de barrière verstoring het epitheel meer gevoelig is voor het irriterend effect van hypochloriet. Bovendien leidde de naftaleen-geïnduceerde epitheeldysfunctie tot rekrutering van monocyt-afgeleide dendritische cellen naar de long en verhoogde het extra insult met hypochloriet de populatie van type 2 aangeboren lymfoïde cellen. Hiermee bevestigden we onze hypothese dat door verstoring van de luchtwegbarrière, met partieel herstel, muizen gevoeliger werden voor een blootstelling aan hypochloriet.

In hoofdstuk 6, implementeerden we een ingrijpender behandelingsprotocol, waarin de muizen tweemaal werden behandeld met naftaleen om de barrière te verstoren, gevolgd door herhaaldelijke endotracheale instillaties met hypochloriet. Ook in dit model vergrootten de functionele longvolumes van de muizen die behandeld werden met naftaleen. In combinatie met de endotracheale instillaties, leidde de herhaaldelijke barrièreverstoring tot een niet-specifieke bronchiale hyperreactiviteit. Verhoging van het aantal neutrofielen in de long en epitheelschade op histologische coupes toonde aan dat op het einde van het experiment de muizen niet volledig hersteld waren van de herhaaldelijke barrièreverstoring. Hypochloriet blootstelling versterkte de luchtwegresponsen en epitheelschade niet, maar leidde wel tot een toename in eosinofielen in de long. Gebruik makend van dit ingrijpender

behandelingsprotocol werd geen specifieke gevoeligheid naar hypochloriet ontwikkeld, maar werden de muizen wel gevoeliger voor luchtwegblootstelling in het algemeen.

Ter conclusie, in deze thesis toonden we aan dat verschillende soorten omgevingsirritantia verschillende effecten hebben op de luchtwegbarrière *in vitro* en dat verstoring van de luchtwegbarrière kan leiden tot de ontwikkeling van luchtwegovergevoeligheid in muizen. Door deze mechanismen te bestuderen, werd aangetoond dat de luchtwegbarrière en de interactie hiervan met irritantia, belangrijke aspecten zijn in de ontwikkeling van IIA.

Scientific acknowledgement, personal contribution and conflict of interest statements

Scientific acknowledgements

I would like to thank Lore Pollaris and Anne-Charlotte Jonckhere for their information on the lung digestion protocol, flow cytometry staining protocol and DC and ILC staining panel. I also express thanks to Stevan Cokic for his acquisition of the TEM images of the G and GO particles. In addition, I would like to thank Dr. Åsa Gustafsson for the experiments with the PreciseInhale system. I would like to mention Mimi Abebe Bogale and Alessandra Pagliaro for their assistance in the TEER and flux experiments during their master project.

Personal contribution

Sofie Van Den Broucke contributed to the design of the studies in close collaboration with her promotor Peter Hoet and co-promoter Jeroen Vanoirbeek. Sofie Van Den Broucke executed the experiments and performed the data analysis. For the phosphoproteomics data, Rita Derua processed the provided membrane fraction cell lysates for LC-MS/MS and identified peptides and proteins. Sofie Van Den Broucke executed the experiments in chapter 4 partly at the research institute Swetox in Sweden in close collaboration with Dr. Ernesto Alfaro-Moreno. Lung function measurements were performed by Sofie Van Den Broucke with the assistance of Jeroen Vanoirbeek, Lore Pollaris or Tatjana Decaesteker. Sofie Van Den Broucke acquired, processed and quantified the micro-CT images of mice. Jonathan Cremer ran the provided lung samples on flow cytometry. Sofie Van Den Broucke wrote the first drafts of the chapters/articles and presented the work at national and international conferences.

Conflicts of interest

There are no conflicts of interest.

List of publications

International peer-reviewed publications

First author

Van Den Broucke S, Vanoirbeek J, Alfaro-Moreno E, and Hoet P. Contribution of mast cells in irritant-induced airway epithelial barrier impairment *in vitro*. *Manuscript submitted.*

Van Den Broucke S, Jonckheere A-C, Pollaris L, Decaesteker T, Cremer J, Nemery B, Hoet P, and Vanoirbeek J. Recruitment of monocyte-derived dendritic cells and type 2 innate lymphoid cells in a mouse model of irritant-induced asthma. *Manuscript submitted.*

Luyts K, **Van Den Broucke S**, Hemmeryckx B, Poels K, Scheers H, Casas L, Vanoirbeek J, Nemery B, and Hoet P. Nanoparticles in the lungs of old mice: Pulmonary inflammation and oxidative stress without procoagulant effects. *Science of the Total Environment*, June 2018.
(First two authours equally contributed)

Van Den Broucke S, Pollaris L, Vande Velde G, Verbeken E, Nemery B, Vanoirbeek J, and Hoet P. Irritant-Induced Asthma to Hypochlorite in Mice due to Impairment of the Airway Barrier. *Archives of Toxicology*, January 2018.

Co-author

Devos F, Pollaris L, **Van Den Broucke S**, Seys S, Goossens A, Nemery B, Hoet P, and Vanoirbeek J. Methylisothiazolinone: Dermal and Respiratory Immune Responses in Mice. *Toxicology Letters*, June 2015.

Pollaris L, **Van Den Broucke S**, Decaesteker T, Cremer J, Devos FC, Verbeken E, Provoost S, MaestT, Nemery B, Hoet P, and Vanoirbeek J. Dermal exposure determines the outcome of repeated airway exposure in a long-term chemical-induced asthma-like mouse model. *Revised manuscript submitted to Toxicological Sciences.*

Manuscripts in preparation

Van Den Broucke S, Derua R, Vanoirbeek J, and Hoet P. Effect of irritants on a co-culture model of the airway barrier.

Van Den Broucke S, Decaesteker T, Verbeken E, Nemery B, Vanoirbeek J, and Hoet P. Airway barrier impairment increases nonspecific airway hyperresponsiveness in mice.

Abstracts presented at conferences

International conferences

Van Den Broucke S, Pollaris L, Vande Velde G, Verbeken E, Nemery B, Vanoirbeek J, and Hoet P. Irritant-Induced Asthma to Hypochlorite in Mice due to Impairment of the Airway Barrier. Poster presentation at the annual Fraunhover seminar on models of lung disease. 18-19 January 2018, Hannover, Germany

Van Den Broucke S, Öner D, Vriens H, Vanoirbeek J, and Hoet P. Effect of Environmental Irritants on the Respiratory Barrier in a 3D-Cell Culture Model. Poster discussion session at American Thoracic Society (ATS) International Conference. 13-18 may 2016, San Francisco, US.

Van Den Broucke S, Devos F, Pollaris L, Seys S, Goossens A, Nemery B, Hoet P, and Vanoirbeek J. Methylisothiazolinone, a strong dermal sensitizer, is a non-asthmogenic irritant. Poster presentation at European Respiratory Society (ERS) Lung Science Conference. 13-15 March 2015, Estoril, Portugal.

National conferences

Van Den Broucke S, Pollaris L, Vande Velde G, Verbeken E, Nemery B, Vanoirbeek J, and Hoet P. Irritant-Induced Asthma to Hypochlorite in Mice due to Impairment of the Airway Barrier. Oral presentation at the BVP, GlaxoSmithKline Awards in Pneumology. 30 May 2018, Brussels.

Van Den Broucke S, Pollaris L, Vande Velde G, Verbeken E, Nemery B, Vanoirbeek J, and Hoet P. Irritant-Induced Asthma to Hypochlorite in Mice due to Impairment of the Airway Barrier. Poster presentation at Beltox Annual Scientific Meeting. 1 December 2017, Leuven.

Van Den Broucke S, Vanoirbeek J, Nemery B, Hoet P. Effect of graphene and graphene oxide on the respiratory barrier in a 3D-cell culture model. Poster presentation at Beltox Annual Scientific Meeting. 9 December 2016, Louvain-la-Neuve.

Van Den Broucke S, Öner D, Vriens H, Vanoirbeek J, Hoet P. Effect of environmental irritants on the respiratory barrier in a 3D-cell culture model. Oral presentation at the annual scientific IUAP meeting. 2 June 2016, Gent.

Van Den Broucke S, Öner D, Vriens H, Hoet P. Effect of environmental irritants on the respiratory barrier in a 3D-cell culture model. Poster presentation at Beltox Annual Scientific Meeting. 26 November 2015, Antwerp.

Van Den Broucke S, Devos F, Pollaris L, Seys S, Goossens A, Nemery B, Hoet P, and Vanoirbeek J. Methylisothiazolinone, a strong dermal sensitizer, is a non-asthmogenic irritant. Poster presentation at the annual scientific IUAP meeting. 12 June 2015, Leuven.

Short curriculum vitae

Sofie Van Den Broucke was born on June 19th 1991 in Turnhout, Belgium. In 2009, she graduated from secondary school at the Sint-Pietersinstituut in Turnhout. After secondary school, she started her training in Biomedical Sciences at the KU Leuven. In 2014, she graduated magna cum laude as Master of Science: Biomedical Sciences, during her master thesis she investigated the dermal and immune responses of methylisothiazolinone in mice. She started, in 2014, her PhD in the Laboratory of Occupational and Environmental Toxicology, at KU Leuven under supervision of Prof. Peter Hoet and Prof. Jeroen Vanoirbeek. She performed *in vitro* as well as *in vivo* (mice) research on the effect of respiratory irritants on the airway epithelial barrier and the development towards airway hypersensitivity.